UNIVERSITÀ DEGLI STUDI DI UDINE
hic sunt futura

www.uniud.it

Corso di dottorato di ricerca in:

Scienze e Biotecnologie Agrarie

Ciclo XXXI

Dissecting the role of iron in the interaction between the host plant tomato and 'Candidatus Phytoplasma solani'

Dottorando

Dott.ssa Sara Buoso

Supervisore

Dott.ssa Simonetta Santi

Anno 2019

Contents

Abstract

Phytoplasmas are prokaryotic plant pathogens that colonize the sieve elements of the host plant, causing alteration in phloem function and impairment of assimilate translocation. Despite the huge impact on agriculture and the lack of effective curative strategies, mechanisms underlying plant host-phytoplasma interaction are still largely unexplored. In particular, no knowledge is available on the role of iron (Fe) in this interaction. Iron is an essential element for most living organisms, and competition for it can lead, as already observed in different pathosystems, to the development of an Fe-withholding response by plants that changes Fe distribution and trafficking. In the current study, we investigated on the role of Fe in the interaction between tomato and '*Candidatus* Phytoplasma solani' by analyzing healthy plants (H/+Fe), Fe-starved plants (H/-Fe), phytoplasma-infected plants (I/+Fe) and phytoplasma-infected/Fe-starved plants (I/-Fe). Firstly, an experimental system was set up so that phytoplasma infection and occurrence of Fe deficiency symptoms were concomitant. Then, high-throughput RNA-sequencing focused on midrib-enriched tissue was conducted to profile leaf transcriptome changes in both stresses. We found that most of differentially regulated genes in common to I/+Fe and H/-Fe plants encode proteins involved in photosynthetic light reactions, in porphyrin and chlorophyll metabolism, and in carotenoid biosynthesis. These similarities supported the hypothesis that phytoplasma might induce alteration in cellular Fe homeostasis. Even if no significant difference in total Fe concentration emerged when comparing H and I plants under both nutritional conditions, the phytoplasma presence caused local modifications of Fe distribution visible by Perls'-DAB staining, with a shift from the leaf lamina to the site of infection (the phloem). Similar to healthy (H/+Fe), Fe dots were localized to the phloem in the infected leaves (I/+Fe), but lacked in xylem parenchyma cells similar to H/-Fe leaves. Moreover, in both stresses the mesophyll palisade cells of the leaf lamina had fewer Fe dots than in H/+Fe condition.

We examined the activity of genes involved in the Fe uptake and Fe homeostasis in roots. Under Fe-sufficient conditions, the phytoplasma apparently did not alter the acquisition mechanism. Under Fe-deficient conditions, the phytoplasma reduced the expression of all the examined genes, except for *FRO1*. These findings suggest that, under Fe-deficient conditions, the presence of phytoplasmas may compromise the communication of the Fe status between leaves and roots, possibly by the interference with the synthesis or transport of a promotive signal.

Keywords: iron deficiency, iron homeostasis, phytoplasma, phloem, tomato, tomato grafting

1. Introduction

1.1. Phytoplasmas

Phytoplasmas are plant pathogenic bacteria belonging to the class *Mollicutes*, a group of wall-less microorganisms phylogenetically related to low G+C Gram-positive bacteria (Weisburg *et al.*, 1989). They are transmitted by insect vectors and are associated with devastating damage to over 700 plant species worldwide, including many economically important crops, fruit trees and ornamental plants (Hogenhout *et al.*, 2008; Oshima *et al.*, 2011). These diseases were initially attributed to plant viruses because their aetiological agents are transmitted by insects, are not cultivable in artificial media, and often cause symptoms similar to those of viral diseases. In 1967, Doi *et al*. discovered small pleomorphic structures that resembled mycoplasmas (bacterial pathogens of humans and animals) in the phloem of plants affected by these diseases (Fig. 1). The associated agents were named mycoplasma-like organisms (MLO) because of their morphology, similar to that described for mycoplasmas, and their sensitivity to tetracycline antibiotics (Ishiie *et al.*, 1967).

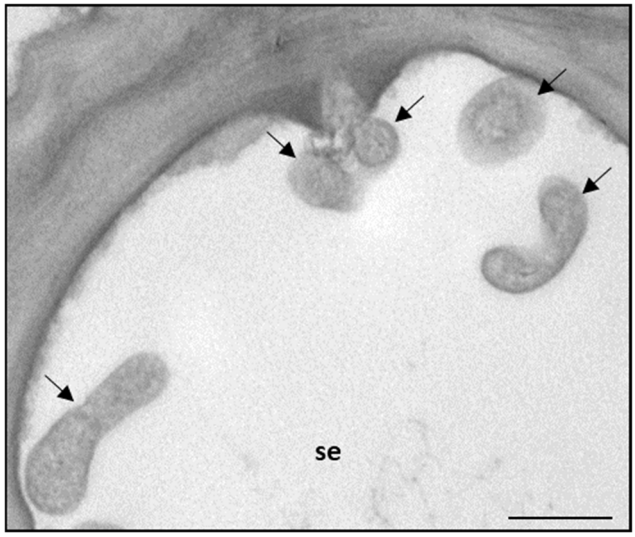

Figure 1. Transmission electron micrographs of phloem tissue of Solanum lycopersicum leaves infected with '*Candidatus* Phytoplasma solani'. Phytoplasmas (arrows), located in sieve elements, show a pleomorphic shape. se: sieve elements. Bar indicates 500 nm.

During the last three decades the application of molecular technologies has provided evidence that these wall-less prokaryotes constitute a large monophyletic group within the class *Mollicutes*, and the name "phytoplasma" followed by designation of '*Candidatus* Phytoplasma' (IRPCM, 2004), were adopted. The comprehensive phytoplasma classification scheme was constructed on restriction fragment length polymorphism (RFLP) patterns of polymerase chain reaction (PCR)-amplified 16S rDNA sequences (Lee *et al.*, 1998; Marcone *et al.*, 2000; Lee *et al.*, 2004a, b; Zhao and Davis, 2016). In this way, the identities of many phytoplasmas associated with hundreds of diseases were determined clearly and 35 ribosomal 16Sr RNA groups have been established (Pérez-López *et al.*, 2016).

Phytoplasmas are similar to bacterial bodies of small dimensions, varying from 200 nm to 800 nm in diameter, delimited only by a plasma membrane (Lee *et al.*, 2000). The absence of a rigid cell wall allows them to be highly pleomorphic and to change shape adapting to the environment (Fig. 1).

Phytoplasma transmission is persistent and propagative. Even if it can occur via vegetative propagation (such as through grafting of infected shoots onto healthy plants, cuttings and by micropropagation practices), in nature phytoplasmas spread mainly through phloem-feeding insects belonging to the families *Cicadellidae* (leafhoppers), *Fulgoridae* (planthoppers), and *Psyllidae* (psyllids) (Weintraub and Beanland, 2006). This means that the feeding preferences of the insect vectors determine the host range of phytoplasmas. Phytoplasma acquisition by insect vector occurs during its feeding activity on the phloem of infected plants, which, to ensure the infection, must last for an extended period (called acquisition access period, AAP) (Fig. 2). During the latent period (LP), phytoplasmas move from the guts of the insect vector, colonize the salivary glands and multiply inside. Then, the insect becomes infective and introduces phytoplasmas in the phloem of healthy plants, through the feeding activity, during the so-called inoculation access period (IAP) (Christensen *et al.*, 2005; Bosco *et al.*, 2007; Hogenhout *et al.*, 2008; Oshima *et al.*, 2011).

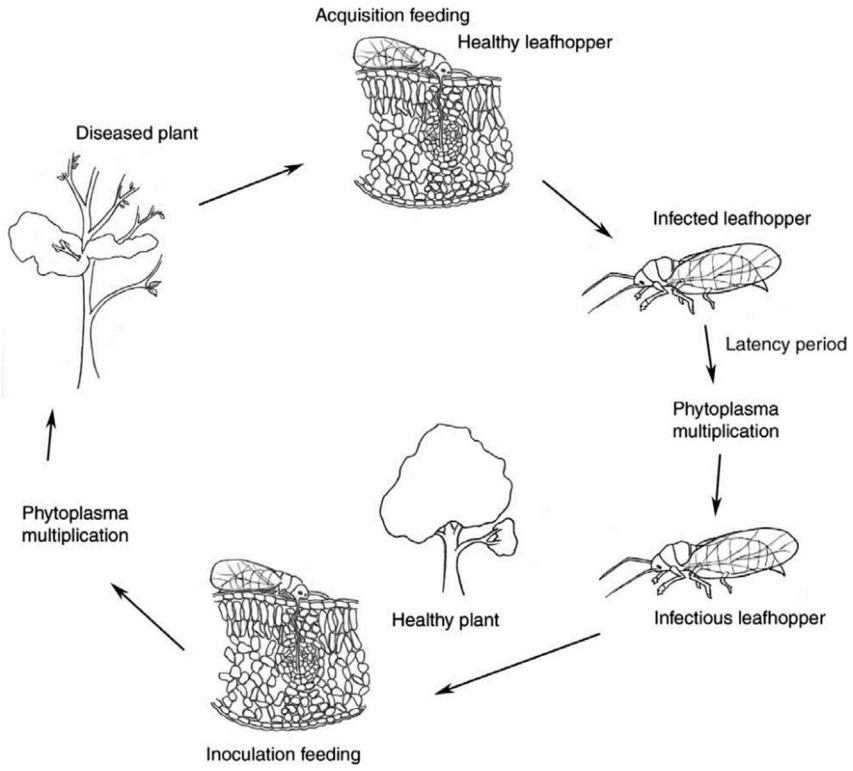

Figure 2. Cycle of phytoplasmas in plant host and insect vector. A healthy leafhopper feeds on a phytoplasma-infected plant (acquisition feeding). A latency period, during which the phytoplasmas multiply within the insect, is necessary before the insect can transmit phytoplasmas to a healthy plant (inoculation feeding). Multiplication and spread of phytoplasmas in the host plant are accompanied by the appearance of disease symptoms (from Christensen *et al.*, 2005).

Phytoplasmas mainly reside in mature sieve tubes (Christensen *et al.*, 2004). Here they can move systemically through the plant, reaching most organs of infected plants (Cordova *et al.*, 2003; Wei *et al.*,2004). Phytoplasmas have not genes coding for cytoskeleton elements or flagella and thus their

active movement seems unlikely (Christensen *et al.*, 2005). On the other hand, phytoplasma spread throughout the plant cannot be explained solely by assimilate flow since some authors demonstrated a deviance between phloem velocity or direction and phytoplasma distribution in the plant (Schaper *et al.*, 1984; Wei *et al.*, 2004). Moreover, phytoplasmas interact with the plant and insect cytoskeleton by the immunodominant membrane proteins (IMP) (Galetto *et al.*, 2011; Boonrod *et al.*, 2012), imposing SE actin reorganization (Buxa *et al.*, 2015). Considering that actin is stimulated by intracellular bacteria for promoting their motility (Borisy and Svitkina, 2000; Opalski *et al.*, 2005; Haglund and Welch, 2011), actin binding could be involved in phytoplasma movement within SEs and through the sieve plates.

Phytoplasmas possess the smallest genome of any plant pathogenic bacteria (530 – 1350 kb), consisting in one chromosome and several small plasmids with a unique replication gene (Nishigawa *et al.*, 2001; Oshima *et al.*, 2001a; Firrao *et al.*, 2007). In 2004, the first complete genomic sequence of a phytoplasma (*Ca*. Phytoplasma asteris OY strain) was published by Oshima *et al.* (2004) and in the following years six other phytoplasma genomes were released (Bai *et al.*, 2006; Tran-Nguyen *et al.*, 2008; Kube *et al.*, 2008; Andersen *et al.*, 2013; Orlovskis *et al.*, 2017; Wang *et al.*, 2018). Phytoplasma genome sequence mostly contains genes for basic cellular functions, such as DNA replication, transcription, translation, and protein translocation (Kakizawa *et al.*, 2001; Jung *et al.*, 2003). On the other hand, it lacks genes for the synthesis of compounds considered necessary for the cell metabolism, such as genes for amino acid biosynthesis, fatty acid biosynthesis, the tricarboxylic acid cycle, and the oxidative phosphorylation (Razin *et al.*, 1998; Oshima *et al.*, 2004; Bai *et al.*, 2006). Owing to the high concentration of C4 compounds in plants, and the presence of malic enzyme (ME) in all phytoplasma genomes so far sequenced, the oxidative decarboxylation of malate and the subsequent conversion to acetate might represent an adaptation to generate energy (Kube *et al.*, 2012). Interesting, the phytoplasma genome encodes multiple copies of transporter-related genes such as malate, metal-ion and amino-acid transporters (Oshima *et al.*, 2004; Arashida *et al.*, 2008). This may indicate that phytoplasmas can survive by means of the absorption of host cell substances and use different transporters in plant and insect hosts (Bai *et al.*, 2006; Oshima *et al.*, 2011; Oshima *et al.*, 2013). The loss of these biosynthetic genes may be the result of a reductive evolution of phytoplasmas, which is common among intracellular parasites adapting to a nutrient-rich environment (Oshima *et al.*, 2004). The profound disturbance caused by phytoplasmas on their plant host is clearly suggested by plant morphology of the infected plants. Apical meristems, which are major determinants of plant morphotype and fertility, are targets of phytoplasmas. Depending upon the developmental stage at the moment of infection, meristems derail from their normal destiny and produce distinct abnormal structures. These modifications correlate with transcriptional

reprogramming of key meristem switching genes. Moreover, disruption of apical dominance by the phytoplasma infection has been reported, resulting in repetitive initiation and outgrowth of axial shoots, witches'-broom growth, a characteristic of many phytoplasma plant diseases that yields no floral meristems (Wei *et al.*, 2013). Symptoms such as virescence, phyllody, sterility of flowers, witches'-broom appearance (proliferation of auxiliary or axillary shoots), abnormal elongation of internodes can indicate an unbalance in plant hormone level and growth regulators. Yellowing of leaves or shoots, leaf curling and generalized stunting is thought to be caused by a modification in carbohydrate synthesis and transportation (Lee *et al.*, 2000; Seemüller *et al.*, 2002; Bertaccini and Duduk, 2009). Also the production of effectors by phytoplasmas can interact directly with vector and host to influence developmental processes (Hogenhout and Loria, 2008; Hogenhout and Segura, 2010; Sugio *et al.*, 2011). The effectors are compounds secreted by the pathogen that share sequence, functional, or structural features with host proteins and thus can interfere with plant or insect cell processes (Desveaux *et al.*, 2006). Effectors could enhance phytoplasma fitness, modifying the plant development in accordance with pathogen needs, for example generating more vegetative tissues to attract the insect vectors, prolonging the vegetative growth phase of the plant to postpone plant death and suppressing inducible plant defence pathways (MacLean *et al.*, 2011; Sugio *et al.*, 2011; Lu *et al.*, 2014; MacLean *et al.*, 2014). Most characterized effectors are the proteins SAP11 of aster yellows witches'-broom phytoplasma (AY-WB) and TENGU of onion yellows phytoplasma (OY) (Bai *et al.*, 2009; Hoshi *et al.*, 2009).

In many phytoplasma-infected plants also photosynthesis is inhibited and a decrease of chlorophyll and carotenoids, together with inhibition of their biosynthesis, has been reported (Bertamini *et al.*, 2002a; Bertamini *et al.*, 2002b; Xue *et al.*, 2018). Though the symptoms induced in diseased plants vary with the phytoplasma and with the stages of infection (Zhang *et al.*, 2004), generally phytoplasma infections have a clearly detrimental effect on plants, causing from partial reduction in yield and quality to nearly total crop loss. For many crops, they even represent the primary limiting factor for the production (McCoy, 1989; Lee, 1992). Nevertheless, due to the extreme difficulty to culture them *in vitro* (Contaldo *et al.*, 2012) and the consequent absence of a clear comprehension of their physiology, no effective way of disease management has been yet developed. In fact, phytoplasma outbreak and spread can be controlled only by the eradication of infective plants and the use of insecticides to reduce insect vector populations. However, these approaches result burdensome both for their economic impact and for health implications to man and his environment (Desneux *et al.*, 2007; Bertaccini *et al.*, 2014). Controlling of disease is slowly shifting from chemical vector treatment to habitat management and the selection and screening of plants resistant to phytoplasma infection (Osler *et al.*, 2014; 2016). The understanding of the fine

mechanisms at the basis of plant responses to phytoplasma infection represents the necessary background for the development of these new strategies.

1.2. '*Candidatus* Phytoplasma solani'

'*Candidatus* Phytoplasma solani ('*Ca*. P. solani') is associated with stolbur disease (Valenta *et al.*, 1961; Quaglino *et al.*, 2013). '*Ca*. P. solani' falls within the 16SrXII group and is naturally transmitted by polyphagous planthoppers of the family *Cixiidae*, mainly *Hyalesthes obsoletus* and *Reptalus panzeri* (Fos *et al.*, 1992; Maixner, 1994; Cvrkovic *et al.*, 2014). '*Ca*. P. solani' is endemic in Europe and infects a wide range of weeds and cultivated plants (Lee *et al.*, 2000), such as solanaceous crops (tomato, tobacco, eggplant), grapevine, celery, maize, sugar beet, strawberry and lavender (reviewed in Garnier, 2000; Gatineau *et al.*, 2002; Duduk and Bertaccini, 2006; Jovic *et al.*, 2007). Infected plants show typical symptoms related to phytoplasma presence: flower malformation, leaf rolling and yellowing, and shoot lignification (Fig. 3). Annual crops develop symptoms a few weeks after insect inoculation, whereas symptoms on perennial hosts, such as grapevine, can appear one or more years after inoculation.

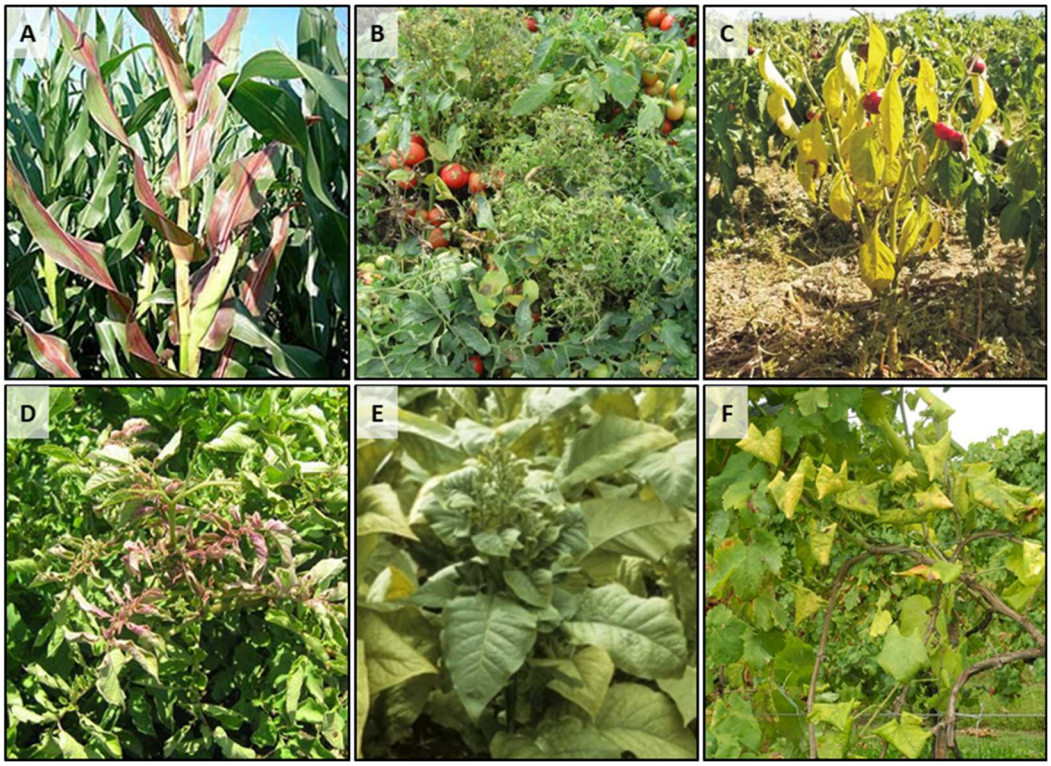

Figure 3. Different symptoms caused by 'Candidatus phytoplasma solany' on (A) maize, (B) tomato, (C) pepper, (D) potato, (E) tobacco and (F) grapevine. Images from: (A) Jović *et al.*, 2007; (B) http://www.fitosanitario.pc.it; (C) Ivanova *et al.*, 2017; (D) Ember *et al.*, 2011; (E) http://ephytia.inra.fr; (F) Courtesy: Alberto Loschi.

'*Ca*. P. solani' infection in grapevine (*Vitis vinifera*), generating the 'so-called' Bois noir disease, is common in European vineyards. This disease affects grapevine at a physiological, yield and fruit quality level, with different degrees of severity according to the cultivars (Garau *et al.*, 2007; Matus *et al.*, 2008; Endeshaw *et al.*, 2012; Rusjan *et al.*, 2012; Romanazzi *et al.*, 2013; Zahavi *et al.*, 2013; Rusjan and Mikulic-Petkovsek, 2015; Ember *et al.*, 2018). While the disease provokes the die of young plants, older plants can recover from the disease spontaneously (Belli *et al.*, 2010; Foissac and Maixner, 2013; Quaglino *et al.*, 2013). '*Ca*. P. solani' infection induces callose deposition and impairs carbohydrate metabolism in grapevine (Santi *et al.*, 2013a; 2013b). These authors showed that phytoplasma causes a switch of leaf function from source to sink of carbohydrates, due to the inhibition of sucrose transport and the increasing of sucrose cleavage activity at the transcriptional level. Photosynthesis is affected, as several genes encoding subunits of Photosystem I complex and other components of the electron transport chain resulted inhibited (Albertazzi *et al.*, 2009; Hren *et al.*, 2009; Punelli *et al.*, 2016). Moreover, key enzymes of flavonoid and stilbenes biosynthetic pathway, defence-related and hormones pathway genes are up-regulated by the infection (Santi *et al.*, 2013a; Paolacci *et al.*, 2017).

In tomato (*Solanum lycopersicum*) plants infected by '*Ca*. P. solani', the characteristic abnormal flowers are associated with changes in the expression of key flower development genes (Pracros *et al.*, 2006). Ahmad *et al.* (2013) showed that salicilate- and jasmonate-mediated defence pathways were activated differently by two strain of '*Ca*. P. solani', suggesting that distinct virulence factors were produce. Some alterations occur in phloem of phytoplasma infected tomato leaves, such as callose deposition and filamentous phloem protein accumulation at the sieve plates (De Marco *et al.*, 2016). This specific plant response to phytoplasma infection might contribute to the impairment of the translocation in the phloem (Furch *et al.*, 2007). Moreover, 'Ca. P. solani' infection leads to a re-organization of the sieve-element ultrastructure in phloem tissue of tomato plants and this changes probably express a transformation that benefits growth, maintenance and transport of phytoplasmas (Buxa *et al.*, 2015).

1.3. Phytoplasma-infection and plant nutrition

Phytoplasmas, as intracellular parasites restricted to phloem tissue, utilize numerous metabolic substances and mineral elements from the host plants. Indeed, the phloem is an environment rich in sugars, nutrients, amino acids, hormones, secondary metabolites, RNA and proteins (Ziegler 1975; Zimmermann and Ziegler 1975; Lohaus *et al.*, 1995; Murray and Christeller, 1995; Christeller *et al.*,

1998; Hartmann, 1999; Hayashi *et al.*, 2000; Dannenhoffer *et al.*, 2001; Ruiz-Medrano *et al.*, 2001; Dinant and Lemoine, 2010; van Bel *et al.*, 2013).

The phloem acts as transport network of some elements with high mobility, such as potassium (K), magnesium (Mg), phosphorus (P), nitrogen (N) and chlorine (Cl) (Marschner, 2011). Phytoplasma infection leads to mass flow impairment (Musetti *et al.*, 2013; Pagliari *et al.*, 2017), that could interfere on the physiological balance of the plants affecting both mineral concentration in the host cells and mineral allocation in the whole plant.

Phytoplasma diseases are often characterized by the presence of symptoms very similar to those displayed in plants subjected to nutritional deficiency, such as chlorosis, curling, and reddening. Nevertheless, there are only few studies on the changes in minerals in plants following phytoplasma infections. Schweigkofler *et al* (2008) showed that Bois noir disease caused a reduction of calcium (Ca) content and of other mineral elements such as N, Mg, P, K, manganese (Mn) and iron (Fe), in different grape cultivars. In phytoplasma infected pear and apricot, Fe/Mn and K/Mg imbalance occurs (Rossi *et al.*, 2010). Mg concentration was reduced in maize tissue infected by phytoplasma (De Oliveira *et al.*, 2002; 2005). Na (sodium), P and K increased, and Ca and B (boron) decreased in leaves of phytoplasma-infected lime (Al-Ghaithi *et al.*, 2016). In jujube infected with witches' broom disease (JWB), the K content in infected leaves was significantly higher than in healthy leaves, while the contents of Ca, Mg and Mn were significantly lower. Fe content was lower in the late growing season (Zhao and Liu, 2009).

1.4. Iron nutrition in plant

Fe is an essential mineral nutrient for most organisms, where can exist in both ferric (Fe^{3+}) and ferrous (Fe^{2+}) form, functioning as a catalytic component of enzymes that mediate redox reactions in key cellular processes, such as DNA replication and energy production. There are two major groups of Fe-containing proteins: heme proteins and Fe–S proteins. Heme proteins include various cytochromes, which contain the heme (a Fe-porphyrin coordination complex) bound as a prosthetic group. Other heme enzymes are catalase and peroxidases. In Fe–S proteins, Fe is coordinated to the thiol group of cysteine or/and to inorganic S as clusters. Several proteins that belong to the electron transport chains contain Fe as cofactor, mainly conjugated with S to form the Fe–S clusters (Johnson *et al.*, 2005; Balk and Pilon, 2011). About 80% of the Fe in leaves is localized in the chloroplasts (Terry and Abadia, 1986), where the most abundant Fe–S proteins are ferredoxin, and electron transport complexes such as photosystem I (PSI) and cytochrome b_6f.

Precisely because of its redox properties, if free, Fe can be very dangerous for the cell. Excess of Fe^{2+} inside a cell leads to the formation of hydroxyl radicals via the so-called Fenton reaction (Fenton, 1894; Haber *et al.*, 1934), which can cause damage to proteins, DNA, and lipids (Luo *et al.*, 1994). Thus, the concentration of free Fe ions must be tightly regulated. In this regard, ferritins in plastids and probably also in mitochondria play a fundamental role in the storage of Fe, preventing photo-oxidative damage (Briat *et al.*, 2010; Tarantino *et al.*, 2010). However, the bulk of Fe is usually bound as metabolically active Fe in Fe–S clusters.

Although Fe is abundantly present in Earth's crust, the bioavailability of this metal is restricted (Guerinot and Yi, 1994). In fact, Fe is mainly present as Fe^{3+}, which is poorly soluble at neutral and basic pH. In soil, Fe^{3+} predominates but is attached to silicate structures and immobilized in hydroxides, limiting Fe availability for plants. In calcareus soil, which covered more than 30% of the Earth's crust, Fe-deficiency is a yield-limiting factor and the most important plant nutritional disorder, (Mortvedt, 1991; Lucena, 2000), due to the high levels of both magnesium carbonate and calcium that reduce soil acidity.

To increase iron uptake under these conditions, non-grass and grass plant species evolved distinct iron-uptake strategies, respectively known as reducing (strategy I) and chelating (strategy II) strategies (Romheld. 1987) (Fig. 4).

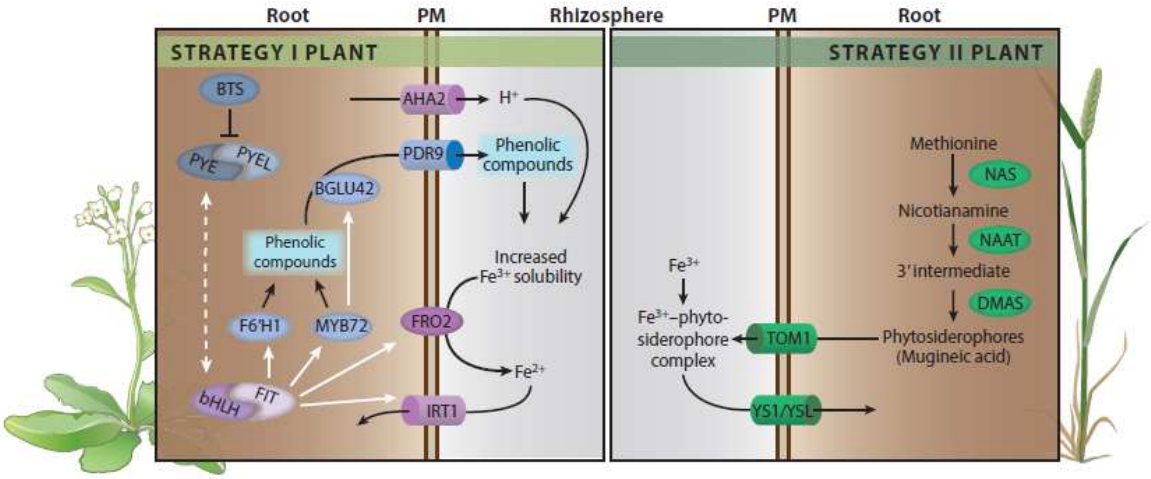

Figure 4. Strategy I and Strategy II iron acquisition in plants (from Verbon et al. Annu Rev Phytopathol, 2017).

When exposed to Fe deficiency condition, non-grass plants, such as the model plant *Arabidopsis thaliana* and tomato, activate a coordinated set of responses in root cells. In Arabidopsis, the solubility of Fe^{3+} in the soil is increased by the activity of the H^+ -ATPase AHA2, which secretes protons into the rhizosphere that lower the pH (Santi and Schmidt, 2009). Solubilized Fe^{3+} is reduced to Fe^{2+} by

the plasma membrane protein FERRIC REDUCTION OXIDASE 2 (FRO2 in *A. thaliana*; SlFRO1 in tomato), after which it is transported from the soil environment to the root epidermis by the high-affinity IRON-REGULATED TRANSPORTER1 (IRT1) (Eide *et al.*, 1996; Robinson *et al.*, 1999; Eckhardt *et al.*, 2001). Iron availability is further enhanced by the release of Fe mobilizing metabolites, including organic acid, phenolics, flavonoids and flavins (Cesco *et al.*, 2010). This release is mediated by the transcription factor MYB72 (Liu and Osbourn, 2015), the coumarin biosynthesis protein FERULOYL-COA 6'-HYDROXYLASE1 (F6'H1), the glucose hydroxylase β-GLUCOSIDASE 42 (BGLU42) (Zamioudis *et al.*, 2014), and the ATP-binding cassette transporter PDR9/ABCG37 (Fourcroy *et al.*, 2014; Schmidt *et al.*, 2014; Zamioudis *et al.*, 2014).

Grass plants, such as maize and wheat, make use of a Fe chelation–based strategy to mobilize and acquire Fe under iron-limiting conditions, through the secretion of phytosiderophores (PS), defined as plant-derived small organic molecules with high affinity for Fe (Römheld and Marschner, 1986). In these so-called Strategy II plants, Fe deficiency triggers the conversion, catalysed by the enzyme NICOTIANAMINE SYNTHASE (NAS), of methionine into nicotianamine (NA). NA is subsequently converted into phytosiderophores by NICOTIANAMINE AMINOTRANSFERASE (NAAT) and DEOXYMUGINEIC ACID SYNTHASE (DMAS) (Ohata *et al.*, 1993; Bashir and Nishizawa, 2006). Deoxymugineic acid, the most abundant phytosiderophore, is released into the rhizosphere by TRANSPORTER OF MUGINEIC ACID1 (TOM1) (Nozoye *et al.*, 2011). The Fe^{3+}-phytosiderophores chelates are taken up from the rhizosphere by the plant by specific transporters, such as YELLOW STRIPE1 (YS1) or YS1-like (YSL) (Curie *et al.*, 2001, Inoue *et al.*, 2009, Kobayashi and Nishizawa, 2012).

The transcriptional regulation of Fe-deficiency response of Strategy I plants has been elucidated in detail, predominantly in Arabidopsis. The basic helix-loop-helix (bHLH) transcription factor FER-LIKE IRON DEFICIENCY INDUCED TRANSCRIPTION FACTOR (FIT) in *A. thaliana* and the LeFER in tomato emerged as the central regulator of the Strategy I iron-uptake response (Ling *et al.*, 2002; Colangelo and Guerinot, 2004; Brumbarova and Bauer, 2005; Yuan *et al.*, 2005; Bauer *et al.*, 2007). Upon iron deprivation, FIT is activated at the transcriptional and post-translational levels in roots only and form a heterodimer with one member of the bHLH Ib subgroup of transcription factors (bHLH038/039/100/101); similarly, FER interacts with SlbHLH068. (Yuan *et al.*, 2008; Sivitz *et al.*, 2012; Wang *et al.*, 2013; Du *et al.*, 2015). In this form, they activate downstream iron-uptake genes, such as AHA2, FRO2 and IRT1 in Arabidopsis (Colangelo and Guerinot 2004; Jakoby *et al.*, 2004; Yuan *et al.*, 2008; Ivanov et al. 2012; Wang *et al.*, 2013). A microarray study of Arabidopsis roots identified another bHLH transcription factor called POPEYE (PYE), which is upregulated upon Fe-deficiency, independently of FIT regulatory network. Like FIT, PYE interacts with other bHLH

transcription factors, such as PYE-like (PYEL), to regulate iron homeostasis (Long *et al.*, 2010). PYE and PYEL are negatively regulated by the E3 ubiquitin-protein ligase BRUTUS (BTS) (Selote *et al.*, 2015). Both networks regulated by PYE and FIT are apparently necessary for efficient Fe-uptake in Strategy I plants. In fact, *pye* and *fit* single mutants in Arabidopsis become chlorotic under Fe-deficient conditions (Colangelo and Guerinot, 2004; Long *et al.*, 2010). Fe-deficiency response results in an increase in Fe-uptake which could lead to overload of Fe. For this reason, several post-transcriptional mechanisms have been observed that rapidly stop Fe-uptake, such as the recycling of IRT1 via ubiquitination (Shin *et al.*, 2013) and BTS which acts as negative regulators of Fe-deficiency response (Selote *et al.*, 2015). In addition to the activation of Strategy I and II in roots, plants that sensing low iron availability initiate a number of morphological changes in the root architecture, including increased root branching and root hair formation, in order to enlarge the ability to take more Fe (Schmidt, 1999; Jin *et al.*, 2008).

Once Fe enters the symplast of the epidermal root cells, it diffuses across the plasmodesmata to reach the vascular tissues for transport to the shoot. Due to its toxicity and low solubility, Fe must be complexed to chelators to be translocated without causing damaging redox reactions. In the xylem vessels, Fe is chelated with citrate and the long-distance transport to the shoot is mediated by FRD3 (FERRIC REDUCTASE DEFECTIVE 3) (Rogers and Guerinot, 2002; Durrett *et al.*, 2007; Rellan-Alvarez *et al.*, 2010). In the phloem, Fe is translocated in complexes with nicotianamine (NA), a non-proteinogenic amino acid (Curie *et al.*, 2008). The lateral distribution of Fe-NA from xylem into neighbouring cells is probably mediated by the transporter YELLOW STRIPE-LIKE 2 (YSL2) (DiDonato *et al.*, 2004). Another transporter implicated in the loading of shoot Fe into the phloem is OLIGOPEPTIDE TRANSPORTER 3 (OPT3) (Mendoza-Còzatl *et al.*, 2014; Zhai *et al.*, 2014; Kumar *et al.*, 2017; Khan *et al.*, 2018). Iron transport and storage are further regulated by iron transporters called NATURAL RESISTANCE-ASSOCIATED MACROPHAGE PROTEINS (NRAMPs), that coordinate iron distribution across the cell and organize iron transport out of vacuoles (Curie *et al.*, 2000; Lanquar *et al.*, 2005). For Fe storage, two major mechanisms are proposed: storage into the vacuoles, due to the VACUOLAR IRON TRANSPORTER (VIT1) (Kim *et al.*, 2006), and into FERRITIN (FER), an important iron storage protein mostly located in chloroplast and mitochondria (Laulhere and Briat, 1993; Deak *et al.*, 1999; Nouet *et al.*, 2011).

1.5. Competition for iron in plant-pathogen interaction

Fe is an essential element for animals, bacteria, fungi, and plants and a competition may be established among different organisms when they live in close relationship. In host–pathogen

interaction a competition for nutrients between host and pathogen is a determinant for an effective immune system and can affect susceptibility and resistance to a pathogen (Payne, 1993; Lemanceau *et al.*, 2009; Narajo-Arcos and Bauer, 2016; Verbon *et al.*, 2017). In vertebrate hosts, iron is sequestered by ferritins in response to microbial invasion as part of a Fe-withholding defence system (Weinberg, 2000). To bypass these processes, microbial pathogen produces siderophores, low molecular weight compounds with high affinity for Fe (Andrews *et al.*, 2003; Winkelmann *et al.*, 2007). In plants, the possibility of a competition for Fe was corroborated by Neema *et al.* (1993), who showed a decrease of Fe incorporated into plant ferritins in soybean cells during *Erwinia chrysanthemi* infection. Phytopathogenic bacteria and fungi can use siderophores to acquire Fe in the host and to promote infection and proliferation (Expert, 1999; Haas *et al.*, 2008). On the other hand, siderophores protect pathogen from plant-derived toxic hydroxyl radicals produced at the site of infections (Dellagi *et al.*, 1998). In the rhizosphere, several bacterial species, called plant growth-promoting rhizobacteria (PGPR), can induce systemic resistance (Induced Systemic Resistance, ISR) and, in this way, can be beneficial to plants and protect them against pathogens (Leeman *et al.*, 1996; Audenaert *et al.*, 2002; Bakker *et al.*, 2007; De Vleesschauwer and Hofte, 2009). For example, *Pseudomonas aeruginosa* produces two siderophores under low Fe conditions, which are involved in protection against pathogens (Buysens *et al.*, 1996). In tomato seedlings, a bacterial mutant unable to produce both pyochelin and pyoverdine is less protective against disease than the wild type strain (Buysens *et al.*, 1996). This finding was attributed to a competition for Fe between *P. aeruginosa* and pathogens, but it also suggested the possibility that plant immunity can be stimulated by siderophores. Indeed, plants are able to activate defence responses in order to decrease Fe availability at the infection site. For example, ferritin gene transcription and protein production are induced after pathogen infection in potato and Arabidopsis (Mata *et al.*, 2001; Dellagi *et al.*, 2005) and the vacuolar transporters NRAMP3 e NRAMP4 are involved in the basal resistance to *Dickeya dadantii* in Arabidopsis (Segond *et al.*, 2009).

Plant Fe status (sufficiency or deficiency) can also influence plant-pathogen interactions acting on both microbial fitness and the activation of plant defence response, preventing or promoting the infection (Anderson and Guerra, 1985; Barash *et al.*, 1988; Macur *et al.*, 1991; Kieu *et al.*, 2012; Nam Phuong, *et al.*, 2012; Ye *et al.*, 2014).

The root mechanism of Fe acquisition and the response to pathogens are closely related in plant, as ISR shares early signalling components with the Fe deficiency response (e.g. the root-specific R2R3-type MYB transcription factor gene MYB72 in Arabidopsis, Pieterse *et al.,* 2014). The defence-related hormones such as salicylic acid, jasmonate, and ethylene are not only involved in activation of immune responses, but also affect important steps in the Fe-uptake response in roots of

Arabidopsis and tomato (Kang *et al.*, 2003; Lucena *et al.*, 2006; Garcia *et al.*, 2010; Maurer *et al.*, 2011; Aznar *et al.*, 2015; Verbon *et al.*, 2017; Cui *et al.*, 2018).

The studies that investigate Fe role in plant-pathogen interactions showed different results according to the pathosystem. Depending on the site of infection, the pathogen infection strategy and the plant host, dissimilar responses can occur concerning Fe homeostasis and activation of plant defence responses. For this reason, no generalization should be made about the role of plant mineral nutrition on microbial disease development.

2. Aims

Field-grown plants are simultaneously exposed to a combination of biotic and abiotic stresses that limit crop yields and quality. Despite the importance of the role that plant nutrition likely plays in plant-pathogen interaction, a wide knowledge has been gained in the separate fields, but little is known about tripartite nutrients-plant-pathogen systems. Phytoplasma-plant host interactions and their relationship with plant nutrition are still largely unexplored. Being the phytoplasma an intracellular parasite adapting to a nutrient-rich environment, such as the phloem, it is possible that plant nutrition can be deeply altered. Besides, the occurrence of nutrient deficiency in field could modify both the plant response to infection and the fitness of the pathogen itself. Among the nutrients, iron (Fe) is an essential element for animals, bacteria, fungi, and plants and a competition for it may establish among organisms when they live in close relationship.

Aimed to study the Fe homeostasis alteration in phytoplasma infected plants, I investigated the response of the tomato plant (Micro-Tom cultivar) as host of '*Candidatus* Phytoplasma solani'.

First, I set up a system where phytoplasma infection and occurrence of Fe-deficiency symptoms could be observed and compared in conditions as much as possible controlled. Second, I carried out experiments to profile gene expression by means of high-throughput RNA-sequencing (RNA-seq) of phytoplasma-infected and healthy/Fe-deficient plants, in comparison to healthy/Fe-sufficient plants. In fact, no wide knowledge was available on the tomato response to '*Ca*. P. solani' infection, nor on the tomato leaf response to Fe deficiency. Plant responses to these stresses were analysed with a multidisciplinary approach, combining microscopy, molecular and biochemical analyses. Overlapping and peculiar aspects of the two stresses were compared to understand if and how phytoplasmas can unbalance Fe homeostasis in the infected plants.

3. Setting of the experimental system

In field, plants have to face with both abiotic and biotic stresses. Among them, nutrient deficiencies and pathogen infection may contemporaneously affect the plant. Despite mineral nutrition has long been recognised as an important component in plant-pathogen interaction (Datnoff *et al.*, 2007; Huber *et al.*, 2012) and in disease control practices (Dordas 2008; Gupta *et al.*, 2017), a wide knowledge has been gained over the years in the separate fields, but little is known about tripartite nutrients-plant-pathogen systems (Huber *et al.*, 2012). As previously described (see chapter 1.3 Phytoplasma-infection and plant nutrition), almost nothing is known about phytoplasma infection and plant nutrition. For this reason, before starting to pursue the aims of my investigation, setting of the experimental system resulted mandatory.

3.1. Plant infection: Micro-Tom tomato grafting for '*Candidatus* Phytoplasma solani' transmission

Dealing with the study of plant-pathogen interaction, investigations in natural plant hosts are often limited by environmental conditions, long plant-host life cycles and poor knowledge of host-plant biology. To overcome these difficulties, also in the case of phytoplasma infection as well as other patho-systems, the use of model plants has been considered. Tomato plant (*Solanum lycopersicum* L.), besides being an economically important crop affected by phytoplasma diseases, is widely investigated in the study on the interaction between the plant and '*Candidatus* Phytoplasma solani' (Pracros *et al.*, 2006; Pracros *et al.*, 2007; Machenaud *et al.*, 2007; Ahmad *et al.*, 2014; Buxa *et al.*, 2015; Aryan *et al.*, 2016; De Marco *et al.*, 2016). '*Ca.* P. solani' has been also associated to Bois noir disease, which is a serious grapevine disease endemic and largely distributed in Europe (Belli *et al.*, 2010).

In general, tomato has been employed as model plant in different research fields (Kimura and Sinha, 2008; Zoroli et al 2007), including plant-pathogen interaction (Arie *et al.*, 2007) and the study of *Strategy I* Fe uptake mechanism (Ivanov *et al.*, 2012). The sequencing of its genome in 2012 (The tomato genome consortium, 2012) has further enforced this trend.

Even if in nature phytoplasmas spread mainly through phloem-feeding insects, their transmission can occur also via vegetative propagation (such as through grafting of infected shoots onto healthy plants, cuttings and by micropropagation practices). In experimental conditions, grafting is the most

rapid and effective method, and the choice of the herbaceous grafting type depends on the kind of experiment to be performed.

Herein, different herbaceous grafting types were performed to reach an efficient '*Ca*. P. solani' transmission in tomato cv. Micro-Tom. To select the best type to use in further experiments, plant and symptom development were observed and, eventually, side graft was selected as the best for our experimental system. Indeed, this kind of grafting guaranteed the best success for phytoplasma transmission and the grafted plant showed harmonic growth and clear symptom development.

In the following part, the protocol for Micro-Tom grafting with infected shoots is presented in form of chapter of "Phytoplasmas: Methods and Protocols" book (2019).

Chapter 2

Micro-Tom Tomato Grafting for Stolbur-Phytoplasma Transmission: Different Grafting Techniques

Sara Buoso and Alberto Loschi

Abstract

Tomato plant, being a model system in scientific research, is widely used to study plant-phytoplasma interaction. Grafting is the faster and most effective method to obtain infected plants. This chapter describes the greenhouse culture of tomato, cv. Micro-Tom, and different herbaceous grafting techniques for efficient stolbur-phytoplasma transmission.

Key words Grafting, Greenhouse maintenance, Micro-Tom, Phytoplasma, Stolbur, Tomato

1 Introduction

Tomato plant (*Solanum lycopersicum* L.), besides being an economically important crop, is a model system in different scientific research [1, 2]. In fact, tomato has many interesting features that other model plants, such as *Arabidopsis*, do not have: fleshy fruit, a sympodial shoot, and compound leaves. The sequencing of tomato genome in 2012 [3] has generated useful biological information and enhanced the use as model plant, especially in relation to the studies about plant-pathogen interactions. Tomato, in fact, is naturally affected by a diversity of diseases, associated with different pathogens. Moreover, resistance to virus and other microorganisms has been largely investigated [4].

Among the different tomato cultivars, Micro-Tom [5] is particularly indicated for scientific investigation due to its small size, high-density culture, and rapid growth [6, 7]. Large collections of Micro-Tom mutants, produced by gamma-ray irradiation and ethylmethanesulfonate (EMS), are available from the National BioResource Project (NBRP) Tomato in Japan via the "TOMATOMA" database [8]. Moreover, Shikata and Ezura [6] have developed an efficient *Agrobacterium*-mediated transformation protocol for Micro-Tom. Successful application of Crispr/Cas9 system in

Rita Musetti and Laura Pagliari (eds.), *Phytoplasmas: Methods and Protocols*, Methods in Molecular Biology, vol. 1875, https://doi.org/10.1007/978-1-4939-8837-2_2,

Micro-Tom for genome editing has been reported in few articles [9–11]. Using this technology, an efficient and site-directed mutagenesis has been achieved to investigate plant functional genomics and crop improvement, without the laborious and time-consuming screening process characterized by traditional mutagenesis methods.

Candidatus Phytoplasma solani ('*Ca*. P. solani', group 16SrXII-A) is an A2 quarantine pathogen in Europe (EPPO, European and Mediterranean Plant Protection Organization) (*see* **Note 1**) and is naturally hosted by a wide range of crops including *Solanaceae* [12] and grapevine, inducing a disease known as stolbur. Therefore, tomato has been used in the study on '*Ca*. P. solani'--plant interaction [13–17], much more than other test plants, such as *Catharanthus roseus* (L.) G. Don, *Vicia faba* (L.), and *Arabidopsis thaliana* [18, 19].

'*Ca*. P. solani' is transmitted by vegetative propagation (grafting and cuttings) and by several insect vector species. In experimental conditions, grafting is the most rapid and effective method. Thus, in this chapter we describe different herbaceous grafting techniques for an efficient stolbur-phytoplasma transmission in tomato cv. Micro-Tom.

All the grafting methods illustrated below can be performed also for the maintenance of phytoplasma in *C. roseus*, the test plant generally used for this purpose. Moreover, some of the described methods can be used in heterologous grafting for the transmission of the phytoplasma from different plant sources to *C. roseus* and tomato plants, as described by Aryan et al. [17].

2 Materials

Considering that '*Ca*. P. solani' is listed as quarantine pest for Europe (*see* **Note 1**), infected plants should be maintained in insect-proof rooms, in confined greenhouse and every experiment should be carried out under safety conditions and according to the local current phytosanitary rules. To reduce the chance of insect-vector casual introduction, few precautions can be adopted such as the use of (1) white net (fine mesh) to protect the entrance of the chamber, (2) chromotropic traps to monitor insect presence, and (3) periodic insecticide treatments.

2.1 Plant Culture

1. Potting substrate mix: peat and perlite (10–15%) (*see* **Note 2**) eventually added with compost.
2. Fertilizers: slow release fertilizers with macro and microelements.
3. Plastic plateaux for seedling.
4. Plastic pots (squared 7 cm × 7 cm, 7 cm high, or bigger).

5. White insect-proof net.
6. Artificial lighting system (lamp *metal-halide* or *light-emitting diodes)*.
7. Plastic film.
8. Bamboo or plastic plant stakes (ca. 30 cm high) (*see* **Note 3**).
9. *Solanum lycopersicum* cv. Micro-Tom seeds (*see* **Note 4**).
10. Sodium hypochlorite solution 1–1.5% (v/v).
11. Broad spectrum fungicide and insecticide (*see* **Note 5**).

2.2 Grafting

1. Healthy tomato cv. Micro-Tom plants.
2. Stolbur-infected tomato.
3. Transparent plastic bags (approximately 20 cm × 15 cm or at least the double height of the scion).
4. Plant ties.
5. Razor blades, scalpels, and cutters (*see* **Note 6**).
6. 90–100% Ethanol.
7. Parafilm.
8. Grafting clip (plastic or silicon).
9. Labels.
10. Pencil.
11. Hole punch.
12. Tubes.

3 Methods

3.1 Growth of Healthy Plants from Seeds

The greenhouse conditions are the same for both healthy and phytoplasma-infected plants. The plants are grown under a long-day photoperiod, with 14–16 h light. During the day, if natural irradiance decreases below 4000 lx, supplementary lighting must be provided (preferably with automatic activation). The daytime temperature should be between 21 and 27 °C, with a night minimum temperature 17 °C. Heating and cooling systems should be automatically activated if the temperature in the greenhouse decreases or increases below the settings. Presence of a data logger for temperature monitoring is recommended.

1. Sterilize seeds soaking in sodium hypochlorite 1–1.5% solution for 3–5 min, then rinse with distilled water.
2. Fill the plastic plateaux with the mix substrate (*see* **Note 7**) and pour out it until saturation with water.
3. Sow seeds with a minimum distance of 1 cm (*see* **Note 8**) from each other, cover with half cm of substrate, and pour out gently (*see* **Note 9**).

4. Cover the plateaux with the plastic film until the plant emerging to maintain high humidity (*see* **Note 10**). Then begin to pierce the film gradually and after 4–5 days cover it off.
5. After ca. 15–20 days from sowing, the plants are ready for transplanting. Prepare some plastic pots (recycled pots should be sterilized with sodium hypochlorite) filled with substrate and transplant the plants individually. After a month, transplant them another time in bigger sterilized pots (*see* **Note 11**).
6. Check daily the plants condition, water gently, and fertilize every 10–15 days switching from N and P rich fertilizers to K and Ca. Pay attention also to the eventual appearance of phytosanitary problems, such as mites, insects, powdery mildew, and *Botrytis*.

3.2 Grafting for Phytoplasma Transmission

About 2 months from the sowing, plants are ready to be grafted for phytoplasma transmission (*see* **Note 12**). The choice of the herbaceous grafting type depends on the kind of experiment to be performed (*see* **Note 13**) and on the available material (healthy and infected plant). Healthy plants, used as rootstock, must have a good vegetative development, lack of visible diseases (*see* **Note 14**) and be cultivated in a controlled area, avoiding insect vector presence. Infected plants, from which scion is taken, must show all the typical disease symptoms (Fig. 1), but not be too old (woody tissues are not suitable for grafting).

It is important to stress the fact that not only phytoplasmas, but also other endophytic microorganisms, may move from the infected scion to the healthy part. Moreover, in grafted plants,

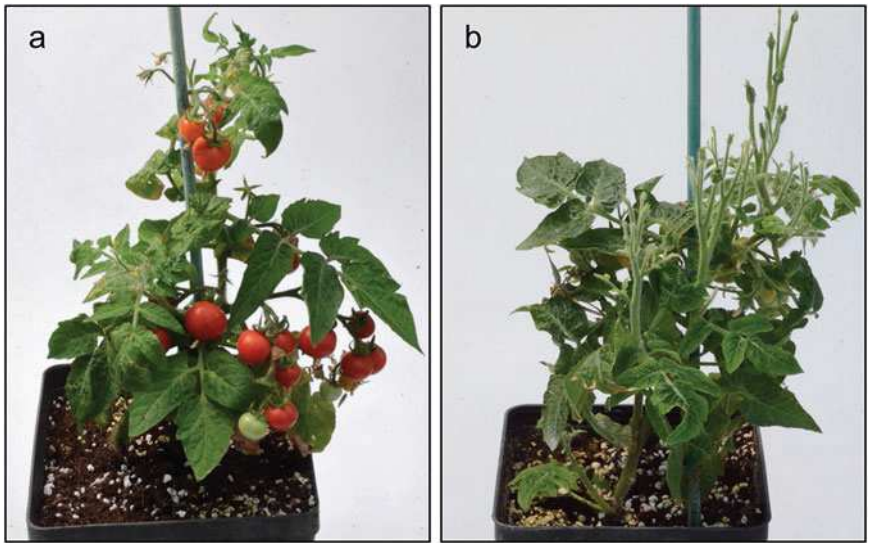

Fig. 1 Phenotypes of healthy and fully symptomatic plants at 90 days after sowing (**a**) normal growth in healthy tomato; (**b**) stolbur-infected tomato with leaf yellowing, flower abnormalities, stunting and reduced leaf area

phytohormone-, long-distance protein-, and small RNA-movement may result altered. For this reason, healthy plant grafted with healthy scion should be used as control in the experiments.

3.2.1 Side Graft

This kind of grafting guarantees the best success both for scion survival and phytoplasma transmission (roughly 95%). Moreover, the grafted plant shows harmonic growth and clear symptom development. The infected scion and the stem of the healthy rootstock need to have approximately the same diameter, to obtain a tight anatomic connection between the tissues.

1. Every cut must be made with razor blades, scalpels, and cutters, sterilized with ethanol. The cutting must be precise, linear, and clear, without remaining lacerated tissues.
2. Cut vertically a portion of stem, with a variable length (from 0.5 cm to 2 cm), in the middle of healthy rootstock (Fig. 2a, b). To better stabilize the scion, it is possible to prepare a little pocket at the end of the cut (Fig. 2c).

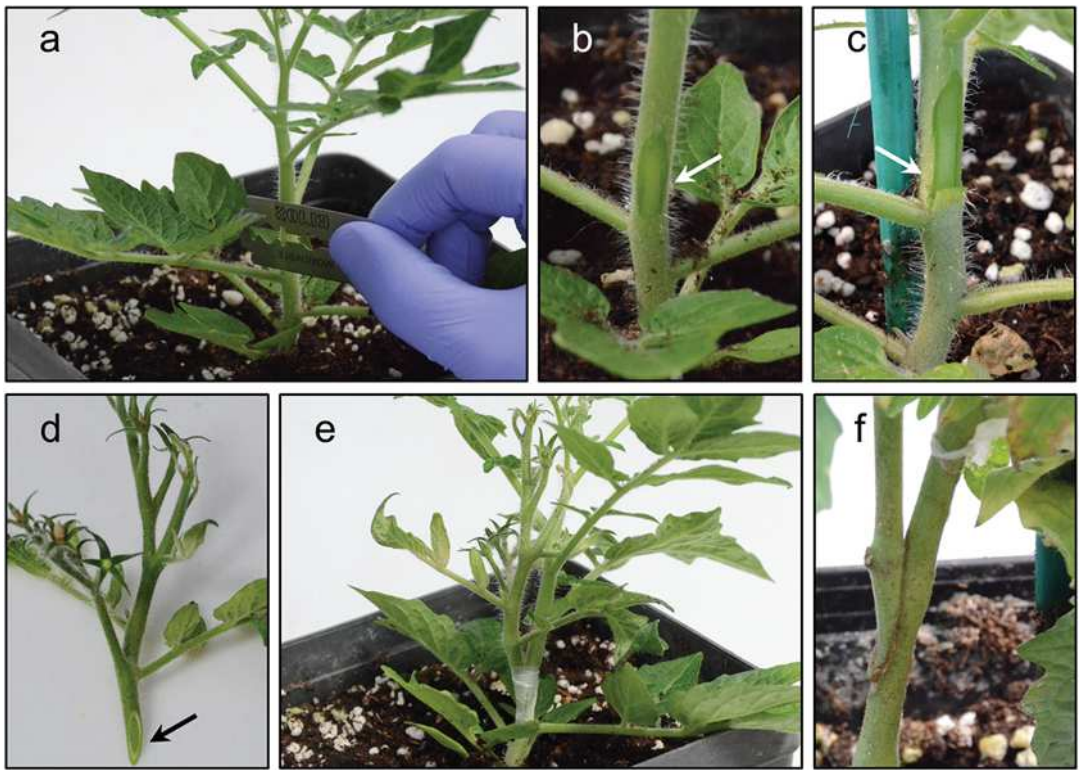

Fig. 2 Side graft stages; (**a–c**) vertical cutting of stem in the healthy rootstock; (**d**) oblique cutting in infected scion; (**e**) completed graft; (**f**) successful rootstock-scion connection 1 month after grafting

3. For the scion, choose a symptomatic shoot from the phytoplasma-infected tomato plant, approximately 7–10 cm long (*see* **Note 15**).
4. In the final part of the scion, make an oblique cut of almost the same size of the cut made on the rootstock plant (Fig. 2d).
5. Insert the scion into the cut of the rootstock plant.
6. Wrap firmly the two parts with parafilm (or grafting clips) to fix the graft (Fig. 2e).
7. Treat with fungicide to avoid the development of *Botrytis*. Place a transparent plastic bag (*see* **Note 16**) over the scions or around the plant (sustained by the stakes) to maintain high humidity.
8. Label all the plants with the phytoplasma name and the grafting date.
9. Keep plants protected from direct light for at least a week; a panel (e.g., Styrofoam™) placed 20–30 cm over the grafted plants could protect them from direct sunlight.
10. Check daily the grafting status to prevent the development of fungal pathogens and, when necessary, open the bag, treat the plants with fungicide, and then close immediately.
11. After 15 days open the bag gradually, for instance cutting the edge corners. Leave the bag open on the plant for other 3 days to permit the scion acclimatization to the environmental conditions.
12. 4–5 weeks after grafting, the symptoms of phytoplasma infections will appear.

3.2.2 Apical Wedge Graft

This grafting technique is very simple to execute and guarantees roughly the complete success of phytoplasma transmission. On the other hand, the harmonic development of the plant will be impaired, so it is preferentially recommended for phytoplasma-maintenance purposes.

Compared to the side graft described here above, the apical wedge graft changes only in the preparation of the rootstock plant:

1. Cut off the top of the main stem of the healthy plant, then make a vertical cut in the middle of the stem (Fig. 3a, b).
2. In the final part of the scion, make an oblique cut on both the sides, to obtain a wedge of almost the same size of the cut made on the rootstock plant (Fig. 3c, d). Insert the scion and wrap firmly to the receiving stem with parafilm (Fig. 3e, f) or grafting clip.
3. Treat with fungicide to avoid the development of *Botrytis* and cover with a transparent plastic bag as described above (Fig. 3g).

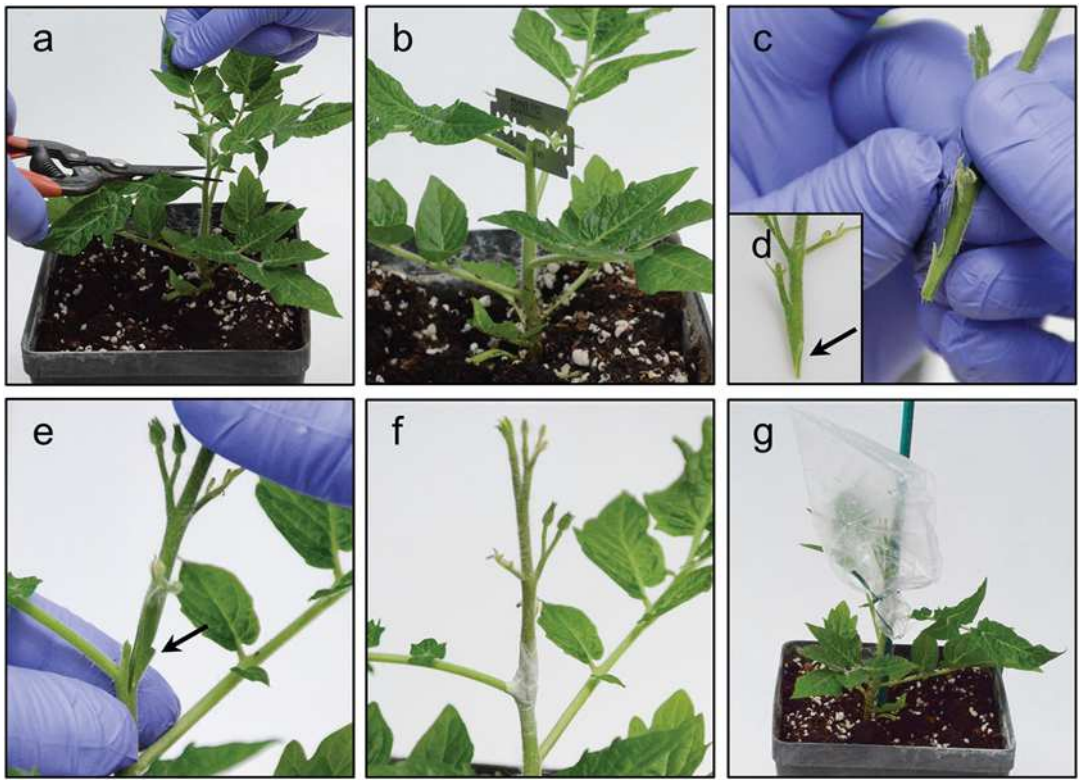

Fig. 3 Apical wedge graft stages; (**a**) removal of the apical stem in healthy rootstock; (**b**) vertical cut of the stem for scion insertion; (**c** and **d**) oblique cutting on both the sides in the infected scion; (**e**) insertion of the scion into the rootstock; (**f**) fixed graft by parafilm; (**g**) graft covering with a transparent plastic bag

4. Label all the grafted plants with the phytoplasma name and the grafting date.
5. After 4–5 weeks, the symptoms of phytoplasma infections will appear.

3.2.3 *Leaf Grafting*

This type of grafting requires precision and care during the execution, because it is necessary that both scion and rootstock midribs fit perfectly together. The success of this kind of grafting is very low but is useful when a poor amount of infected material is available, or when it is recommended to reduce the damage produced by the impact of the previous described grafting techniques.

1. Cut a disc from the midrib section of the infected leaf with a hole punch. The leaf must be well developed but not too old (*see* **Note 17**).
2. Cut the healthy leaf with the hole punch and discard the leaf disk (Fig. 4a).
3. Take the infected disc and put it on the hole of the healthy leaf (Fig. 4b). The midribs should be aligned as best as possible,

Fig. 4 Leaf grafting stages; (**a**) cutting of healthy leaf; (**b**) infected disc; (**c**) insertion of infected disk in the healthy leaves; (**d**) sealing with tape

and the disc should carefully match the hole. Put a piece of adhesive tape at the bottom of the receiving leaf to hold the scion leaf disc in place while necessary adjustments are made.

4. Take another piece of tape of similar length and place it above the leaf, then press it firmly (Fig. 4c).
5. Treat with fungicide to avoid the development of *Botrytis* or other fungal disease and place a transparent plastic bag over the leaf. Fix it around the plant or the stick.
6. Label plant with phytoplasma name and date of grafting.
7. After 1–2 weeks will be possible to determine the disc scion survival, as dead leaf will turn into browny colour. Symptoms occur 4–5 weeks after grafting.

3.2.4 *Approach Grafting*

This type of grafting is characterized by the use of a scion that remains attached to its own root system at the time of grafting. Approach grafting should be used in heterologous grafting for transmission of the stolbur phytoplasma from different plant sources to tomato plants. Unlike all other methods, the scion is less prone to become water stressed, resulting in a high probability of success. Alternatively, the scion could be cut off from its own root and put in a tube with water (Fig. 5c).

1. Cut vertically a portion of stem with the same length in healthy and infected plants (Fig. 5a).
2. Tying the two stems together at cut site with parafilm (Fig. 5b).
3. After 4–5 weeks, the symptoms of phytoplasma infections will appear.

4 Notes

1. For more information refer to EPPO website (https://www.eppo.int/QUARANTINE/quarantine.html), which every year provides updated lists of quarantine pests within the European and Mediterranean region.

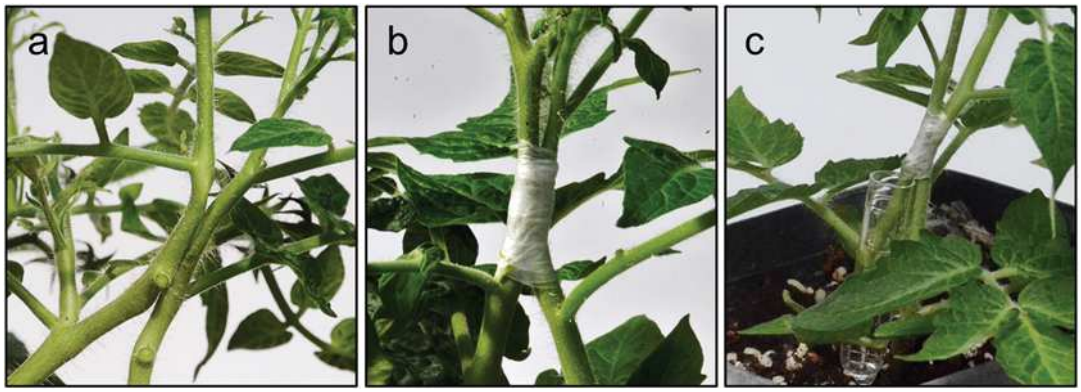

Fig. 5 Approach grafting stages; (**a**) vertical cutting of stem in the healthy and infected plant; (**b**) complete graft union; (**c**) approach grafting with scion cut and insertion in a tube for hydration

2. A good substrate for tomato growth must ensure a good soil aeration and structural stability (low slumping effect). The ideal pH should be between 5.7 and 6.5. Commercial horticulture mixes for professional use can guarantee high quality substrates.
3. The plastic support stakes are to be preferred to woody ones, to avoid mold development. Nevertheless, woody stakes can be treated with an appropriate fungicide.
4. Micro-Tom wild-type seeds can be purchased in the "TOMA-TOMA" database (http://tomatoma.nbrp.jp/), where a rich collection of mutant lines is also provided. Seeds can be produced and collected by fully developed plants. When plants reach the anthesis phase (fully open flower), shake the flower individually to replace the natural self-pollination by insect or wind. At red ripe stage, harvest the fruits and collect seeds in a tissue net (ca. 0.5 mm mesh), close it with tie and submerge it in a water bath to remove locular tissue. Then proceed with a 5–10 min wash in hypochlorite solution (1–1.5%) and rinse in water to eliminate the remaining locular tissue. Dry the seeds overnight on a clean net tissue. Transfer the dried seeds to a paper bag and store in dry and cool conditions.
5. If you use a new active ingredient, check the potential harmful effect on few plants before spraying it on the test plants and use pesticides according to label information.
6. The blades must be very sharp to obtain plain cut surfaces and to minimize the tissues damages. Before every use, sterilize the blades with ethanol.
7. For sowing use a fine substrate which provides optimum condition for seed germination and root growth.
8. The distance between the seeds must be suitable for the next transplanting operation and to facilitate the right development of the roots and the plant in general.

9. If the watering is too violent, it could disturb the regular seed germination.
10. The maintenance of humidity is essential to guarantee seed germination. A too high level of humidity can lead to the development of root pathogens (*Phythium* spp. and *Phythophthora* spp.). Therefore, treatments with fungicide are recommended to avoid the development of root rots.
11. Tomato plants can be also grown in hydroponic condition [20]. Hydroponic system may be helpful to study the interactions among phytoplasmas and specific nutrients or to survey plant response at root level.
12. When request by the experimental conditions, it is possible to use a younger healthy plant as rootstock. Younger plants ensure quicker symptom development and clearer symptoms. On the other hand, the younger is the plant, the more difficult will be the grafting operation, because of the tight diameter of the stem.
13. An experiment planning is mandatory for research success. Some experimentation requires the use of healthy plants deriving from seeds produced by a single plant.
14. The sanitary status of the plants must be checked by symptom appearance and molecular detection analyses, also to exclude mixed infections with viruses or other phytoplasmas (*Cfr* Chapter 5).
15. The stem scion of infected plant must match in diameter with the stem of rootstock plant.
16. The plastic bag is used to maintain the scion hydrated to ensure the grafting success. The plastic bag must be at least twice bigger than the scion. It is possible to cover the whole plant, even if it is not recommended for a proper plant development.
17. Leaves of healthy plants must be well developed and not too young; the use of young leaves makes difficult to cut and manipulate the discs. For a successful match of tissues, the punched discs of the scion need to be slightly bigger than the rootstock plant hole diameter.

References

1. Kimura S, Sinha N (2008) Tomato (Solanum lycopersicum): a model fruit-bearing crop. CSH Protoc 2008(11):pdb-emo105
2. Zorzoli R, Pratta GR, Rodríguez GR, Picardi LA (2007) Advances in biotechnology: tomato as a plant model system. Funct Plant Sci Biotechnol 1(1):146–159
3. The Tomato Genome Consortium (2012) The tomato genome sequence provides insights into fleshy fruit evolution. Nature 485:635–641
4. Arie T, Takahashi H, Kodama M, Teraoka T (2007) Tomato as a model plant for plant-pathogen interactions. Plant Biotechnol 24 (1):135–147
5. Scott JW, Harbaugh BK (1989) Micro-tom. A miniature dwarf tomato, vol S-370. FL Agric Exp Sta Circ, Florida, pp 1–6

6. Shikata M, Ezura H (2016) Micro-tom tomato as an alternative plant model system: mutant collection and efficient transformation. In: Botella JR, Botella MA (eds) Plant signal transduction. Methods in molecular biology, vol 1363. Humana Press, New York
7. Meissner R, Jacobson Y, Melamed S, Levyatuv S, Shalev G, Ashri A, Elkind Y, Levy A (1997) A new model system for tomato genetics. Plant J 12:1465–1472
8. Saito T, Ariizumi T, Okabe Y, Asamizu E, Hiwasa-Tanase K, Fukuda N, Mizoguchi T, Yamazaki Y, Aoki K, Ezura H (2011) TOMA-TOMA: a novel tomato mutant database distributing micro-tom mutant collections. Plant Cell Physiol 52:283–296
9. Ueta R, Abe C, Watanabe T et al (2017) Rapid breeding of parthenocarpic tomato plants using CRISPR/Cas9. Sci Rep 7:507
10. Pan C, Ye L, Qin L et al (2016) CRISPR/Cas9-mediated efficient and heritable targeted mutagenesis in tomato plants in the first and later generations. Sci Rep 6:24765
11. Brooks C, Nekrasov V, Lippman ZB, Van Eck J (2014) Efficient gene editing in tomato in the first generation using the clustered regularly interspaced short palindromic repeats/CRISPR-associated9 system. Plant Physiol 166(3):1292–1297
12. Quaglino F, Zhao Y, Casati P, Bulgari D, Bianco PA, Wei W, Davis RE (2013) "Candidatus Phytoplasma solani", a novel taxon associated with stolbur and bois noir related diseases of plants. Int J Syst Evol Microbiol 63:2879–2894
13. Pracros P, Renaudin J, Eveillard S, Mouras A, Hernould M (2006) Tomato flower abnormalities induced by stolbur phytoplasma infection are associated with changes of expression of floral development genes. Mol Plant-Microbe Interact 19(1):62–68
14. Pracros P, Hernould M, Teyssier E, Eveillard S, Renaudin J (2007) Stolbur phytoplasma-infected tomato showed alteration of SlDEF methylation status and deregulation of methyltransferase genes expression. B Insectol 60 (2):221–222
15. Machenaud J, Henri R, Dieuaide-Noubhani M, Pracros P, Renaudin J, Eveillard S (2007) Gene expression and enzymatic activity of invertases and sucrose synthase in Spiroplasma citri or stolbur phytoplasma infected plants. B Insectol 60(2):219–220
16. Buxa SV, Degola F, Polizzotto R et al (2015) Phytoplasma infection in tomato is associated with re-organization of plasma membrane, ER stacks and actin filaments in sieve elements. Front Plant Sci 6:650
17. Aryan A, Musetti R, Riedle-Bauer M, Brader G (2016) Phytoplasma transmission by heterologous grafting influences viability of the scion and results in early symptom development in periwinkle rootstock. J Phytopathol 164 (9):631–640
18. Choi YH, Tapias EC, Kim HK et al (2004) Metabolic discrimination of Catharanthus roseus leaves infected by phytoplasma using 1H-NMR spectroscopy and multivariate data analysis. Plant Physiol 135(4):2398–2410
19. Riedle-Bauer M, Sára A, Regner F (2008) Transmission of a stolbur phytoplasma by the Agalliinae leafhopper Anaceratagallia ribauti (Hemiptera, Auchenorrhyncha, Cicadellidae). J Phytopathol 156(11–12):687–690
20. Motohashi R, Enoki H, Fukazawa C, Kiriiwa Y (2015) Hydroponic culture of 'micro-tom' tomato. Bio-Protoc 5(19):e1613

3.2. Induction of plant iron starvation

One major problem in studying the interaction between plant growth and nutrient deficiency is the uncertainty of the soil nutrient supply in the field. The examination of nutrient deficiency under controlled conditions in hydroponic systems represents a valuable alternative approach (Jones, 1982). Many investigations on tomato plant has been carried out under Fe starvation in hydroponics. Nevertheless, young tomato seedlings and an Fe deficiency induction prolonged for a few days (7-10 days) are generally used (Li *et al.*, 2008; Ling *et al.*, 2002; Zamboni *et al.*, 2012; Lucena *et al.*, 2006; Zouari *et al.*, 2001; Schikora and Schmidt, 2002). With the aim to set up a system where phytoplasma infection and occurrence of Fe deficiency symptoms were concomitant, in our experiment we have grown plants older than usually. In fact, for the achievement of high infection rate and low plant-death rate, 4-week-old plants were used for grafting and other 5 weeks were necessary for full phytoplasma symptom development. Thus, Fe deficiency was induced on 6-week-old plants (two weeks after grafting), as described in Table 1 and in more detail in Chapter 4.

Table 1. Main steps for plant material preparation.

Condition	**Phytoplasma infection** (w.a.s.*)	**Fe starvation induction** (w.a.s.*)	**Harvest** (w.a.s.*)
H/+Fe Healthy/ Fe-sufficient	-	-	9
I/+Fe Phytoplasma-infected/ Fe-sufficient	4	-	9
H/-Fe Healthy/ Fe-starved	-	6	9
I/-Fe Phytoplasma-infected/ Fe-starved	4	6	9

*w.a.s.: weeks after sowing

4. On the role of iron in the interaction between '*Candidatus* Phytoplasma solani' and tomato

After setting the system for infection and induction of Fe deficiency in tomato plants, it has been proceeded with the study on the role of Fe in the interaction between '*Ca.* P. solani' and tomato plants. It has been hypothesised that also between plants and phytoplasma a competition for Fe may occur, leading to an alteration of Fe homeostasis in plant.

Manuscript ready to be submitted.

On the role of iron in the interaction between '*Candidatus* Phytoplasma solani' and tomato

Sara Buoso[1], Laura Pagliari[1], Rita Musetti[1], Marta Martini[1], Fabio Marroni[1,2], Wolfgang Schmidt[3], Simonetta Santi[1*]

[1]Department of Agricultural, Food, Environmental and Animal Sciences, University of Udine, 33100 Udine.

[2]IGA Technology Services, Via Jacopo Linussio, 51, 33100 Udine.

[3]Institute of Plant and Microbial Biology, Academia Sinica, 11529 Taipei, Taiwan.

[*]Correspondence to: Simonetta.Santi@uniud.it

Abstract

Phytoplasmas are prokaryotic plant pathogens that colonize the sieve elements of the host plant, causing alterations in phloem function and impairment of assimilate translocation. Despite the huge impact on agriculture and the lack of effective curative strategies, the mechanisms underlying plant host-phytoplasma interaction are still largely unexplored. As observed in different pathosystems, competition for iron is an essential component of the interplay between host and pathogen and may lead to the development of an Fe-withholding response by plants that changes Fe distribution and trafficking. Here we report that phytoplasma infection of tomato plants (*Solanum lycopersicum* cv. Micro-Tom) by '*Candidatus* Phytoplasma solani' leads to the development of chlorotic leaves and alters the local distribution of Fe in leaves. Both phytoplasma infection and exposure of plants to Fe-deficient conditions altered the expression of genes involved in photosynthetic light reactions, porphyrin and chlorophyll metabolism, and carotenoid biosynthesis. In Fe-deficient plants, phytoplasma infection perturbed the Fe deficiency response in roots, possibly by interference with the synthesis or transport of a promotive signal transmitted from the leaves to the roots. It is concluded that phytoplasma infection does not interfere directly with the Fe uptake mechanisms of the host plant, but affects the orchestration of root-mediated transport processes by compromising shoot-to-root communication.

Keywords: iron deficiency, iron homeostasis, phytoplasma, phloem, tomato

4.1. Introduction

Phytoplasmas are associated with devastating damage to over 700 plant species worldwide, including many economically important crops, fruit trees and ornamental plants (Hougenhout and Loria, 2008; Oshima *et al.*, 2013). Phytoplasmas are plant pathogenic bacteria belonging to the class *Mollicutes*, a group of wall-less, minute, pleomorphic microorganisms, phylogenetically related to low G+C Gram-positive bacteria (Weisburg *et al.*, 1989). Phytopasmas live a trans-kingdom parasitic life, infecting plant and phloem-feeding insect hosts (Weintraub and Beanland, 2006). In infected plants, phytoplasmas reside in sieve elements of the phloem (Christensen *et al.*, 2004), where spread is reaching most organs (Cordova *et al.*, 2003; Wei *et al.*, 2004). Phytoplasmas possess the smallest genome of any plant pathogenic bacteria (530 – 1350 kb), believed to have evolved from an ancestor

via genomic reduction and fusion (Oshima *et al.*, 2004; Wei *et al.*, 2008), possibly due to adaptation to a nutrient-rich environment. Because of the difficulties associated with their isolation and *in vitro* culture, phytoplasmas remain one of the least characterized plant pathogens (Contaldo *et al.*, 2012). Complete genomic sequences obtained from a few phytoplasmas (Oshima *et al.*, 2004; Bai *et al.*, 2006; Tran-Nguyen *et al.*, 2008; Kube *et al.*, 2008; Andersen *et al.*, 2013, Orlovskis *et al.*, 2017; Wang *et al.*, 2018b) show the presence of genes for basic cellular functions such as DNA replication, transcription, translation, and protein translocation. Notably, the genome lacks genes encoding proteins involved in essential metabolic pathways, such as the biosynthesis of amino fatty acids, the tricarboxylic acid cycle, and oxidative phosphorylation. Thus, phytoplasmas have strongly reduced metabolic capabilities and must absorb essential compounds from their hosts. This observation is supported by the presence of multiple copies of transport-related genes such as malate, metal-ion, and amino acid transporters in the phytoplasma genome (Kube *et al.*, 2012). Moreover, phytoplasmas secrete proteins that may directly interact, manipulate, or weaken their hosts. Examples are the secreted protein TENGU and SAP11 of '*Candidatus* Phytoplasma asteris' (Bai *et al.*, 2009; Hoshi *et al.*, 2009).

Phytoplasma-infected plants often exhibit symptoms of virescence, phyllody, witches'-broom growth (proliferation of auxiliary or axillary shoots), abnormal elongation of internodes, flower malformation, and sterility. Some symptoms represent a derailment of programmed meristem fate and a modified pattern of growth due to pathogen-affected key meristem switch genes (Pracros *et al.*, 2006; Wei *et al.*, 2013). At the ultrastructural level, infected plant shows occlusions in sieve elements due to phloem-protein agglutination and callose deposition, which impair phloem mass flow (Pagliari *et al.*, 2017) and often result in hyperplasia, necrosis, and collapse of sieve elements (Musetti *et al.*, 2005; Santi *et al.*, 2013; Buxa *et al.*, 2015; De Marco *et al.* 2016; Pagliari *et al.*, 2016).

Moreover, yellowing of leaves or shoots, leaf curling, and general stunting are typical symptoms, which have been found to be associated with reduced content of chlorophyll, carotenoids and antenna proteins of photosystem II (Bertamini *et al.*, 2003; Liu *et al.* 2016). In addition, several genes encoding photosystem I subunits and other components of the electron transport chain were found to be inhibited by the infection (Albertazzi *et al.*, 2009; Hren *et al.*, 2009; Wang *et al.*, 2018c). Photosynthesis is heavily affected in many phytoplasma-infected plants, but the molecular mechanisms underlying these changes are still unclear (Albertazzi *et al.*, 2009; Hren *et al.* 2009; Liu *et al.* 2013; Mou *et al.* 2013, Nejat *et al.*, 2015; Xue *et al.*, 2018; Wang *et al.*, 2018c). Besides photosynthesis, key enzymes of the flavonoid and stilbene biosynthetic pathways, defence-related genes, and hormones signalling pathway are modulated by the infection (Albertazzi *et al.*, 2009; Hren *et al.*, 2009; Mou *et al.*, 2013; Santi *et al.*, 2013; Paolacci *et al.*, 2017; Wang *et al.*, 2018c).

Leaf chlorosis has been described as a diagnostic value of symptom for iron (Fe) deficiency, caused by compromised chloroplast development and impaired chlorophyll biosynthesis, and is associated with decreased photosynthetic rates (Terry, 1980). Enzymes taking part in the oxygen-dependent photosynthetic electron transport are Fe-requiring proteins that possess Fe as either Fe-S clusters or heme groups. Fe deficiency not only decreases the activity of genes related to electron transport complexes, but also causes downregulation of genes encoding proteins of light-harvesting complexes (LHC), or enzymes involved in porphyrin, chlorophyll, and carotenoid metabolism (Rodriguez-Celma *et al.*, 2013; Wang *et al.*, 2018a). Chloroplasts contain 80% of the leaf Fe (Terry and Abadia, 1986), a part of which is buffered by ferritin, a storage protein of key importance in the protection of oxidative stress induced by free Fe (Ravet *et al.*, 2009). If free, Fe can react with oxygen and generate harmful free radicals, in particular hydroxyl radicals via the so-called Fenton reaction (Fenton, 1894; Haber *et al.*, 1934), which cause damage to proteins, DNA, and lipids (Luo *et al.*, 1994). Therefore, plants strictly control Fe concentrations through the regulation of uptake, transport, utilization, and storage. Plants have evolved complex strategies to acquire Fe from soils (Römheld and Marschner, 1986). Although abundantly present in Earth's crust, the bioavailability of Fe is restricted, due to the poor solubility of hydroxides that control Fe activity in aerated soils (Guerinot and Yi, 1994; Schmidt, 1999). All non-grass species, including tomato, employ a reduction-based Fe acquisition mechanism (strategy I), in which Fe^{3+} is reduced by the Fe^{3+}-chelate reductase (FRO2 in Arabidopsis, FRO1 in tomato; Robinson *et al.*, 1999; Ling *et al.*, 2002). The reduced Fe^{2+} is then transported across the plasma membrane by the transporter IRON-REGULATED TRANSPORTER 1 (IRT1; Eide *et al.*, 1996; Eckhardt *et al.*, 2001). Solubilisation of scarcely available Fe pools in soil is supported by P-type ATPase-driven proton extrusion (AHA2 in Arabidopsis; Santi and S□hmidt, 2009). Similar to grasses, which rely on the secretion of Fe^{3+}-binding phytosiderophores (PS) that are taken up after binding to Fe^{3+} (Strategy II; Römheld and Marschner, 1986), Arabidopsis and other non-graminaceous species secrete Fe^{3+}-mobilizing compounds such as flavins and coumarins (Cesco *et al.*, 2010; Tsai and Schmidt, 2017). In contrast to grasses, which take up the Fe^{3+}-phystosiderophore complex without prior reduction of Fe, reduction of Fe^{3+} mobilized by secreted metabolites is obligatory in Strategy I plants. The transcriptional regulation of Fe-deficiency response of Strategy I plants has been elucidated in detail, predominantly in Arabidopsis. The basic helix-loop-helix (bHLH) transcription factor LeFER in tomato and its Arabidopsis ortholog FER-LIKE IRON DEFICIENCY INDUCED TRANSCRIPTION FACTOR (FIT) emerged as the central regulator of the Strategy I response (Ling *et al.*, 2002; Colangelo and Guerinot, 2004; Brumbarova and Bauer, 2005; Yuan *et al.*, 2005; Bauer *et al.*, 2007). Upon Fe deprivation, FIT is activated in roots at the transcriptional and post-translational level and forms heterodimers with members of the bHLH lb

subgroup of transcription factors (bHLH038/039/100/101). Similarly, FER interacts with SlbHLH068 (Yuan *et al.*, 2008; Sivitz *et al.*, 2012; Wang *et al.*, 2013; Du *et al.*, 2015). The heterodimers activate a suite of downstream genes such as *AHA2*, *FRO2*, and *IRT1* in Arabidopsis (Colangelo and Guerinot 2004; Jakoby *et al.*, 2004; Yuan *et al.*, 2008; Ivanov *et al.* 2012; Wang *et al.*, 2013). Another Arabidopsis bHLH transcription factor, POPEYE (PYE), is upregulated upon Fe-deficiency and acts independently of the FIT regulatory network. Similar to FIT, PYE interacts with other bHLH transcription factors, such as PYE-like (PYEL), to negatively regulate a distinct subset of genes involved in Fe acquisition and mobilization (Long *et al.*, 2010). *Vice versa*, the E3 ubiquitin-protein ligase BRUTUS (BTS) interacts with PYE and PYEL to positively regulate the same set of genes (Selote *et al.*, 2015). This dual regulation seems to be necessary to avoid overload of Fe and to control cellular homeostasis (Long *et al.*, 2010). Transcriptional activation of the Fe deficiency response in both Strategy I and Strategy II plants is also dependent on the presence of IRON MAN, a family of peptides that accumulate in leaves and roots of Fe-deficient plants (Grillet *et al.*, 2018).

In host–pathogen interactions, competition for nutrients is a determinant for an effective immune system and can affect susceptibility and resistance to a pathogen (Payne, 1993; Narajo-Arcos and Bauer, 2016; Verbon *et al.*, 2017). In vertebrate hosts, ferritin sequesters Fe in response to microbial invasion as part of a Fe-withholding defence system (Weinberg, 2000). To bypass these processes, microbial pathogen produces siderophores, low molecular weight compounds with high affinity for Fe (Andrews *et al.*, 2003; Winkelmann *et al.*, 2007). In plant hosts, different dynamics have been observed. Neema *et al.* (1993) showed a decrease of Fe incorporated into plant ferritins in soybean cells during *Erwinia chrysanthemi* infection. *Vice versa*, ferritin gene transcription and protein production were induced after pathogen infection in potato and Arabidopsis (Mata *et al.*, 2001; Dellagi *et al.*, 2005). Moreover, the vacuolar Fe transporters NRAMP3 and NRAMP4 were involved in the basal resistance to *Dickeya dadantii* in *Arabidopsis* (Segond *et al.*, 2009). Phytopathogenic bacteria and fungi can use siderophores to acquire Fe from the host and to promote infection and proliferation (Expert *et al.*, 1999; Haas *et al.*, 2008), but plants can respond by activating a systemic resistance mechanism (Leeman *et al.*, 1996; Audenaert *et al.*, 2002; Bakker *et al.*, 2007; De Vleesschauwer and Hoefte, 2009). Moreover, pathogen-secreted siderophores can trigger an Fe deficiency response in roots (Dellagi *et al.*, 2009; Segond *et al.*, 2009).

Induced systemic resistance and Fe uptake shares early signalling components such as the Myb-type transcription factor MYB72 (Zamioudis *et al.*, 2014). The defence-related hormones salicylic acid, jasmonate, and ethylene are not only involved in activation of immune responses, but also affect important steps in the Fe-uptake responses (Kang *et al.*, 2003; Lucena *et al.*, 2006; Garcia *et al.*, 2010; Maurer *et al.*, 2011; Aznar *et al.*, 2015; Verbon *et al.*, 2017; Cui *et al.*, 2018).

Phytoplasma diseases are often related to symptoms of nutritional deficiency, such as chlorosis, curling, and reddening. However, only few studies addressed the imbalance of mineral nutrients in plants following phytoplasma infections. Schweigkofler *et al.* (2008) showed that the Bois noir disease caused a reduction of the content of Ca and other mineral elements such as N, Mg, P, K, Mn, and Fe in different grape cultivars. In phytoplasma infected pear and apricot, imbalances in Fe/Mn and K/Mg ratio were reported (Rossi *et al.*, 2010).

Here, we dissected the role of Fe in the interaction between '*Candidatus* Phytoplasma solani' ('*Ca*. P. solani'), a phytoplasma belonging to the 16SrXII group associated with stolbur disease (Valenta *et al.*, 1961) and tomato plants (Micro-Tom cultivar) as hosts. '*Ca*. P. solani' is endemic in Europe and infects a wide range of weeds and cultivated plants, such as solanaceous crops (tomato, tobacco, eggplant), grapevine, celery, maize, sugar beet, strawberry, lavender, and peonia trees (reviewed in Garnier, 2000; Gatineau *et al.*, 2002; Duduk and Bertaccini, 2006; Jovic *et al.*, 2007; Gao *et al.*, 2013). '*Ca*. P. solani' is naturally transmitted by polyphagous planthoppers of the family *Cixiidae*, mainly *Hyalesthes obsoletus* and *Reptalus panzeri* (Fos *et al.*, 1992; Maixner, 1994; Cvrkovic *et al.*, 2014). Fe content and allocation were examined in leaves upon phytoplasma transmission and upon Fe deficiency, imposed both on healthy and infected plants. Effects on Fe acquisition machinery were investigated by means of expression analysis of key genes. Moreover, we compared transcriptome changes upon phytoplasma infection and upon Fe deficiency to discover common and specific gene networks.

Our data are consistent with a model in which phytoplasma competes for Fe and perturbs the long-distance signalling of Fe status that is transmitted to the roots.

4.2. Materials and methods

Plant material and growth conditions

Tomato (*Solanum lycopersicum* L., cv. Micro-Tom) seeds were collected from fruits of one single plant and germinated for 7 days in the dark at 22 °C between two layers of filter paper soaked with 1 mM $CaSO_4$. Homogenous seedlings were transferred into hydroponic nutrient solution containing 1.5 mM K_2S0_4, 3 mM KNO_3, 0.5 mM $MgSO_4$, 1.5 mM $CaCl_2$, 0.5 mM NaH_2PO_4, 25 µM H_3BO_3, 1 µM $MnSO_4$, 0.5 µM $ZnSO_4$, 0.3 µM $CuSO_4$, 0.05 µM $(NH_4)_6Mo_7O_{24}$, and 20 µM Fe-EDTA. The pH was adjusted to 6.0 with KOH. The aerated nutrient solution was replaced every four days. Plants were grown in a greenhouse at 20-25 °C with a 16 h light photoperiod. After four weeks, half of the plants were infected with '*Candidatus* Phytoplasma solani' ('*Ca.* P. solani'), belonging to the

stolbur group, subgroup 16SrXII-A (Quaglino *et al.*, 2013), by grafting shoot tips from phytoplasma-infected tomato plants onto healthy tomato plants. Healthy shoot tips were grafted onto the remaining half of the plants. Two weeks after grafting, Fe starvation was induced in one half of the healthy plants and one half of the infected plants by growing plants in Fe-free nutrient solution during the last three weeks of the experiment. All plant samples were collected five weeks after grafting. Plants were grown in four different conditions: healthy or phytoplasma-infected plants grown with full nutrient solution containing Fe (H/+Fe and I/+Fe, respectively), and healthy or phytoplasma-infected plants grown during the last three weeks in Fe-free nutrient solution (H/-Fe and I/-Fe, respectively). For transcriptome profiling by RNA-seq, we omitted the double-stress condition (I/-Fe) and comparisons were carried out among three conditions: H/+Fe, I/+Fe and H/-Fe.

Plant biometrics and phytoplasma detection

Biometric analyses were performed on six plants per condition. Total plant fresh weight was recorded at the end of the experimental period. Chlorophyll was indirectly determined by measuring leaf light transmittance with a portable chlorophyll meter (SPAD-502; Minolta, Osaka, Japan). The SPAD-502 meter measures the transmittance of red (650 nm) and infrared (940 nm) radiation through the leaf and calculates a relative SPAD index that corresponds to the amount of chlorophyll present in the sample leaf (Minolta 1989). For each plant, five SPAD measurements were taken on five leaves (150 measures in total per condition). Average leaf area was determined by analysing five leaves per plant. Leaf area was calculated using the ImageJ 1.49m software package (National Institutes of Health, Bethesda, MD, USA).

The presence of phytoplasma was assessed in healthy and symptomatic plants by qPCR analysis. Total genomic DNA was extracted as described in phytoplasma relative quantification. Phytoplasma detection was carried out using specific primers designed on the 16SrRNA gene of '*Ca.* P. solani' (GenBank accession no. AF248959) according to Santi *et al.* (2013).

Phytoplasma relative quantification

Phytoplasma titre was determined in eight plants per condition (I/+Fe and I/-Fe). Total genomic DNA was extracted from approximately 800 mg of leaf tissue enriched in midribs according to Doyle and Doyle (1990) modified by Martini *et al.* (2009). DNA concentration and purity were verified using a NanoDrop 1000 spectrophotometer (Thermo Fisher Scientific, Wilmington, DE, USA). qPCR analysis of '*Ca.* P. solani' and relative quantification of specific DNA levels were performed. In each experiment, duplicate samples were amplified in a qPCR reaction targeting the 16SrRNA gene of

'*Ca.* P. solani' and the single-copy tomato gene (Ling *et al.*, 1999) nicotianamine synthase (Chloronerva, CHLN) as internal positive reference. The primers for the 16SrRNA gene of '*Ca.* P. solani' (SP-16S) were the same than those used for phytoplasma detection (see above). The nicotianamine synthase gene was targeted by the primer pair list in Supplemental Table 2. For each gene, qPCR analysis was performed in triplicates in a 15 µL reaction mix, containing 7.5 µL of 2x SsoAdvanced Universal SYBR Green Supermix (Bio-Rad Laboratories), 400 nM of primers 16Sstol(RT)F2 and 16Sstol(RT)R3 or 300 nM of primers CHLN (forward and reverse), and 2 µL template DNA normalised to 5 ng/µL. The reactions were performed as described above. A positive and a negative control were run on every plate. To correct for inter-plate variation, a calibrator sample was run on every plate, allowing manual adjustment of the threshold level in order to maintain the threshold cycle (Ct) values of the calibrator sample constant. For each sample, phytoplasma DNA was determined by normalizing *16SrRNA* gene relative to the tomato *SCHLN* gene.

Transmission electron microscopy

To preserve phloem tissue structures, a specifically adapted protocol was used to prepare samples for transmission electron microscopy (TEM) observation, modifying the methods by Ehlers *et al.* (2000). Thirty mm long midrib segments were excised from three leaves of five plants per experimental condition. The midrib portions were immediately immersed in MES buffer for 2 h at room temperature, and the buffer was subsequently replaced by fixation solution consisting of 3% (w/v) paraformaldehyde and 4% (v/v) glutaraldehyde. The fixative was replaced every 30 min for 6 h. Samples were post-fixed overnight with 2% (w/v) OsO_4 at 4 °C, dehydrated in a graded ethanol series, and then transferred into propylene oxide. From the central part of each midrib, a 6-7 mm long piece was excised and embedded in Epon/Araldite epoxy resin (Electron Microscopy Sciences, Fort Washington, PA, USA). Ultrathin sections (60-70 nm in thickness) were cut using an ultramicrotome (Reichert Leica Ultracut E ultramicrotome, Leica Microsystems, Wetzlar, Germany), and collected on uncoated copper grids. Sections were then stained with UAR-EMS uranyl acetate replacement stain (Electron Microscopy Sciences, Fort Washington, PA, USA), and observed under a PHILIPS CM 10 (FEI, Eindhoven, The Netherlands) transmission electron microscope (TEM) operated at 80 kV, equipped with a Megaview G3 CCD camera (EMSIS GmbH, Münster, Germany). Three non-serial cross sections from each sample were analysed.

RNA-sequencing

Single-end stranded RNA-seq transcriptome analysis was performed on tomato leaves. Two leaves from three plants each were pooled and considered as one biological replicate. Three biological replicates for each of three conditions (H/+Fe, I/+Fe and H/-Fe) were analysed. In total, nine libraries were prepared as follows. Circa 1 g of leaf tissue enriched in midribs was ground in liquid nitrogen, and total RNA was extracted from approximately 100 mg of powder with the Spectrum Plant Total RNA Kit (Sigma-Aldrich, St Louis, MO, USA) according to the manufacturer's instructions. DNA was removed using the TURBO DNA-free™ Kit (Life Technologies, Carlsbad, CA, USA). The quality of RNA was evaluated using a Bioanalyzer 2100 (Agilent Technologies, Santa Clara, CA, USA). RIN scores ranged from 6.0 to 7.8. Libraries were prepared from 200 ng of total RNA with the TruSeq stranded Total RNA library Prep Plant Kit (Illumina Inc., San Diego, CA, USA) following the manufacturer's instructions. This kit enables bead-based depletion of cytoplasmic, mitochondrial, and chloroplast ribosomal RNA in multiple plant species. Libraries were sequenced on the Illumina NextSeq500 platform. Quality analysis of RNA, library construction, and RNA-seq were carried out at IGA Technology Services (Udine, Italy), who provided adapter-trimmed sequences and raw reads in Fastq-files. For each library, more than 45 million of 75 bp single-end reads were obtained.

RNA-seq data analysis

Reads quality was analysed by FastQC (URL: www.bioinformatics.babraham.ac.uk/projects/fastqc). The first six bases, which showed anomalous enrichments, were trimmed by FASTX_trimmer, and reads with a quality score below 30 (50%) were removed by FASTX quality filter application (URL: http://hannonlab.cshl.edu/fastx_toolkit), both available at CyVerse cyberinfrastructure (URL*:* www.cyverse.org). The same bioinformatics platform was used for RNA-seq data analysis. Clean reads were mapped to the reference genome of the cultivar Heinz 1706, Build SL3.0 and gene annotation ITAG3.20 (downloaded from Sol Genomics Network: https://solgenomics.net/organism/Solanum_lycopersicum/genome), by TopHat 2.0.9 (Kim *et al.*, 2013). Default parameters were used except for segment mismatch that was set to no more than 1, minimum intron length set to 25 bp, and maximum intron length set to 200,000. Anchor length was set to 8, and maximum number of mismatches that can appear on the anchor region was set to zero. Differentially expressed genes (DEGs) were identified by Cuffdiff 2.1.1 (Trapnell *et al.*, 2013), using multiple-hit correction, min-alignment-count 10, normalization to known transcripts and a False Discovery Rate (FDR) set to 0.05. The expression levels for gene models from ITAG3.20 were measured and normalized as fragments per kilobase of exon model per million mapped reads

(FPKM) (Mortazavi *et al.*, 2008). Visualization of read densities from RNA-seq was performed using the Integrated Genome Browser (Nicol *et al.*, 2009). The high-quality reads of this study were deposited in the NCBI SRA database (accession number: ****). The DEGs among the comparisons were graphically represented by Venn diagram entering the DEGs identifiers in VennPlex (Cai *et al.*,2013).

For functional annotation of sequences and data mining, the PANTHER (Protein Analysis Through Evolutionary Relationships) classification system was used to classify genes and their proteins in families, subfamilies, and molecular function. NCBI Entrez was used to retrieve further functional annotation. Further information on genes for which no annotation was available was retrieved by aligning all the protein sequences available in the tomato annotation against the NCBI database with the software Blastp (restricted to viridiplantae to reduce computation time), considering matches with an e-value lower than 10^-9.

Gene ontology classifications (GO) of DEGs in the three comparisons were downloaded from Sol Genomics Network FTP site for the ITAG3.20 annotation release. The enrichment analysis for the differential gene ontology (GO) term distribution in DEGs was tested by Fisher's exact test, implemented in the R package topGO with a P value significance cut-off value of 0.05.

Metabolic pathway analysis was performed using the KEGGenrich function in the R package clusterProfiler (Yu *et al.*, 2012). For functional characterization of genes and their organization in metabolic pathways, the KEGG database was used (Kanehisa *et al*., 2010).

RNA-seq data validation

To validate RNA-seq expression profiles, expression patterns of genes that were differentially expressed between different conditions were analysed by qRT-PCR. RNA used for library construction and sequencing was used to validate gene expression observed in the RNA-seq experiment. Primers were designed on the corresponding sequences retrieved from SGN (Supplemental Table 2). The reactions were performed as described below (Gene expression analyses).

ICP-OES analysis

Fe concentration was measured by Inductively Coupled Plasma–Optical Emission Spectroscopy (ICP-OES) analysis in both leaves and roots, in six plants for each condition. Root apoplastic Fe pools were removed as described by Bienfait *et al.* (1985), by rinsing roots in a solution containing

1.2 g L^{-1} sodium dithionite, 1.5 mM 2,2'-bipyridyl, and 1 mM $Ca(NO_3)^2$ under bubbling N_2 gas. Root and leaf tissues were dried at 65 °C for 48 h, then at 105 °C for 24 h. Dried samples (200 mg) were then suspended in 10 ml of concentrated HNO_3 [65% (v/v)] in teflon vessels, and digested in a microwave oven (CEM Mars Xpress Matthews, NC, USA), according to the USEPA 3052 method "Plant Xpress" (USEPA, 1995). The microwave temperature was increased to 180 °C for 10 min at 1,600 W (ramp time 30 min). Samples were than diluted to 20 ml with ultrapure deionized water and filtered with 0.45 µm PTFE filters. Elemental concentration was subsequently determined by ICP-OES (Varian Vista Pro axial) after dilution of the samples [8.8 ml of ultrapure deionized water, 0.2 ml Yttrium (Y) standard solution 50 mg L^{-1} as internal standard, and 1 ml of filtered sample]. Mineral quantifications were carried out using certified multi-element standard. Tomato leaves (NIST SRM 1573a) were used as external certified reference material. Mineral nutrient concentration in leaves was expressed on a dry weight (DW) basis.

Perls'-DAB staining

For *in situ* Perls'-DAB Fe staining intensification, leaves were fixed in a solution containing 2% (w/v) paraformaldehyde, 1% (v/v) glutaraldehyde, 1% (w/v) caffeine, and 0.01% triton X-100 in 0.1 M phosphate buffer (pH 7) for 24 h. Fixed tissue was dehydrated in 10, 30, 50, 60, 70, 80, 90, and 100% ethanol for 1 h at each concentration and then embedded in paraffin. Sections (7 µm) were obtained using a microtome (Leica, Milan, Italy), placed on poly-l-lysine-coated slides (Menzel-Glaser, Braunschweig, Germany), and dried at 30 °C for 1 h. Before staining, sections were dewaxed and rehydrated. Leaves sections were incubated for 45 min in 4% (v/v) HCl and 4% w/v K-ferrocyanide (Perls stain solution) for 45 min (Stacey *et al.*, 2008), except for negative controls which were incubated in 4% (v/v) HCl. After washing with deionized water, glass slides were incubated in a methanol solution containing 0.01 M NaN_3 and 0.3% (v/v) H_2O_2 for 1 h and then washed with 0.1 M phosphate buffer (pH 7.4). For the intensification reaction, samples were then incubated between 10 and 30 min in a 0.1 M phosphate buffer (pH 7.4) solution containing 0.025% (w/v) DAB (Sigma), 0.005% (v/v) H_2O_2, and 0.005% (w/v) $CoCl_2$ (intensification solution) (Roschzttardtz et al, 2009). Rinsing with distilled water stopped the reaction. Samples were observed by a light microscope (Nikon Eclipse Ni microscope, Tokyo, Japan).

To quantify Perls'-DAB Fe staining in the leaf lamina, 5 randomly-selected 10x images per sample were captured (3 samples per experimental condition, n=15). Image analysis was carried out using the open-source ImageJ 1.49m software package (National Institutes of Health, Bethesda, MD, USA). Image analysis was coded in ImageJ macro-language, thresholding the region of interest with

Maximum Entropy algorithm, selecting dots with a diameter ranging from 1 to 5 µm (Roschzttardtz *et al.*, 2011; 2013) and measuring their area.

Gene expression analyses

To investigate the expression of genes involved in the Fe uptake of strategy I plants and other genes modulated by Fe deficiency in roots, qRT-PCR experiments were performed on samples from H/+Fe, I/+Fe, H/-Fe and I/-Fe plants on a CFX96 instrument (Bio-Rad Laboratories, Richmond, CA, USA). About 1 g of root tissue for each plant was homogenized by mortar and liquid nitrogen, and RNA was extracted from approximately 100 mg of powder with the Spectrum Plant Total RNA Kit (Sigma-Aldrich, St Louis, MO, USA) according to the manufacturer's instructions. Extracted RNA was reverse-transcribed into complementary DNA (cDNA) with the QuantiTect Reverse Transcription Kit (Qiagen GmbH, Hilden, Germany) following the manufacturer's instructions, which include an incubation step in gDNA Wipeout Buffer to eliminate genomic DNA. *UPL3* (E3 ubiquitin-protein ligase UPL3), *EF-1* (elongation factor 1-alpha), *ACT-7 like* (actin-7-like), and *TUB* (beta-tubulin) were used as reference genes (Supplemental Table 1). Gene stability measures (M values) were calculated according to the geNorm program (Vandesompele *et al.*, 2002). The *UPL3* gene was found to be one of the most stably expressed genes in both leaves and roots (M=0.303 and M=0.357, respectively) and thus the most suitable reference gene.

SsoFast EvaGreen Supermix 2x (Bio-Rad Laboratories Inc., Hercules, CA, USA), cDNA obtained from 2.5 ng of RNA, and specific primers (final concentration 300 nM of each primers) were used in a total volume of 15 µL for all genes analysed. Every reaction was performed at 95°C for 3 min, 40 cycles of 95°C for 5 sec and 57°C for 5 sec, followed by a melting curve analysis from 65°C to 95°C to validate primer specificity. Primers were designed on the sequences retrieved from NCBI RefSeq database using Primer3 software (http://bioinfo.ut.ee/primer3-0.4.0/primer3/), and primer specificity was evaluated with the BLASTN (Nucleotide Basic Local Alignment Search Tool) algorithm (Altschul *et al.,*1997). Primer pair efficiency (E) was evaluated as described by Pfaffl (2001) on the standard curves of different dilutions of pooled cDNA. Gene and primer sequences for expression analysis are reported in Supplemental Table 2. Mean normalized expression (MNE) for each gene of interest (Muller *et al.,* 2002) was calculated by normalizing its mean expression level to the level of the *UPL3* gene. Three technical repeats and five individuals were used for MNE determination.

Fe(III)-chelate reduction activity

FCR activity in the roots was assayed by the method described in Welch *et al.* (1993). Briefly, lateral roots were excised from five plants per condition and embedded in a gel consisting of 0.2 mM $CaSO_4$, 1 % (w/v) agarose, 5 mM MES buffer (pH 5.5), 0.1 mM Fe(III)-EDTA, and 0.3 mM Na_2-bathophenanthrolinedisulfonic acid (BPDS). The reddish coloured staining, which is related to the reduction activity of Fe(III) to Fe(II), and the simultaneous Fe(II)-BPDS complex formation, developed in 30 min.

Statistical analysis

Data are expressed as mean values ±SD. Statistical analyses were performed by SigmaPlot 12.0 (SigmaPlot Software, CA, USA), using one-way ANOVA with a Holm-Sidak's test as *post hoc* test for multiple comparisons.

4.3. Results

Iron deficiency and phytoplasma infection induce leaf chlorosis

Plant responses to the different stress conditions (Fe starvation, phytoplasma-infection and phytoplasma-infection concurrent with Fe starvation) were first studied considering whole plant morphology and plant biometric parameters (Fig. 1). Plants were analysed five weeks after grafting, when healthy plants showed regular growth, and typical symptoms developed in both phytoplasma-infected and Fe-starved plants (Fig. 1). Plant morphology was severely affected by both Fe deficiency and infection by phytoplasma, although plant weight was not significantly altered by either treatment (Fig. 1E). Infected plants grown on Fe-replete media (I/+Fe plants) developed leaf chlorosis caused by decreased chlorophyll content (Fig. 1B and F). Yellowing was particularly pronounced in the leaf edges (Fig 1B). Infected plants produced smaller leaves with reduced leaf area when compared to healthy plants (Fig. 1B and G). Symptoms of infected plants included swollen flower buds and malformed flowers with green petals (Fig. 1B). Root morphology remained unaffected by the infection (Fig. 1B). Non-infected Fe-deficient (H/-Fe) plants developed interveinal chlorosis on young leaves, which did not differ in size from leaves of control plants (Fig. 1C, F and G). Roots of Fe-starved plants formed short lateral roots, extra root hairs, and swollen tips (Fig. 1C). No alterations were observed in shoot and flowers (Fig. 1C). Upon infection, Fe-starved plants developed symptoms of both stresses, *i.e.* yellowing and surface reduction of leaves, the typical phytoplasma-induced

alterations of the shoot and of the flowers, as well as the root modifications caused by Fe deficiency (Fig. 1D, F and G). Notably, the combination of the two stresses intensified the chlorosis symptoms with interveinal chlorosis appearing together with yellowing of the leaf edges (Fig. 1D). Phytoplasma infection and Fe starvation had additive effects on the chlorophyll content (Fig. 1 F).

The presence of '*Ca*. P. solani' in all plants grafted with phytoplasma-infected scions was validated by qPCR in leaf and root samples. To investigate the impact of Fe deficiency on pathogen replication capability, phytoplasma titre was quantified by qPCR in eight I/+Fe and eight I/-Fe plants. The phytoplasma concentration was determined by measuring phytoplasma 16SrRNA gene levels relative to the tomato Chloronerva gene (Fig. 2). In leaves of I/-Fe plants, the amount of phytoplasma was 1.7-fold reduced compared to leaves of I/+Fe.

Iron deficiency and phytoplasma infection compromise chloroplast ultrastructure

To visualize changes in cellular ultrastructure following pathogen infection or Fe starvation, leaf tissue was examined by TEM. Since phytoplasmas were mostly confined to the sieve elements, observations were focused on the midribs of the leaves. In samples from healthy (H/+Fe) plants, TEM images revealed well-structured cells (Fig. 3A). Sieve elements developed plasma membranes with a regular profile and tiny protein filaments occurring in the lumen of sieve element. The chloroplasts of companion and phloem parenchyma cells were large and oval shaped, containing fully developed grana with numerous layers and well-developed stroma lamellae (Fig. 3B). In infected (I/+Fe) plants, phytoplasmas with their typical pleomorphic profile were detected exclusively in the lumen of the sieve elements and were surrounded by a pronounced accumulation of protein filaments (Fig. 3C). In companion and phloem parenchyma cells, chloroplasts showed irregular arrangements of thylakoid stacks, associated to the presence of large starch grains that caused a distortion of the parallel pattern of the lamellae (Fig. 3D). Fe starvation did not alter the sieve element ultrastructure (Fig. 3E) but affected thylakoid organization in companion and phloem parenchyma cells. Similar to what has been observed in infected plants, Fe-deficient plants showed disorganization of grana and stroma lamellae, and starch accumulation (Fig. 3F). Also in phytoplasma-infected Fe-starved tissues, phytoplasmas were exclusively detected in sieve elements, plugged by a massive presence of phloem protein filaments (Fig. 3G). Chloroplasts were disorganized with severely altered ultrastructure (Fig. 3H).

Fe starvation and phytoplasma infection induce specific changes in the transcriptome of tomato leaves

To gain insights into the transcriptomic response to infection by phytoplasma or Fe deficiency, single-end stranded RNA-seq transcriptome profiling was performed on midrib-enriched leaves. No information was available on the effect of each single stress (phytoplasma infection or Fe deficiency) on the leaf transcriptome in tomato, thus the study of the double stress was considered too complex to be addressed in this stage, and we limited our analysis to control (H/+Fe), infected Fe-sufficient (I/+Fe), and Fe-deficient (H/-Fe) plants. Three biological replicates for each condition were analysed by RNA-seq and mapped to the ITAG3.20 (release date: June 15, 2017) annotation of the tomato reference genome (SL3.0), covering a total of 35,768 genes. After quality filtering, approximately 38 million reads on average for each of nine libraries (three conditions, three biological replicates) were mapped to the reference genome, corresponding to a mean mapping rate of 83.1 ± 1.2 %. Assembling of transcripts from the mapped reads, estimating transcript abundance, and identifying differentially expressed genes (DEGs) were conducted using the TopHat2 and Cuffdiff2 software. On average, 20,463 ± 90 genes were considered as being expressed in midrib-enriched leaves with FPKM >1 in at least one condition of each pairwise comparison. DEGs were defined by a FDR<0.05 and FPKM >1 in at least one condition. In the Cuffdiff2 outputs, each DEG corresponded to only one transcript and one coding sequence. Venn diagrams show the number of up-, down- and anti-directionally regulated transcripts that were common and specific for the various pairwise comparisons (Fig. 4). Phytoplasma infection altered the expression of 2,773 genes relative to non-infected controls (H/+Fe). Among this subset, 1,120 DEGs (including 5 genes not expressed in H/+Fe) were upregulated in infected plants, while 1,653 (including 9 genes expressed only in H/+Fe) were downregulated. A subset of 1,846 genes was considered as being differentially expressed in healthy Fe-deficient (H/-Fe) plants compared to healthy Fe-sufficient (H/+Fe). Among them, 656 (including 11 genes not expressed in H/+Fe) were upregulated in H/-Fe, while 1190 (including 4 genes not expressed in H/-Fe) were downregulated. Comparing I/+Fe and H/-Fe plants yielded 2,908 DEGs. A suite of 824 common DEGs were identified in the comparison between I/+Fe vs H/+Fe and H/-Fe vs H/+Fe. Among this subset, only 89 DEGs were anti-directionally regulated by phytoplasma-infection and Fe-starvation, suggesting generally similar effects of phytoplasma infection and Fe deficiency on commonly targeted genes.

qRT-PCR was performed to confirm the results of RNA-seq on 10 genes affected by phytoplasma-infection and/or Fe starvation. This validation confirmed expression directionality and showed similar levels of regulation for all genes examined, indicating that fold-change values obtained from RNA-seq were accurate (Supplemental Table 3). To determine differences and

similarities between phytoplasma-infected and Fe-starved leaves, DEGs were used to perform GO classification and KEGG functional enrichment analyses (Fig. 5 and Fig. 6). For the genes that were differentially expressed between infected and non-infected plants, the most significant enriched GO terms ($P<0.05$) were 'photosynthesis', 'generation of precursor metabolites and energy' and 'cellular homeostasis' in the biological process (BP) category, 'thylakoid', 'plastid' and 'membrane' in the cellular component (CC) category, and 'DNA-binding transcription factor activity' in the molecular function (MF) category (Fig. 5). The GO categories significantly enriched in phytoplasma-infected samples indicated that photosynthesis-related processes represent the major changes caused by the infection, which was confirmed by the most enriched KEGG pathways ($P<0.05$), i.e. photosynthesis (antenna proteins), porphyrin and chlorophyll metabolism, and carotenoid metabolism. Moreover, KEGG enrichment listed several DEGs involved in carbon metabolism, specifically carbon fixation and C2 cycle (Fig. 6). For the DEGs in the H/-Fe vs H/+Fe comparison, the terms 'generation of precursor metabolites and energy', 'response to endogenous stimulus' and 'cellular homeostasis' were mostly enriched in the BP category. Most DEGs in the cellular component category were assigned to 'thylakoid' and 'extracellular region' terms. The most significant GO term in the molecular function category was 'transferase activity (Fig. 5). In sum, similar to what has been observed in phytoplasma-infected plants, the enrichment analysis suggests that light harvesting and light reactions as major targets of Fe deficiency. Moreover, Fe starvation affected the expression of genes involved in photosynthesis (in particular antenna proteins), porphyrin and chlorophyll metabolism, and carotenoid metabolism pathways (Fig. 6). In addition, KEGG enrichment revealed several DEGs involved in carbon metabolism, specifically in carbon fixation, pentose phosphate pathway and photorespiration (glyoxylate and dicarboxylate metabolism). When comparing infected Fe-sufficient (I/+Fe) with healthy Fe-deficient (H/-Fe) plants, the terms 'photosynthesis', 'generation of precursor metabolites and energy' and 'cellular homeostasis' were again mostly enriched in the BP category. With regard to the cellular component category, most of the DEGs were assigned to 'thylakoid', 'extracellular matrix' and 'membrane'. The most significant GO terms in the MF category were 'DNA-binding transcription factor activity' (Fig.5). Interesting, the most enriched group of phytoplasma-enriched genes was the antenna protein cluster (pathway sly00196) (Fig. 6, Fig. 7, Supplementary Table 4). Following infection (I/+Fe), a general downregulation of several genes encoding antenna proteins associated with photosystem I (clustered in the orthologues group Lhca) and photosystem II (Lhcb group) was observed. Most DEGs were specific to this condition. Fe starvation (H/-Fe) induced the expression of some antenna proteins genes belonging to the Lhca and Lhcb groups. Some antenna proteins, Solyc06g069730 (Lcha4 group), Solyc02g070970, and Solyc03g005770 (both Lchb1 group) were down-regulated in I/+Fe plants and induced in H/-Fe

leaves. Comparing the two stresses yielded a large suite of antenna proteins of all subgroups that were all downregulated. Thus, phytoplasma infection and Fe starvation exert opposite effects to a similar group of genes.

When examining genes associated with porphyrin and chlorophyll metabolism (sly00860), genes involved in chlorophyll biosynthetic pathway such as the glutamyl-tRNA reductase 1 (Solyc04g076870 and Solyc01g106390), the magnesium chelatase subunit H (Solyc04g015750, ChlH), and the putative magnesium-protoporphyrin monomethyl ester cyclase (Solyc10g077040, at103), were down-regulated upon Fe deficiency, indicating that, as anticipated, chlorophyll biosynthesis was affected by the Fe regime (Fig. 8 and Supplemental Table 5). A similar trend was observed in I/+Fe plants. Similar to what was observed for genes encoding antenna proteins, some genes involved in porphyrin metabolism were anti-directionally regulated by phytoplasma infection and Fe starvation. For example, one of the two genes encoding glutamyl-tRNA reductase (Solyc01g106390), which represents a key step for the biosynthesis of both heme and chlorophyll, was 2-fold induced in I/+Fe leaves but downregulated in H/-Fe plants. Also, a chlorophyllide a oxygenase gene (CAO; Solyc06g060310) was down-regulated in I/+Fe plants, while up-regulated in H/-Fe. Moreover, ChlH gene activity appeared more heavily compromised in I/+Fe compared to H/-Fe leaves. All genes involved in chlorophyll turnover where affected by both stresses. Changes in the abundance of LHC apoproteins are generally accompanied by parallel changes in chlorophyll content to prevent the production of excess pigment without the corresponding binding protein and *vice versa*. Accordingly, a synchronisation was observed between lhcb and CAO gene expression in response to irradiance (Masuda *et al.*, 2003). Also carotenoid biosynthesis was affected in both conditions. Here, a similar trend was observed, i.e. downregulation of the genes encoding key enzymes involved in the biosynthesis of alpha- and beta-carotene and their oxidized forms from geranylgeranyl bisphosphate, through phytoene and lycopene intermediates synthesis. Among these genes, beta-carotene hydroxylase (Solyc06g036260) was strongly downregulated by infection (I/+Fe): 19.2 times, compared to 2.8 times of Fe starvation (H/-Fe) (Fig. 9). In I/+Fe plants, also the expression of zeaxanthin epoxidase (ZEP; Solyc02g090890) was reduced, suggesting a deep impairment of zeaxanthin and violaxanthin production from beta-carotene (Fig. 9 and Supplemental Table 6). While the light harvesting apparatus appeared compromised in all components, i.e. antenna proteins synthesis and pigment biosynthesis, also several clusters of genes associated with photosynthetic light reactions (sly00195) were down-regulated in the two conditions. Common targets of both stressors were the two ferredoxin genes (PetF; Solyc10g075160, Solyc11g006910) and two genes associated with photosystem II (PsbS and Psb28). In addition, phytoplasma infection targeted genes of the electron transport (i.e. the plastocianin encoding gene Solyc04g082010 and a ferredoxin-$NADP^+$

reductase gene Solyc02g083810), and several genes encoding proteins of other thylakoid complexes, photosystem I, the cytochrome b_6/f complex and the F-type ATP synthase complex (subunit gamma and b) (Fig. 10 and Supplemental Table 7).

Transcriptional profiling revealed robust regulation of genes involved in flowering time, transport, and photosynthesis

To identify genes that are massively regulated by Fe starvation or phytoplasma infection and possibly play key roles in the plant responses to these cues, we considered the top 100 up- or downregulated genes in plants subjected to either stress condition (total FPKM expression levels >10). In leaves of Fe-deficient plants, a putative Arabidopsis *IRON MAN* (*IMA*) ortholog (Solyc12g006770) was most strongly induced (Supplementary Table 8). IMA is a family of Fe deficiency-induced peptides associated with the communication of the Fe status from leaves to roots via the phloem recently identified in Arabidopsis (Grillet *et al.*, 2018). Several other genes encoding IMA peptides were also strongly induced upon Fe deficiency but were not expressed in leaves of Fe-sufficient plants. Similarly, *bHLH68* (Solyc10g079680), an ortholog of *AtbHLH38/39* was strongly induced upon Fe deficiency and not expressed under control conditions. Another gene encoding a protein that has been implicated in long-distance signaling, OLIGOPEPTIDE TRANSPORTER 3 (Solyc11g012700) (Stacey *et al.*, 2008; Mendoza-Cózatl *et al.*, 2014), was also robustly induced upon Fe starvation. Further, several transcription factors of the bHLH (Solyc11g056650; Solyc10g008270; Solyc10g006640; Solyc07g063830) and NAC (Solyc05g007770) families were in the group of strongly upregulated genes in leaves of Fe-deficient plants (Supplemental Table 8).

A gene encoding the Fe sequestration protein ferritin (Solyc06g050980) was downregulated under Fe-deficient conditions. The expression of the putative tomato *NEET* ortholog (Solyc03g007030), a protein with a conserved role in Fe metabolism reactive oxygen homeostasis, decreased in response to Fe starvation, a response that has also been observed in Arabidopsis leaves (Rodiguez-Celma *et al.*, 2013). In addition, three genes encoding proteins with similarity to vacuolar iron transporters of the VIT (Solyc04g071165; Solyc04g051180; Solyc01g104780) family were among the list, indicating reduced vacuolar sequestration of Fe. Also, two other genes associated with cellular Fe homeostasis, the nicotianamine synthase *chloronerva* (Solyc01g100490), the ferric reductase *FRO6* (Solyc01g102610), and several genes involved in the transport of mineral nutrients such as Pi and boron showed reduced expression in Fe-deficient leaves. A massive downregulation upon Fe deficiency was observed for RuBisCO activase 1 (RCA1; Solyc09g011080), suggesting strongly reduced photosynthetic activity in Fe-deficient plants. Reduced expression involved in

flowering control, *EARLY FLOWERING 4* (Solyc06g051680) and three CONSTANS-LIKE proteins (Solyc07g045180; Solyc07g045185; Solyc02g093590) are indicative of delayed flowering of Fe-deficient plants. Several transcripts of genes encoding transcription factors of the zinc finger family (Solyc02g084420; Solyc07g045185; Solyc07g045180; Solyc02g093590), MYB (Solyc10g084370; Solyc02g036370; Solyc06g005320), and bHLH (Solyc03g114230) showed reduced abundance upon Fe starvation.

Similar to Fe-deficient plants, *RCA1* was strongly downregulated by phytoplasma infection. In diseased plants, a second RuBisCO activase (Solyc10g086580) was massively downregulated. In addition, the gene encoding *PROTON GRADIENT REGULATION 5* (Solyc09g090570), a protein required for electron transport and in preventing of oxidative damage to photosystem I (Munekage *et al.*, 2002), showed reduced activity in infected plants. Associated with a supposedly reduced photosynthetic rate, *SUGAR TRANSPORT PROTEIN 8* (Solyc06g054270) and a sugar transporter with similarity to SWEET proteins (Solyc05g024260) were downregulated upon pathogen infection. Also similar to Fe-deficient plants, several genes putatively related to flowering (Solyc06g073180; Solyc02g089540; Solyc07g053140; Solyc12g005660; Solyc04g054800) showed reduced expression in diseased plants. Further, a suite of genes encoding proteins involved in the transport of boron (Solyc01g079150), Pi (Solyc05g010060; Solyc01g091870), sulfate (Solyc04g072740; Solyc09g082550), ammonium (Solyc04g050440), nitrate (Solyc08g077170) potassium (Solyc07g014680), and a ferric reductase (FRO6, Solyc01g102610) showed reduced transcript abundance, indicating a generally reduced translocation of mineral nutrients in diseased plants. Upregulated in infected plants were several proteins related to pathogen defense, the chitinase Solyc02g082960, the pathogenesis-related thaumatin superfamily protein Solyc11g066130, and DEFENSIN-LIKE PROTEIN 3 (Solyc07g007760). Several other pathogen defense-related genes were expressed at high levels and significantly but only moderately upregulated and were thus not included in the list of the top 100 upregulated genes. Among these genes, several chitinases (*CHI3*, Solyc02g082920; *CHI9*, Solyc10g055810; *CHI17*, Solyc02g082930; *endochitinase 4*, Solyc10g055800; *acidic endochitinase* Solyc05g050130), and pathogenesis-related proteins such as pathogenesis-related leaf protein 6 (PR1b1, Solyc00g174340) and pathogenesis-related protein P4 (P4/pr1a, Solyc09g007010). Among these moderately induced genes were also other thaumatin-like proteins such as osmotin-like protein *OSML13* (TPM-1, Solyc08g080650).

Iron distribution is altered by phytoplasma infection

To investigate a possible effect of the infection on Fe uptake and translocation, the Fe content of leaves and roots was quantified by ICP-OES. In leaves of infected plants, the Fe concentration was similar to that of healthy plants, whereas a significant decrease was observed in healthy Fe-starved (H/-Fe) and phytoplasma-infected/Fe-starved (I/-Fe) plants (Fig. 11A). Following Fe starvation, the Fe concentration decreased by 57% in H/-Fe plants and by 75% in I/-Fe plants. Notably, in spite of lack of difference in Fe concentration between I/+Fe and H/+Fe plants, the Fe concentration in infected Fe-deficient plants was significantly lower than in H/-Fe plants. In roots, infected (I/+Fe) plants showed a reduction of the Fe concentration of 15% in comparison to H/+Fe plants. As expected, Fe starvation caused a strong decrease in Fe concentration in roots of both H/-Fe and I/-Fe plants (60% and 65%, respectively, compared to H/+Fe) (Fig. 11B).

Next, we investigated whether the presence of pathogens altered the distribution of Fe in leaves using Perls'-DAB staining. Healthy (H/+Fe) plants showed pronounced Fe staining in the phloem area (Fig. 12A; Supplemental Fig. 1), clearly visible in the longitudinal sections (Fig. 12E). Tiny Fe dots were also present in xylem parenchyma cells (Fig. 12I). Fe dots in the phloem area were also observed in midribs of infected plants (Fig. 12B). However, no Fe deposit in xylem parenchyma cells was observed in infected plants (Fig. 12L). Mesophyll palisade cells of the lamina exhibited a non-uniform distribution of the Fe dots. Quantification of Perls'-DAB staining in leaf parenchyma revealed that the leaf lamina of I/+Fe plants was characterized by less intense DAB staining when compared to H/+Fe plants (Fig. 12O). Independently on the infection, in Fe-deficient plants Fe dots were neither detected in midrib cells nor in xylem or phloem tissue (Fig. 12C, D, G, H, M and N). Quantification of the Fe staining confirmed the decreased frequency of Fe dots in the mesophyll palisade cells of the lamina of both healthy and infected Fe-deficient plants (Fig. 12O).

Phytoplasma infection perturbs the Fe deficiency response of tomato roots

To investigate if phytoplasma infection affects the Fe acquisition mechanism at the root level, the expression of the Iron-Regulated Transporter 1 (*LeIRT1,* Solyc02g069200; Eckhardt *et al.*, 2001), the Ferric Reduction Oxidase 1 (*LeFRO1,* Solyc07g017780; Li *et al.*, 2004) and the *AtAHA2* orthologue plasma membrane H^+-ATPase 4 (*LHA4,* Solyc07g017780; Morsomme and Boutry, 2000) was analysed by qRT-PCR (Fig.13). Expression analysis involved also two transcription factors known to act upstream in the regulation of Fe uptake genes, the *AtFIT* orthologue *FER* (*FER,* Solyc06g051550; Ling *et al.*, 2002) and *SlbHLH068* (Solyc10g079680), which interacts with FER to regulate the Fe deficiency response in tomato (Du *et al.* 2015) (Fig. 13). In addition, we quantified

the transcripts level of other genes known to be involved in intra-cellular metal transport and mobilization of metal pools, i.e. *LeNRAMP1* (Solyc11g018530; Bereczky *et al.*, 2003) and *LeNRAMP3* (Solyc02g092800; Bereczky *et al.*, 2003) (Fig. 13). We further explored the tomato genome database for genes possibly involved in the synthesis and activation of Fe-mobilizing coumarins (see Tsai and Schmidt, 2017 for a review). *SlF6'H1* (Solyc11g045520), which is annotated as Feruloyl CoA ortho-hydroxylase 1 in the NCBI gene database, shares 63% identity at the amino acid level with AtS8H (AT3G12900), which encodes a Scopoletin 8-hydroxylase involved in fraxetin biosynthesis (Tsai *et al.*, 2018). Arabidopsis *MYB72* is a root-specific transcription factor functioning as a node of convergence in the induced systemic resistance and iron starvation signalling pathways, triggering the activation of coumarins *via* β-glucosidase BGLU42 (Segarra *et al.*, 2009; Zamioidis *et al.*, 2014). In the Hierarchical Catalog of Orthologs (OrthoDB URL: https://www.orthodb.org), the *Solanum lycopersicum* orthologue of *AtMYB72* is the Myb domain protein 58 (*SlMYB58;* Solyc10g005550) gene, which possesses a homeobox domain-like, a Myb and a SANT/Myb domain (InterPro Domain IPR009057, 017930 and 001005, respectively) similar to AtMYB72. Finally, we analysed the expression of a phospho*enol*pyruvate carboxylase (*PEPC*) gene. PEPC is involved in C fixation and subsequent synthesis of organic acids, especially citrate, that transport Fe to leaves via xylem sap and contribute with other organic molecules to the mobilization of Fe from the apoplast in roots (Lopez-Millan *et al.*, 2009; Schmidt, 1999). The protein of the *SlPEPC* (Solyc10g007290) gene aligns with the highest score and 88% identity to Arabidopsis PPC3 (AT3G14940), the PEPC isoform most abundantly expressed in Arabidopsis roots.

In the presence of Fe, the expression level of every gene under investigation was not significantly modified by phytoplasma infection (I/+Fe plants), although high variability among individuals has potentially masked possible differences between infected and non-infected plants (Fig 13). As expected, all investigated gene were up-regulated upon Fe deficiency. However, the degree of the induction greatly varied among genes. In fact, some genes, such as *LHA4, NRAMP3*, *PEPC* and *FER,* exhibited an expression that was several times higher in H/-Fe plants than in H/+Fe plants (ranging from roughly 1.5-fold to 8-fold). The up-regulation of other genes was even higher (15-fold *IRT1,* 30-fold *FRO1*, 19.5-fold *NRAMP1*, 39-fold *MYB58*, 76-fold *F6'H1*), reaching a peak for *bHLH068,* which was induced by a factor of 139. When examining I/-Fe plants, an increase in the expression of most of the genes under investigation was observed, but, unexpectedly, the extent of such an induction was not similar to H/-Fe plants, as expression levels stood at intermediate values between the two Fe conditions. Thus, the general Fe deficiency-induced up-regulation that characterized both healthy and infected plants differed in a significant manner according to the sanitary status of the plants, as for almost every investigated gene transcript abundance was reduce by the presence of phytoplasma. The

containment of the up-regulation varied according to the gene considered, ranging from a decrease in expression of 36.8% (*IRT1*) to 80% (*bHLH068*). A notable exception to this trend was the expression of *FRO1*, which was induced by growth on Fe-free media regardless of the sanitary status. This result was confirmed by the Fe(III)-chelate reduction activity survey that was performed on excised roots (Supplemental Fig. 2). In accordance with gene expression analysis of *FRO1*, reductase activity was induced by Fe deficiency but remained unaffected by phytoplasma infection.

4.4. Discussion

The transcriptional response of phytoplasma-infected tomato leaves mirrors Fe deficiency

Phytoplasmas are prokaryotic plant pathogens that colonize the sieve elements of the host plant's phloem. Alteration in phloem function and impairment of assimilate translocation are the most dramatic effects of the infection, but the mechanisms underlying plant host-phytoplasma interaction are still largely unexplored. Fe appears to play a central role in the interaction between pathogens and their plant hosts. Plants are infected by a variety of microorganisms that produce siderophores, secreted in response to Fe deficiency to provide Fe to the microorganism (Andrews *et al.*, 2003; Winkelmann, 2007). In fact, in different pathosystems, competition for Fe can take place, forcing the plant to develop a Fe withholding response and change the distribution and trafficking of Fe (Dellagi *et al.*, 2005). For some pathogens, such as *Erwinia chrysanthemi*, the control of Fe homeostasis is central to pathogenicity (Expert *et al.*, 1996).

Previous plant-phytoplasma interaction studies have shown changes in the expression level of genes involved in photosynthesis (Albertazzi *et al.*, 2009; Hren *et al.*, 2009; Liu *et al.*, 2013; Mou *et al.*, 2013, Nejat *et al.*, 2015; Xue *et al.*, 2018; Wang *et al.*, 2018c). In the current study, plants grown in an environment-controlled hydroponic system displayed the symptoms normally occurring in field: in both infected (I/+Fe) and Fe-starved (H/-Fe) plants, leaves appeared to be chlorotic and yellowish, and a concomitant decrease in the total chlorophyll content was measured. Transcriptional analyses of Arabidopsis leaves and apple seedlings showed that, in the case of Fe deficiency, the chlorosis is accompanied by alterations in the expression of genes involved in photosynthesis and chlorophyll metabolism (Wang *et al.*, 2018a; Rodriguez-Celma *et al.*, 2013). This global rearrangement is not surprising if considering that the largest sinks for Fe are the photosystems, and the major fraction of Fe is located in the chloroplasts (Briat and Lobreaux 1997; Briat *et al.*, 2007). Fe deficiency was shown to decrease the abundance of proteins involved in photosynthesis and of components of the electron transport chain and the photosystems (Pushnik and Miller, 1982; Andaluz *et al.*, 2006;

Msilini *et al.*, 2011). As previously reported, both Fe deficiency and phytoplasma infection alter the ultrastructure of chloroplasts, causing disorganization of thylakoids (Briat *et al.*, 1995; Stocking, 1975; Vigani *et al.*, 2015; Pagliari *et al.*, 2016; Xue *et al.*, 2018). Photosynthetic pigments such as chlorophylls are embedded in the thylakoid membrane, the site of the light-dependent reactions in photosynthesis. The stacked coil shape of the grana gives the chloroplast a high surface area to volume ratio, contributing to the photosynthetic efficiency (Tikkanen and Aro, 2012).

The fact that both Fe deficiency and phytoplasma infection are characterized by leaf yellowing and alteration of expression of genes involved in photosynthesis, let us to speculate that phytoplasma may cause an alteration of Fe homeostasis. Both stresses compromised photosystem II, the soluble component of the electron transport, and the light harvesting complexes through a modulation of several antenna proteins and an impairment of key steps in the biosynthesis of chlorophyll and carotenoids. This scenario suggests that plants have evolved control mechanisms to avoid deleterious reactions of light absorption when the photosynthetic activity is impaired. For example, in Fe-deficient Arabidopsis leaves, a downregulation of key steps of tetrapyrrole biosynthesis such as ALA synthesis was observed (Rodriguez-Celma *et al.*, 2013). Chlorophyll precursors such as Mg-protoporphyrin IX (Mg-PPIX) were proposed to be directly involved in retrograde signalling, since its accumulation caused by disturbance of the chlorophyll biosynthesis pathway provokes downregulation of the LHC genes (Strand *et al.*, 2003). In tomato, the Mg chelatase subunit H gene (Solyc04g015750), involved in the biosynthesis of Mg-PPIX, and the magnesium-protoporphyrin IX monomethyl ester cyclase gene (at103; Solyc10g077040), mediating protochlorophyllide synthesis from Mg-PPIX, were dramatically downregulated in both Fe-deficient and infected plants, suggesting a decrease in the amount of Mg-PPIX. Notably, while LHC genes were upregulated in Fe-deficient plants, the same genes were dramatically downregulated in infected plants, suggesting different cause-effect scenarios under pathogen infection and Fe deficiency. In both cases, altered dissipation of light energy might lead to the accumulation of reactive oxygen species (ROS). In Arabidopsis, a potential candidate that links photosynthetic ROS and Fe metabolism is a NEET protein (Nechushtai *et al.*, 2012). NEET proteins are involved in Fe, Fe-S, and reactive oxygen homeostasis in cells. A putative orthologous gene in tomato is the CDGSH iron-sulfur domain-containing protein gene (Solyc03g007030), which was downregulated in H/-Fe and I/+Fe leaves, -7.3 and -3.8 times respectively.

Besides antenna proteins genes, also other components of the photosynthetic apparatus were modulated in a partly overlapping manner in Fe-deficient and infected plants. Noteworthy is the downregulation of genes encoding components of the photosystem I, the cytochrome b_6f complex, the F-type ATPase and the LHC antenna proteins lhcb in infected (I/+Fe) plants. Thus, the effects of

infection on the photosynthetic apparatus was even more devastating than in H/-Fe plants. The inhibition of the expression of genes involved in photosynthesis is in accordance with results of plant-phytoplasma interaction studies previously reported (Albertazzi *et al.*, 2009; Hren *et al.* 2009; Liu *et al.* 2013; Mou *et al.* 2013, Nejat *et al.*, 2015; Xue *et al.*, 2018; Wang *et al.*, 2018c). However, most genes encoding proteins involved in photosynthetic light reactions, porphyrin and chlorophyll metabolism, and in carotenoid biosynthesis had comparable expression changes in both I/+Fe and H/-Fe plants.

Phytoplasma infection alters the local distribution of Fe

Considering that phytoplasma infection and Fe starvation seem to induce similar alteration in the transcriptome regarding photosynthesis, chlorophyll and carotenoid metabolism, we investigated if in I/+Fe plants this response was induced by a phytoplasma-induced alteration in cellular Fe homeostasis. An ICP-OES survey of the Fe concentration in leaves and roots did not reveal an interference with Fe uptake by phytoplasmas. Considering that, different from other pathogens, phytoplasmas are strictly restricted to phloem tissues, it is rather likely that due to the locally restricted demand of the pathogen, infection alters the spatial distribution of Fe. Perls'-DAB staining and Fe dots quantification confirmed this supposition. Indeed, similar to Fe-deficient conditions, xylem parenchyma cells of infected leaves were characterized by a total absence of Fe dots. Moreover, the leaf lamina of infected (I/+Fe) and Fe-deficient (H/-Fe) plants had fewer Fe dots in the mesophyll palisade cells than control plants (H/+Fe), while similar to healthy (H/+Fe) plants Fe dots were visible in the phloem of the infected (I/+Fe) plants. These findings suggest a spatial shift of Fe from the leaf lamina to the infection site. This phenomenon has been observed in other plant-pathogen systems such as Arabidopsis infected by *Dickeya dadantii*. Here, a loss of Fe from leaf cellular compartments and the cell wall, in the latter case caused by pectin degradation, was associated with the concomitant accumulation of Fe inside and around the bacteria (Aznar *et al.*, 2015). These observations are consistent with a scenario in which the presence of Fe in the phloem tissue modifies the perception of the plant's Fe status and its communication to the roots. While little knowledge is available regarding the involvement of Fe in phytoplasma metabolism, it appears that Fe starvation imposed on infected plants reduced the phytoplasma titre, corroborating the assumption that phytoplasmas must acquire Fe from the phloem, converting the phloem into a sink tissue for Fe.

In plant-pathogen interactions, the secretion of siderophores by the pathogen is an efficient mechanism to acquire Fe from the host and to promote infection (Expert, 1999; Haas *et al.*, 2008). No information about the ability of phytoplasmas to produce siderophore is available, but it may be

assumed that effectors are secreted that act as or similar to bacterial siderophores. Rosa *et al* (2017) identified a putative effector with high similarity with the siderophore-protein hupB. Moreover, phytoplasmas secrete effectors directly into the host sieve elements and then the effectors are unloaded from the phloem to target other plant cells via symplastic transport (Bai *et al.,* 2009; Hoshi *et al.*, 2009; Sugio *et al.*, 2011). Similar to our results on phytoplasma infection, Aznar *et al.* (2014) observed modifications in Fe localization in Arabidopsis leaves upon siderophore treatment, without concomitant changes in total leaf Fe content. However, whereas siderophore treatment caused a rapid transient increase of Fe and zinc content in Arabidopsis roots, in our experiments infection was associated with a decrease in root Fe content. Our conditions may represent a late response to pathogen infection, masking transient changes in Fe concentrations following infection. The effector SAP11 expressed in transgenic plants was found to induce a small subset of genes involved in Fe deficiency responses (Lu *et al.*, 2014). Thus, we might speculate that phytoplasma siderophore-like effectors could compete with the plant for Fe and locally alter Fe homeostasis in the leaf. Whereas these changes appear to have relatively minor effects on the overall Fe metabolism of the host plant when sufficient Fe is available, under Fe-deficient conditions the presence of phytoplasma appear to impair the efficiency of root Fe acquisition, reducing furthermore the fitness of both the plant and the pathogen.

Phytoplasma infection perturbs the Fe deficiency response in roots

Little is known about the mechanisms by which plants communicate the Fe status among tissues and organs internally. Several lines of evidence point to the idea that shoots can signal their Fe status to the roots, tuning Fe uptake from the soil (Kobayashi and Nishizawa, 2014). Hormones, Fe-binding ligands, and recycling Fe ions have been proposed to act as signals promoting Fe deficiency responses in the roots (Kobayashi and Nishizawa, 2014). Under Fe-sufficient conditions, phytoplasma infection had no effect on the gene expression of Fe acquisition in roots. This is consistent with the lack of change in the Fe concentration in both leaves and roots, suggesting that the pathogen mobilizes Fe in the phloem but does not interfere with root Fe uptake. In healthy plants, Fe starvation led to a considerable upregulation of the genes of Fe uptake in roots increasing Fe acquisition. Also infected Fe-starved (I/-Fe) plants induced the upregulation of the same genes, although the entity of their expression was lower in comparison to Fe-starved (H/-Fe) plants. This finding could be interpreted as an interference of phytoplasmas with the transport of a promotive long-distance signal in the phloem that modulates root Fe acquisition. This presumptive restriction of shoot-to-root signalling is in line with the phloem mass flow impairment by phytoplasma infection demonstrated *in vivo*

(Pagliari *et al.*, 2017; Musetti *et al.*, 2013). A recent work (Grillet *el al.*, 2018) had identified a novel family of peptides (IRON MAN, IMA), expressed preferentially in leaves and associated with the phloem, in the regulation of Fe responses in roots by acting upstream of the master transcription factor FIT. The transcription, phloem loading, or the transport of IMA peptides or other yet unidentified mobile promotive signals could be altered in infected plants. Split-root experiments showed that the expression of *IRT1* and *FRO2* is controlled by both local and systemic signalling pathways and both signals being integrated to tightly control the production of the root iron uptake proteins (Vert *et al.*, 2003; Schikora and Schmidt, 2001; Schmidt *et al.*, 1996; Romera *et al.*, 1992). Notably, in our system FRO1 seemed to respond chiefly to a local signal, suggesting multi-level regulation of Fe acquisition.

4.5. Conclusions

In the current study, we analysed the effects of phytoplasma infection concurrent with Fe deficiency stress, conditions that mimic the simultaneous exposure to biotic and abiotic stresses that may normally occur in the field. We found that photosynthesis and porphyrin synthesis are the main targets of both stresses, leading to the development of chlorotic leaves, and, presumably, reduced photosynthetic rates and a concomitant imbalance of ROS species. While Fe deficiency directly affects chlorophyll synthesis, in infected plants chlorosis and impaired photosynthesis may rather be related to impaired signalling and subsequent deregulation of the genes involved in these processes. Under Fe-sufficient conditions, phytoplasma do not appear to interfere with the acquisition, uptake, or long-distance transport of Fe. However, phytoplasma infection alters the distribution of Fe within the leaf, leading to a probable increase of Fe in the phloem. Under Fe-deficient conditions, the presence of phytoplasmas may compromise the communication of the Fe status between leaves and roots, possibly by interference with the synthesis or transport of a promotive signal. It may be assumed that interference with phloem-based long-distance signalling has far-reaching consequences for the orchestration of root-mediated transport processes. Moreover, restricted source-sink transport of various classes of compounds such as carbohydrates and hormones may cause short circuits and negatively feed-back on metabolic and physiologic processes of leaves.

4.6. Acknowledgements

We are grateful to Alberto Loschi, for his help in plant rearing and infection, and Carla Calligaro, for technical support in the sample preparation for Perls'-DAB staining. RNA sequencing was performed by IGA Technologies Service, Udine, Italy. Most of bioinformatics work was allowed thanks to the CyVerse cyberinfrastructure (URL: www.cyverse.org) that is supported by

the USA National Science Foundation's Directorate for Biological Sciences under Award Numbers DBI-0735191 and DBI-1265383. This work was supported by FFABR_2017 (Italian MIUR) and RICLIB founds to Simonetta Santi and an Academia Sinica Investigator Award to Wolfgang Schmidt.

4.7. Figure

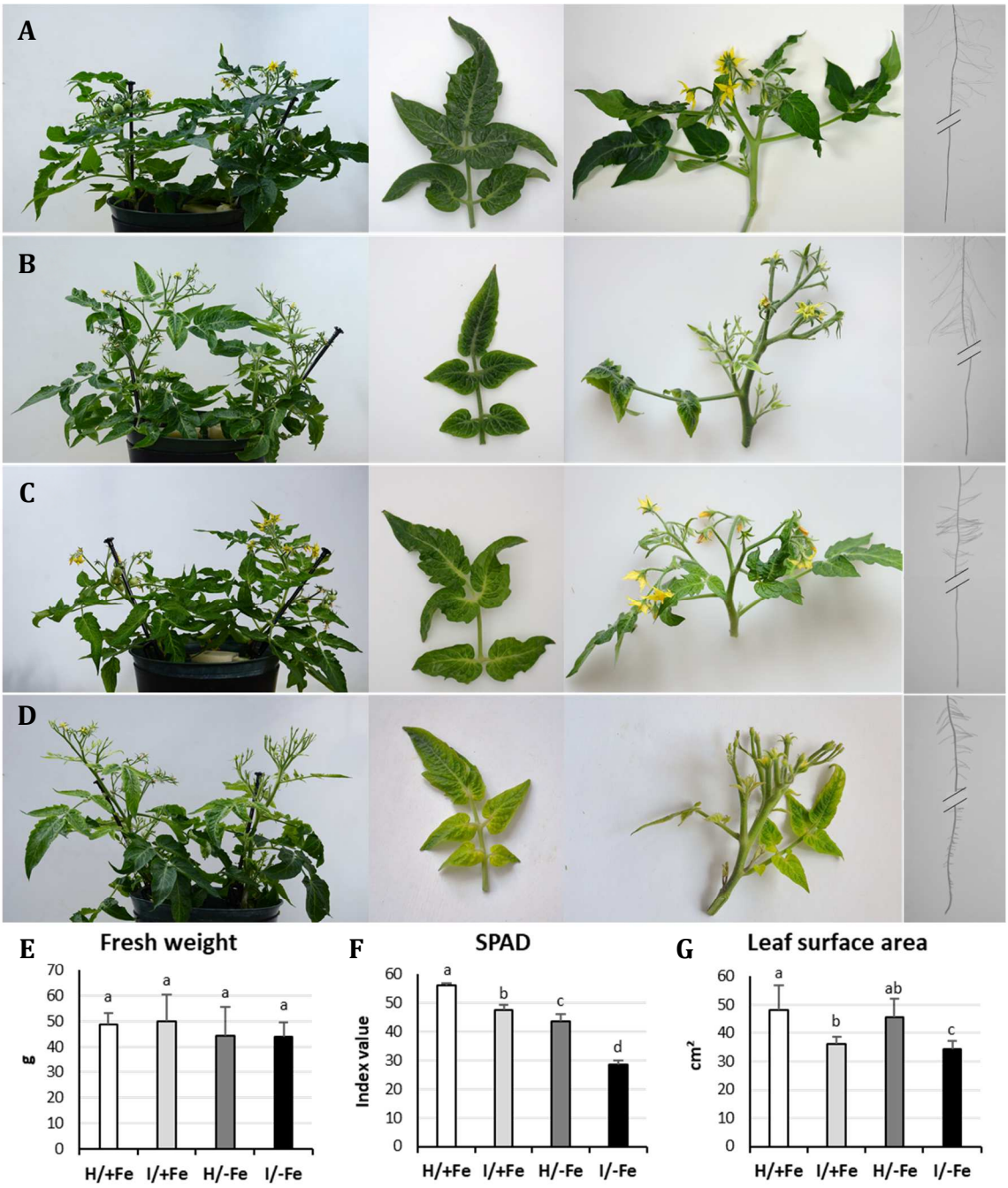

Figure 1. Phenotypes of representative tomato plants grown under different experimental conditions. Whole plants, leaves, shoots, and roots of (A) healthy Fe-sufficient (H/+Fe) plants, (B) infected Fe-sufficient (I/+Fe) plants (C) healthy Fe-deficient (H/-Fe) plants, and (D) infected Fe-deficient plants, (I/-Fe). (E) Total plant fresh weight. Results are expressed as mean ±SD (n= 6). (F) Leaf SPAD index values of fully expanded leaves. Results are expressed as mean ±SD (n= 150). (G) Leaf surface area. Results are expressed as mean ±SD (n= 30). Different letters indicate statistically significant differences ($P<0.05$) among conditions (one-way ANOVA followed by Holm-Sidak's test).

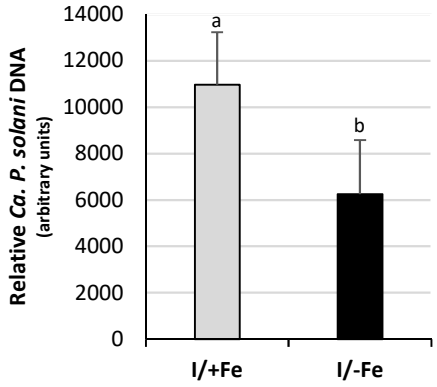

Figure 2. Quantification of '*Ca*. P. solani' in infected Fe-sufficient and Fe-deficient tomato leaves. Relative amount of '*Ca*. P. solani' DNA was determined by qPCR analysis of the *16SrRNA* gene of '*Ca*. P. solani' relative to the tomato single-copy gene *Chloronerva*. Results are expressed as mean ±SD (n= 8). Different letters indicate statistically significant differences ($P<0.05$) among conditions (one-way ANOVA followed by Holm-Sidak's test).

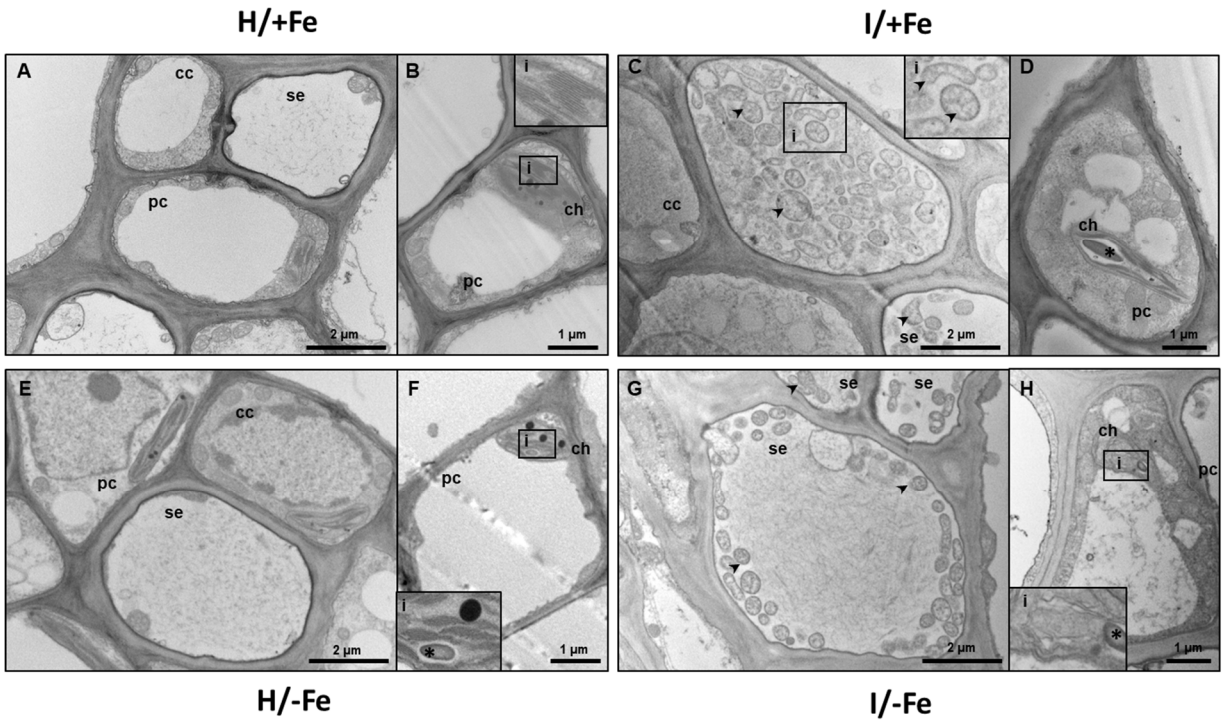

Figure 3. Effects of Fe starvation and phytoplasma infection on phloem ultrastructure.
In control samples (H/+Fe), sieve elements and surroundings cells presented a regular subcellular organization. (A, B). In infected plants (I/+Fe), phytoplasmas were detected, as expected, exclusively in the lumen of the sieve elements (C). Companion and mesophyll cells presented chloroplasts with distorted arrangement of thylakoid stacks and significative accumulation of starch (D). Healthy Fe-starved tissues (H/-Fe) were characterized by sieve elements with a regular ultrastructure (E) and companion and parenchyma cells with altered chloroplasts (F). Large starch grains impaired the correct organization of granal and stromal lamellae (F). In phytoplasma-infected/Fe-starved plants (I/-Fe), phytoplasma were detected in sieve elements (G) and chloroplasts ultrastructure appeared severely altered (H), as seen in both single stresses. cc: companion cell; ch: chloroplast; i: inset; pc: parenchyma cell; se: sieve element; *: starch; arrowheads indicate phytoplasmas. Three non-serial cross sections from five plants were analysed for each condition (n= 15).

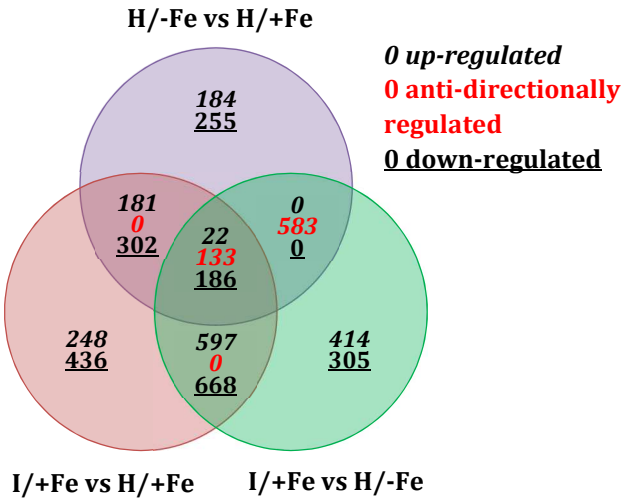

Figure 4. Venn diagrams. The number of up-, down- and anti-directionally regulated differentially expressed genes (DEGs) that were common and specific for the pairwise comparisons are shown: I/+Fe vs H/+Fe, H/-Fe vs H/+Fe, and I/+Fe vs H/-Fe.

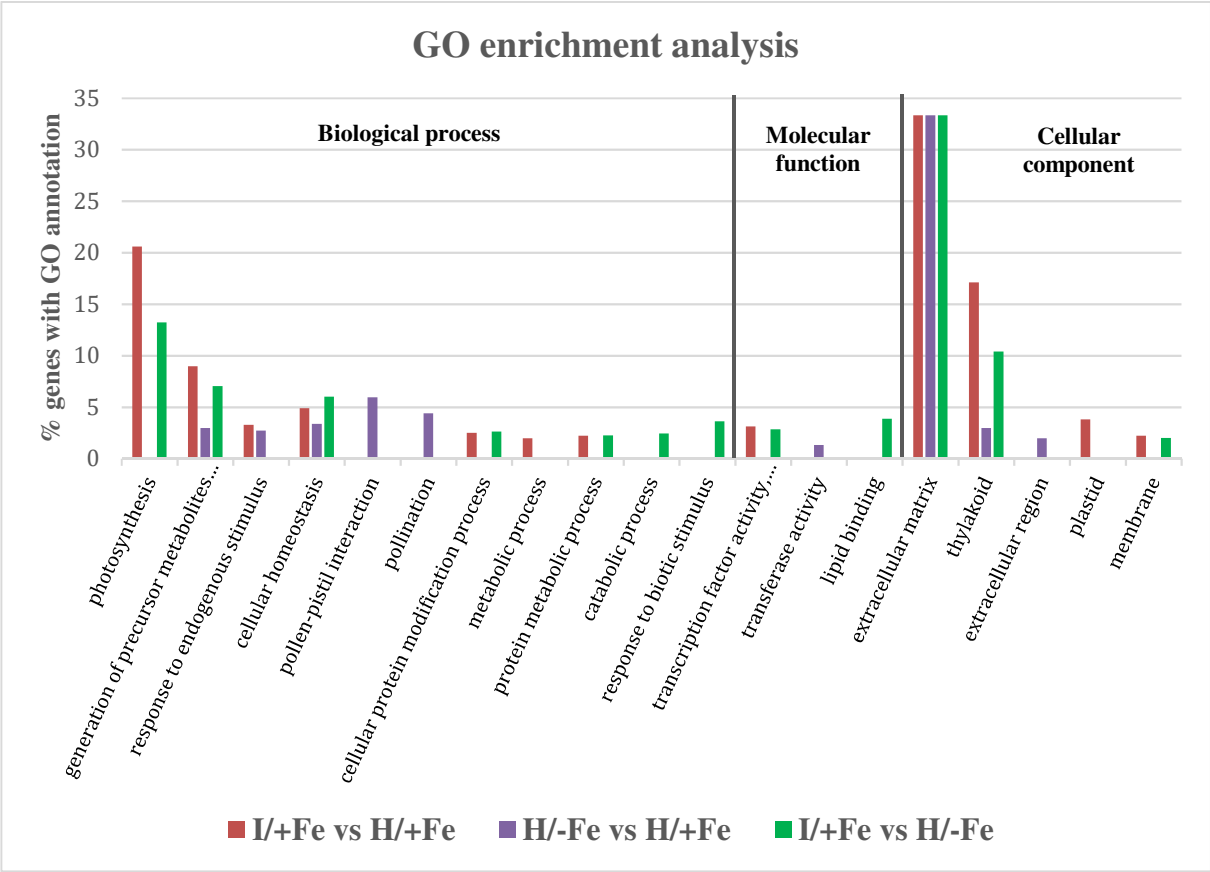

Figure 5. Gene Ontology Enrichment Analysis of differentially expressed genes (DEGs) in the three comparison groups. The y-axis indicates the percentage of significant DEGs corresponding to the total number of genes annotated in each GO categories (P<0.05). DEGs were grouped into three major functional categories: biological process, cellular component, and molecular function.

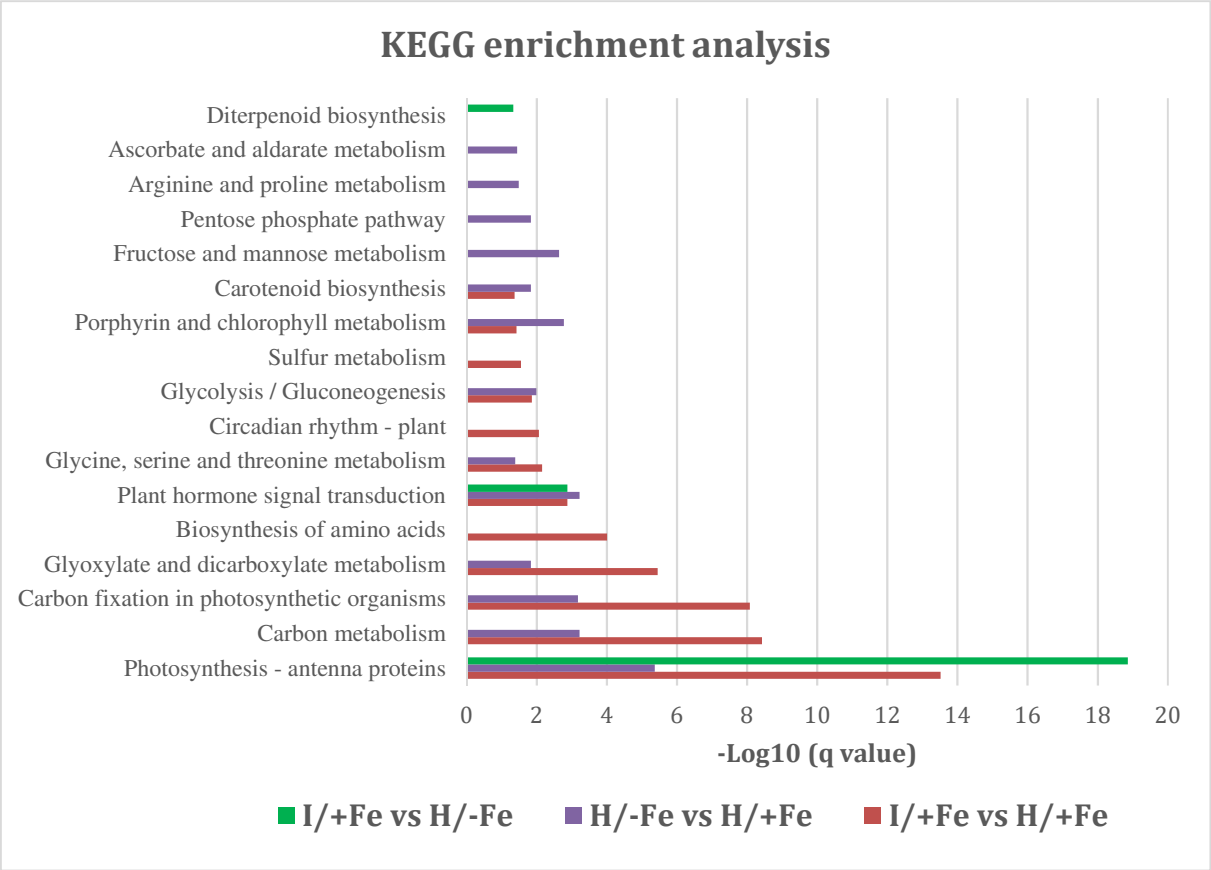

Figure 6. KEGG pathway enrichment analyses of differentially expressed genes (DEGs). X-axis indicates the value of -Log10 (q value).

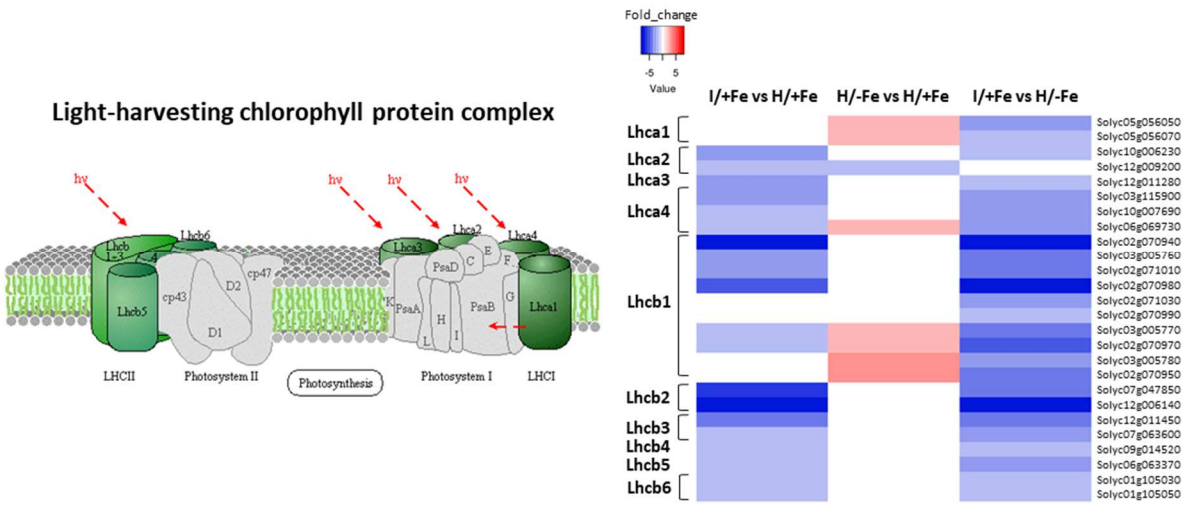

Figure 7. Heat map analysis showing the fold change of DEGs in the three comparison groups involved in antenna protein cluster (KEGG sly00196).

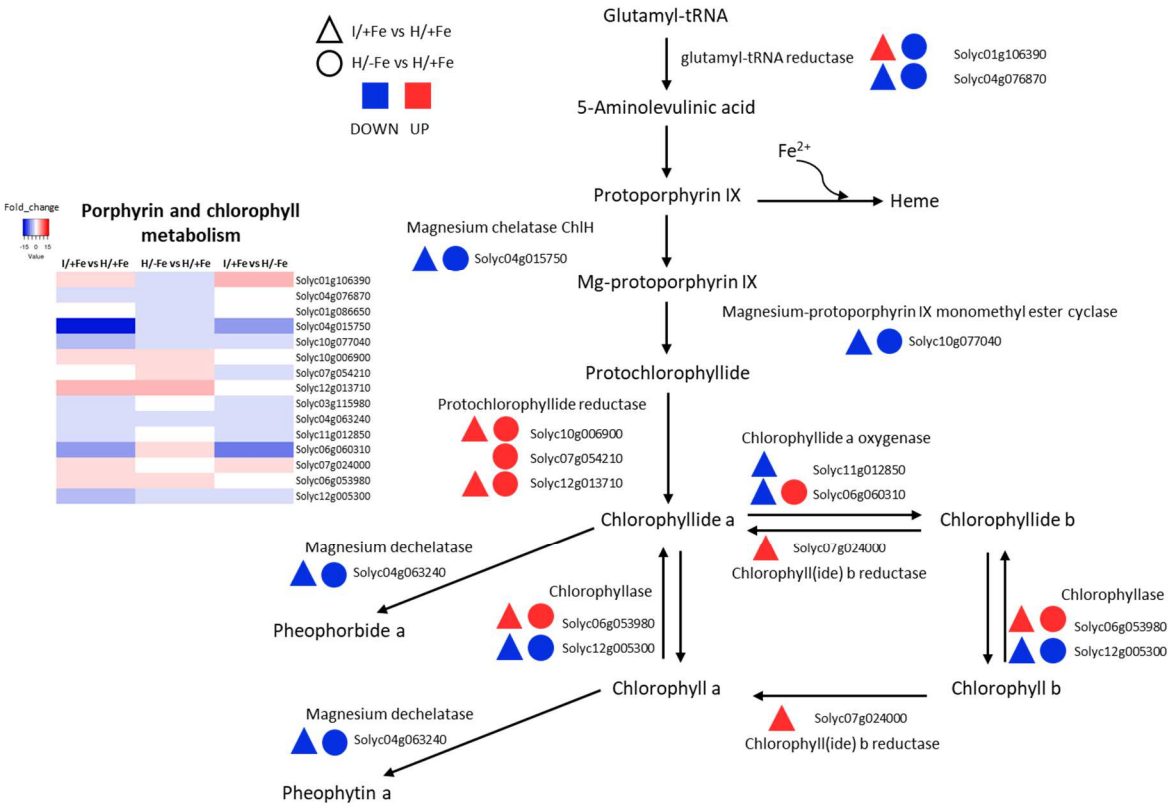

Figure 8. Heat map analysis showing the fold change of DEGs in the three comparison groups associated with porphyrin and chlorophyll metabolism (KEGG sly00860) with partial pathway representation.

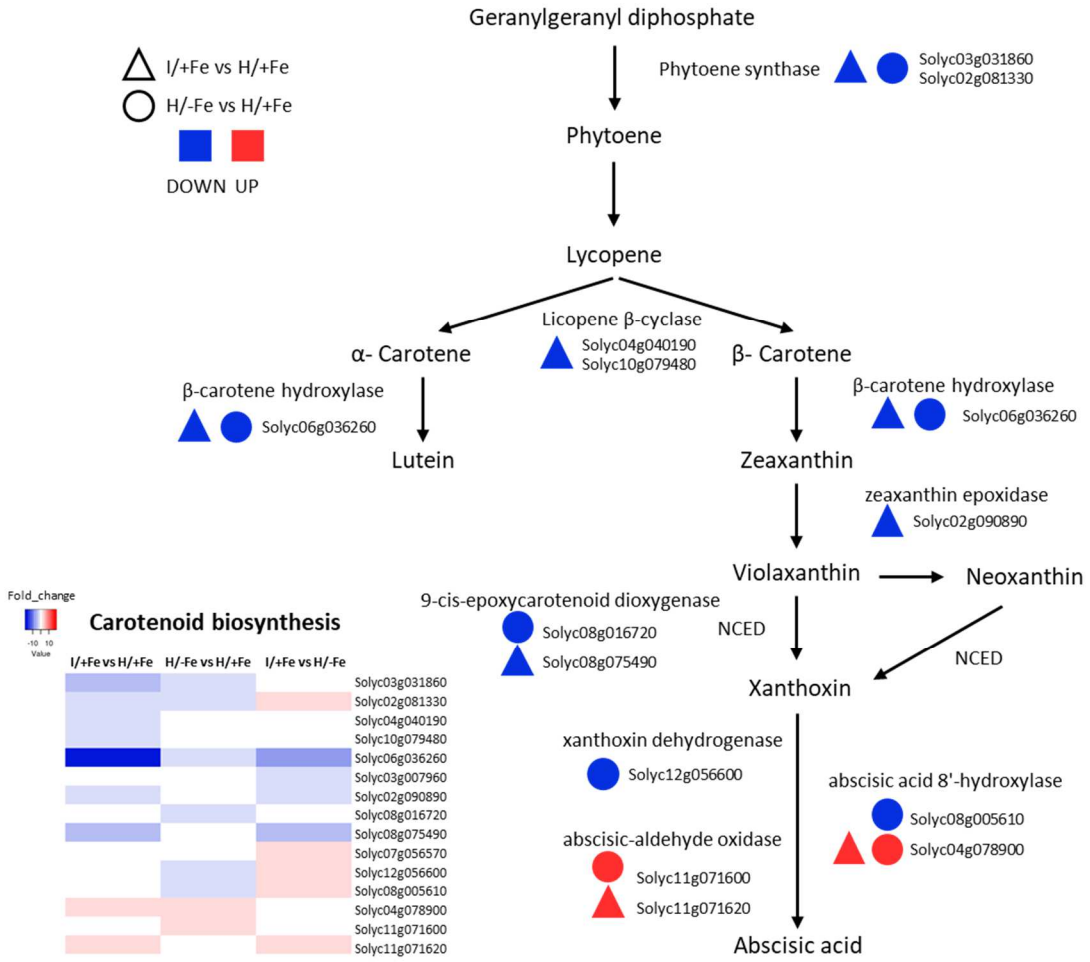

Figure 9. Heat map analysis showing the fold change of DEGs in the three comparison groups associated with carotenoid biosynthesis (KEGG sly00906) with partial pathway representation.

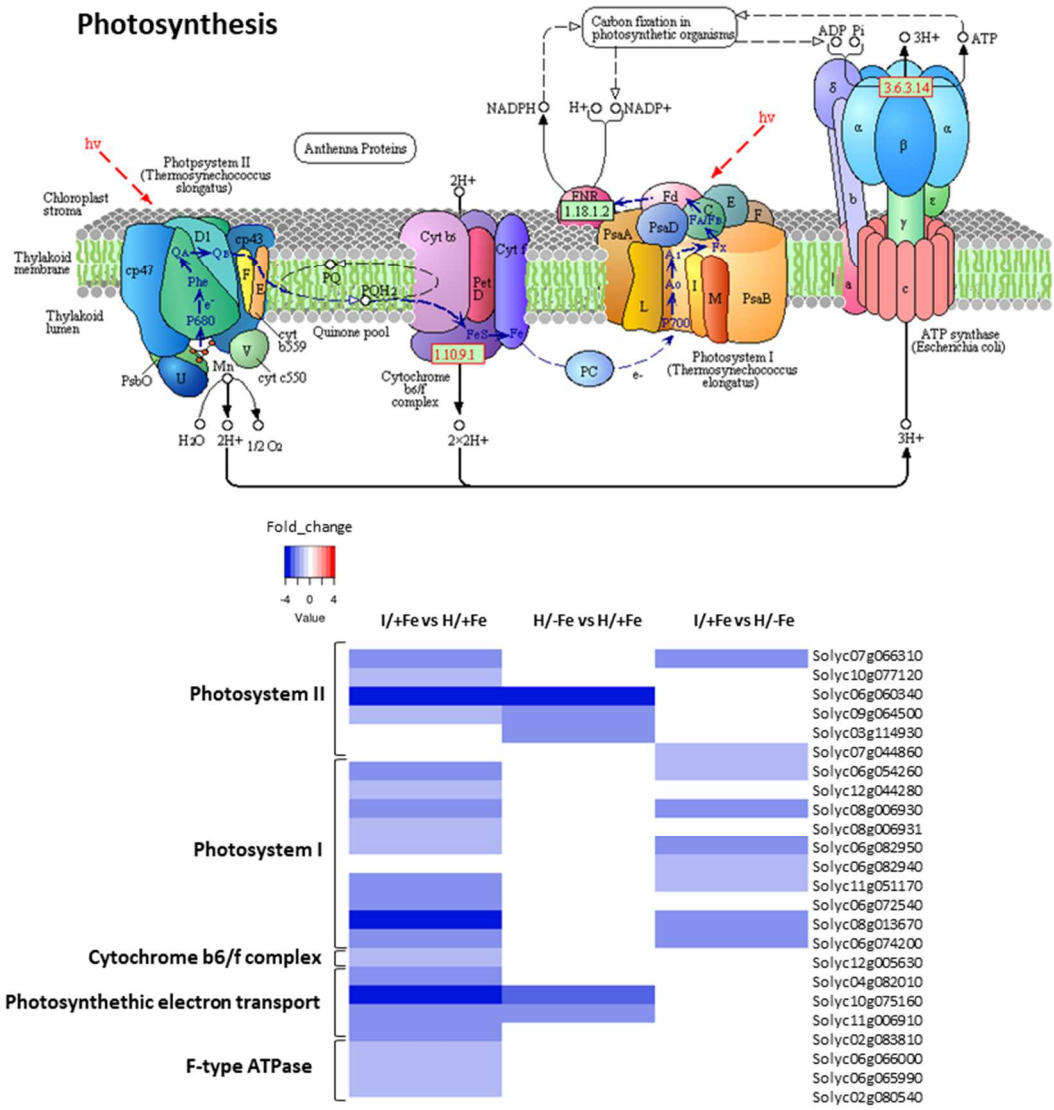

Figure 10. Heat map analysis showing the fold change of DEGs in the three comparison groups involved in photosynthesis-light reactions (KEGG sly00195).

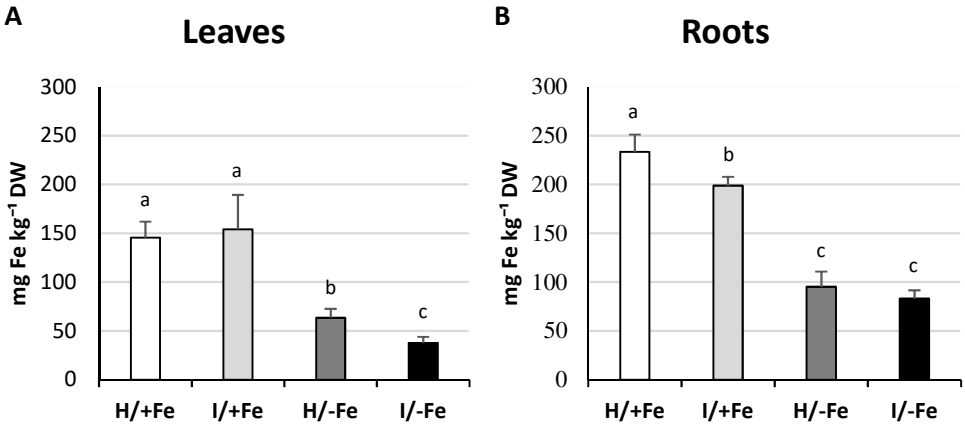

Figure 11. Effects of phytoplasma infection and Fe starvation on iron concentration in leaves and roots. Fe concentration in leaves (A) and roots (B) of H/+Fe, I/+Fe, H/-Fe, and I/-Fe tomato plants. Fe concentration was determined by ICP-OES. Results are expressed as mean ±SD (n= 6). DW: dry weight. Different letters indicate statistically significant differences ($P<0.05$) among conditions (one-way ANOVA followed by Holm-Sidak's test).

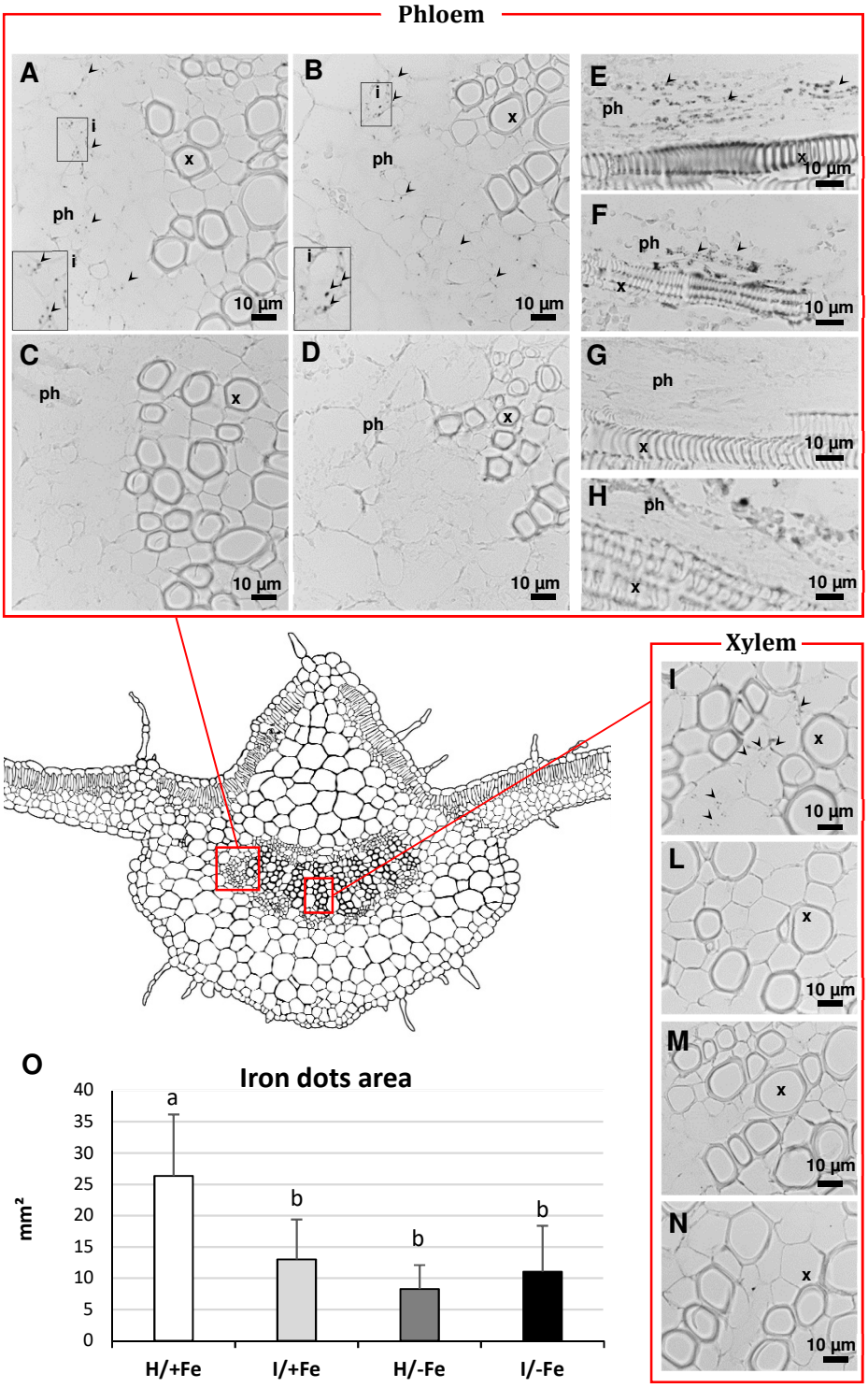

Figure 12. Effects of phytoplasma infection and Fe starvation on Fe distribution in leaf midrib. For Perls'-DAB staining: (A-D) transversal sections of leaf tissues in the phloem area, (E-H) longitudinal sections of leaf tissues in the phloem area, (I-N) transversal sections of the xylem area. (A, E, I): H/+Fe; (B, F, L): I/+Fe; (C, G, M): H/-Fe; (D, H, N): I/-Fe. ph: phloem; x: xylem; arrowheads indicate Fe dots. Scale bars: 10 µm. (O) Quantification of Fe dots in leaf lamina sections after Perls-DAB staining. Five randomly-selected 10x images per sample were captured, and Fe dots (diameter ranging from 1 to 5 µm) were selected and quantified with ImageJ 1.49m software. For each condition three samples were analysed. The results are expressed as the mean ±SD (n=15). Different letters indicate statistically significant differences ($P<0.05$) among the conditions (one-way ANOVA followed by Holm-Sidak's test).

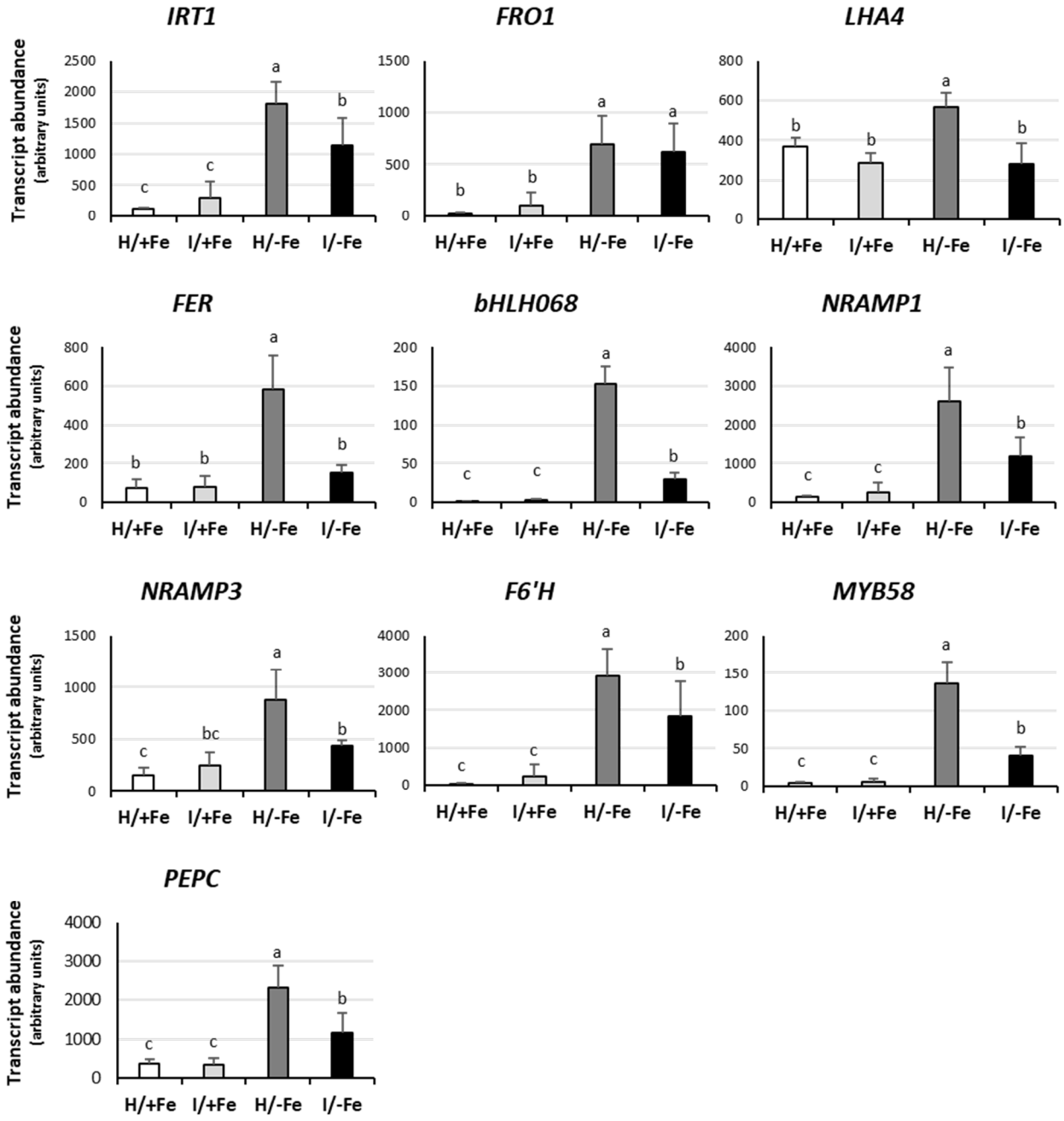

Figure 13. Expression analysis of Fe-related genes in tomato roots by real-time RT-PCR. The mean normalized expression (MNE) of each gene is plotted as the transcript abundance compared with the *UPL3* expression level (set at 100). Results are expressed as mean ±SD (n= 5). Different letters indicate statistically significant differences (P<0.05) among the conditions (one-way ANOVA followed by Holm-Sidak's test).

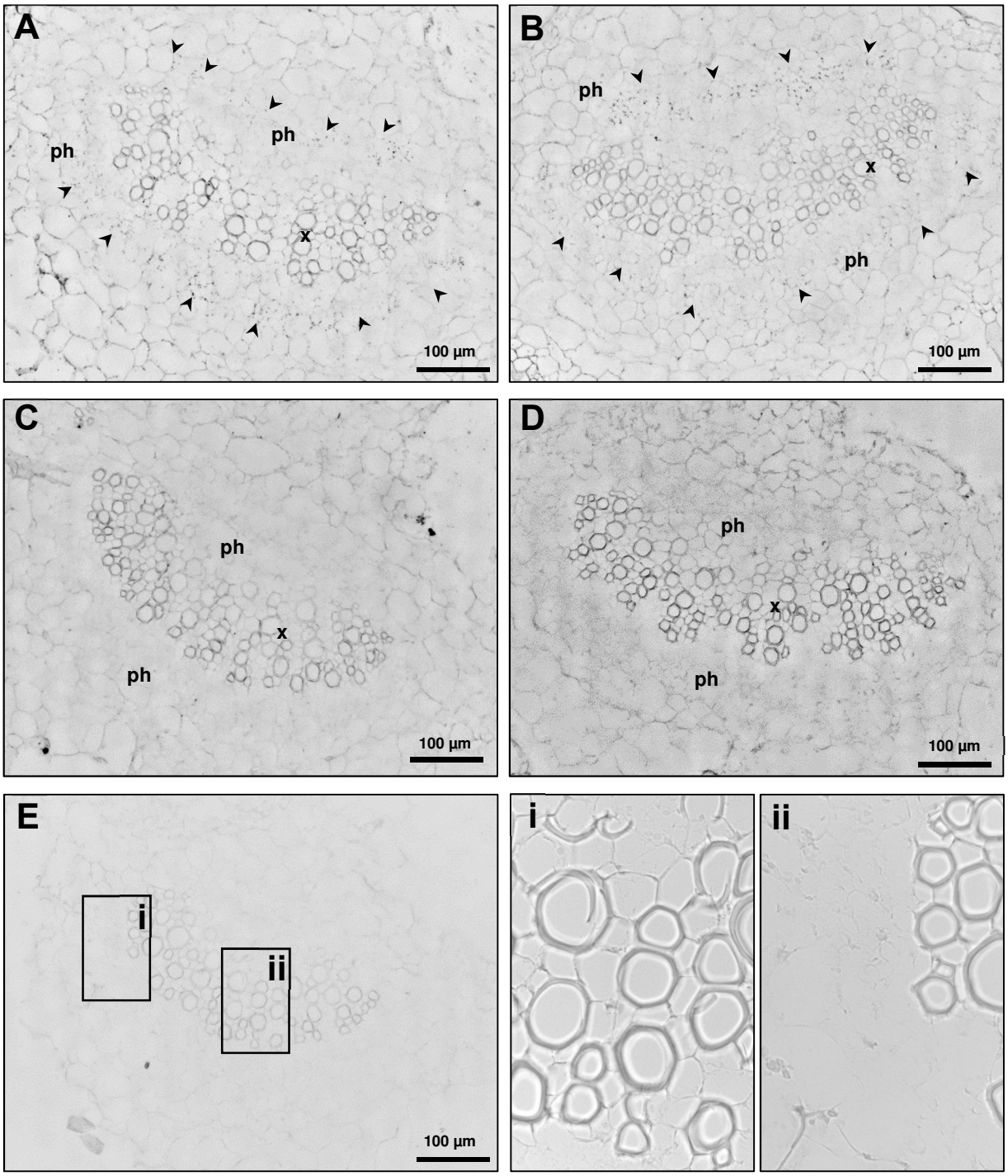

Supplemental Figure 1. Iron detection in tomato leaf midribs. Perls'-DAB staining on 7 µm-thick sections of leaf midribs in (A) H/+Fe, (B) I/+Fe, (C) H/-Fe, and (D) I/-Fe tomato plants. Small Fe dots are visible in H/+Fe and I/+Fe conditions in the phloem area (A, B). (E) Control sections with DAB without previous Perls reaction. ph: phloem; x: xylem; arrowheads indicate Fe dots. Scale bars: 100 µm.

H/+Fe **I/+Fe** **H/-Fe** **I/-Fe**

Supplemental Figure 2 Qualitative visualization of Fe(III) reduction activity along lateral tomato roots.

Roots were placed in 1% agarose containing 0.2 mM $CaSO_4$, 5 mM Mes buffer (pH 5.5), 0.1 mM Fe(III)-EDTA and 0.3 mM Na_2-bathophenanthrolinedisulfonic acid (BPDS). The reddish coloration, corresponding to Fe(II)-BPDS complex, revealed the regions of Fe(III) reduction only in H/-Fe and I/-Fe roots. Gel shown is representative of five independent experiments. For each condition, H/+Fe, I/+Fe, H/-Fe, and I/-Fe, five plants were examined, using two lateral roots (n= 5).

4.8. Supplemental table

Supplemental Table 1. List of primers and accession number of sequences used for housekeeping individuation.

Gene	Forward primer 5'-3'	Reverse primer 5'-3'	NCBI ID	SGN Gene ID
UPL3*	TGTGAGGACTGGAATTGGGC	CAAGCGTCTCAGCCTTCCAT	XM_004230989.3 XM_010317077.2 101264868	Solyc10g055450
EF-1	GAGGCAAACTGTTGCTGTGG	TCCGTGCTCATCAAATGCA	XM_004240531.3 101244084	Solyc06g009970
ACT-7 like	TAGCACCTTCCAGCAGATGT	CAGCAGACCCGAGTTCACTT	NM_001321306.1 101262163	Solyc11g005330
TUB	TCCAAGTTTTGGTGACTTGAACC	ACAGCCAATTTCCTCAGGTCT	NM_001247878.2 778227	Solyc04g081490

*This primer pair amplifies every gene transcript variant.

Supplemental Table 2. Gene and primer sequences for root expression analysis and RNA-seq validation.

Gene	Forward primer 5'-3'	Reverse primer 5'-3'	NCBI Gene ID	SGN Gene ID
IRT1	GGGCTATCACTAGGTGCGTC	ATACTCCGCCTGTAGGATGC	543597	Solyc02g069200
FER	CAAAGGGCGACACATTGCAG	TCTCTCACATAAAGAGTGAAGGTGA	543705	Solyc06g051550
bHLH068	TGCAAGTGTAGAGGAAGATGGA	TCAATTGGTCCTTGCATCTGA	101258211	Solyc10g079680
LHA4	GCTTTGATTTTCGTGACCCGT	TGGCAACCAATTGGGCAATCA	101263827	Solyc07g017780
FRO1	AAGGGTGAAGGAAGTTGGTCC	ATCATGCCTTAGAAAATGTGTGGAA	543871	Solyc01g094910
F6'H1	AGGAAATGGCTTTGGAATGGA	TCAAGAGCCACATCCTTGCAT	101262174	Solyc11g045520
NRAMP1	TGGCCAATTTATCATGCAAGGATT	GCTCCTGACGATCCTCCAAT	543868	Solyc11g018530
NRAMP3	TTTTGCCCTGATCCCCCTTC	GCTACTAGCCATGATATCACCTTCA	544257	Solyc02g092800
MYB58	AGCTGGGTTATTGAGGTGTGG	GGTGTCTTCTTCTTGTGGGG	104649494	Solyc10g005550
PEPC	GACCCGGGTATTGCAGCTC	CCAGCAATCTGGAGAAGGAGG	101261166	Solyc10g007290
ERF017	TTTTTCCGGGGTTCGATGACT	GGTGATGGTTGTGGTGACGA	101253257	Solyc12g009240
PECTINESTERASE	CCTCTACGTCCACTCACTTCG	GAACAACAGCTGCATTACCAAAAA	101260941	Solyc06g009190
REVEILLE8	CCCGGACTTTGAACCCATTAAAAA	ACCACCTGTAGGAAGACCGA	101253545	Solyc10g084370
FRO6	CAGCCTTCATTGGAGGAGGG	ACATCCTTTGAAGCCAGGGG	101246763	Solyc01g102610
JAR1*	GCAAATTCTCCAGTCGGCCT	ACGATATAAACCTGCGAAATTGGT	101262053	Solyc10g011660
Ferritin-1	AACGTCCATGCTGTAGCCTC	CCATGTCCTTGGCCAACTCT	104647958	Solyc06g050980
ChlH	GAACCTCAGGAAGGATGGCA	ACAACGTACGTACCTGAGCA	101244176	Solyc04g015750
CHLN	TGCTCTGGAGGAGTGAGTGA	AGACACACAAATAGGACACACTGA	101248619	Solyc01g100490
OPT3	GTGGGGCTTGTTGTTTGCAT	TGTCATATCCGGGTTGCTGATT	101265194	Solyc11g012700

*This primer pair amplifies every gene transcript variant.

Supplemental Table 3. Experimental validation of a subset of genes regulated by phytoplasma-infection and/or Fe-starvation. Shown are the log2 fold-change values from RNA-seq and qRT-PCR for each gene in the three comparisons: phytoplasma-infected versus healthy Fe-sufficient plants (I/+Fe vs H/+Fe), healthy Fe-starved versus Fe-sufficient (H/-Fe vs H/+Fe) and phytoplasma-infected Fe-sufficient versus Fe-starved plants (I/+Fe vs H/-Fe).

			LOG_2(FOLD-CHANGE)	
GENE	**DESCRIPTION**	**COMPARISON**	**RNA-seq**	**qRT-PCR**
Solyc12g009240	Ethylene-responsive transcription factor 17 (*ERF017*)	I/+Fe vs H/+Fe	3,49	3,51
		H/-Fe vs H/+Fe	1,23	1,15
		I/+Fe vs H/-Fe	2,27	2,36
Solyc06g009190	Pectinesterase	I/+Fe vs H/+Fe	2,77	2,46
		H/-Fe vs H/+Fe	0,77	0,30
		I/+Fe vs H/-Fe	2,00	2,16
Solyc10g084370	MYB transcription factor (*REVEILLE 8*)	I/+Fe vs H/+Fe	-8,27	-8,22
		H/-Fe vs H/+Fe	-2,10	-2,02
		I/+Fe vs H/-Fe	-6,17	-6,19
Solyc01g102610	Ferric reduction oxidase 6 (*FRO6*)	I/+Fe vs H/+Fe	-5,41	-5,12
		H/-Fe vs H/+Fe	-2,45	-2,20
		I/+Fe vs H/-Fe	-2,96	-2,92
Solyc10g011660	Jasmonic acid-amido synthetase (*JAR1*)	I/+Fe vs H/+Fe	0,03	-0,29
		H/-Fe vs H/+Fe	0,81	0,56
		I/+Fe vs H/-Fe	-0,78	-0,85
Solyc02g092800	*NRAMP3*	I/+Fe vs H/+Fe	0,27	-0,16
		H/-Fe vs H/+Fe	1,00	0,73
		I/+Fe vs H/-Fe	-0,73	-0,90
Solyc06g050980	Ferritin-1	I/+Fe vs H/+Fe	-0,20	-1,69
		H/-Fe vs H/+Fe	-2,81	-2,62
		I/+Fe vs H/-Fe	2,61	0,93
Solyc04g015750	Magnesium chelatase H subunit (*ChlH*)	I/+Fe vs H/+Fe	-4,07	-5,10
		H/-Fe vs H/+Fe	-1,20	-0,89
		I/+Fe vs H/-Fe	-2,86	-4,21
Solyc01g100490	Nicotianamine synthase-like (*CHLN*)	I/+Fe vs H/+Fe	-1,39	-1,12
		H/-Fe vs H/+Fe	-2,33	-1,90
		I/+Fe vs H/-Fe	0,94	0,78
Solyc11g012700	Oligopeptide transporter 3 (*OPT3*)	I/+Fe vs H/+Fe	-0,22	-0,19
		H/-Fe vs H/+Fe	2,25	2,36
		I/+Fe vs H/-Fe	-2,47	-2,55

Supplemental Table 4. Genes associated with Photosynthesis-Antenna Proteins KEGG pathway (00196) in all pairwise comparisons.

In the I versus H (+Fe) comparison, fold-change is the ratio of I/+Fe FPKM on H/+Fe FPKM; similarly, in the comparison -Fe versus +Fe (H), fold-change is the ratio of H/-Fe FPKM on H/+Fe FPKM, and in I/+Fe versus H/-Fe the ratio is calculated as I/+Fe FPKM on H/-Fe FPKM.

Lhca: Light-harvesting chlorophyll protein complexes associated to the Photosystem I. Lhcb: Light-harvesting chlorophyll protein complexes associated to the Photosystem II. In bold, DEGs specific for the indicated pairwise comparison. Contra-regulated genes in Infected and Fe deficient samples are underlined. In bold italic, one Gene ID that NCBI associates to different genes annotated in the Solgenomics ITAG3.0 assembly. Total FPKM corresponds to the sum of FPKM expression of the corresponding gene in the two compared conditions.

Ortholog group	Gene Name	NCBI Gene ID	Fold-change	direction	Total FPKM
I/+Fe versus H/+Fe					
Lhca2	**Solyc10g006230**	101264376	3.2	DOWN	1097.3
Lhca2	Solyc12g009200	101252151	2.2	DOWN	35.3
Lhca3	**Solyc12g011280**	101265617	3.2	DOWN	105.5
Lhca4	**Solyc10g007690**	101253628	2.6	DOWN	1228.4
Lhca4	**Solyc03g115900**	101268669	2.7	DOWN	328.0
Lhca4	Solyc06g069730	101256006	2.0	DOWN	13.7
Lhcb1	**Solyc02g070940**	***101264784***	8.1	DOWN	921.9
Lhcb1	**Solyc03g005760**	101267774	2.7	DOWN	885.6
Lhcb1	**Solyc02g071010**	***101264784***	2.7	DOWN	670.1
Lhcb1	Solyc02g070970	***101264784***	2.3	DOWN	205.7
Lhcb1	Solyc03g005770	101245729	2.4	DOWN	134.1
Lhcb1	**Solyc02g070980**	104645884	5.5	DOWN	72.9
Lhcb2	**Solyc07g047850**	543975	6.0	DOWN	781.1
Lhcb2	**Solyc12g006140**	543976	7.1	DOWN	249.7
Lhcb3	**Solyc12g011450**	101243766	3.9	DOWN	740.0
Lhcb3	**Solyc07g063600**	101268123	2.0	DOWN	269.9
Lhcb4	**Solyc09g014520**	101249002	2.4	DOWN	1076.2
Lhcb5	**Solyc06g063370**	101266527	2.6	DOWN	645.4
Lhcb6	**Solyc01g105030**	101256629	2.3	DOWN	364.8
Lhcb6	**Solyc01g105050**	101256131	2.2	DOWN	87.4
H/-Fe versus H/+Fe					
Lhca1	**Solyc05g056070**	544310	1.9	UP	907.3
Lhca1	**Solyc05g056050**	101253380	1.9	UP	219.3
Lhca2	Solyc12g009200	101252151	2.1	DOWN	35.7
Lhca4	Solyc06g069730	101256006	1.9	UP	26.3
Lhcb1	Solyc02g070970	***101264784***	2.5	UP	499.4
Lhcb1	Solyc03g005770	101245729	1.7	UP	254.2
Lhcb1	**Solyc03g005780**	108491835	3.0	UP	246.5
Lhcb1	**Solyc02g070950**	***101264784***	3.2	UP	221.4
I/+Fe versus H/-Fe					
Lhca1	Solyc05g056070	544310	2.4	DOWN	844.6
Lhca1	Solyc05g056050	101253380	2.7	DOWN	195.6

Lhca2	Solyc10g006230	101264376	2.6	DOWN	950.9
Lhca3	Solyc12g011280	101265617	2.5	DOWN	88.3
Lhca4	Solyc10g007690	101253628	3.1	DOWN	1403.4
Lhca4	Solyc03g115900	101268669	3.8	DOWN	425.8
Lhca4	Solyc06g069730	101256006	3.7	DOWN	21.7
Lhcb1	**Solyc02g071030**	***101264784***	3.2	DOWN	1823.1
Lhcb1	Solyc03g005760	101267774	4.8	DOWN	1392.0
Lhcb1	Solyc02g071010	***101264784***	4.3	DOWN	956.9
Lhcb1	Solyc02g070940	***101264784***	7.2	DOWN	825.2
Lhcb1	Solyc02g070970	***101264784***	5.7	DOWN	417.6
Lhcb1	Solyc03g005780	108491835	3.4	DOWN	239.6
Lhcb1	Solyc02g070950	***101264784***	4.2	DOWN	208.7
Lhcb1	Solyc03g005770	101245729	4.0	DOWN	199.3
Lhcb1	Solyc02g070980	104645884	7.1	DOWN	90.2
Lhcb1	**Solyc02g070990**	101266182	2.0	DOWN	64.5
Lhcb2	Solyc07g047850	543975	4.7	DOWN	630.7
Lhcb2	Solyc12g006140	543976	7.4	DOWN	258.7
Lhcb3	Solyc12g011450	101243766	4.7	DOWN	857.4
Lhcb3	Solyc07g063600	101268123	2.9	DOWN	351.0
Lhcb4	Solyc09g014520	101249002	2.0	DOWN	931.2
Lhcb5	Solyc06g063370	101266527	2.7	DOWN	669.9
Lhcb6	Solyc01g105030	101256629	2.4	DOWN	379.9
Lhcb6	Solyc01g105050	101256131	2.2	DOWN	87.8

Supplemental Table 5. Genes associated with 'Porphyrin and chlorophyll metabolism' KEGG pathway (00860) in all pairwise comparisons.
In the I/+Fe versus H/+Fe comparison, fold-change is the ratio of I/+Fe FPKM on H/+Fe FPKM; similarly, in the comparison H/-Fe versus H/+Fe, fold-change is the ratio of H/-Fe FPKM on H/+Fe FPKM, and in I/+Fe versus H/-Fe the ratio is calculated as I/+Fe FPKM on H/-Fe FPKM.
Total FPKM corresponds to the sum of FPKM expression of the corresponding gene in the two compared conditions.
In bold, DEGs specific for the indicated pairwise comparison. Contra-regulated genes in Infected and Fe deficient samples are underlined.

Gene Name	NCBI Gene ID	Gene description KEGG | NCBI RefSeq	Fold-change	direction	Total FPKM
I/+Fe versus H/+Fe					
Solyc10g077040	101257518	magnesium-protoporphyrin IX monomethyl ester (oxidative) cyclase [EC:1.14.13.81] | at103; putative magnesium-protoporphyrin monomethyl ester cyclase	4.7	DOWN	258.2
Solyc04g015750	101244176	magnesium chelatase subunit H [EC:6.6.1.1] | magnesium-chelatase subunit ChlH, chloroplastic	16.7	DOWN	221.7
Solyc04g076870	101266935	glutamyl-tRNA reductase [EC:1.2.1.70] | glutamyl-tRNA reductase 1, chloroplastic	2.0	DOWN	156.2
Solyc03g115980	101262299	geranylgeranyl diphosphate/geranylgeranyl-bacteriochlorophyllide a reductase [EC:1.3.1.83 1.3]	2.7	DOWN	140.8
Solyc04g063240	101252980	magnesium dechelatase [EC:4.99.1.10] | protein STAY-GREEN LIKE, chloroplastic	3.2	DOWN	71.3
Solyc11g012850	101244441	chlorophyllide a oxygenase [EC:1.14.13.122] | chlorophyllide a oxygenase, chloroplastic	2.6	DOWN	31.8
Solyc06g060310	101261422	chlorophyllide a oxygenase [EC:1.14.13.122] | chlorophyllide a oxygenase, chloroplastic	5.6	DOWN	20.6
Solyc12g005300	101263579	chlorophyllase [EC:3.1.1.14] | chlorophyllase-2, chloroplastic	3.7	DOWN	19.8
Solyc07g024000	101258872	chlorophyll(ide) b reductase [EC:1.1.1.294] | probable chlorophyll(ide) b reductase	1.7	UP	94.4
Solyc12g013710	101248079	protochlorophyllide reductase [EC:1.3.1.33] | protochlorophyllide reductase-like	3.6	UP	92.8

Solyc01g106390	101252440	glutamyl-tRNA reductase [EC:1.2.1.70] | glutamyl-tRNA reductase 1, chloroplastic-like	1.9	UP	62.9
Solyc10g006900	101244717	protochlorophyllide reductase [EC:1.3.1.33] | light dependent NADH:protochlorophyllide	2.4	UP	53.2
Solyc06g053980	101258376	chlorophyllase [EC:3.1.1.14] | chlorophyllase-2, chloroplastic-like	2.9	UP	41.6
H/-Fe versus H/+Fe					
Solyc10g077040	101257518	magnesium-protoporphyrin IX monomethyl ester (oxidative) cyclase [EC:1.14.13.81] | at103, putative magnesium-protoporphyrin monomethyl ester cyclase	1.9	DOWN	328.5
Solyc04g015750	101244176	magnesium chelatase subunit H [EC:6.6.1.1] | magnesium-chelatase subunit ChlH, chlor	2.3	DOWN	299.9
Solyc04g076870	101266935	glutamyl-tRNA reductase [EC:1.2.1.70] | glutamyl-tRNA reductase 1, chloroplastic	2.0	DOWN	157.4
Solyc04g063240	101252980	magnesium dechelatase [EC:4.99.1.10] | protein STAY-GREEN LIKE, chloroplastic	1.9	DOWN	82.5
Solyc01g106390	101252440	glutamyl-tRNA reductase [EC:1.2.1.70] | glutamyl-tRNA reductase 1, chloroplastic-like	2.3	DOWN	30.8
Solyc12g005300	101263579	chlorophyllase [EC:3.1.1.14] | chlorophyllase-2, chloroplastic	1.8	DOWN	24.0
Solyc01g086650	101261158	uroporphyrin-III C-methyltransferase [EC:2.1.1.107] | siroheme synthase	1.8	DOWN	10.2
Solyc07g054210	543647	protochlorophyllide reductase [EC:1.3.1.33] | POR2; protochlorophyllide reductase	1.8	UP	148.9
Solyc12g013710	101248079	protochlorophyllide reductase [EC:1.3.1.33] | protochlorophyllide reductase-like	4.5	UP	110.4
Solyc10g006900	101244717	protochlorophyllide reductase [EC:1.3.1.33] | light dependent NADH:protochlorophyllide	3.3	UP	66.6
Solyc06g060310	101261422	chlorophyllide a oxygenase [EC:1.14.13.122] | chlorophyllide a oxygenase, chloroplas	1.8	UP	47.9

Solyc06g053980	101258376	chlorophyllase [EC:3.1.1.14] | chlorophyllase-2, chloroplastic-like	2.8	UP	40.8
I/+Fe versus H/-Fe					
Solyc10g077040	101257518	magnesium-protoporphyrin IX monomethyl ester (oxidative) cyclase [EC:1.14.13.81] | at103, putative magnesium-protoporphyrin monomethyl ester cyclase	2.6	DOWN	160.6
Solyc07g054210	543647	protochlorophyllide reductase [EC:1.3.1.33] | POR2; protochlorophyllide reductase	1.9	DOWN	144.8
Solyc03g115980	101262299	geranylgeranyl diphosphate/geranylgeranyl-bacteriochlorophyllide a reductase [EC:1.3.1.83 1.3	2.5	DOWN	135.7
Solyc04g015750	101244176	magnesium chelatase subunit H [EC:6.6.1.1] | magnesium-chelatase subunit ChlH, chlor	7.3	DOWN	103.2
Solyc04g063240	101252980	magnesium dechelatase [EC:4.99.1.10] | protein STAY-GREEN LIKE, chloroplastic	1.7	DOWN	45.2
Solyc06g060310	101261422	chlorophyllide a oxygenase [EC:1.14.13.122] | chlorophyllide a oxygenase, chloroplast	9.8	DOWN	33.6
Solyc11g012850	101244441	chlorophyllide a oxygenase [EC:1.14.13.122] | chlorophyllide a oxygenase, chloroplastic	2.0	DOWN	26.4
Solyc12g005300	101263579	chlorophyllase [EC:3.1.1.14] | chlorophyllase-2, chloroplastic	2.0	DOWN	12.7
Solyc07g024000	101258872	chlorophyll(ide) b reductase [EC:1.1.1.294] | probable chlorophyll(ide) b reductase	1.8	UP	93.7
Solyc01g106390	101252440	glutamyl-tRNA reductase [EC:1.2.1.70] | glutamyl-tRNA reductase 1, chloroplastic-like	4.5	UP	50.5

Supplemental Table 6. Genes associated with Carotenoid Biosynthesis KEGG pathway (00906) in the pairwise comparisons.
In the I/+Fe versus H/+Fe comparison, fold-change is the ratio of I/+Fe FPKM on H/+Fe FPKM; similarly, in the comparison H/-Fe versus H/+Fe, fold-change is the ratio of H/-Fe FPKM on H/+Fe FPKM, and in I/+Fe versus H/-Fe the ratio is calculated as I/+Fe FPKM on H/-Fe FPKM.
Total FPKM corresponds to the sum of FPKM expression of the corresponding gene in the two compared conditions. In bold, DEGs specific for the indicated pairwise comparison.

Gene Name	NCBI Gene ID	Gene description KEGG | NCBI RefSeq	Fold-change	direction	Total FPKM
I/+Fe versus H/+Fe					
Solyc08g075490	101250535	9-cis-epoxycarotenoid dioxygenase [EC:1.13.11.51] | probable carotenoid cleavage dioxygenase	4.7	DOWN	191.9
Solyc02g090890	544162	zeaxanthin epoxidase [EC:1.14.15.21] | ZEP, ZE; zeaxanthin epoxidase, chloroplastic	3.0	DOWN	101.0
Solyc04g040190	544104	lycopene beta-cyclase [EC:5.5.1.19] | LCY1, CrtL-1, LCY-B; lycopene beta-cyclase	3.6	DOWN	68.5
Solyc06g036260	544133	beta-carotene 3-hydroxylase [EC:1.14.15.24] | CrtR-b1; beta-carotene hydroxylase	19.2	DOWN	64.9
Solyc03g031860	543988	15-cis-phytoene synthase [EC:2.5.1.32] | Psy1, GTOM5, psy; phytoene synthase 1, chloroplastic	5.2	DOWN	33.2
Solyc02g081330	543964	15-cis-phytoene synthase [EC:2.5.1.32] | PSY2; phytoene synthase 2, chloroplastic	1.6	DOWN	28.1
Solyc10g079480	101267662	lycopene beta-cyclase [EC:5.5.1.19] | lycopene beta cyclase, chloroplastic	1.9	DOWN	21.4
Solyc04g078900	100136887	(+)-abscisic acid 8'-hydroxylase [EC:1.14.14.137] | CYP707A1; ABA 8'-hydroxylase	2.0	UP	110.6
Solyc11g071620	543650	abscisic-aldehyde oxidase [EC:1.2.3.14] | AO1, TAO1; aldehyde oxidase	1.7	UP	29.2

H/-Fe versus H/+Fe					
Solyc06g036260	544133	beta-carotene 3-hydroxylase [EC:1.14.15.24] | CrtR-b1; beta-carotene hydroxylase	2.8	DOWN	83.8
Solyc08g005610	101249565	(+)-abscisic acid 8'-hydroxylase [EC:1.14.14.137] | CYP707A2; abscisic acid 8'-hydroxylase	2.3	DOWN	46.1
Solyc03g031860	543988	15-cis-phytoene synthase [EC:2.5.1.32] | Psy1, GTOM5, psy; phytoene synthase 1, chloroplastic	3.6	DOWN	35.5
Solyc02g081330	543964	15-cis-phytoene synthase [EC:2.5.1.32] | PSY2; phytoene synthase 2, chloroplastic	3.0	DOWN	23.2
Solyc12g056600	100750250	xanthoxin dehydrogenase [EC:1.1.1.288] | SlscADH1; short-chain dehydrogenase-reductase	2.6	DOWN	4.2
Solyc08g016720	100316877	9-cis-epoxycarotenoid dioxygenase [EC:1.13.11.51] | NCED2; 9-cis-epoxycarotenoid dioxygenase	2.1	DOWN	2.7
Solyc04g078900	100136887	(+)-abscisic acid 8'-hydroxylase [EC:1.14.14.137] | CYP707A1; ABA 8'-hydroxylase	1.6	UP	96.5
Solyc11g071600	543652	abscisic-aldehyde oxidase [EC:1.2.3.14] | TAO3, AO3; aldehyde oxidase	1.7	UP	18.7

I/+Fe versus H/-Fe					
Solyc08g075490	101250535	9-cis-epoxycarotenoid dioxygenase [EC:1.13.11.51] | probable carotenoid cleavage dioxygenase	4.9	DOWN	198.7
Solyc02g090890	544162	zeaxanthin epoxidase [EC:1.14.15.21] | ZEP, ZE; zeaxanthin epoxidase, chloroplastic	3.2	DOWN	106.5
Solyc06g036260	544133	beta-carotene 3-hydroxylase [EC:1.14.15.24] | CrtR-b1; beta-carotene hydroxylase	6.9	DOWN	25.3
Solyc03g007960	544297	beta-carotene 3-hydroxylase [EC:1.14.15.24] | CrtR-b2; beta-carotene hydroxylase	2.1	DOWN	17.7
Solyc08g005610	101249565	(+)-abscisic acid 8'-hydroxylase [EC:1.14.14.137] | CYP707A2; abscisic acid 8'-hydroxylase	3.4	UP	60.8
Solyc11g071620	543650	abscisic-aldehyde oxidase [EC:1.2.3.14] | AO1, TAO1; aldehyde oxidase	1.8	UP	28.8
Solyc07g056570	544163	9-cis-epoxycarotenoid dioxygenase [EC:1.13.11.51] | LeNCED1; nine-cis-epoxycarotenoid dioxygenase	1.8	UP	24.1
Solyc02g081330	543964	15-cis-phytoene synthase [EC:2.5.1.32] | PSY2; phytoene synthase 2, chloroplastic	1.8	UP	16.4
Solyc12g056600	100750250	xanthoxin dehydrogenase [EC:1.1.1.288] | SlscADH1;short-chain dehydrogenase-reductase	3.8	UP	5.7

Supplemental Table 7. Genes associated with Photosynthesis-light reactions KEGG pathway (00195) in all pairwise comparisons.
In the I/+Fe versus H/+Fe comparison, fold-change is the ratio of I/+Fe FPKM on H/+Fe FPKM; similarly, in the comparison H/-Fe versus H/+Fe, fold-change corresponds to the ratio of H/-Fe FPKM on H/+Fe FPKM, and in I/+Fe versus H/-Fe the ratio is calculated as I/+Fe FPKM on H/-Fe FPKM. Total FPKM corresponds to the sum of FPKM expression of the corresponding gene in the two compared conditions. In bold, DEGs specific for the indicated pairwise comparison.

Gene Name	NCBI Gene ID	Gene description KEGG | NCBI RefSeq	Fold-change	direction	Total FPKM
I/+Fe versus H/+Fe					
Solyc07g066310	778297	photosystem II 10kDa protein | PSBR; PSII polypeptide	2.0	DOWN	8353.3
Solyc11g051170	101265249	photosystem I subunit XI | photosystem I reaction center subunit XI, chloroplastic	1.9	DOWN	5134.8
Solyc06g072540	101268297	photosystem I subunit PsaN | photosystem I reaction center subunit	2.3	DOWN	4944.3
Solyc04g082010	544053	plastocyanin | PETE; plastocyanin, chloroplastic	1.9	DOWN	1296.6
Solyc06g054260	543978	photosystem I subunit II | PSI-D, psaD; photosystem I reaction center subunit II, chloroplastic	1.9	DOWN	1279.6
Solyc08g006930	101255222	photosystem I subunit X | photosystem I reaction center subunit psaK, chloroplastic	2.5	DOWN	1071.9
Solyc06g074200	101254806	photosystem I subunit PsaO | photosystem I subunit O	2.0	DOWN	1070.0
Solyc10g077120	101259494	photosystem II PsbY protein | photosystem II core complex proteins psbY, chloroplast	1.6	DOWN	854.7
Solyc08g013670	101268297	photosystem I subunit PsaN | photosystem I reaction center subunit	3.4	DOWN	760.7
Solyc02g083810	101261284	ferredoxin--NADP+ reductase [EC:1.18.1.2] | ferredoxin--NADP reductase, leaf-type isozyme, chloroplastic	1.9	DOWN	446.4
Solyc12g005630	101243864	cytochrome b6-f complex iron-sulfur subunit [EC:1.10.9.1] | cytochrome b6-f complex	1.8	DOWN	434.0

Solyc06g082950	101265555	photosystem I subunit XI | photosystem I reaction center subunit XI, chloroplastic	1.6	DOWN	427.7
Solyc02g080540	101253342	F-type H+-transporting ATPase subunit gamma | ATP synthase gamma chain, chloroplasti	1.7	DOWN	316.3
Solyc10g075160	101265784	ferredoxin | ferredoxin	4.1	DOWN	268.6
Solyc06g066000	109120519	F-type H+-transporting ATPase subunit b | ATP synthase subunit b', chloroplastic-like	1.7	DOWN	147.7
Solyc06g060340	101260830	photosystem II 22kDa protein | psbS, CP22; photosystem II subunit S	4.1	DOWN	111.9
Solyc12g044280	101244751	photosystem I subunit VI | photosystem I reaction center subunit VI, chloroplastic-l	1.7	DOWN	71.5
Solyc06g065990	101263124	F-type H+-transporting ATPase subunit b | ATP synthase subunit b', chloroplastic	1.8	DOWN	65.9
Solyc09g064500	101245880	photosystem II 13kDa protein | photosystem II reaction center Psb28 protein	1.7	DOWN	49.1
Solyc11g006910	101266472	ferredoxin | ferredoxin, root R-B2-like	2.4	DOWN	9.5
H/-Fe versus H/+Fe					
Solyc10g075160	101265784	ferredoxin | ferredoxin	3.0	DOWN	286.7
Solyc06g060340	101260830	photosystem II 22kDa protein | (RefSeq) psbS, CP22; photosystem II subunit S	3.6	DOWN	115.4
Solyc09g064500	101245880	photosystem II 13kDa protein | photosystem II reaction center Psb28 protein	2.3	DOWN	44.4
Solyc03g114930	101259227	photosystem II oxygen-evolving enhancer protein 2 | psbP-like protein 1, chloroplast	1.9	DOWN	12.3
Solyc11g006910	101266472	ferredoxin | ferredoxin, root R-B2-like	2.3	DOWN	9.6
I/+Fe versus H/-Fe					
Solyc07g066310	778297	photosystem II 10kDa protein | (RefSeq) PSBR; PSII polypeptide	2.2	DOWN	8955.4

Solyc11g051170	101265555	photosystem I subunit XI | (RefSeq) photosystem I reaction center subunit XI, chloroplastic	1.6	DOWN	4610.9
Solyc06g054260	543978	photosystem I subunit II | (RefSeq) PSI-D, psaD; photosystem I reaction center subunit II, ch	1.8	DOWN	1240.7
Solyc06g074200	101254806	photosystem I subunit PsaO | (RefSeq) photosystem I subunit O	2.3	DOWN	1152.6
Solyc07g044860	544077	photosystem II oxygen-evolving enhancer protein 2 | (RefSeq) PSBP, OEE2, psbX; photosystem II	1.7	DOWN	1000.9
Solyc08g006930	101255222	photosystem I subunit X | (RefSeq) photosystem I reaction center subunit psaK, chloroplastic	1.9	DOWN	878.3
Solyc06g082940	101265249	photosystem I subunit XI | (RefSeq) photosystem I reaction center subunit XI, chloroplastic	1.6	DOWN	835.2
Solyc08g013670	101268297	photosystem I subunit PsaN | (RefSeq) photosystem I reaction center subunit	2.1	DOWN	539.5
Solyc06g082950	101265555	photosystem I subunit XI | (RefSeq) photosystem I reaction center subunit XI, chloroplastic	1.9	DOWN	476.8

Supplemental Table 8. Top 100 up- or downregulated DEGs in all pairwise comparisons. In the I/+Fe versus H/+Fe comparison, fold-change means the ratio of I/+Fe FPKM on H/+Fe FPKM. Similarly, in the comparison H/-Fe versus H/+Fe, fold-change is the ratio of H/-Fe FPKM on H/+Fe FPKM. In I/+Fe versus H/-Fe the ratio is calculated as I/+Fe FPKM on H/-Fe FPKM. Total FPKM corresponds to the sum of FPKM expression of the corresponding gene in the indicated pairwise comparison. Genes with total fpkm expression values under 10 were discarded. FDR (q) <0.01.

SGN locus	Gene_name Gene ID	ITAG3.0 gene description	NCBI GeneID	NCBI Symbol	NCBI description / 1st blastp hit / 2nd blastp hit	fold_ change	direction	total_ fpkm
I /+Fe versus H/+Fe_UP								
Solyc02g065570	Solyc02g065570.1	LOW QUALITY:Rotundifolia-like protein (AHRD V3.3	104645948	LOC104645948	uncharacterized LOC104645948	4,03	UP	2445,28
Solyc07g007760	Solyc07g007760.3	defensin-like protein	101263826	DEFL1	defensin-like protein	4,9	UP	1534,15
Solyc07g041900	Solyc07g041900.3	cysteine proteinase	101252505	Cyp-3	cysteine proteinase 3	3,49	UP	715,76
Solyc08g016150	Solyc08g016150.1	LOW QUALITY:Avr9/Cf-9 rapidly elicited protein		#N/D	gb|AAG43556.1|AF211538_1 Avr9/Cf-9 rapidly elicited protein 180 [Nicotiana tabacum]	3,23	UP	440,74
Solyc04g071890	Solyc04g071890.3	Peroxidase (AHRD V3.3 *** K4BTH6_SOLLC)	101253377	LOC101253377	peroxidase 12	3,49	UP	396,39
Solyc05g008895	Solyc05g008895.1	Lipid transfer protein (AHRD V3.3 ***		#N/D	ref|XP_010320740.1| PREDICTED: non-specific lipid-transfer protein 2-like [Solanum	5,82	UP	356,28
Solyc06g074030	Solyc06g074030.1	Polynucleotidyl transferase, ribonuclease H-like	101258270	LOC101258270	probable CCR4-associated factor 1 homolog 9	3,32	UP	315,69
Solyc10g075090	Solyc10g075090.2	Non-specific lipid-transfer protein (AHRD V3.3		#N/D	ref|NP_001233953.1| non-specific lipid-transfer protein 2 precursor [Solanum lycopersicum]	3,35	UP	276,16
Solyc09g015300	Solyc09g015300.1	Photosystem I P700 chlorophyll a apoprotein A1		#N/D	ref|XP_006445529.1| hypothetical protein CICLE_v10004112mg, partial [Citrus clementina]	3,3	UP	224,92
Solyc06g024210	Solyc06g024210.2	LOW QUALITY:Senescence-associated protein (AHRD		#N/D	ref|XP_010315002.1| PREDICTED: uncharacterized protein LOC101254183, partial [Solanum	3,23	UP	216,24
Solyc03g093800	Solyc03g093800.1	glycine-rich protein (AHRD V3.3 *-* AT5G61660.1)		#N/D	ref|XP_004235193.1| PREDICTED: glycine-rich cell wall structural protein 2-like [Solanum	4,4	UP	186,17
Solyc11g027645	Solyc11g027645.1	Ribosomal RNA small subunit methyltransferase B		#N/D	gb|KRH17867.1| hypothetical protein GLYMA_13G0231001, partial [Glycine max]	3,45	UP	185,41
Solyc02g087350	Solyc02g087350.2	Hexosyltransferase (AHRD V3.3 *** K4BBP2_SOLLC)	101265190	LOC101265190	probable galacturonosyltransferase-like 10	3,63	UP	162,82
Solyc08g082680	Solyc08g082680.3	RING/U-box superfamily protein (AHRD V3.3 ***	101250143	LOC101250143	probable E3 ubiquitin-protein ligase RHA4A	3,9	UP	159,52
Solyc02g091180	Solyc02g091180.1	LOW QUALITY:DUF4228 domain protein (AHRD V3.3 ***	104645686	LOC104645686	uncharacterized LOC104645686	3,82	UP	155,9
Solyc02g084850	Solyc02g084850.3	Abscisic acid and environmental stress-inducible	544056	TAS14	TAS14 peptide (AA 1-130)	4,61	UP	141,97
Solyc08g077900	Solyc08g077900.3	Expansin-like protein (AHRD V3.3 ***	101247647	LOC101247647	expansin-like B1	5,37	UP	135,32
Solyc12g009240	Solyc12g009240.1	Ethylene-responsive transcription factor ERF017	101253257	LOC101253257	ethylene-responsive transcription factor ERF017	11,26	UP	134,8
Solyc00g272810	Solyc00g272810.1	Tyramine N-feruloyltransferase 4/11, putative		#N/D	ref|XP_004253515.1| PREDICTED: probable acetyltransferase NATA1-like [Solanum lycopersicum]	4,09	UP	129,56
Solyc06g076570	Solyc06g076570.3	class I small heat shock protein	101264936	Hsp20.0	class I small heat shock protein	3,4	UP	126,34
Solyc06g053220	Solyc06g053220.3	Homeobox leucine zipper protein (AHRD V3.3 ***	101264731	LOC101264731	homeobox-leucine zipper protein ATHB-12-like	3,33	UP	124,32
Solyc01g109250	Solyc01g109250.2	LOW QUALITY:DUF4228 domain protein (AHRD V3.3 ***	101261073	LOC101261073	uncharacterized LOC101261073	3,62	UP	119,27
Solyc01g005305	Solyc01g005305.1	Eukaryotic aspartyl protease family protein (AHRD		#N/D	0	3,79	UP	116,73
Solyc01g005290	Solyc01g005290.3	Sec14p-like phosphatidylinositol transfer family		#N/D	ref|XP_010316439.1| PREDICTED: LOW QUALITY PROTEIN: sec14 cytosolic factor-like [Solanum	3,34	UP	115,16
Solyc05g051480	Solyc05g051480.2	DNA-directed RNA polymerase subunit beta (AHRD		#N/D	0	3,2	UP	114,4
Solyc10g081980	Solyc10g081980.2	Late embryogenesis abundant (LEA)	101249973	LOC101249973	NDR1/HIN1-Like protein 3-like	3,18	UP	108,21
Solyc01g005300	Solyc01g005300.3	Flavin-binding kelch domain F box protein (AHRD		#N/D	ref|XP_004228739.1| PREDICTED: adagio protein 3 [Solanum lycopersicum]	3,64	UP	102,05
Solyc08g007240	Solyc08g007240.3	Nudix hydrolase (AHRD V3.3 *** A0A061G4C5_THECC)	101261537	LOC101261537	nudix hydrolase 8	3,62	UP	96,18
Solyc12g013710	Solyc12g013710.2	light dependent NADH:protochlorophyllide	101248079	LOC101248079	protochlorophyllide reductase-like	3,63	UP	92,82
Solyc10g049420	Solyc10g049420.2	TRAF-like superfamily protein (AHRD V3.3 --*		#N/D	0	12,4	UP	91,81
Solyc06g051680	Solyc06g051680.1	Protein EARLY FLOWERING 4 (AHRD V3.3 *-*		#N/D	ref|XP_009629950.1| PREDICTED: protein EARLY FLOWERING 4-like [Nicotiana tomentosiformis]	4,5	UP	89,11
Solyc02g094000	Solyc02g094000.1	Calcium-binding protein (AHRD V3.3 ***	101245711	LOC101245711	putative calcium-binding protein CML19	4,19	UP	84,06
Solyc05g009610	Solyc05g009610.1	Alpha/beta-Hydrolases superfamily protein (AHRD		#N/D	ref|XP_004238946.1| PREDICTED: probable carboxylesterase 6 [Solanum lycopersicum]	3,6	UP	83,03
Solyc06g059740	Solyc06g059740.3	Alcohol dehydrogenase (AHRD V3.3 *** ADH_MALDO)	544074	ADH2	alcohol dehydrogenase	4,75	UP	79,21
Solyc10g081970	Solyc10g081970.2	Late embryogenesis abundant (LEA)		#N/D	ref|XP_004249776.1| PREDICTED: protein YLS9-like, partial [Solanum lycopersicum]	3,71	UP	77,5
Solyc12g094380	Solyc12g094380.2	Thioredoxin superfamily protein (AHRD V3.3 ***	101254074	LOC101254074	uncharacterized LOC101254074	3,5	UP	76,81
Solyc06g076580	Solyc06g076580.1	Minichromosome maintenance (MCM2/3/5) family		#N/D	0	3,58	UP	67,05
Solyc04g054990	Solyc04g054990.3	PLAT domain-containing protein 1 (AHRD V3.3 ***	101262509	LOC101262509	PLAT domain-containing protein 2-like	4,01	UP	64,72
Solyc01g007030	Solyc01g007030.3	U-box domain-containing family protein (AHRD V3.3		#N/D	ref|XP_010315681.1| PREDICTED: LOW QUALITY PROTEIN: E3 ubiquitin-protein ligase PUB22-like	3,6	UP	56,92
Solyc05g052520	Solyc05g052520.3	Protein phosphatase 2C family protein (AHRD V3.3	101258862	LOC101258862	putative protein phosphatase 2C 53	4,62	UP	55
Solyc09g009530	Solyc09g009530.3	alpha/beta-Hydrolases superfamily protein (AHRD	101261737	LOC101261737	alpha/beta-Hydrolases superfamily protein	3,63	UP	49,76
Solyc10g008910	Solyc10g008910.1	Histone H3 (AHRD V3.3 *** A0A068VC55_COFCA)	101252717	LOC101252717	histone H3.2	3,64	UP	44,16
Solyc08g006770	Solyc08g006770.3	2-oxoglutarate and Fe(II)-dependent oxygenase	101250715	LOC101250715	protein DMR6-LIKE OXYGENASE 2	4,04	UP	43,65

SGN locus	Gene_name Gene ID	ITAG3.0 gene description	NCBI GeneID	NCBI Symbol	NCBI description / 1st blastp hit / 2nd blastp hit	fold_ change	direction	total_ fpkm
Solyc01g087990	Solyc01g087990.3	MADS-box transcription factor AGAMOUS-like	101260573	LOC101260573	agamous-like MADS-box protein AGL15	4,08	UP	41,39
Solyc01g096420	Solyc01g096420.3	NADPH:quinone oxidoreductase (AHRD V3.3 ***	101265773	LOC101265773	NAD(P)H:quinone oxidoreductase	5,09	UP	40,82
Solyc01g006680	Solyc01g006680.3	2-oxoglutarate (2OG) and Fe(II)-dependent		#N/D	ref|NP_001306150.1| JmjC-domain protein JMJ524 [Solanum lycopersicum]	5,37	UP	40,73
Solyc03g043860	Solyc03g043860.2	NUDIX hydrolase (AHRD V3.3 *** A0A118K334_CYNCS)	101265208	LOC101265208	nudix hydrolase 1-like	5,11	UP	39,9
Solyc02g086810	Solyc02g086810.1	LOW QUALITY:DUF1645 family protein (AHRD V3.3 ***	101250946	LOC101250946	uncharacterized LOC101250946	3,57	UP	38,83
Solyc05g055540	Solyc05g055540.2	Major facilitator superfamily protein (AHRD V3.3	101262315	LOC101262315	uncharacterized LOC101262315	3,39	UP	38,68
Solyc02g079700	Solyc02g079700.1	Serine/threonine-protein kinase (AHRD V3.3 *-*		#N/D	ref|XP_010317320.1| PREDICTED: LOW QUALITY PROTEIN: receptor-like serine/threonine-protein	5,16	UP	37,15
Solyc12g009800	Solyc12g009800.2	Purple acid phosphatase (AHRD V3.3 ***	101262785	LOC101262785	bifunctional purple acid phosphatase 26	4,05	UP	36,98
Solyc04g081910	Solyc04g081910.3	Calcium-dependent protein kinase, putative (AHRD	101246133	LOC101246133	calcium-dependent protein kinase 29	3,35	UP	34,35
Solyc06g009190	Solyc06g009190.3	Pectinesterase (AHRD V3.3 *** K4C3U9_SOLLC)	101260941	LOC101260941	pectinesterase	6,83	UP	31,66
Solyc01g095930	Solyc01g095930.3	O-acyltransferase WSD1-like protein (AHRD V3.3		#N/D	ref|XP_010315460.1| PREDICTED: LOW QUALITY PROTEIN: O-acyltransferase WSD1 [Solanum	4,73	UP	31,36
Solyc08g074620	Solyc08g074620.3	polyphenol oxidase precursor	101259357	LOC101259357	polyphenol oxidase E, chloroplastic	3,17	UP	30,67
Solyc04g008730	Solyc04g008730.3	Alpha-galactosidase (AHRD V3.3 *** K4BP29_SOLLC)	101249542	LOC101249542	alpha-galactosidase 1	3,28	UP	30,01
Solyc06g069070	Solyc06g069070.1	Lipid transfer protein (AHRD V3.3 ***		#N/D	ref|XP_004241634.1| PREDICTED: non-specific lipid-transfer protein 2-like [Solanum	5,12	UP	29,71
Solyc02g037495	Solyc02g037495.1	AMP-dependent synthetase and ligase family		#N/D	ref|XP_004231632.1| PREDICTED: probable acyl-activating enzyme 6 [Solanum lycopersicum]	3,21	UP	29,11
Solyc05g055080	Solyc05g055080.1	LOW QUALITY:P-loop containing nucleoside		#N/D	0	5,03	UP	29,09
Solyc06g053640	Solyc06g053640.1	RING/U-box superfamily protein (AHRD V3.3 ***	101249928	LOC101249928	RING-H2 finger protein ATL16-like	3,62	UP	28,02
Solyc09g089580	Solyc09g089580.3	2-oxoglutarate (2OG) and Fe(II)-dependent	101268031	ACO3	1-aminocyclopropane-1-carboxylate oxidase homolog	4,48	UP	26,72
Solyc11g020050	Solyc11g020050.1	LOW QUALITY:Cytosolic Fe-S cluster assembly		#N/D	gb|AFK43595.1| unknown [Lotus japonicus]	3,56	UP	25,94
Solyc07g053230	Solyc07g053230.3	R2R3MYB transcription factor 83		#N/D	ref|XP_004243413.1| PREDICTED: myb-related protein Myb4-like [Solanum lycopersicum]	4,2	UP	23,76
Solyc03g081240	Solyc03g081240.3	Two-component response regulator-like protein	101250283	LOC101250283	two-component response regulator-like APRR5	6,4	UP	21,87
Solyc08g062960	Solyc08g062960.3	SolycHsfA2	101255223	LOC101255223	heat stress transcription factor HsfA2	3,77	UP	21,51
Solyc02g080120	Solyc02g080120.2	Gibberellin 2-beta- dioxygenase 7	101263073	LOC101263073	gibberellin 2-beta-dioxygenase 8	4,33	UP	20,88
Solyc02g071700	Solyc02g071700.3	Lipase, GDSL (AHRD V3.3 *** A0A103XTV4_CYNCS)		#N/D	ref|XP_004233010.2| PREDICTED: uncharacterized protein LOC101263269 [Solanum lycopersicum]	4,1	UP	20,05
Solyc04g063210	Solyc04g063210.3	Caffeoyl-CoA O-methyltransferase (AHRD V3.3 ***	101252173	LOC101252173	probable caffeoyl-CoA O-methyltransferase At4g26220	6,71	UP	19,65
Solyc04g008100	Solyc04g008100.2	U-box domain-containing protein (AHRD V3.3 ***	101262803	LOC101262803	U-box domain-containing protein 21-like	3,78	UP	19,59
Solyc01g079110	Solyc01g079110.3	Histone H3 (AHRD V3.3 *** A0A0V0H170_SOLCH)	101260571	LOC101260571	histone H3.2-like	3,81	UP	19,37
Solyc09g009810	Solyc09g009810.1	LOW QUALITY:TSA: Wollemia nobilis	101255524	LOC101255524	uncharacterized LOC101255524	5,1	UP	19,11
Solyc11g066130	Solyc11g066130.1	osmotin	543971	LOC543971	osmotin-like protein	5,2	UP	18,81
Solyc01g006240	Solyc01g006240.3	Mannose-binding lectin superfamily protein (AHRD		#N/D	ref|XP_004228728.1| PREDICTED: inactive protein RESTRICTED TEV MOVEMENT 1-like [Solanum	4,41	UP	18,74
Solyc03g079880	Solyc03g079880.3	Protease inhibitor/seed storage/lipid transfer		#N/D	ref|NP_001306089.1| xylem sap protein 10 kDa precursor [Solanum lycopersicum]	3,22	UP	18,11
Solyc01g010390	Solyc01g010390.3	Beta-glucosidase, putative (AHRD V3.3 ***	101256510	LOC101256510	beta-glucosidase 40	3,54	UP	18,01
Solyc12g005940	Solyc12g005940.2	1-aminocyclopropane-1-carboxylate oxidase 1 (AHRD	101251255	LOC101251255	1-aminocyclopropane-1-carboxylate oxidase	3,74	UP	17,53
Solyc10g009410	Solyc10g009410.1	Eukaryotic aspartyl protease family protein (AHRD	101264466	LOC101264466	aspartyl protease family protein 2	4,46	UP	17,43
Solyc10g050970	Solyc10g050970.1	Ethylene Response Factor D.4	101246484	LOC101246484	ethylene-responsive transcription factor ERF109-like	3,99	UP	16,53
Solyc05g009480	Solyc05g009480.1	LOW QUALITY:NIM1-interacting 2 (AHRD V3.3 -**	104647288	LOC104647288	uncharacterized LOC104647288	3,64	UP	15,57
Solyc02g038740	Solyc02g038740.3	3-hydroxy-3-methylglutaryl coenzyme A reductase		#N/D	ref|NP_001296119.1| 3-hydroxy-3-methylglutaryl-coenzyme A reductase 2 [Solanum lycopersicun	4,25	UP	15,5
Solyc03g117800	Solyc03g117800.3	Fatty acid hydroxylase superfamily (AHRD V3.3 ***	101251368	LOC101251368	protein ECERIFERUM 3	3,75	UP	15,19
Solyc02g077060	Solyc02g077060.2	LOW QUALITY:RPW8.2-like protein (AHRD V3.3 *-*	104645842	LOC104645842	uncharacterized LOC104645842	4,47	UP	14,82
Solyc01g057910	Solyc01g057910.3	R2R3MYB transcription factor 2	101246560	LOC101246560	transcription factor MYB108-like	3,65	UP	14,11
Solyc03g006210	Solyc03g006210.2	Cysteine protease (AHRD V3.3 *** J7GPZ5_SOLCI)	101249528	LOC101249528	zingipain-2-like	18,73	UP	14,1
Solyc03g111820	Solyc03g111820.3	Sieve element occlusion a (AHRD V3.3 ***		#N/D	ref|XP_004236294.1| PREDICTED: uncharacterized protein LOC101251765 [Solanum lycopersicum]	3,33	UP	13,98
Solyc03g026000	Solyc03g026000.3	cold regulated protein 27 (AHRD V3.3 --*	101244747	LOC101244747	uncharacterized LOC101244747	5,53	UP	13,62
Solyc06g083650	Solyc06g083650.3	GDSL esterase/lipase (AHRD V3.3 ***	101267033	LOC101267033	GDSL esterase/lipase At5g33370	4,73	UP	13,18
Solyc01g066570	Solyc01g066570.3	senescence-associated family protein (DUF581)	101258100	LOC101258100	uncharacterized LOC101258100	8,37	UP	12,86
Solyc08g063130	Solyc08g063130.3	FAD/NAD(P)-binding oxidoreductase family protein	101258393	LOC101258393	FAD-dependent urate hydroxylase-like	6,84	UP	12,73
Solyc01g087785	Solyc01g087785.1	Subtilisin-like protease SDD1 (AHRD V3.3 *-*		#N/D	ref|XP_016489542.1| PREDICTED: subtilisin-like protease SBT1.9 [Nicotiana tabacum]	3,88	UP	12,19
Solyc07g045350	Solyc07g045350.3	Acetoacetyl-CoA thiolase (AHRD V3.3 ***	101262830	LOC101262830	acetyl-CoA acetyltransferase, cytosolic 1	4,69	UP	12,09
Solyc11g021060	Solyc11g021060.2	TOMARPIX proteinase inhibitor	543962	ARPI	proteinase inhibitor	5,6	UP	11,99
Solyc12g099160	Solyc12g099160.2	serine carboxypeptidase family protein	101244564	LOC101244564	serine carboxypeptidase-like 33	4,33	UP	11,8
Solyc02g082240	Solyc02g082240.1	LOW QUALITY:UDP-N-acetylenolpyruvoylglucosamine		#N/D	emb|CDP01750.1| unnamed protein product [Coffea canephora]	3,32	UP	11,76
Solyc08g067510	Solyc08g067510.1	Non-specific lipid-transfer protein (AHRD V3.3	101246456	LOC101246456	non-specific lipid-transfer protein 1-like	18,66	UP	11,75
Solyc08g074630	Solyc08g074630.2	polyphenol oxidase precursor	101259064	LOC101259064	polyphenol oxidase F, chloroplastic	4,81	UP	11,27
Solyc06g051800	Solyc06g051800.3	expansin 1	544035	EXP1	expansin	4,02	UP	11,12
Solyc08g006790	Solyc08g006790.3	Early nodulin-like protein (AHRD V3.3 ***	101251307	LOC101251307	early nodulin-like protein 3	3,22	UP	11
Solyc05g007300	Solyc05g007300.3	HVA22-like protein (AHRD V3.3 *** K4BWQ6_SOLLC)	101263114	LOC101263114	HVA22-like protein c	12,02	UP	10,48
Solyc07g043480	Solyc07g043480.1	Glycosyltransferase (AHRD V3.3 ***	101254402	LOC101254402	zeatin O-xylosyltransferase-like	4,73	UP	10,3

SGN locus	Gene_name Gene ID	ITAG3.0 gene description	NCBI GeneID	NCBI Symbol	NCBI description / 1st blastp hit / 2nd blastp hit	fold_ change	direction	total_ fpkm
I /+Fe versus H/+Fe_DOWN								
Solyc10g086580	Solyc10g086580.2	Ribulose bisphosphate carboxylase/oxygenase	#N/D	#N/D	ref|XP_010312360.1| ribulose bisphosphate carboxylase/oxygenase activase, chloroplastic LOC10	9,0	DOWN	3523,3
Solyc05g051850	Solyc05g051850.3	putative myo-inositol-1-phosphatase	543809	LOC543809	inositol-3-phosphate synthase	11,7	DOWN	585,1
Solyc06g053260	Solyc06g053260.1	SAUR-like auxin-responsive family protein (AHRD	101055583	LOC101055583	small auxin-up protein 58	19,7	DOWN	398,6
Solyc07g043130	Solyc07g043130.3	Phototropic-responsive NPH3 family protein (AHRD	101259171	LOC101259171	root phototropism protein 2	13,6	DOWN	362,4
Solyc11g012360	Solyc11g012360.2	Tonoplast dicarboxylate transporter (AHRD V3.3	101257524	LOC101257524	ref|NP_001266027.1| tonoplast dicarboxylate transporter-like [Solanum lycopersicum]	60,9	DOWN	329,0
Solyc06g054270	Solyc06g054270.3	Sugar transporter protein 11	101261239	STP11	sugar transport protein 8-like	9,9	DOWN	297,4
Solyc09g090570	Solyc09g090570.2	proton gradient regulation 5 (AHRD V3.3 ***	101262255	LOC101262255	protein PROTON GRADIENT REGULATION 5, chloroplastic	18,8	DOWN	229,3
Solyc04g015750	Solyc04g015750.3	Magnesium chelatase H subunit (AHRD V3.3 ***	101244176	LOC101244176	magnesium-chelatase subunit ChlH, chloroplastic	16,7	DOWN	221,7
Solyc02g080640	Solyc02g080640.3	adenylyl-sulfate reductase	544267	LOC544267	adenylyl-sulfate reductase	9,4	DOWN	221,4
Solyc06g073180	Solyc06g073180.3	CONSTANS interacting protein 1	778334	CIP1	CONSTANS interacting protein 1	16,3	DOWN	220,1
Solyc11g013810	Solyc11g013810.2	Nitrate reductase (AHRD V3.3 *** K4D6I5_SOLLC)	100736473	NR	nitrate reductase [NADH] E value 0.0	26,1	DOWN	205,7
Solyc10g085140	Solyc10g085140.1	Alkyl transferase (AHRD V3.3 *-* K7X479_SOLLC)		#N/D	ref|XP_010312432.1| PREDICTED: dehydrodolichyl diphosphate synthase 2-like [Solanum	9,1	DOWN	182,3
Solyc09g089730	Solyc09g089730.3	2-oxoglutarate (2OG) and Fe(II)-dependent	101244528	LOC101244528	1-aminocyclopropane-1-carboxylate oxidase homolog	14,5	DOWN	179,3
Solyc09g011080	Solyc09g011080.3	Ribulose bisphosphate carboxylase/oxygenase	101250725	LOC101250725	ribulose bisphosphate carboxylase/oxygenase activase 1, chloroplastic	209,3	DOWN	170,3
Solyc10g079620	Solyc10g079620.2	haloacid dehalogenase	100316880	LOC100316880	haloacid dehalogenase	99,7	DOWN	157,1
Solyc01g080870	Solyc01g080870.3	Peptide transporter, putative (AHRD V3.3 ***	101250924	LOC101250924	protein NRT1/ PTR FAMILY 7.3	13,3	DOWN	152,0
Solyc01g102610	Solyc01g102610.3	Ferric reduction oxidase 7 (AHRD V3.3 ***	101246763	LOC101246763	ref|XP_004230384.1| PREDICTED: ferric reduction oxidase 6-like [Solanum lycopersicum]	42,4	DOWN	145,5
Solyc00g136560	Solyc00g136560.3	Alkyl transferase (AHRD V3.3 *** K7X479_SOLLC)		#N/D	ref|XP_004253464.1| PREDICTED: dehydrodolichyl diphosphate synthase 2-like [Solanum	12,8	DOWN	135,8
Solyc09g018640	Solyc09g018640.1	LOW QUALITY:phosphatidylinositol-glycan		#N/D		nan	DOWN	123,9
Solyc01g107460	Solyc01g107460.2	LOW QUALITY:neuronal PAS domain protein (AHRD		#N/D	ref|XP_004230726.1| PREDICTED: uncharacterized protein LOC101248432 [Solanum lycopersicum]	129,3	DOWN	105,2
Solyc02g084420	Solyc02g084420.3	B-box zinc finger family protein (AHRD V3.3 ***		#N/D	ref|XP_015066178.1| PREDICTED: B-box zinc finger protein 19-like [Solanum pennellii]	60,5	DOWN	92,1
Solyc03g111120	Solyc03g111120.3	Malate synthase (AHRD V3.3 *** M1B824_SOLTU)	101267395	LOC101267395	ref|XP_004236346.1| PREDICTED: malate synthase, glyoxysomal [Solanum lycopersicum]	38,3	DOWN	89,8
Solyc01g105120	Solyc01g105120.3	Dentin sialophosphoprotein-related, putative		#N/D	ref|XP_010315092.1| PREDICTED: uncharacterized protein LOC101244909 isoform X2 [Solanum	10,3	DOWN	82,3
Solyc02g071380	Solyc02g071380.2	2-oxoglutarate (2OG) and Fe(II)-dependent	101262071	LOC101262071	protein SRG1	14,2	DOWN	81,1
Solyc07g005390	Solyc07g005390.3	aldehyde dehydrogenase 11A3 (AHRD V3.3 ***	101262732	SlALDH11A3a	NADP-dependent glyceraldehyde-3-phosphate dehydrogenase,	10,7	DOWN	75,4
Solyc05g012030	Solyc05g012030.1	LOW QUALITY:Protein BIG GRAIN 1-like E (AHRD V3.3		#N/D	ref|XP_004239030.1| PREDICTED: histone-lysine N-methyltransferase, H3 lysine-79 specific	41,0	DOWN	69,8
Solyc03g059260	Solyc03g059260.3	Carboxyl-terminal-processing protease (AHRD V3.3	101257542	LOC101257542	carboxyl-terminal-processing peptidase 3, chloroplastic	9,2	DOWN	69,7
Solyc10g084370	Solyc10g084370.2	MYB transcription factor (AHRD V3.3 ***	101253545	LOC101253545	protein REVEILLE 8	308,5	DOWN	68,6
Solyc02g084430	Solyc02g084430.3	B-box type zinc finger family protein (AHRD V3.3		#N/D	ref|XP_015066178.1| PREDICTED: B-box zinc finger protein 19-like [Solanum pennellii]	58,5	DOWN	67,1
Solyc03g116630	Solyc03g116630.3	cytochrome P450 family protein (AHRD V3.3 ***	101253674	LOC101253674	uncharacterized LOC101253674	17,9	DOWN	66,8
Solyc03g098320	Solyc03g098320.3	Myb transcription factor (AHRD V3.3 ***	101255972	LOC101255972	ref|XP_004235390.1| PREDICTED: protein REVEILLE 7 [Solanum lycopersicum]	69,3	DOWN	66,2
Solyc09g007760	Solyc09g007760.3	plasma membrane intrinsic protein 2.10		#N/D	ref|XP_010325988.1| PREDICTED: aquaporin PIP2-1-like [Solanum lycopersicum]	11,0	DOWN	65,6
Solyc06g036260	Solyc06g036260.3	beta-carotene hydroxylase-1	544133	CrtR-b1	beta-carotene hydroxylase	19,2	DOWN	64,9
Solyc04g040160	Solyc04g040160.3	Pheophorbide A oxygenase, putative (AHRD V3.3 ***	101255583	LOC101255583	protochlorophyllide-dependent translocon component 52, chloroplastic	8,8	DOWN	61,5
Solyc02g089540	Solyc02g089540.3	CONSTANS 1	778253	CO1	CONSTANS 1;CO1;ortholog	66,2	DOWN	60,2
Solyc05g007880	Solyc05g007880.3	Dof zinc finger protein (AHRD V3.3 ***	101248009	LOC101248009	cyclic dof factor 1	15,6	DOWN	58,6
Solyc05g011890	Solyc05g011890.1	Sulfotransferase (AHRD V3.3 *** K4BXR2_SOLLC)	101259437	LOC101259437	ref|XP_004239020.1| PREDICTED: cytosolic sulfotransferase 12-like [Solanum lycopersicum]	37,2	DOWN	57,9
Solyc08g082590	Solyc08g082590.3	Glutaredoxin (AHRD V3.3 *** A0A103XR19_CYNCS)	101252103	LOC101252103	ref|XP_004245502.1| PREDICTED: glutaredoxin domain-containing cysteine-rich protein	85,9	DOWN	57,7
Solyc03g007370	Solyc03g007370.3	Sigma factor (AHRD V3.3 *** A0A0G2STU5_9ROSI)	101252660	LOC101252660	RNA polymerase sigma factor sigE, chloroplastic/mitochondrial	11,5	DOWN	55,7
Solyc01g079150	Solyc01g079150.3	Boron transporter (AHRD V3.3 *** B6V758_VITVI)	101260863	LOC101260863	ref|XP_004229368.1| PREDICTED: boron transporter 1 [Solanum lycopersicum]	69,4	DOWN	53,7
Solyc09g007765	Solyc09g007765.1	Aquaporin-like protein (AHRD V3.3 *-*		#N/D	ref|XP_010325988.1| PREDICTED: aquaporin PIP2-1-like [Solanum lycopersicum]	14,4	DOWN	52,0
Solyc07g051820	Solyc07g051820.3	Cellulose synthase family protein (AHRD V3.3 ***	101259456	LOC101259456	cellulose synthase-like protein H1	15,0	DOWN	49,2
Solyc10g050670	Solyc10g050670.1	LOW QUALITY:LOB domain-containing protein 7 (AHRD		#N/D		nan	DOWN	45,9
Solyc01g068560	Solyc01g068560.3	Agglutinin-like protein ALA1, putative isoform 3		#N/D	ref|XP_010320656.1| PREDICTED: uncharacterized protein LOC101268608 [Solanum lycopersicum]	9,1	DOWN	45,5
Solyc08g007130	Solyc08g007130.3	Beta-amylase (AHRD V3.3 *** K4CIK0_SOLLC)	101259175	LOC101259175	beta-amylase 3, chloroplastic-like	21,2	DOWN	43,6
Solyc01g110940	Solyc01g110940.3	SAUR-like auxin-responsive protein family (AHRD		#N/D	ref|XP_016539874.1| PREDICTED: auxin-induced protein 15A-like [Capsicum annuum]	8,9	DOWN	42,9
Solyc05g012230	Solyc05g012230.3	Protein POLAR LOCALIZATION DURING ASYMMETRIC	101267310	LOC101267310	ref|XP_004239047.1| PREDICTED: uncharacterized protein LOC101267310 [Solanum lycopersicum]	34,5	DOWN	42,5
Solyc02g092110	Solyc02g092110.3	Phytosulfokines 3 family protein (AHRD V3.3 ***	101268443	PSK4	phytosulfokines 3	12,8	DOWN	40,6
Solyc09g010530	Solyc09g010530.3	Cation/H(+) antiporter (AHRD V3.3 ***	101249848	LOC101249848	cation/H(+) antiporter 20	282,5	DOWN	40,5
Solyc10g005080	Solyc10g005080.3	Late elongated hypocotyl (AHRD V3.3 ***	101261662	LOC101261662	ref|XP_004248416.1| PREDICTED: protein LHY [Solanum lycopersicum]	91,2	DOWN	40,3

SGN locus	Gene_name Gene ID	ITAG3.0 gene description	NCBI GeneID	NCBI Symbol	NCBI description / 1st blastp hit / 2nd blastp hit	fold_ change	direction	total_ fpkm
Solyc01g009080	Solyc01g009080.3	Zeaxanthin epoxidase, chloroplastic (AHRD V3.3	101252420	LOC101252420	uncharacterized LOC101252420	9,2	DOWN	38,6
Solyc04g080040	Solyc04g080040.3	Heat shock protein binding protein, putative		#N/D	ref|XP_004238235.1| PREDICTED: J domain-containing protein required for chloroplast	29,6	DOWN	38,5
Solyc07g053140	Solyc07g053140.3	Zinc finger, B-box (AHRD V3.3 ***	101265452	LOC101265452	ref|XP_004243424.1| PREDICTED: zinc finger protein CONSTANS-LIKE 4-like [Solanum	33,9	DOWN	38,4
Solyc03g096760	Solyc03g096760.1	Response to low sulfur protein, putative (AHRD	101268660	LOC101268660	ref|XP_004235266.1| PREDICTED: uncharacterized protein LOC101268660 [Solanum lycopersicum]	36,7	DOWN	38,1
Solyc10g005030	Solyc10g005030.3	Pseudo-response regulator 9 (AHRD V3.3 ***	101262866	LOC101262866	two-component response regulator-like APRR9	9,6	DOWN	36,7
Solyc07g040680	Solyc07g040680.3	SolycHsfA9	101266046	LOC101266046	heat stress transcription factor A-2-like	8,8	DOWN	36,4
Solyc06g081990	Solyc06g081990.2	LOW QUALITY:Dynein light chain type 1 family		#N/D		nan	DOWN	36,4
Solyc03g116910	Solyc03g116910.3	cinnamoyl-CoA reductase 2	778359	CCR2	cinnamoyl-CoA reductase	19,4	DOWN	36,2
Solyc01g096630	Solyc01g096630.3	Dentin sialophosphoprotein-related, putative		#N/D		16,5	DOWN	36,1
Solyc07g014680	Solyc07g014680.3	sodium transporter HKT1,2		#N/D	emb|CCJ09642.1| Na+ transporter [Solanum lycopersicum var. cerasiforme]	10,1	DOWN	34,1
Solyc01g110370	Solyc01g110370.3	Zinc finger, B-box (AHRD V3.3 ***		#N/D	ref|XP_004230952.1| PREDICTED: B-box zinc finger protein 19-like [Solanum lycopersicum]	18,5	DOWN	33,7
Solyc12g015630	Solyc12g015630.2	transmembrane protein (AHRD V3.3 *** AT5G55570.1)	101246694	LOC101246694	uncharacterized LOC101246694	10,9	DOWN	30,4
Solyc01g007895	Solyc01g007895.1	basic helix-loop-helix (bHLH) DNA-binding		#N/D	ref|XP_004228559.1| PREDICTED: putative uncharacterized protein DDB_G0282499 [Solanum	13,7	DOWN	30,2
Solyc03g093140	Solyc03g093140.3	Glycerol-3-phosphate transporter, putative (AHRD	101259222	LOC101259222	putative glycerol-3-phosphate transporter 1	8,9	DOWN	29,5
Solyc08g067540	Solyc08g067540.1	Non-specific lipid-transfer protein (AHRD V3.3	101256205	LOC101256205	non-specific lipid-transfer protein 1-like	8,9	DOWN	29,4
Solyc11g006290	Solyc11g006290.2	3-oxo-5-alpha-steroid 4-dehydrogenase family	101255051	LOC101255051	3-oxo-5-alpha-steroid 4-dehydrogenase 1-like	23,8	DOWN	28,9
Solyc07g063120	Solyc07g063120.3	Ubiquitin ligase protein cop1, putative (AHRD		#N/D	ref|XP_004244232.1| PREDICTED: protein SPA1-RELATED 4-like [Solanum lycopersicum]	9,2	DOWN	28,8
Solyc04g009795	Solyc04g009795.1	EEIG1/EHBP1 N-terminal domain-containing protein		#N/D	ref|XP_004236801.1| PREDICTED: uncharacterized protein LOC101251972 [Solanum lycopersicum]	12,7	DOWN	27,3
Solyc02g072540	Solyc02g072540.3	Non-specific serine/threonine protein kinase	101251538	LOC101251538	CBL-interacting serine/threonine-protein kinase 20	8,6	DOWN	26,2
Solyc01g096620	Solyc01g096620.3	MATH and LRR domain-containing protein PFE0570w,		#N/D	ref|XP_010324123.1| PREDICTED: ACI112 protein isoform X1 [Solanum lycopersicum]	15,0	DOWN	25,4
Solyc04g082290	Solyc04g082290.3	At1g76250 (AHRD V3.3 *-* Q8GX25_ARATH)	101255492	LOC101255492	uncharacterized LOC101255492	15,7	DOWN	24,7
Solyc07g056240	Solyc07g056240.3	TRNA-methyltransferase (AHRD V3.3 ***	101250133	LOC101250133	uncharacterized LOC101250133	10,3	DOWN	24,3
Solyc04g011780	Solyc04g011780.1	Glutaredoxin (AHRD V3.3 *** A0A103XEX1_CYNCS)		#N/D	ref|XP_004236715.1| PREDICTED: monothiol glutaredoxin-S1-like [Solanum lycopersicum]	11,9	DOWN	24,0
Solyc10g083940	Solyc10g083940.1	Nodulin-like / Major Facilitator Superfamily	101244136	LOC101244136	uncharacterized LOC101244136	18,5	DOWN	23,7
Solyc06g068970	Solyc06g068970.3	3-oxo-5-alpha-steroid 4-dehydrogenase (AHRD V3.3	101250128	LOC101250128	uncharacterized LOC101250128	11,3	DOWN	20,2
Solyc08g077170	Solyc08g077170.3	Peptide transporter, putative (AHRD V3.3 ***	101263538	LOC101263538	ref|XP_004245877.1| PREDICTED: protein NRT1/ PTR FAMILY 7.3 [Solanum lycopersicum]	42,5	DOWN	19,9
Solyc12g005660	Solyc12g005660.2	Zinc finger, B-box (AHRD V3.3 *-*	101055534	LOC101055534	Hop-interacting protein THI121	13,1	DOWN	19,9
Solyc09g092490	Solyc09g092490.3	Glycosyltransferase (AHRD V3.3 *-* B6EWX4_LYCBA)		#N/D	ref|XP_004247896.2| PREDICTED: crocetin glucosyltransferase, chloroplastic-like [Solanum	34,5	DOWN	19,7
Solyc06g049050	Solyc06g049050.3	expansin 2	543582	EXP2	expansin	9,7	DOWN	19,6
Solyc02g093720	Solyc02g093720.3	TPX2 (Targeting protein for Xklp2) family		#N/D	ref|XP_004231816.1| PREDICTED: histone H3.v1-like [Solanum lycopersicum]	14,6	DOWN	18,7
Solyc01g110720	Solyc01g110720.2	SAUR-like auxin-responsive protein family (AHRD	109118704	LOC109118704	auxin-induced protein 15A-like	10,0	DOWN	18,1
Solyc09g056000	Solyc09g056000.1	LOW QUALITY:30S ribosomal protein S4,		#N/D		nan	DOWN	17,2
Solyc11g042630	Solyc11g042630.2	DUF506 family protein (AHRD V3.3 ***		#N/D	ref|XP_004250717.2| PREDICTED: uncharacterized protein LOC101267284 [Solanum lycopersicum]	42,5	DOWN	17,0
Solyc08g005100	Solyc08g005100.3	PLATZ transcription factor family protein (AHRD	101268014	LOC101268014	uncharacterized LOC101268014	9,3	DOWN	16,0
Solyc07g005370	Solyc07g005370.3	Pathogenesis-related (PR)-10-related	101262127	LOC101262127	S-norcoclaurine synthase 1-like	21,1	DOWN	13,5
Solyc05g010060	Solyc05g010060.3	Phosphate transporter PHO1-like protein (AHRD	101244953	LOC101244953	phosphate transporter PHO1 homolog 1	10,8	DOWN	13,3
Solyc04g050440	Solyc04g050440.3	ammonium transporter	544110	AMT1-2	ammonium transporter	19,1	DOWN	13,2
Solyc10g007110	Solyc10g007110.3	Tyrosine aminotransferase (AHRD V3.3 ***		#N/D	ref|XP_004248255.1| PREDICTED: probable aminotransferase TAT2 [Solanum lycopersicum]	11,4	DOWN	12,9
Solyc11g006300	Solyc11g006300.2	3-oxo-5-alpha-steroid 4-dehydrogenase family	101255353	LOC101255353	ref|XP_004249926.1| PREDICTED: very-long-chain enoyl-CoA reductase-like [Solanum	81,6	DOWN	12,8
Solyc09g091960	Solyc09g091960.3	High mobility group B-like protein (AHRD V3.3 ***	101265586	LOC101265586	ref|XP_004247860.1| PREDICTED: high mobility group B protein 15 [Solanum lycopersicum]	41,9	DOWN	12,7
Solyc05g024260	Solyc05g024260.3	Bidirectional sugar transporter SWEET (AHRD V3.3	101255592	LOC101255592	bidirectional sugar transporter N3	20,1	DOWN	12,4
Solyc03g096770	Solyc03g096770.1	Response to low sulfur protein, putative (AHRD	101243684	LOC101243684	uncharacterized LOC101243684	8,9	DOWN	12,2
Solyc12g094580	Solyc12g094580.2	AT hook motif DNA-binding family protein (AHRD		#N/D	ref|XP_008358871.1| PREDICTED: uncharacterized protein LOC103422586 [Malus domestica]	8,6	DOWN	11,9
Solyc09g082550	Solyc09g082550.3	Sulfate transporter (AHRD V3.3 *** D7LTZ8_ARALL)	101253320	LOC101253320	ref|XP_004247591.1| PREDICTED: sulfate transporter 3.1-like [Solanum lycopersicum]	41,5	DOWN	11,9
Solyc10g054820	Solyc10g054820.2	X-intrinsic protein 1.2	101251423	LOC101251423	probable aquaporin TIP3-1	9,7	DOWN	11,6
Solyc12g094585	Solyc12g094585.1	inactive purple acid phosphatase-like protein		#N/D	ref|XP_004253200.1| PREDICTED: uncharacterized protein LOC101248373 [Solanum lycopersicum]	10,0	DOWN	10,9
Solyc08g007540	Solyc08g007540.3	ACT domain-containing family protein (AHRD V3.3	101243731	LOC101243731	ACT domain-containing protein ACR8	10,0	DOWN	10,9
Solyc04g072740	Solyc04g072740.3	Sulfate transporter, putative (AHRD V3.3 ***	101245940	LOC101245940	low affinity sulfate transporter 3	10,2	DOWN	10,8
Solyc01g006790	Solyc01g006790.2	BnaAnng41820D protein (AHRD V3.3 ***	101264148	LOC101264148	uncharacterized LOC101264148	9,1	DOWN	10,5
Solyc07g055560	Solyc07g055560.3	Cytochrome P450 (AHRD V3.3 *** A0A124SAX2_CYNCS)	101262533	LOC101262533	ref|XP_004243253.1| PREDICTED: cytochrome P450 CYP72A219 [Solanum lycopersicum]	84,1	DOWN	10,2

SGN locus	Gene_name Gene ID	ITAG3.0 gene description	NCBI GeneID	NCBI Symbol	NCBI description / 1st blastp hit / 2nd blastp hit	fold_ change	direction	total_ fpkm
H/-Fe versus H/+Fe_UPREGULATED								
Solyc07g044910	Solyc07g044910.1	LOW QUALITY:NAC domain containing protein 90		#N/D	putative IRON MAN peptide	nan	UP	4564,8
Solyc07g044900	Solyc07g044900.1	LOW QUALITY:AP2/B3-like transcriptional factor		#N/D	putative IRON MAN peptide	nan	UP	3226,0
Solyc09g092110	Solyc09g092110.3	Light-regulated (AHRD V3.3 *** A0A0B0P5I2_GOSAR)	101268227	LOC101268227	light-regulated protein	8,1	UP	3207,7
Solyc07g064160	Solyc07g064160.3	Thiamine thiazole synthase, chloroplastic (AHRD	101257192	LOC101257192	thiamine thiazole synthase, chloroplastic	3,5	UP	1283,6
Solyc09g015300	Solyc09g015300.1	Photosystem I P700 chlorophyll a apoprotein A1		psaA LyesC2p065	ref|XP_006445529.1| hypothetical protein CICLE_v10004112mg, partial [Citrus clementina]	11,7	UP	665,7
Solyc07g054760	Solyc07g054760.1	LOW QUALITY:Wound-responsive family protein (AHRD	101254813	LOC101254813	uncharacterized LOC101254813	3,9	UP	442,1
Solyc12g098850	Solyc12g098850.2	ethylene-forming enzyme		#N/D	ref|XP_004252959.1| PREDICTED: UPF0396 protein CG6066 [Solanum lycopersicum]	3,1	UP	428,3
Solyc12g006770	Solyc12g006770.1	glutathione S-transferase zeta 1 (AHRD V3.3 --*		#N/D	putative IRON MAN peptide	75,2	UP	405,5
Solyc07g054780	Solyc07g054780.1	LOW QUALITY:Wound-responsive family protein (AHRD	544070	LOC544070	uncharacterized LOC544070	5,7	UP	391,1
Solyc09g092430	Solyc09g092430.3	Selenium binding family protein (AHRD V3.3 ***	101249583	LOC101249583	selenium-binding protein 2	3,0	UP	389,0
Solyc03g083420	Solyc03g083420.3	OBP3-responsive protein 1 (AHRD V3.3 ***	101254880	LOC101254880	probable plastid-lipid-associated protein 14, chloroplastic	10,5	UP	275,0
Solyc12g006750	Solyc12g006750.1	glutathione S-transferase zeta 1 (AHRD V3.3 --*		#N/D	putative IRON MAN peptide	nan	UP	271,1
Solyc03g005780	Solyc03g005780.3	chlorophyll a/b-binding protein Cab-3C	108491835	Cab-3C	chlorophyll a/b-binding protein Cab-3C	3,0	UP	246,5
Solyc06g049020	Solyc06g049020.1	Sorghum bicolor protein targeted either to	101254906	LOC101254906	uncharacterized LOC101254906	3,8	UP	227,2
Solyc02g070950	Solyc02g070950.1	Chlorophyll a-b binding protein, chloroplastic	101264784	CAB1B	chlorophyll a/b-binding protein Cab-1B	3,2	UP	221,4
Solyc10g045530	Solyc10g045530.1	LOW QUALITY:Diacylglycerol kinase family protein		#N/D		nan	UP	217,8
Solyc01g006020	Solyc01g006020.3	6,7-dimethyl-8-ribityllumazine synthase (AHRD	101264357	LOC101264357	uncharacterized LOC101264357	3,2	UP	207,9
Solyc11g012700	Solyc11g012700.2	oligopeptide transporter (AHRD V3.3 ***	101265194	LOC101265194	oligopeptide transporter 3	4,8	UP	207,9
Solyc02g077430	Solyc02g077430.3	Phospholipase A1 (AHRD V3.3 *** A5YW95_CAPAN)		#N/D	ref|XP_004232942.2| PREDICTED: phospholipase A1-IIgamma-like [Solanum lycopersicum]	3,4	UP	180,1
Solyc08g082680	Solyc08g082680.3	RING/U-box superfamily protein (AHRD V3.3 ***	101250143	LOC101250143	probable E3 ubiquitin-protein ligase RHA4A	4,3	UP	173,5
Solyc06g071820	Solyc06g071820.3	BTB/POZ and TAZ domain protein (AHRD V3.3 ***	101263123	LOC101263123	BTB/POZ and TAZ domain-containing protein 1-like	3,9	UP	170,0
Solyc01g103590	Solyc01g103590.3	Lactoylglutathione lyase / glyoxalase I family	101243831	LOC101243831	uncharacterized LOC101243831	3,2	UP	167,7
Solyc02g079240	Solyc02g079240.1	LOW QUALITY:Wound-responsive family protein (AHRD		#N/D	ref|XP_010316669.1| PREDICTED: uncharacterized protein LOC104645811 [Solanum lycopersicum	3,9	UP	166,9
Solyc04g080540	Solyc04g080540.2	DNA polymerase epsilon catalytic subunit A,	101245159	LOC101245159	uncharacterized LOC101245159	7,3	UP	150,6
Solyc04g071800	Solyc04g071800.3	Cytochrome P450 (AHRD V3.3 *** A0A0B0NSU6_GOSAR)	101251878	LOC101251878	cytochrome P450 71A1-like	3,4	UP	141,1
Solyc01g017710	Solyc01g017710.1	LOW QUALITY:ferredoxin-fold anticodon-binding		#N/D		4,7	UP	138,8
Solyc03g093800	Solyc03g093800.1	glycine-rich protein (AHRD V3.3 *-* AT5G61660.1)		#N/D	ref|XP_004235193.1| PREDICTED: glycine-rich cell wall structural protein 2-like [Solanum	2,9	UP	134,6
Solyc02g062890	Solyc02g062890.2	polyol monosaccharide transporter 5		#N/D	ref|XP_004233513.1| PREDICTED: probable polyol transporter 6 isoform X2 [Solanum	2,9	UP	128,9
Solyc09g089510	Solyc09g089510.3	Proteinase inhibitor I (AHRD V3.3 ***		#N/D	ref|XP_004247691.2| PREDICTED: proteinase inhibitor I-B [Solanum lycopersicum]	8,6	UP	127,5
Solyc05g051720	Solyc05g051720.1	Glutaredoxin family protein (AHRD V3.3 ***	101252183	LOC101252183	monothiol glutaredoxin-S1-like	4,2	UP	122,5
Solyc05g007770	Solyc05g007770.3	NAC domain TF	101244582	LOC101244582	NAC transcription factor family protein	3,6	UP	117,0
Solyc06g076570	Solyc06g076570.3	class I small heat shock protein	101264936	Hsp20.0	class I small heat shock protein	3,0	UP	113,9
Solyc02g083310	Solyc02g083310.3	Wound-responsive family protein, putative (AHRD	101247280	LOC101247280	bifunctional nuclease 2	3,5	UP	113,8
Solyc06g053220	Solyc06g053220.3	Homeobox leucine zipper protein (AHRD V3.3 ***	101264731	LOC101264731	homeobox-leucine zipper protein ATHB-12-like	2,9	UP	110,9
Solyc12g013710	Solyc12g013710.2	light dependent NADH:protochlorophyllide	101248079	LOC101248079	protochlorophyllide reductase-like	4,5	UP	110,4
Solyc07g044970	Solyc07g044970.1	LOW QUALITY:P-loop containing nucleoside		#N/D	ref|XP_016580390.1| PREDICTED: uncharacterized protein LOC107878034 isoform X1 [Capsicum	3,1	UP	106,6
Solyc04g050620	Solyc04g050620.3	Cytochrome P450 family protein (AHRD V3.3 ***	101245153	LOC101245153	cytochrome P450 CYP736A12-like	3,4	UP	106,5
Solyc08g007240	Solyc08g007240.3	Nudix hydrolase (AHRD V3.3 *** A0A061G4C5_THECC)	101261537	LOC101261537	nudix hydrolase 8	4,0	UP	103,1
Solyc09g083440	Solyc09g083440.3	PIN-I protein (AHRD V3.3 *** Q4FE22_SOLTU)	101246961	LOC101246961	wound-induced proteinase inhibitor 1	6,0	UP	101,3
Solyc09g084470	Solyc09g084470.3	Wound-induced proteinase inhibitor 1 (AHRD V3.3	543954	LOC543954	wound-induced proteinase inhibitor 1	9,0	UP	100,8
Solyc07g043420	Solyc07g043420.3	2-oxoglutarate-dependent dioxygenase 2	544002	LOC544002	2-oxoglutarate-dependent dioxygenase 2	3,0	UP	97,3
Solyc12g006740	Solyc12g006740.1	LOW QUALITY:RING/U-box superfamily protein (AHRD		#N/D	putative IRON MAN peptide	nan	UP	89,7
Solyc02g088345	Solyc02g088345.1	Transcription factor (AHRD V3.3 ***		#N/D	ref|XP_004232197.1| PREDICTED: probable WRKY transcription factor 3 [Solanum lycopersicum]	3,1	UP	78,7
Solyc10g006900	Solyc10g006900.3	light dependent NADH:protochlorophyllide	101244717	LOC101244717	light dependent NADH:protochlorophyllide oxidoreductase 3	3,3	UP	66,6
Solyc12g089240	Solyc12g089240.2	Zinc finger, B-box (AHRD V3.3 ***	101247504	LOC101247504	B-box zinc finger protein 20	2,9	UP	63,3
Solyc03g098780	Solyc03g098780.2	Cathepsin D Inhibitor	101262903	LOC101262903	aspartic protease inhibitor 1-like	3,9	UP	62,8
Solyc05g055540	Solyc05g055540.2	Major facilitator superfamily protein (AHRD V3.3	101262315	LOC101262315	uncharacterized LOC101262315	5,5	UP	56,8
Solyc09g091810	Solyc09g091810.1	LOW QUALITY:CLAVATA3/ESR-related protein (AHRD		#N/D		3,4	UP	50,6
Solyc07g043400	Solyc07g043400.1	LOW QUALITY:C2H2 and C2HC zinc fingers		#N/D		11,4	UP	48,7

SGN locus	Gene_name Gene ID	ITAG3.0 gene description	NCBI GeneID	NCBI Symbol	NCBI description / 1st blastp hit / 2nd blastp hit	fold_ change	direction	total_ fpkm
Solyc01g066190	Solyc01g066190.1	LOW QUALITY:Splicing factor 3B subunit 3 (AHRD		#N/D		7,5	UP	47,0
Solyc05g011980	Solyc05g011980.3	Photosystem II reaction center protein M (AHRD		#N/D	ref|XP_004239026.1| PREDICTED: uncharacterized protein LOC101261117 [Solanum lycopersicum	3,0	UP	45,7
Solyc08g006770	Solyc08g006770.3	2-oxoglutarate and Fe(II)-dependent oxygenase	101250715	LOC101250715	protein DMR6-LIKE OXYGENASE 2	4,2	UP	45,1
Solyc09g009530	Solyc09g009530.3	alpha/beta-Hydrolases superfamily protein (AHRD	101261737	LOC101261737	alpha/beta-Hydrolases superfamily protein	2,9	UP	41,5
Solyc01g066270	Solyc01g066270.3	LOW QUALITY:AT-hook motif nuclear-localized		#N/D		4,3	UP	41,1
Solyc07g008440	Solyc07g008440.3	Purine permease-like protein (AHRD V3.3 ***	101252698	LOC101252698	purine permease 3-like	4,2	UP	38,4
Solyc01g096420	Solyc01g096420.3	NADPH:quinone oxidoreductase (AHRD V3.3 ***	101265773	LOC101265773	NAD(P)H:quinone oxidoreductase	4,5	UP	36,9
Solyc07g066010	Solyc07g066010.3	Amino acid transporter, putative (AHRD V3.3 ***	101267140	LOC101267140	probable amino acid permease 7	3,9	UP	36,8
Solyc12g098110	Solyc12g098110.1	LOW QUALITY:Self-incompatibility S1 family	109119116	LOC109119116	uncharacterized LOC109119116	3,1	UP	35,4
Solyc11g056650	Solyc11g056650.2	bHLH transcription factor 096	101263275	LOC101263275	transcription factor bHLH81	3,5	UP	35,2
Solyc10g008270	Solyc10g008270.3	bHLH transcription factor 094	101265482	LOC101265482	uncharacterized LOC101265482	3,2	UP	34,7
Solyc10g079680	Solyc10g079680.2	bHLH transcription factor 068	101258211	LOC101258211	putative transcription factor SlbHLH068	nan	UP	33,1
Solyc06g064500	Solyc06g064500.2	O-methyltransferase (AHRD V3.3 *** F6M2M1_VITPS)		#N/D	ref|XP_004241912.1| PREDICTED: trans-resveratrol di-O-methyltransferase-like [Solanum	3,2	UP	32,7
Solyc01g017720	Solyc01g017720.2	Maturase K (AHRD V3.3 --* H9NKB3_9ASTR)		#N/D		5,2	UP	32,3
Solyc10g086380	Solyc10g086380.1	GAI-like protein 1 (AHRD V3.3 *** A1YWN9_9ROSI)	101265384	LOC101265384	DELLA protein GAI	2,9	UP	31,6
Solyc09g074600	Solyc09g074600.1	Glutaredoxin (AHRD V3.3 *** A0A103Y7J3_CYNCS)	101257598	LOC101257598	monothiol glutaredoxin-S2-like	8,6	UP	28,6
Solyc12g010020	Solyc12g010020.2	Leucine aminopeptidase A1		#N/D		10,2	UP	28,3
Solyc02g079700	Solyc02g079700.1	Serine/threonine-protein kinase (AHRD V3.3 *-*		#N/D	ref|XP_010317320.1| PREDICTED: LOW QUALITY PROTEIN: receptor-like serine/threonine-protei	3,4	UP	26,6
Solyc11g072480	Solyc11g072480.2	Tetraspanin (AHRD V3.3 *** A0A103XGG0_CYNCS)	101249329	LOC101249329	tetraspanin-3	3,1	UP	25,6
Solyc11g022590	Solyc11g022590.1	trypsin inhibitor-like protein precursor	544001	LOC544001	uncharacterized LOC544001	9,0	UP	25,1
Solyc09g084480	Solyc09g084480.3	Type I serine protease inhibitor (AHRD V3.3 ***	101247857	LOC101247857	wound-induced proteinase inhibitor 1-like	22,2	UP	24,7
Solyc01g006400	Solyc01g006400.3	Extensin-like protein (AHRD V3.3 ***	101055528	LOC101055528	Hop-interacting protein THI101	3,3	UP	23,5
Solyc07g007250	Solyc07g007250.3	Metallocarboxypeptidase inhibitor (AHRD V3.3 ***	544286	mcpi	metallocarboxypeptidase inhibitor	4,0	UP	23,3
Solyc05g047590	Solyc05g047590.3	Sl Pectinesterase	101261415	LOC101261415	probable pectinesterase/pectinesterase inhibitor 12	3,3	UP	22,6
Solyc02g090120	Solyc02g090120.1	LOW QUALITY:Inositol 1,4,5-trisphosphate		#N/D	ref|XP_009625215.1| PREDICTED: uncharacterized protein LOC104116127 [Nicotiana tomentosifo	4,1	UP	22,0
Solyc02g080120	Solyc02g080120.2	Gibberellin 2-beta- dioxygenase 7	101263073	LOC101263073	gibberellin 2-beta-dioxygenase 8	4,4	UP	21,3
Solyc11g005650	Solyc11g005650.1	Ubiquitin family protein (AHRD V3.3 *-*		#N/D	dbj|BAJ61942.1| ubiquitin, partial [Nymphaea hybrid cultivar]	3,3	UP	21,3
Solyc07g007150	Solyc07g007150.1	LOW QUALITY:Guanine nucleotide-binding protein	104648246	LOC104648246	uncharacterized LOC104648246	4,2	UP	21,0
Solyc12g087860	Solyc12g087860.2	RING/U-box superfamily protein, putative (AHRD	101250098	LOC101250098	E3 ubiquitin-protein ligase ATL6-like	2,9	UP	20,8
Solyc09g089580	Solyc09g089580.3	2-oxoglutarate (2OG) and Fe(II)-dependent	101268031	ACO3	1-aminocyclopropane-1-carboxylate oxidase homolog	3,1	UP	19,9
Solyc03g006410	Solyc03g006410.3	DUF506 family protein (AHRD V3.3 ***		#N/D	ref|XP_004234117.1| PREDICTED: uncharacterized protein LOC101259314 [Solanum lycopersicum	4,7	UP	18,9
Solyc10g006640	Solyc10g006640.3	bHLH transcription factor153	101264865	LOC101264865	transcription factor bHLH123-like	3,3	UP	18,8
Solyc01g007980	Solyc01g007980.3	Protein kinase family protein (AHRD V3.3 ***		#N/D	ref|XP_015066642.1| PREDICTED: cysteine-rich receptor-like protein kinase 2 isoform	2,9	UP	17,6
Solyc02g087740	Solyc02g087740.3	2-aminoethanethiol dioxygenase (AHRD V3.3 ***	101258715	LOC101258715	plant cysteine oxidase 2	3,6	UP	17,0
Solyc05g046270	Solyc05g046270.3	Protein Ycf2 (AHRD V3.3 --* YCF2_OENGL)	101266224	LOC101266224	uncharacterized LOC101266224	2,9	UP	16,7
Solyc07g063830	Solyc07g063830.3	bHLH transcription factor142	101263532	LOC101263532	transcription factor bHLH123	3,9	UP	16,4
Solyc07g054430	Solyc07g054430.3	Glutamate formiminotransferase 1 (AHRD V3.3 ***	101260836	LOC101260836	formimidoyltransferase-cyclodeaminase	3,3	UP	16,4
Solyc08g008140	Solyc08g008140.3	Sumo ligase, putative (AHRD V3.3 --*		#N/D	ref|XP_010324635.1| PREDICTED: uncharacterized protein LOC101255315 isoform X2 [Solanum	2,9	UP	15,8
Solyc07g054790	Solyc07g054790.1	Wound-responsive family protein (AHRD V3.3 ***	101253603	LOC101253603	uncharacterized LOC101253603	5,1	UP	15,6
Solyc03g081240	Solyc03g081240.3	Two-component response regulator-like protein	101250283	LOC101250283	two-component response regulator-like APRR5	4,1	UP	15,0
Solyc09g008830	Solyc09g008830.3	Transcription factor, putative (AHRD V3.3 ***		#N/D	ref|XP_010325945.1| PREDICTED: putative DNA helicase INO80 [Solanum lycopersicum]	3,7	UP	13,9
Solyc09g008670	Solyc09g008670.3	threonine deaminase	543983	LOC543983	threonine dehydratase biosynthetic, chloroplastic	7,3	UP	13,5
Solyc01g091170	Solyc01g091170.3	arginase 2 ARG2	544271	ARG2	arginase 2	3,2	UP	13,2
Solyc12g006730	Solyc12g006730.1	LOW QUALITY:glutathione S-transferase zeta 1		#N/D	putative IRON MAN peptide	nan	UP	13,1
Solyc05g009860	Solyc05g009860.2	Leucoanthocyanidin reductase (AHRD V3.3 *-*		#N/D	ref|XP_006362568.1| PREDICTED: leucoanthocyanidin reductase-like [Solanum tuberosum]	6,5	UP	12,3
Solyc01g017730	Solyc01g017730.1	LOW QUALITY:ARM repeat superfamily protein (AHRD		#N/D		4,9	UP	11,5
Solyc03g005330	Solyc03g005330.1	Non-specific serine/threonine protein kinase	101258333	LOC101258333	CBL-interacting serine/threonine-protein kinase 7	4,4	UP	10,9
Solyc07g043390	Solyc07g043390.3	Cellulose synthase (AHRD V3.3 ***		#N/D	ref|XP_004243640.1| PREDICTED: cellulose synthase-like protein G2 [Solanum lycopersicum]	14,6	UP	10,8
Solyc01g087785	Solyc01g087785.1	Subtilisin-like protease SDD1 (AHRD V3.3 *-*		#N/D	ref|XP_016489542.1| PREDICTED: subtilisin-like protease SBT1.9 [Nicotiana tabacum]	3,1	UP	10,1
Solyc07g043480	Solyc07g043480.1	Glycosyltransferase (AHRD V3.3 ***	101254402	LOC101254402	zeatin O-xylosyltransferase-like	4,6	UP	10,1
Solyc08g074630	Solyc08g074630.2	polyphenol oxidase precursor	101259064	LOC101259064	polyphenol oxidase F, chloroplastic	4,2	UP	10,1

SGN locus	Gene_name Gene ID	ITAG3.0 gene description	NCBI GeneID	NCBI Symbol	NCBI description / 1st blastp hit / 2nd blastp hit	fold_ change	direction	total_ fpkm
H/-Fe versus H/+Fe_DOWNREGULATED								
Solyc03g083770	Solyc03g083770.1	Plant invertase/pectin methylesterase inhibitor	101248367	LOC101248367	21 kDa protein-like	4,6	DOWN	655,5
Solyc12g006260	Solyc12g006260.1	L-fucokinase/GDP-L-fucose pyrophosphorylase (AHRD		#N/D	ref|XP_006352002.1| PREDICTED: uncharacterized protein LOC102602513 [Solanum tuberosum]	5,6	DOWN	593,7
Solyc02g089350	Solyc02g089350.3	Gibberellin-regulated family protein (AHRD V3.3	101248254	LOC101248254	protein GAST1-like	6,4	DOWN	450,2
Solyc09g092520	Solyc09g092520.3	xyloglucan endotransglycosylase	543637	LOC543637	brassinosteroid-regulated protein BRU1	14,4	DOWN	422,9
Solyc07g054470	Solyc07g054470.1	methionyl-tRNA synthetase (AHRD V3.3 -**	101259953	LOC101259953	uncharacterized LOC101259953	5,7	DOWN	321,6
Solyc06g050980	Solyc06g050980.3	Ferritin (AHRD V3.3 *** K4C5P1_SOLLC)	104647958	LOC104647958	ferritin-1, chloroplastic	7,0	DOWN	306,6
Solyc02g080640	Solyc02g080640.3	adenylyl-sulfate reductase	544267	LOC544267	adenylyl-sulfate reductase	4,7	DOWN	242,7
Solyc11g013810	Solyc11g013810.2	Nitrate reductase (AHRD V3.3 *** K4D6I5_SOLLC)	100736473	NR	nitrate reductase [NADH] E value 0.0	8,1	DOWN	222,5
Solyc06g076790	Solyc06g076790.1	LOW QUALITY:Thylakoid soluble phosphoprotein	101259757	LOC101259757	uncharacterized LOC101259757	5,9	DOWN	219,3
Solyc09g011080	Solyc09g011080.3	ribulose bisphosphate carboxylase/oxygenase activase 1, chlo	101250725	LOC101250725	ribulose bisphosphate carboxylase/oxygenase activase 1, chloroplastic	7,4	DOWN	192,4
Solyc08g077020	Solyc08g077020.1	Auxin responsive SAUR protein (AHRD V3.3 ***	101266965	LOC101266965	uncharacterized LOC101266965	4,3	DOWN	188,7
Solyc03g113910	Solyc03g113910.3	Snakin-2-like protein (AHRD V3.3 ***	101256861	LOC101256861	gibberellin-regulated protein 10	4,2	DOWN	184,0
Solyc01g102610	Solyc01g102610.3	Ferric reduction oxidase 7 (AHRD V3.3 ***	101246763	LOC101246763	ferric reduction oxidase 6	5,5	DOWN	168,1
Solyc05g007830	Solyc05g007830.3	expansin12	543795	LOC543795	expansin12	7,2	DOWN	136,7
Solyc04g074410	Solyc04g074410.2	Phosphate-responsive 1 family protein (AHRD V3.3	101260427	LOC101260427	protein EXORDIUM-like	4,4	DOWN	128,0
Solyc03g111120	Solyc03g111120.3	Malate synthase (AHRD V3.3 *** M1B824_SOLTU)	101267395	LOC101267395	malate synthase, glyoxysomal	4,9	DOWN	105,4
Solyc01g100490	Solyc01g100490.3	chloronerva	101248619	CHLN	nicotianamine synthase-like	5,0	DOWN	105,4
Solyc02g084420	Solyc02g084420.3	B-box zinc finger family protein (AHRD V3.3 ***		#N/D	B-box zinc finger protein 19? E value 3e-78	7,3	DOWN	103,1
Solyc04g082140	Solyc04g082140.3	pectinesterase	778302	LOC778302	multicopper oxidase-like protein	4,4	DOWN	101,5
Solyc06g061230	Solyc06g061230.3	Metallocarboxypeptidase inhibitor (AHRD V3.3 -**		#N/D		4,5	DOWN	90,0
Solyc10g084370	Solyc10g084370.2	MYB transcription factor (AHRD V3.3 ***	101253545	LOC101253545	protein REVEILLE 8	4,3	DOWN	84,3
Solyc02g083880	Solyc02g083880.3	Gibberellin-regulated protein 2, putative (AHRD	101259800	LOC101259800	gibberellin-regulated protein 11	4,8	DOWN	83,7
Solyc02g032840	Solyc02g032840.1	CDP-diacylglycerol--glycerol-3-phosphate		#N/D		8,7	DOWN	81,8
Solyc02g084430	Solyc02g084430.3	B-box type zinc finger family protein (AHRD V3.3		#N/D	ref|XP_015066178.1| PREDICTED: B-box zinc finger protein 19-like [Solanum pennellii]	7,6	DOWN	74,7
Solyc12g005750	Solyc12g005750.1	LOW QUALITY:Zinc finger protein CONSTANS-LIKE 14		#N/D	ref|XP_009802590.1| PREDICTED: probable salt tolerance-like protein At1g75540 [Nicotiana	4,1	DOWN	69,1
Solyc01g079150	Solyc01g079150.3	Boron transporter (AHRD V3.3 *** B6V758_VITVI)	101260863	LOC101260863	boron transporter 1	4,2	DOWN	65,7
Solyc08g082590	Solyc08g082590.3	Glutaredoxin (AHRD V3.3 *** A0A103XR19_CYNCS)	101252103	LOC101252103	glutaredoxin domain-containing cysteine-rich protein 1	6,7	DOWN	65,5
Solyc05g007880	Solyc05g007880.3	Dof zinc finger protein (AHRD V3.3 ***	101248009	LOC101248009	cyclic dof factor 1	8,2	DOWN	61,9
Solyc05g011890	Solyc05g011890.1	Sulfotransferase (AHRD V3.3 *** K4BXR2_SOLLC)	101259437	LOC101259437	cytosolic sulfotransferase 12-like	10,4	DOWN	61,8
Solyc09g092500	Solyc09g092500.1	Glycosyltransferase (AHRD V3.3 *** K4CWS6_SOLLC)	101250450	SlUGT75C1	ABA uridine diphosphate glucosyltransferase	5,3	DOWN	61,7
Solyc03g083560	Solyc03g083560.1	Phosphate-responsive 1 family protein (AHRD V3.3	101250380	LOC101250380	protein EXORDIUM-like 3	12,8	DOWN	60,2
Solyc12g019700	Solyc12g019700.1	Protein Ycf2 (AHRD V3.3 --* YCF2_CHLSC)		#N/D		4,4	DOWN	59,6
Solyc02g036370	Solyc02g036370.3	Myb family transcription factor	101261079	LOC101261079	protein REVEILLE 1	5,7	DOWN	58,0
Solyc01g086640	Solyc01g086640.2	LOW QUALITY:O-fucosyltransferase family protein	101260866	LOC101260866	uncharacterized protein At1g04910-like	6,5	DOWN	50,1
Solyc08g007130	Solyc08g007130.3	Beta-amylase (AHRD V3.3 *** K4CIK0_SOLLC)	101259175	LOC101259175	beta-amylase 3, chloroplastic-like	5,2	DOWN	49,7
Solyc02g092110	Solyc02g092110.3	Phytosulfokines 3 family protein (AHRD V3.3 ***	101268443	PSK4	phytosulfokines 3	4,2	DOWN	46,7
Solyc10g050670	Solyc10g050670.1	LOW QUALITY:LOB domain-containing protein 7 (AHRD		#N/D		nan	DOWN	45,9
Solyc02g088390	Solyc02g088390.3	Blue copper protein, putative (AHRD V3.3 ***		#N/D	ref|XP_004232193.1| PREDICTED: lamin-like protein [Solanum lycopersicum]	4,7	DOWN	45,5
Solyc09g010530	Solyc09g010530.3	Cation/H(+) antiporter (AHRD V3.3 ***	101249848	LOC101249848	cation/H(+) antiporter 20	9,5	DOWN	44,5
Solyc03g096760	Solyc03g096760.1	Response to low sulfur protein, putative (AHRD	101268660	LOC101268660	uncharacterized LOC101268660	6,0	DOWN	43,3
Solyc01g079580	Solyc01g079580.3	DNAJ heat shock N-terminal domain-containing	101245693	LOC101245693	uncharacterized LOC101245693	6,2	DOWN	39,7
Solyc11g006290	Solyc11g006290.2	3-oxo-5-alpha-steroid 4-dehydrogenase family	101255051	LOC101255051	3-oxo-5-alpha-steroid 4-dehydrogenase 1-like	4,8	DOWN	33,5
Solyc03g025720	Solyc03g025720.3	4-coumarate:CoA ligase-like protein (AHRD V3.3	101251259	LOC101251259	oxalate--CoA ligase-like	4,3	DOWN	32,8
Solyc01g065700	Solyc01g065700.3	Protein phosphatase 2C family protein (AHRD V3.3	101265959	LOC101265959	probable protein phosphatase 2C 34	8,5	DOWN	32,5
Solyc03g093140	Solyc03g093140.3	Glycerol-3-phosphate transporter, putative (AHRD	101259222	LOC101259222	putative glycerol-3-phosphate transporter 1	5,5	DOWN	31,4
Solyc06g064610	Solyc06g064610.1	LOW QUALITY:Glucan endo-1,3-beta-glucosidase		#N/D	ref|XP_016558456.1| PREDICTED: uncharacterized protein LOC107858292 [Capsicum annuum]	8,8	DOWN	31,3
Solyc04g074165	Solyc04g074165.1	Hydroxyproline-rich glycoprotein (AHRD V3.3 -**		#N/D	ref|XP_009586797.1| PREDICTED: classical arabinogalactan protein 25-like [Nicotiana	6,2	DOWN	30,5
Solyc08g079090	Solyc08g079090.3	Monocopper oxidase-like protein SKU5 (AHRD V3.3	101247352	LOC101247352	monocopper oxidase-like protein SKU5	4,2	DOWN	30,2
Solyc03g025710	Solyc03g025710.3	Acyl-CoA N-acyltransferases-like protein (AHRD	101251856	LOC101251856	uncharacterized LOC101251856	14,7	DOWN	29,1
Solyc03g097050	Solyc03g097050.3	Cellulose synthase-like protein (AHRD V3.3 ***		#N/D	ref|XP_004235281.1| PREDICTED: cellulose synthase-like protein D3 [Solanum lycopersicum]	4,1	DOWN	29,1
Solyc06g008990	Solyc06g008990.1	LOW QUALITY:Fantastic four-like protein (AHRD	101268871	LOC101268871	protein FANTASTIC FOUR 1-like	4,8	DOWN	28,1
Solyc02g089620	Solyc02g089620.3	proline dehydrogenase	778202	PDH	proline dehydrogenase	13,1	DOWN	27,9

SGN locus	Gene_name Gene ID	ITAG3.0 gene description	NCBI GeneID	NCBI Symbol	NCBI description / 1st blastp hit / 2nd blastp hit	fold_ change	direction	total_ fpkm
Solyc03g093180	Solyc03g093180.1	Peroxisomal membrane protein 11-4 (AHRD V3.3 ***	101259820	LOC101259820	peroxisomal membrane protein 11B	4,3	DOWN	26,0
Solyc10g083940	Solyc10g083940.1	Nodulin-like / Major Facilitator Superfamily	101244136	LOC101244136	uncharacterized LOC101244136	7,7	DOWN	25,4
Solyc04g071165	Solyc04g071165.1	Vacuolar iron transporter (AHRD V3.3 ***		#N/D	ref|XP_004237778.1| PREDICTED: vacuolar iron transporter homolog 1-like [Solanum	6,8	DOWN	25,1
Solyc03g007760	Solyc03g007760.3	P-loop containing nucleoside triphosphate	101260609	LOC101260609	uncharacterized LOC101260609	4,1	DOWN	23,4
Solyc05g006510	Solyc05g006510.1	Hexosyltransferase (AHRD V3.3 *** K4BWH7_SOLLC)		#N/D	ref|XP_004238733.1| PREDICTED: probable galacturonosyltransferase-like 9 [Solanum	5,2	DOWN	22,9
Solyc02g088240	Solyc02g088240.3	Phosphate transporter PHO1-like protein (AHRD		#N/D	ref|XP_004232204.1| PREDICTED: phosphate transporter PHO1 homolog 3 [Solanum lycopersicur	9,2	DOWN	22,6
Solyc01g089850	Solyc01g089850.3	cyclinU4_1	101251921	LOC101251921	cyclin-U4-1	6,4	DOWN	22,6
Solyc07g006040	Solyc07g006040.3	DNA-directed RNA polymerase subunit beta (AHRD		#N/D	ref|XP_016554707.1| PREDICTED: uncharacterized protein LOC107854224 [Capsicum annuum]	6,2	DOWN	22,4
Solyc01g102350	Solyc01g102350.3	Pectinacetylesterase family protein (AHRD V3.3	101268518	LOC101268518	pectin acetylesterase 12	4,6	DOWN	22,3
Solyc07g045185	Solyc07g045185.1	CONSTANS-like zinc finger protein (AHRD V3.3 *-*		#N/D	ref|XP_004243599.1| PREDICTED: zinc finger protein CONSTANS-LIKE 10 [Solanum lycopersicum]	10,0	DOWN	22,1
Solyc09g092490	Solyc09g092490.3	Glycosyltransferase (AHRD V3.3 *-* B6EWX4_LYCBA)		#N/D	ref|XP_004247896.2| PREDICTED: crocetin glucosyltransferase, chloroplastic-like [Solanum	7,7	DOWN	21,7
Solyc03g097170	Solyc03g097170.3	Cinnamoyl-CoA reductase, putative (AHRD V3.3 ***	101262601	LOC101262601	cinnamoyl-CoA reductase-like SNL6	4,2	DOWN	21,4
Solyc02g093720	Solyc02g093720.3	TPX2 (Targeting protein for Xklp2) family		#N/D	ref|XP_004231816.1| PREDICTED: histone H3.v1-like [Solanum lycopersicum]	4,9	DOWN	21,1
Solyc06g049050	Solyc06g049050.3	expansin 2	543582	EXP2	expansin	5,5	DOWN	21,0
Solyc06g007160	Solyc06g007160.3	Internal alternative NAD(P)H-ubiquinone	101266519	LOC101266519	internal alternative NAD(P)H-ubiquinone oxidoreductase A1, mitochondrial	4,2	DOWN	20,7
Solyc06g030470	Solyc06g030470.3	Domain of Uncharacterized protein function,	101255003	LOC101255003	protein UPSTREAM OF FLC	4,1	DOWN	20,5
Solyc02g092580	Solyc02g092580.3	Peroxidase (AHRD V3.3 *** K4BD54_SOLLC)	101257228	LOC101257228	peroxidase 51	8,1	DOWN	20,3
Solyc07g045180	Solyc07g045180.3	CONSTANS-like zinc finger protein (AHRD V3.3 ***		#N/D	ref|XP_004243599.1| PREDICTED: zinc finger protein CONSTANS-LIKE 10 [Solanum lycopersicum]	11,4	DOWN	19,6
Solyc06g051680	Solyc06g051680.1	Protein EARLY FLOWERING 4 (AHRD V3.3 *-*		#N/D	ref|XP_009629950.1| PREDICTED: protein EARLY FLOWERING 4-like [Nicotiana tomentosiformis]	5,3	DOWN	19,2
Solyc02g063000	Solyc02g063000.3	Glycosyltransferase (AHRD V3.3 *** K4B6I8_SOLLC)	101261193	LOC101261193	ref|XP_004233506.1| PREDICTED: anthocyanidin 3-O-glucosyltransferase 5-like [Solanum	46,9	DOWN	18,3
Solyc06g053700	Solyc06g053700.1	ATBET12, putative (AHRD V3.3 *** B9STJ3_RICCO)	101250806	LOC101250806	uncharacterized protein At4g14450, chloroplastic-like	4,1	DOWN	18,2
Solyc06g076350	Solyc06g076350.3	LePCL1		#N/D	ref|NP_001308215.1| transcription factor PCL1 [Solanum lycopersicum]	4,5	DOWN	17,7
Solyc05g005760	Solyc05g005760.3	NHL repeat-containing family protein (AHRD V3.3	101255990	LOC101255990	uncharacterized LOC101255990	4,2	DOWN	17,2
Solyc04g007470	Solyc04g007470.3	Drought responsive Zinc finger protein	101253772	LOC101253772	ref|XP_004236980.1| PREDICTED: putative zinc finger protein At1g68190 isoform X2	85,8	DOWN	16,7
Solyc02g089420	Solyc02g089420.1	BZIP transcription factor family protein (AHRD	101260992	LOC101260992	basic leucine zipper 43	4,5	DOWN	16,5
Solyc01g110880	Solyc01g110880.1	SAUR-like auxin-responsive protein family (AHRD	101251524	LOC101251524	auxin-responsive protein SAUR21-like	4,5	DOWN	16,2
Solyc11g005350	Solyc11g005350.2	WAT1-related protein (AHRD V3.3 *** K4D4E8_SOLLC)	101261286	LOC101261286	WAT1-related protein At1g68170	5,1	DOWN	15,8
Solyc03g097230	Solyc03g097230.1	AIG2-like (avirulence induced gene) family	101245930	LOC101245930	putative gamma-glutamylcyclotransferase At3g02910	7,2	DOWN	15,6
Solyc02g094390	Solyc02g094390.3	S-acyltransferase (AHRD V3.3 *** K4BDN4_SOLLC)	101261378	LOC101261378	probable protein S-acyltransferase 7	5,5	DOWN	15,5
Solyc06g005320	Solyc06g005320.1	MYB-related transcription factor (AHRD V3.3 *-*		#N/D	ref|XP_015077550.1| PREDICTED: transcription factor MYB48-like [Solanum pennellii]	6,2	DOWN	15,5
Solyc04g051180	Solyc04g051180.1	Vacuolar iron transporter family protein (AHRD		#N/D	ref|XP_015072233.1| PREDICTED: vacuolar iron transporter homolog 1-like [Solanum	5,8	DOWN	15,5
Solyc03g007030	Solyc03g007030.3	CDGSH iron-sulfur domain-containing protein	101244055	LOC101244055	CDGSH iron-sulfur domain-containing protein	7,6	DOWN	15,5
Solyc09g091960	Solyc09g091960.3	High mobility group B-like protein (AHRD V3.3 ***	101265586	LOC101265586	high mobility group B protein 15	4,2	DOWN	15,4
Solyc06g007165	Solyc06g007165.1	Internal alternative NAD(P)H-ubiquinone		#N/D	ref|XP_004240404.1| PREDICTED: internal alternative NAD(P)H-ubiquinone oxidoreductase	4,2	DOWN	15,2
Solyc04g077140	Solyc04g077140.3	DUF1005 family protein (AHRD V3.3 ***	101246921	LOC101246921	uncharacterized LOC101246921	4,3	DOWN	14,1
Solyc03g093080	Solyc03g093080.3	Xyloglucan endotransglucosylase/hydrolase (AHRD	101258345	LOC101258345	probable xyloglucan endotransglucosylase/hydrolase protein 23	5,8	DOWN	13,9
Solyc11g069960	Solyc11g069960.2	RLK-1	101246212	LOC101246212	probable leucine-rich repeat receptor-like protein kinase At1g68400	7,7	DOWN	13,2
Solyc09g082550	Solyc09g082550.3	Sulfate transporter (AHRD V3.3 *** D7LTZ8_ARALL)	101253320	LOC101253320	sulfate transporter 3.1-like	9,2	DOWN	12,9
Solyc04g074310	Solyc04g074310.3	RNA-binding family protein, putative (AHRD V3.3	101258063	LOC101258063	RNA-binding protein 24-B	6,6	DOWN	12,5
Solyc11g008140	Solyc11g008140.2	Pectate lyase (AHRD V3.3 *** K4D575_SOLLC)		#N/D	ref|XP_004250039.1| PREDICTED: probable pectate lyase 13 isoform X1 [Solanum lycopersicum]	5,9	DOWN	12,5
Solyc10g054720	Solyc10g054720.1	Small auxin up-regulated RNA78	101250847	LOC101250847	auxin-induced protein 15A-like	4,9	DOWN	12,0
Solyc03g093130	Solyc03g093130.3	xyloglucan endotransglucosylase-hydrolase 3	543914	XTH3	xyloglucan endotransglucosylase-hydrolase XTH3	8,7	DOWN	11,5
Solyc07g055560	Solyc07g055560.3	Cytochrome P450 (AHRD V3.3 *** A0A124SAX2_CYNCS)		#N/D	cytochrome P450 CYP72A219	8,9	DOWN	11,2
Solyc03g083720	Solyc03g083720.1	LOW QUALITY:Plant invertase/pectin methylesterase	101248953	LOC101248953	21 kDa protein-like	4,0	DOWN	10,9
Solyc01g104780	Solyc01g104780.3	Vacuolar iron transporter family protein (AHRD	101246768	LOC101246768	vacuolar iron transporter homolog 4-like	11,3	DOWN	10,8
Solyc10g084430	Solyc10g084430.2	RING/U-box superfamily protein (AHRD V3.3 ***	101254650	LOC101254650	E3 ubiquitin-protein ligase SGR9, amyloplastic-like	23,1	DOWN	10,5
Solyc07g055690	Solyc07g055690.1	Serine/threonine-protein kinase (AHRD V3.3 ***	101260448	LOC101260448	epidermis-specific secreted glycoprotein EP1-like	6,6	DOWN	10,1
Solyc02g093590	Solyc02g093590.3	Zinc finger CONSTANS-LIKE 7-like protein (AHRD	101256821	LOC101256821	zinc finger protein CONSTANS-LIKE 16	5,7	DOWN	10,0

SGN locus	Gene_name Gene ID	ITAG3.0 gene description	NCBI GeneID	NCBI Symbol	NCBI description / 1st blastp hit / 2nd blastp hit	fold_ change	direction	total_ fpkm
I/+Fe versus H/-Fe_UPREGULATED								
Solyc07g007760	Solyc07g007760.3	defensin-like protein	101263826	DEFL1	defensin-like protein	6,43	UP	1472,11
Solyc03g083770	Solyc03g083770.1	Plant invertase/pectin methylesterase inhibitor	101248367	0	21 kDa protein-like	6,88	UP	921,32
Solyc12g006260	Solyc12g006260.1	L-fucokinase/GDP-L-fucose pyrophosphorylase (AHRD		#N/D	ref|XP_006352002.1| PREDICTED: uncharacterized protein LOC102602513 [Solanum	7,74	UP	788,64
Solyc08g016150	Solyc08g016150.1	LOW QUALITY:Avr9/Cf-9 rapidly elicited protein		#N/D	gb|AAG43556.1|AF211538_1 Avr9/Cf-9 rapidly elicited protein 180 [Nicotiana tabacum]	4,6	UP	409,54
Solyc04g071890	Solyc04g071890.3	Peroxidase (AHRD V3.3 *** K4BTH6_SOLLC)	101253377	LOC101253377	peroxidase 12	6,55	UP	355,21
Solyc05g008895	Solyc05g008895.1	Lipid transfer protein (AHRD V3.3 ***		#N/D	ref|XP_010320740.1| PREDICTED: non-specific lipid-transfer protein 2-like [Solanum	9,44	UP	336,22
Solyc06g050980	Solyc06g050980.3	Ferritin (AHRD V3.3 *** K4C5P1_SOLLC)	104647958	LOC104647958	ferritin-1, chloroplastic	6,11	UP	271,67
Solyc09g092520	Solyc09g092520.3	xyloglucan endotransglycosylase	543637	LOC543637	brassinosteroid-regulated protein BRU1	7,51	UP	234,35
Solyc04g074430	Solyc04g074430.1	Phosphate-responsive 1 family protein (AHRD V3.3		#N/D	ref|XP_004253500.2| PREDICTED: protein EXORDIUM-like [Solanum lycopersicum]	4,95	UP	209,94
Solyc04g074450	Solyc04g074450.1	Phosphate-responsive 1 family protein (AHRD V3.3	104644303	LOC104644303	protein EXORDIUM-like	4,73	UP	169,2
Solyc05g009310	Solyc05g009310.3	CONSTANS-like zinc finger protein (AHRD V3.3 ***	101253781	LOC101253781	zinc finger protein CONSTANS-LIKE 16-like	4,33	UP	159,63
Solyc02g091180	Solyc02g091180.1	LOW QUALITY:DUF4228 domain protein (AHRD V3.3 ***	104645686	LOC104645686	uncharacterized LOC104645686	4,18	UP	153,12
Solyc12g009240	Solyc12g009240.1	Ethylene-responsive transcription factor ERF017	101253257	LOC101253257	ethylene-responsive transcription factor ERF017	4,81	UP	149,54
Solyc04g074410	Solyc04g074410.2	Phosphate-responsive 1 family protein (AHRD V3.3	101260427	LOC101260427	protein EXORDIUM-like	5,24	UP	148,79
Solyc02g084850	Solyc02g084850.3	Abscisic acid and environmental stress-inducible	544056	TAS14	TAS14 peptide (AA 1-130)	4,92	UP	140,37
Solyc11g013310	Solyc11g013310.2	SlLAX3	100736478	LOC100736478	LAX3 protein	4,28	UP	115,37
Solyc01g109250	Solyc01g109250.2	LOW QUALITY:DUF4228 domain protein (AHRD V3.3 ***	101261073	LOC101261073	uncharacterized LOC101261073	5,1	UP	111,8
Solyc06g061230	Solyc06g061230.3	Metallocarboxypeptidase inhibitor (AHRD V3.3 -**		#N/D		5,43	UP	104,4
Solyc10g049420	Solyc10g049420.2	TRAF-like superfamily protein (AHRD V3.3 --*		#N/D		7,29	UP	96,62
Solyc03g026280	Solyc03g026280.3	CBF	543826	CBF1	CBF1 protein	5,45	UP	91,81
Solyc02g089990	Solyc02g089990.1	HTH-type transcriptional regulator (AHRD V3.3 ***	101260191	LOC101260191	uncharacterized LOC101260191	6,34	UP	91,46
Solyc02g094000	Solyc02g094000.1	Calcium-binding protein (AHRD V3.3 ***	101245711	LOC101245711	putative calcium-binding protein CML19	7,04	UP	77,5
Solyc06g051680	Solyc06g051680.1	Protein EARLY FLOWERING 4 (AHRD V3.3 *-*		#N/D	ref|XP_009629950.1| PREDICTED: protein EARLY FLOWERING 4-like [Nicotiana	23,99	UP	75,94
Solyc06g051660	Solyc06g051660.1	Early flowering 4 (AHRD V3.3 ***	101267898	LOC101267898	protein EARLY FLOWERING 4	5,47	UP	68,16
Solyc03g124110	Solyc03g124110.2	CBF	101263186	LOC101263186	dehydration-responsive element-binding protein 1A	4,47	UP	60,86
Solyc12g057150	Solyc12g057150.1	transmembrane protein (AHRD V3.3 --* AT2G46550.3)		#N/D		6,08	UP	55,88
Solyc01g007030	Solyc01g007030.3	U-box domain-containing family protein (AHRD V3.3		#N/D	ref|XP_010315681.1| PREDICTED: LOW QUALITY PROTEIN: E3 ubiquitin-protein ligase PUB22-	5,78	UP	52,25
Solyc07g006890	Solyc07g006890.1	Cytochrome P450, putative (AHRD V3.3 ***	101246836	LOC101246836	cytochrome P450 94A1-like	5,35	UP	51,06
Solyc05g052280	Solyc05g052280.3	Peroxidase (AHRD V3.3 *** K4C1Q9_SOLLC)	101264425	LOC101264425	peroxidase P7	4,81	UP	50,73
Solyc01g106390	Solyc01g106390.3	Glutamyl-tRNA reductase (AHRD V3.3 ***	101252440	LOC101252440	glutamyl-tRNA reductase 1, chloroplastic-like	4,48	UP	50,52
Solyc01g086640	Solyc01g086640.2	LOW QUALITY:O-fucosyltransferase family protein	101260866	LOC101260866	uncharacterized protein At1g04910-like	6,41	UP	49,42
Solyc01g079660	Solyc01g079660.2	LOW QUALITY:cotton fiber protein (AHRD V3.3 ***	101247750	LOC101247750	uncharacterized LOC101247750	7,88	UP	47,17
Solyc03g093360	Solyc03g093360.3	PLAT domain-containing protein 1 (AHRD V3.3 ***		#N/D	ref|XP_004235174.1| PREDICTED: lipoxygenase homology domain-containing protein 1-like	4,68	UP	46,07
Solyc07g054850	Solyc07g054850.3	transmembrane protein (AHRD V3.3 *** AT4G28100.1)	101252410	LOC101252410	uncharacterized GPI-anchored protein At4g28100	4,58	UP	45,39
Solyc03g114030	Solyc03g114030.3	PermeaseI-like protein	101253471	SlPer1	permease I-like protein	4,28	UP	45,32
Solyc03g082530	Solyc03g082530.1	Small auxin up-regulated RNA37		#N/D	ref|XP_015164315.1| PREDICTED: auxin-responsive protein SAUR32-like [Solanum	4,49	UP	42,21
Solyc06g030470	Solyc06g030470.3	Domain of Uncharacterized protein function,	101255003	LOC101255003	protein UPSTREAM OF FLC	8,94	UP	39,89
Solyc01g006680	Solyc01g006680.3	2-oxoglutarate (2OG) and Fe(II)-dependent		#N/D	ref|NP_001306150.1| JmjC-domain protein JMJ524 [Solanum lycopersicum]	6,77	UP	39,41
Solyc03g043860	Solyc03g043860.2	NUDIX hydrolase (AHRD V3.3 *** A0A118K334_CYNCS)	101265208	LOC101265208	nudix hydrolase 1-like	9,93	UP	36,72
Solyc06g007190	Solyc06g007190.3	Protein phosphatase 2C (AHRD V3.3 ***	101267711	LOC101267711	putative protein phosphatase 2C 53	7,5	UP	36,47
Solyc01g103470	Solyc01g103470.2	Cytosolic Fe-S cluster assembly factor nar-1		#N/D	gb|KZM81565.1| hypothetical protein DCAR_029178 [Daucus carota subsp. sativus]	4,58	UP	34,82
Solyc03g114860	Solyc03g114860.3	UDP-arabinose mutase-like protein		#N/D	ref|XP_004236070.1| PREDICTED: alpha-1,4-glucan-protein synthase [UDP-forming] 2-like	4,33	UP	33,62
Solyc12g057160	Solyc12g057160.1	Arabinogalactan protein (AHRD V3.3 ***	101246031	LOC101246031	classical arabinogalactan protein 5	5,63	UP	33,14
Solyc03g031420	Solyc03g031420.1	LOW QUALITY:Molybdenum cofactor sulfurase (AHRD	101250087	LOC101250087	molybdenum cofactor sulfurase-like	8,98	UP	32,9
Solyc11g005350	Solyc11g005350.2	WAT1-related protein (AHRD V3.3 *** K4D4E8_SOLLC)	101261286	LOC101261286	WAT1-related protein At1g68170	11,67	UP	32,77
Solyc05g051870	Solyc05g051870.3	Pollen Ole e 1 allergen/extensin (AHRD V3.3 ***	101247921	LOC101247921	anther-specific protein LAT52-like	10,53	UP	30,15
Solyc04g071165	Solyc04g071165.1	Vacuolar iron transporter (AHRD V3.3 ***		#N/D	ref|XP_004237778.1| PREDICTED: vacuolar iron transporter homolog 1-like [Solanum	8,29	UP	30,05
Solyc11g012980	Solyc11g012980.1	Ethylene-responsive transcription factor (AHRD	101253047	LOC101253047	ethylene-responsive transcription factor ERF014	8,34	UP	29,34
Solyc03g083560	Solyc03g083560.1	Phosphate-responsive 1 family protein (AHRD V3.3	101250380	LOC101250380	protein EXORDIUM-like 3	5,43	UP	28,12

SGN locus	Gene_name Gene ID	ITAG3.0 gene description	NCBI GeneID	NCBI Symbol	NCBI description / 1st blastp hit / 2nd blastp hit	fold_ change	direction	total_ fpkm
Solyc04g074165	Solyc04g074165.1	Hydroxyproline-rich glycoprotein (AHRD V3.3 -**		#N/D	ref|XP_009586797.1| PREDICTED: classical arabinogalactan protein 25-like [Nicotiana	5,5	UP	27,45
Solyc04g076730	Solyc04g076730.1	LOW QUALITY:Transmembrane protein, putative (AHRD		#N/D	emb|CDP22061.1| unnamed protein product [Coffea canephora]	4,88	UP	26,78
Solyc05g055080	Solyc05g055080.1	LOW QUALITY:P-loop containing nucleoside		#N/D		11,16	UP	26,44
Solyc03g121340	Solyc03g121340.1	LOW QUALITY:isopentenyltransferase 5 (AHRD V3.3		#N/D	gb|EYU21402.1| hypothetical protein MIMGU_mgv1a021570mg, partial [Erythranthe	5,32	UP	26,38
Solyc06g053640	Solyc06g053640.1	RING/U-box superfamily protein (AHRD V3.3 ***	101249928	LOC101249928	RING-H2 finger protein ATL16-like	5,93	UP	25,67
Solyc08g068600	Solyc08g068600.3	Aromatic amino acid decarboxylase 1B (AHRD V3.3	101264847	LOC101264847	histidine decarboxylase-like	4,17	UP	25,2
Solyc06g076350	Solyc06g076350.3	LePCL1		#N/D	ref|NP_001308215.1| transcription factor PCL1 [Solanum lycopersicum]	6,5	UP	24,28
Solyc05g006510	Solyc05g006510.1	Hexosyltransferase (AHRD V3.3 *** K4BWH7_SOLLC)		#N/D	ref|XP_004238733.1| PREDICTED: probable galacturonosyltransferase-like 9 [Solanum	5,49	UP	24,05
Solyc04g015360	Solyc04g015360.3	GATA transcription factor (AHRD V3.3 ***	101250294	LOC101250294	GATA transcription factor 8	4,95	UP	24,02
Solyc01g007020	Solyc01g007020.3	U-box domain-containing family protein (AHRD V3.3	101266548	LOC101266548	E3 ubiquitin-protein ligase PUB23-like	4,71	UP	23,76
Solyc07g053230	Solyc07g053230.3	R2R3MYB transcription factor 83		#N/D	ref|XP_004243413.1| PREDICTED: myb-related protein Myb4-like [Solanum lycopersicum]	4,35	UP	23,6
Solyc01g079110	Solyc01g079110.3	Histone H3 (AHRD V3.3 *** A0A0V0H170_SOLCH)	101260571	LOC101260571	histone H3.2-like	4,52	UP	18,73
Solyc03g006260	Solyc03g006260.3	Calcium-binding EF-hand (AHRD V3.3 *-*	101254062	LOC101254062	uncharacterized LOC101254062	6,6	UP	18,72
Solyc07g045185	Solyc07g045185.1	CONSTANS-like zinc finger protein (AHRD V3.3 *-*		#N/D	ref|XP_004243599.1| PREDICTED: zinc finger protein CONSTANS-LIKE 10 [Solanum	8,24	UP	18,49
Solyc06g035700	Solyc06g035700.1	Dehydration responsive element binding	101268109	LOC101268109	ethylene-responsive transcription factor ERF025-like	4,39	UP	18,46
Solyc02g094390	Solyc02g094390.3	S-acyltransferase (AHRD V3.3 *** K4BDN4_SOLLC)	101261378	LOC101261378	probable protein S-acyltransferase 7	6,35	UP	17,64
Solyc04g008100	Solyc04g008100.2	U-box domain-containing protein (AHRD V3.3 ***	101262803	LOC101262803	U-box domain-containing protein 21-like	7,52	UP	17,55
Solyc05g005760	Solyc05g005760.3	NHL repeat-containing family protein (AHRD V3.3	101255990	LOC101255990	uncharacterized LOC101255990	4,25	UP	17,23
Solyc03g079880	Solyc03g079880.3	Protease inhibitor/seed storage/lipid transfer		#N/D	ref|NP_001306089.1| xylem sap protein 10 kDa precursor [Solanum lycopersicum]	4,42	UP	16,95
Solyc03g093080	Solyc03g093080.3	Xyloglucan endotransglucosylase/hydrolase (AHRD	101258345	LOC101258345	probable xyloglucan endotransglucosylase/hydrolase protein 23	7,22	UP	16,85
Solyc03g115200	Solyc03g115200.3	Glucan endo-1,3-beta-glucosidase-like protein	101245933	LOC101245933	beta-1,3-glucanase family protein	6,07	UP	16,85
Solyc07g045180	Solyc07g045180.3	CONSTANS-like zinc finger protein (AHRD V3.3 ***		#N/D	ref|XP_004243599.1| PREDICTED: zinc finger protein CONSTANS-LIKE 10 [Solanum	9,51	UP	16,68
Solyc02g093590	Solyc02g093590.3	Zinc finger CONSTANS-LIKE 7-like protein (AHRD	101256821	LOC101256821	zinc finger protein CONSTANS-LIKE 16	10,12	UP	16,55
Solyc03g096550	Solyc03g096550.3	PLAT domain-containing protein 1 (AHRD V3.3 ***	101267006	LOC101267006	PLAT domain-containing protein 3-like	4,48	UP	15,75
Solyc04g051180	Solyc04g051180.1	Vacuolar iron transporter family protein (AHRD		#N/D	ref|XP_015072233.1| PREDICTED: vacuolar iron transporter homolog 1-like [Solanum	5,89	UP	15,7
Solyc10g050970	Solyc10g050970.1	Ethylene Response Factor D.4	101246484	LOC101246484	ethylene-responsive transcription factor ERF109-like	6,29	UP	15,32
Solyc02g038740	Solyc02g038740.3	3-hydroxy-3-methylglutaryl coenzyme A reductase		#N/D	ref|NP_001296119.1| 3-hydroxy-3-methylglutaryl-coenzyme A reductase 2 [Solanum	5,62	UP	14,78
Solyc03g006210	Solyc03g006210.2	Cysteine protease (AHRD V3.3 *** J7GPZ5_SOLCI)	101249528	LOC101249528	zingipain-2-like	9,97	UP	14,73
Solyc01g100010	Solyc01g100010.3	F-box protein (AHRD V3.3 *** W9RMP6_9ROSA)	101262356	LOC101262356	F-box protein PP2-B15-like	4,33	UP	14,71
Solyc07g008103	Solyc07g008103.1	Blue copper protein (AHRD V3.3 *-*		#N/D		4,41	UP	14,27
Solyc02g077060	Solyc02g077060.2	LOW QUALITY:RPW8.2-like protein (AHRD V3.3 *-*	104645842	LOC104645842	uncharacterized LOC104645842	5,67	UP	14,24
Solyc01g066570	Solyc01g066570.3	senescence-associated family protein (DUF581)	101258100	LOC101258100	uncharacterized LOC101258100	4,54	UP	14,02
Solyc03g006980	Solyc03g006980.3	Alpha-L-fucosidase 1 (AHRD V3.3 *** W9SQK3_9ROSA)		#N/D	ref|XP_010317463.1| PREDICTED: alpha-L-fucosidase 1 [Solanum lycopersicum]	4,87	UP	13,7
Solyc08g067510	Solyc08g067510.1	Non-specific lipid-transfer protein (AHRD V3.3	101246456	LOC101246456	non-specific lipid-transfer protein 1-like	4,44	UP	13,67
Solyc05g051860	Solyc05g051860.3	senescence-associated family protein, putative	101248202	LOC101248202	uncharacterized LOC101248202	4,68	UP	13,32
Solyc06g083650	Solyc06g083650.3	GDSL esterase/lipase (AHRD V3.3 ***	101267033	LOC101267033	GDSL esterase/lipase At5g33370	4,74	UP	13,17
Solyc08g068610	Solyc08g068610.3	Decarboxylase family protein IPR002129	778255	AADC1B	aromatic amino acid decarboxylase 1B	4,58	UP	13,16
Solyc04g007470	Solyc04g007470.3	Drought responsive Zinc finger protein	101253772	LOC101253772	putative zinc finger protein At1g68190	66,01	UP	12,86
Solyc06g005680	Solyc06g005680.3	Two-component response regulator (AHRD V3.3 ***		#N/D	ref|XP_004240372.1| PREDICTED: transcription factor PCL1 [Solanum lycopersicum]	47,53	UP	12,85
Solyc03g093110	Solyc03g093110.3	xyloglucan endotransglucosylase-hydrolase	101258632	LOC101258632	probable xyloglucan endotransglucosylase/hydrolase protein 23	7,14	UP	12,81
Solyc05g009490	Solyc05g009490.2	DNA polymerase epsilon catalytic subunit (AHRD		#N/D		5,6	UP	12,36
Solyc01g104780	Solyc01g104780.3	Vacuolar iron transporter family protein (AHRD	101246768	LOC101246768	vacuolar iron transporter homolog 4-like	13,01	UP	12,35
Solyc02g076850	Solyc02g076850.2	Dof zinc finger protein4	104645845	LOC104645845	dof zinc finger protein DOF1.5	9,11	UP	11,68
Solyc11g008140	Solyc11g008140.2	Pectate lyase (AHRD V3.3 *** K4D575_SOLLC)		#N/D	ref|XP_004250039.1| PREDICTED: probable pectate lyase 13 isoform X1 [Solanum	5,41	UP	11,62
Solyc06g061010	Solyc06g061010.3	senescence-associated family protein (DUF581)	101246541	LOC101246541	uncharacterized LOC101246541	4,77	UP	11,45
Solyc03g093130	Solyc03g093130.3	xyloglucan endotransglucosylase-hydrolase 3	543914	XTH3	xyloglucan endotransglucosylase-hydrolase XTH3	8,5	UP	11,31
Solyc02g089620	Solyc02g089620.3	proline dehydrogenase	778202	PDH	proline dehydrogenase	4,55	UP	11,01
Solyc10g084023	Solyc10g084023.1	SAUR-like auxin-responsive protein family (AHRD		#N/D	ref|XP_015055099.1| PREDICTED: auxin-responsive protein SAUR32-like [Solanum pennellii]	4,57	UP	10,89
Solyc06g051800	Solyc06g051800.3	expansin 1	544035	EXP1	expansin	5,13	UP	10,64
Solyc05g007300	Solyc05g007300.3	HVA22-like protein (AHRD V3.3 *** K4BWQ6_SOLLC)	101263114	LOC101263114	HVA22-like protein c	11,77	UP	10,49
Solyc10g050220	Solyc10g050220.2	cold regulated protein 27 (AHRD V3.3 ***	101251726	LOC101251726	uncharacterized LOC101251726	8,14	UP	10,31

SGN locus	Gene_name Gene ID	ITAG3.0 gene description	NCBI GeneID	NCBI Symbol	NCBI description / 1st blastp hit / 2nd blastp hit	fold_ change	direction	total_ fpkm
I/+Fe versus H/-Fe_DOWNREGULATED								
Solyc07g044910	Solyc07g044910.1	LOW QUALITY:NAC domain containing protein 90		#N/D	putative IRON MAN peptide	nan	DOWN	4564,78
Solyc07g044900	Solyc07g044900.1	LOW QUALITY:AP2/B3-like transcriptional factor		#N/D	putative IRON MAN peptide	nan	DOWN	3226,01
Solyc02g070940	Solyc02g070940.1	Chlorophyll a-b binding protein, chloroplastic	101264784	CAB1B	chlorophyll a/b-binding protein Cab-1B blastx E=0	7,17	DOWN	825,21
Solyc12g006760	Solyc12g006760.1	glutathione S-transferase zeta 1 (AHRD V3.3 --*		#N/D	putative IRON MAN peptide	210,6	DOWN	457,08
Solyc02g070970	Solyc02g070970.1	Chlorophyll a-b binding protein, chloroplastic	101264784	CAB1B	chlorophyll a/b-binding protein Cab-1B	5,74	DOWN	417,57
Solyc12g006770	Solyc12g006770.1	glutathione S-transferase zeta 1 (AHRD V3.3 --*		#N/D	putative IRON MAN peptide	27,88	DOWN	414,58
Solyc03g117590	Solyc03g117590.3	Heat shock protein binding protein (AHRD V3.3 ***	100736525	LOC100736525	heat shock protein binding protein	7,84	DOWN	332,86
Solyc05g051850	Solyc05g051850.3	putative myo-inositol-1-phosphatase	543809	LOC543809	inositol-3-phosphate synthase	5,98	DOWN	320,48
Solyc11g073120	Solyc11g073120.2	R2R3MYB transcription factor 58	101262486	LOC101262486	transcription factor MYB48	6,89	DOWN	312,33
Solyc06g054270	Solyc06g054270.3	Sugar transporter protein 11	101261239	STP11	sugar transport protein 8-like	9,89	DOWN	297,07
Solyc03g083420	Solyc03g083420.3	OBP3-responsive protein 1 (AHRD V3.3 ***	101254880	LOC101254880	probable plastid-lipid-associated protein 14, chloroplastic	8,94	DOWN	279,05
Solyc12g006750	Solyc12g006750.1	glutathione S-transferase zeta 1 (AHRD V3.3 --*		#N/D	putative IRON MAN peptide	220,5	DOWN	272,35
Solyc12g006140	Solyc12g006140.2	Cab-5 gene encoding chlorophyll a/b-binding	543976	CAB5	chlorophyll a-b binding protein 5, chloroplastic	7,39	DOWN	258,67
Solyc05g053760	Solyc05g053760.3	Chaperone protein DNAj, putative (AHRD V3.3 ***	101257564	LOC101257564	chaperone protein dnaJ 20, chloroplastic-like	5,36	DOWN	255,3
Solyc06g053840	Solyc06g053840.3	auxin-regulated IAA4	101255303	IAA4	auxin-responsive protein IAA4	6,55	DOWN	246,08
Solyc10g045530	Solyc10g045530.1	LOW QUALITY:Diacylglycerol kinase family protein		#N/D		nan	DOWN	217,817
Solyc11g012700	Solyc11g012700.2	oligopeptide transporter (AHRD V3.3 ***	101265194	LOC101265194	oligopeptide transporter 3	5,54	DOWN	202,81
Solyc03g096780	Solyc03g096780.1	Response to low sulfur protein, putative (AHRD	101243970	LOC101243970	uncharacterized LOC101243970	5,54	DOWN	195,09
Solyc07g043130	Solyc07g043130.3	Phototropic-responsive NPH3 family protein (AHRD	101259171	LOC101259171	root phototropism protein 2	6,42	DOWN	184,08
Solyc04g080540	Solyc04g080540.2	DNA polymerase epsilon catalytic subunit A,	101245159	LOC101245159	uncharacterized LOC101245159	6,34	DOWN	153,41
Solyc08g078870	Solyc08g078870.2	14 kDa proline-rich protein DC2.15, putative	101251407	LOC101251407	14 kDa proline-rich protein DC2.15-like	6,07	DOWN	152,95
Solyc02g079240	Solyc02g079240.1	LOW QUALITY:Wound-responsive family protein (AHRD		#N/D	ref|XP_010316669.1| PREDICTED: uncharacterized protein LOC104645811 [Solanum lycopersicu	7,99	DOWN	149,26
Solyc10g085140	Solyc10g085140.1	Alkyl transferase (AHRD V3.3 *-* K7X479_SOLLC)		#N/D	ref|XP_010312432.1| PREDICTED: dehydrodolichyl diphosphate synthase 2-like [Solanum	7,19	DOWN	148,35
Solyc02g092700	Solyc02g092700.3	DUF1230 family protein (DUF1230) (AHRD V3.3 ***	101254550	LOC101254550	uncharacterized LOC101254550	8,24	DOWN	142,08
Solyc06g053260	Solyc06g053260.1	SAUR-like auxin-responsive family protein (AHRD	101055583	LOC101055583	small auxin-up protein 58	5,99	DOWN	134,56
Solyc09g089510	Solyc09g089510.3	Proteinase inhibitor I (AHRD V3.3 ***		#N/D	ref|XP_004247691.2| PREDICTED: proteinase inhibitor I-B [Solanum lycopersicum]	8,23	DOWN	128,06
Solyc05g051720	Solyc05g051720.1	Glutaredoxin family protein (AHRD V3.3 ***	101252183	LOC101252183	monothiol glutaredoxin-S1-like	5,18	DOWN	117,78
Solyc11g012360	Solyc11g012360.2	Tonoplast dicarboxylate transporter (AHRD V3.3	101257524	LOC101257524	tonoplast dicarboxylate transporter-like	20,77	DOWN	115,65
Solyc07g008240	Solyc07g008240.3	Non-symbiotic hemoglobin 1 (AHRD V3.3 ***	100736435	Glb1	non-symbiotic hemoglobin class 1	5,28	DOWN	115,08
Solyc06g007440	Solyc06g007440.3	Non-specific serine/threonine protein kinase	101247723	LOC101247723	CBL-interacting serine/threonine-protein kinase 11-like	5,78	DOWN	112,12
Solyc04g015750	Solyc04g015750.3	Magnesium chelatase H subunit (AHRD V3.3 ***	101244176	LOC101244176	magnesium-chelatase subunit ChlH, chloroplastic	7,26	DOWN	103,23
Solyc09g083440	Solyc09g083440.3	PIN-I protein (AHRD V3.3 *** Q4FE22_SOLTU)	101246961	LOC101246961	wound-induced proteinase inhibitor 1	5,8	DOWN	101,83
Solyc09g084470	Solyc09g084470.3	Wound-induced proteinase inhibitor 1 (AHRD V3.3	543954	LOC543954	wound-induced proteinase inhibitor 1	10,21	DOWN	99,62
Solyc06g073180	Solyc06g073180.3	CONSTANS interacting protein 1	778334	CIP1	CONSTANS interacting protein 1	6,36	DOWN	93,77
Solyc02g070980	Solyc02g070980.1	Chlorophyll a-b binding protein, chloroplastic	104645884	Cab-1A	chlorophyll a/b-binding protein Cab-1A	7,08	DOWN	90,15
Solyc09g089730	Solyc09g089730.3	2-oxoglutarate (2OG) and Fe(II)-dependent	101244528	LOC101244528	1-aminocyclopropane-1-carboxylate oxidase homolog	6,17	DOWN	83,14
Solyc00g136560	Solyc00g136560.3	Alkyl transferase (AHRD V3.3 *** K7X479_SOLLC)		#N/D	ref|XP_004253464.1| PREDICTED: dehydrodolichyl diphosphate synthase 2-like [Solanum	7,07	DOWN	79,36
Solyc07g006630	Solyc07g006630.3	CONSTANS-like protein (AHRD V3.3 ***	100191137	LOC100191137	CONSTANS-like protein	11,65	DOWN	75,12
Solyc07g055260	Solyc07g055260.3	DnaJ (AHRD V3.3 *** A0A126DIH0_ARAHY)	101268200	LOC101268200	DNAJ heat shock N-terminal domain-containing protein	11,18	DOWN	73,17
Solyc01g080870	Solyc01g080870.3	Peptide transporter, putative (AHRD V3.3 ***		#N/D	protein NRT1/ PTR FAMILY 7.3	5,72	DOWN	71,5
Solyc01g105120	Solyc01g105120.3	Dentin sialophosphoprotein-related, putative		#N/D	ref|XP_010315092.1| PREDICTED: uncharacterized protein LOC101244909 isoform X2 [Solanum	8,8	DOWN	71,23
Solyc12g098910	Solyc12g098910.2	Non-specific serine/threonine protein kinase	101249805	LOC101249805	CBL-interacting serine/threonine-protein kinase 1	7,14	DOWN	68,7
Solyc09g009420	Solyc09g009420.1	LOW QUALITY:AMP-dependent synthetase and ligase		#N/D	ref|XP_004246546.1| PREDICTED: uncharacterized protein LOC101264052 [Solanum lycopersicu	6,32	DOWN	68,3
Solyc10g079620	Solyc10g079620.2	haloacid dehalogenase	100316880	LOC100316880	ref|XP_004249222.1| PREDICTED: haloacid dehalogenase-like hydrolase domain-containing	37,13	DOWN	59,51
Solyc05g012030	Solyc05g012030.1	LOW QUALITY:Protein BIG GRAIN 1-like E (AHRD V3.3		#N/D	ref|XP_004239030.1| PREDICTED: histone-lysine N-methyltransferase, H3 lysine-79 specific	30,03	DOWN	51,61
Solyc03g119910	Solyc03g119910.3	Le3OH-23b-hydroxylase	543504	3OH-2	3b-hydroxylase	5,64	DOWN	51,09
Solyc10g005030	Solyc10g005030.3	Pseudo-response regulator 9 (AHRD V3.3 ***	101262866	LOC101262866	two-component response regulator-like APRR9	13	DOWN	48,56
Solyc03g059260	Solyc03g059260.3	Carboxyl-terminal-processing protease (AHRD V3.3	101257542	LOC101257542	carboxyl-terminal-processing peptidase 3, chloroplastic	5,98	DOWN	47,54
Solyc01g066190	Solyc01g066190.1	LOW QUALITY:Splicing factor 3B subunit 3 (AHRD		#N/D		12,49	DOWN	44,83
Solyc04g009050	Solyc04g009050.3	Dentin sialophosphoprotein-related, putative		#N/D	ref|XP_010319337.1| PREDICTED: uncharacterized protein LOC101266410 isoform X2 [Solanum	5,52	DOWN	43,48
Solyc03g116630	Solyc03g116630.3	cytochrome P450 family protein (AHRD V3.3 ***	101253674	LOC101253674	uncharacterized LOC101253674	10,74	DOWN	41,56
Solyc07g014680	Solyc07g014680.3	sodium transporter HKT1,2		#N/D	emb|CCJ09642.1| Na+ transporter [Solanum lycopersicum var. cerasiforme]	12,24	DOWN	40,73

SGN locus	Gene_name Gene ID	ITAG3.0 gene description	NCBI GeneID	NCBI Symbol	NCBI description / 1st blastp hit / 2nd blastp hit	fold_ change	direction	total_ fpkm
Solyc03g007370	Solyc03g007370.3	Sigma factor (AHRD V3.3 *** A0A0G2STU5_9ROSI)	101252660	LOC101252660	RNA polymerase sigma factor sigE, chloroplastic/mitochondrial	6,71	DOWN	34,28
Solyc06g060310	Solyc06g060310.3	Chlorophyllide a oxygenase (AHRD V3.3 ***	101261422	LOC101261422	chlorophyllide a oxygenase, chloroplastic	9,75	DOWN	33,57
Solyc10g079680	Solyc10g079680.2	bHLH transcription factor 068	101258211	LOC101258211	putative transcription factor SlbHLH068	nan	DOWN	33,1349
Solyc01g068560	Solyc01g068560.3	Agglutinin-like protein ALA1, putative isoform 3		#N/D	ref|XP_010320656.1| PREDICTED: uncharacterized protein LOC101268608 [Solanum lycopersicu	6,33	DOWN	32,94
Solyc12g098110	Solyc12g098110.1	LOW QUALITY:Self-incompatibility S1 family	109119116	LOC109119116	uncharacterized LOC109119116	5,17	DOWN	32,02
Solyc11g005190	Solyc11g005190.2	Transducin/WD40 repeat-like superfamily protein	101259391	LOC101259391	COP1-like protein	6,17	DOWN	30,04
Solyc01g102610	Solyc01g102610.3	Ferric reduction oxidase 7 (AHRD V3.3 ***	101246763	LOC101246763	ferric reduction oxidase 6	7,76	DOWN	29,36
Solyc01g017720	Solyc01g017720.2	Maturase K (AHRD V3.3 --* H9NKB3_9ASTR)		#N/D		15,64	DOWN	28,82
Solyc12g005660	Solyc12g005660.2	Zinc finger, B-box (AHRD V3.3 *-*	101055534	LOC101055534	Hop-interacting protein THI121	19,26	DOWN	28,71
Solyc01g107460	Solyc01g107460.2	LOW QUALITY:neuronal PAS domain protein (AHRD		#N/D	ref|XP_004230726.1| PREDICTED: uncharacterized protein LOC101248432 [Solanum lycopersicu	33,25	DOWN	27,67
Solyc12g010020	Solyc12g010020.2	Leucine aminopeptidase A1		#N/D		13,67	DOWN	27,67
Solyc07g051820	Solyc07g051820.3	Cellulose synthase family protein (AHRD V3.3 ***	101259456	LOC101259456	cellulose synthase-like protein H1	7,39	DOWN	25,78
Solyc09g084480	Solyc09g084480.3	Type I serine protease inhibitor (AHRD V3.3 ***	101247857	LOC101247857	wound-induced proteinase inhibitor 1-like	13	DOWN	25,45
Solyc06g036260	Solyc06g036260.3	beta-carotene hydroxylase-1	544133	CrtR-b1	beta-carotene hydroxylase	6,88	DOWN	25,29
Solyc04g011780	Solyc04g011780.1	Glutaredoxin (AHRD V3.3 *** A0A103XEX1_CYNCS)		#N/D	ref|XP_004236715.1| PREDICTED: monothiol glutaredoxin-S1-like [Solanum lycopersicum]	12,59	DOWN	25,16
Solyc11g022590	Solyc11g022590.1	trypsin inhibitor-like protein precursor	544001	LOC544001	uncharacterized LOC544001	19,01	DOWN	23,74
Solyc09g011080	Solyc09g011080.3	Ribulose bisphosphate carboxylase/oxygenase activase	101250725	LOC101250725	ribulose bisphosphate carboxylase/oxygenase activase 1, chloroplastic	28,27	DOWN	23,7
Solyc01g100910	Solyc01g100910.3	WAT1-related protein (AHRD V3.3 *** K4B1C2_SOLLC)	101257305	LOC101257305	WAT1-related protein At1g09380	6,38	DOWN	23,33
Solyc09g007765	Solyc09g007765.1	Aquaporin-like protein (AHRD V3.3 *-*		#N/D	ref|XP_010325988.1| PREDICTED: aquaporin PIP2-1-like [Solanum lycopersicum]	5,23	DOWN	21
Solyc03g111120	Solyc03g111120.3	Malate synthase (AHRD V3.3 *** M1B824_SOLTU)	101267395	LOC101267395	malate synthase, glyoxysomal	7,86	DOWN	20,26
Solyc01g096630	Solyc01g096630.3	Dentin sialophosphoprotein-related, putative		#N/D		8,72	DOWN	20,06
Solyc04g058100	Solyc04g058100.3	Metallothionein-like protein type 2 (AHRD V3.3	778300	MT3	type 2 metallothionein MT3	10,32	DOWN	19,55
Solyc03g098320	Solyc03g098320.3	Myb transcription factor (AHRD V3.3 ***	101255972	LOC101255972	protein REVEILLE 7	18,95	DOWN	18,77
Solyc08g067540	Solyc08g067540.1	Non-specific lipid-transfer protein (AHRD V3.3	101256205	LOC101256205	non-specific lipid-transfer protein 1-like	5,23	DOWN	18,58
Solyc01g007895	Solyc01g007895.1	basic helix-loop-helix (bHLH) DNA-binding		#N/D	ref|XP_004228559.1| PREDICTED: putative uncharacterized protein DDB_G0282499 [Solanum	7,34	DOWN	17,11
Solyc12g042100	Solyc12g042100.2	RING/FYVE/PHD zinc finger superfamily protein		#N/D		9,37	DOWN	16,22
Solyc10g084370	Solyc10g084370.2	MYB transcription factor (AHRD V3.3 ***	101253545	LOC101253545	ref|XP_004249508.1| PREDICTED: protein REVEILLE 8-like [Solanum lycopersicum]	71,89	DOWN	16,15
Solyc07g053140	Solyc07g053140.3	Zinc finger, B-box (AHRD V3.3 ***	101265452	LOC101265452	zinc finger protein CONSTANS-LIKE 4-like	12,23	DOWN	14,58
Solyc07g056240	Solyc07g056240.3	TRNA-methyltransferase (AHRD V3.3 ***	101250133	LOC101250133	uncharacterized LOC101250133	5,74	DOWN	14,53
Solyc10g019050	Solyc10g019050.2	LOW QUALITY:Farnesyl pyrophosphate synthase 1		#N/D		nan	DOWN	14,1822
Solyc05g052240	Solyc05g052240.3	Chalcone-flavonone isomerase family protein (AHRD	101266223	LOC101266223	probable chalcone--flavonone isomerase 3	11,64	DOWN	14,13
Solyc03g117580	Solyc03g117580.3	GAG1At protein (AHRD V3.3 *** AT1G16000.1)	101256860	LOC101256860	uncharacterized LOC101256860	5,87	DOWN	14,02
Solyc02g084420	Solyc02g084420.3	B-box zinc finger family protein (AHRD V3.3 ***		#N/D	B-box zinc finger protein 19? E value 3e-78	8,32	DOWN	13,96
Solyc09g008670	Solyc09g008670.3	threonine deaminase	543983	LOC543983	threonine dehydratase biosynthetic, chloroplastic	5,61	DOWN	13,95
Solyc09g090300	Solyc09g090300.3	DCTP pyrophosphatase 1 (AHRD V3.3 ***		#N/D	ref|XP_004247743.1| PREDICTED: dCTP pyrophosphatase 1-like isoform X1 [Solanum lycopersi	9,69	DOWN	13,69
Solyc01g079150	Solyc01g079150.3	Boron transporter (AHRD V3.3 *** B6V758_VITVI)	101260863	LOC101260863	boron transporter 1	16,67	DOWN	13,49
Solyc03g116910	Solyc03g116910.3	cinnamoyl-CoA reductase 2	778359	CCR2	cinnamoyl-CoA reductase	6,53	DOWN	13,32
Solyc12g006730	Solyc12g006730.1	LOW QUALITY:glutathione S-transferase zeta 1		#N/D	putative IRON MAN peptide	nan	DOWN	13,1393
Solyc05g052230	Solyc05g052230.1	LOW QUALITY:Pentatricopeptide repeat (PPR)		#N/D	ref|XP_015074437.1| PREDICTED: uncharacterized protein LOC107018461 [Solanum pennellii]	nan	DOWN	13,0928
Solyc03g096770	Solyc03g096770.1	Response to low sulfur protein, putative (AHRD	101243684	LOC101243684	uncharacterized LOC101243684	8,93	DOWN	12,3
Solyc05g012230	Solyc05g012230.3	Protein POLAR LOCALIZATION DURING ASYMMETRIC	101267310	LOC101267310	uncharacterized LOC101267310	9,23	DOWN	12,25
Solyc04g080040	Solyc04g080040.3	Heat shock protein binding protein, putative		#N/D	ref|XP_004238235.1| PREDICTED: J domain-containing protein required for chloroplast	8,75	DOWN	12,25
Solyc01g096620	Solyc01g096620.3	MATH and LRR domain-containing protein PFE0570w,		#N/D	ref|XP_010324123.1| PREDICTED: ACI112 protein isoform X1 [Solanum lycopersicum]	6,72	DOWN	12,23
Solyc12g096210	Solyc12g096210.2	F-box/RNI-like superfamily protein (AHRD V3.3 --*		#N/D		7,68	DOWN	12,02
Solyc05g010060	Solyc05g010060.3	Phosphate transporter PHO1-like protein (AHRD	101244953	LOC101244953	phosphate transporter PHO1 homolog 1	9,5	DOWN	11,83
Solyc10g005080	Solyc10g005080.3	Late elongated hypocotyl (AHRD V3.3 ***	101261662	LOC101261662	protein LHY	24,74	DOWN	11,25
Solyc08g077170	Solyc08g077170.3	Peptide transporter, putative (AHRD V3.3 ***	101263538	LOC101263538	protein NRT1/ PTR FAMILY 7.3	23,14	DOWN	11,05
Solyc01g017730	Solyc01g017730.1	LOW QUALITY:ARM repeat superfamily protein (AHRD		#N/D		9,65	DOWN	10,49

4.9. Literature

Albertazzi, G., Milc, J., Caffagni, A., Francia, E., Roncaglia, E., Ferrari, F., ... & Pecchioni, N. (2009). Gene expression in grapevine cultivars in response to Bois Noir phytoplasma infection. *Plant Science*, *176*(6), 792-804.

Altschul, S. F., Madden, T. L., Schäffer, A. A., Zhang, J., Zhang, Z., Miller, W., & Lipman, D. J. (1997). Gapped BLAST and PSI-BLAST: a new generation of protein database search programs. *Nucleic acids research*, *25*(17), 3389-3402.

Andaluz, S., López-Millán, A. F., De las Rivas, J., Aro, E. M., Abadía, J., & Abadía, A. (2006). Proteomic profiles of thylakoid membranes and changes in response to iron deficiency. *Photosynthesis research*, *89*(2-3), 141-155.

Andersen, M. T., Liefting, L. W., Havukkala, I., & Beever, R. E. (2013). Comparison of the complete genome sequence of two closely related isolates of 'Candidatus Phytoplasma australiense' reveals genome plasticity. *BMC genomics*, *14*(1), 529.

Andrews, S. C., Robinson, A. K., & Rodríguez-Quiñones, F. (2003). Bacterial iron homeostasis. *FEMS microbiology reviews*, *27*(2-3), 215-237.

Audenaert, K., Pattery, T., Cornelis, P., & Hofte, M. (2002). Induction of systemic resistance to Botrytis cinerea in tomato by Pseudomonas aeruginosa 7NSK2: role of salicylic acid, pyochelin, and pyocyanin. *Mol. Plant Microbe Interact.*, *11*, 1147–1156.

Aznar, A., Chen, N. W., Rigault, M., Riache, N., Joseph, D., Desmaële, D., ... & Thomine, S. (2014). Scavenging iron: a novel mechanism of plant immunity activation by microbial siderophores. *Plant physiology*, pp-113.

Aznar, A., Chen, N. W., Thomine, S., & Dellagi, A. (2015). Immunity to plant pathogens and iron homeostasis. *Plant Science*, *240*, 90-97.

Bai, X., Correa, V. R., Toruño, T. Y., Ammar, E. D., Kamoun, S., & Hogenhout, S. A. (2009). AY-WB phytoplasma secretes a protein that targets plant cell nuclei. *Molecular Plant-Microbe Interactions*, *22*(1), 18-30.

Bai, X., Zhang, J., Ewing, A., Miller, S. A., Radek, A. J., Shevchenko, D. V., ... & Hogenhout, S. A. (2006). Living with genome instability: the adaptation of phytoplasmas to diverse environments of their insect and plant hosts. *Journal of bacteriology*, *188*(10), 3682-3696.

Bakker, P. A., Pieterse, C. M., & Van Loon, L. C. (2007). Induced systemic resistance by fluorescent Pseudomonas spp. *Phytopathology*, *97*(2), 239-243.

Bauer, P., Ling, H. Q., & Guerinot, M. L. (2007). FIT, the FER-like iron deficiency induced transcription factor in Arabidopsis. *Plant Physiology and Biochemistry*, *45*(5), 260-261.

Bereczky, Z., Wang, H. Y., Schubert, V., Ganal, M., & Bauer, P. (2003). Differential regulation of nramp and irt metal transporter genes in wild type and iron uptake mutants of tomato. *Journal of Biological Chemistry*.

Bertamini, M., Grando, M. S., & Nedunchezhian, N. (2003). Effects of phytoplasma infection on pigments, chlorophyll-protein complex and photosynthetic activities in field grown apple leaves. *Biologia plantarum*, *47*(2), 237-242.

Bienfait, H. F., van den Briel, W., & Mesland-Mul, N. T. (1985). Free space iron pools in roots: generation and mobilization. *Plant Physiology*, *78*(3), 596-600.

Briat, J. F., & Lobréaux, S. (1997). Iron transport and storage in plants. *Trends in plant science*, *2*(5), 187-193.

Briat, J. F., Curie, C., & Gaymard, F. (2007). Iron utilization and metabolism in plants. *Current opinion in plant biology*, *10*(3), 276-282.

Briat, J. F., Fobis-Loisy, I., Grignon, N., Lobréaux, S., Pascal, N., Savino, G., ... & Van Wuytswinkel, O. (1995). Cellular and molecular aspects of iron metabolism in plants. *Biology of the Cell*, *84*(1-2), 69-81.

Brumbarova, T., & Bauer, P. (2005). Iron-mediated control of the basic helix-loop-helix protein FER, a regulator of iron uptake in tomato. *Plant Physiology*, *137*(3), 1018-1026.

Buxa, S. V., Degola, F., Polizzotto, R., De Marco, F., Loschi, A., Kogel, K. H., ... & Musetti, R. (2015). Phytoplasma infection in tomato is associated with re-organization of plasma membrane, ER stacks, and actin filaments in sieve elements. *Frontiers in plant science*, *6*, 650.

Cai, H., Chen, H., Yi, T., Daimon, C. M., Boyle, J. P., Peers, C., ... & Martin, B. (2013). VennPlex–a novel Venn diagram program for comparing and visualizing datasets with differentially regulated datapoints. *PloS one*, *8*(1), e53388.

Cesco, S., Neumann, G., Tomasi, N., Pinton, R., & Weisskopf, L. (2010). Release of plant-borne flavonoids into the rhizosphere and their role in plant nutrition. *Plant and Soil*, *329*(1-2), 1-25.

Christensen, N. M., Nicolaisen, M., Hansen, M., & Schulz, A. (2004). Distribution of phytoplasmas in infected plants as revealed by real-time PCR and bioimaging. *Molecular Plant–Microbe Interactions*, *17*,1175–1184.

Colangelo, E. P., & Guerinot, M. L. (2004). The essential basic helix-loop-helix protein FIT1 is required for the iron deficiency response. *The Plant Cell*, *16*(12), 3400-3412.

Contaldo, N., Bertaccini, A., Paltrinieri, S., Windsor, H. M., & Windsor, G. D. (2012). Axenic culture of plant pathogenic phytoplasmas. *Phytopathol. Mediterr.*, *51*, 607–617.

Cordova, I., Jones, P., Harrison, N. A., & Oropeza, C. (2003). In Situ Detection of Phytoplasma DNA in Embryos from Coconut Palms with Lethal Yellowing Disease. *Molecular Plant Pathology*, *4*, 99-108.

Cui, Y., Chen, C. L., Cui, M., Zhou, W. J., Wu, H. L., & Ling, H. Q. (2018). Four IVa bHLH Transcription Factors Are Novel Interactors of FIT and Mediate JA Inhibition of Iron Uptake in Arabidopsis. *Molecular plant*, *11*(9), 1166-1183.

Cvrkovic, T., Jovic, J., Mitrovic, M., Krstic, O., & Tosevski I. (2014). Experimental and molecular evidence of Reptalus panzeri as a natural vector of bois noir. *Plant Pathology*, *63*, 42–53.

De Marco, F., Pagliari, L., Degola, F., Buxa, S. V., Loschi, A., Dinant, S., ... & Musetti, R. (2016). Combined microscopy and molecular analyses show phloem occlusions and cell wall modifications in tomato leaves in response to 'Candidatus Phytoplasma solani'. *Journal of microscopy*, *263*(2), 212-225.

De Vleesschauwer, D., & Höfte, M. (2009). Rhizobacteria-induced systemic resistance. *Advances in botanical research*, *51*, 223-281.

Dellagi, A., Rigault, M., Segond, D., Roux, C., Kraepiel, Y., Cellier, F., ... & Expert, D. (2005). Siderophore-mediated upregulation of Arabidopsis ferritin expression in response to Erwinia chrysanthemi infection. *The Plant Journal*, *43*(2), 262-272.

Dellagi, A., Segond, D., Rigault, M., Fagard, M., Simon, C., Saindrenan, P., & Expert, D. (2009). Microbial siderophores exert a subtle role in Arabidopsis during infection by manipulating the immune response and the iron status. *Plant physiology*, *150*(4), 1687-1696.

Doyle, J. J., & Doyle, J. L. (1990). DNA extraction from Arabidopsis. *Focus*, *12*, 13-15.

Du, J., Huang, Z., Wang, B., Sun, H., Chen, C., Ling, H. Q., & Wu, H. (2015). SlbHLH068 interacts with FER to regulate the iron-deficiency response in tomato. *Annals of botany*, *116*(1), 23-34.

Duduk, B., & Bertaccini, A. (2006). Corn with symptoms of reddening: new host of stolbur phytoplasma. *Plant Disease*, *90*(10), 1313-1319.

Eckhardt, U., Marques, A. M., & Buckhout, T. J. (2001). Two iron-regulated cation transporters from tomato complement metal uptake-deficient yeast mutants. *Plant molecular biology*, *45*(4), 437-448.

Ehlers, K., Knoblauch, M., & Van Bel, A. J. E. (2000). Ultrastructural features of well-preserved and injured sieve elements: minute clamps keep the phloem transport conduits free for mass flow. *Protoplasma*, *214*(1-2), 80-92.

Eide, D., Broderius, M., Fett, J., & Guerinot, M. L. (1996). A novel iron-regulated metal transporter from plants identified by functional expression in yeast. *Proceedings of the National Academy of Sciences*, *93*(11), 5624-5628.

Expert, D. (1999). Withholding and exchanging iron: interactions between Erwinia spp. and their plant hosts. *Annual review of phytopathology*, *37*(1), 307-334.

Expert, D., Enard, C., & Masclaux, C. (1996). The role of iron in plant host-pathogen interactions. *Trends in microbiology*, *4*(6), 232-237.

Fenton, H. (1894). Oxidation of tartaric acid in presence of iron. *J. Chem. Soc. Trans.*, *65*, 899–910.

Fos, A., Danet, J. L., Zreik, L., Garnier, M., & Bové, J. M. (1992). Use of a monoclonal-antibody to detect the stolbur mycoplasma-like organism in plants and insects and to identify a vector in France. *Plant Disease*, *76*, 1092–1096.

Gao, Y., Qiu, P. P., Liu, W. H., Su, W. M., Gai, S. P., Liang, Y. C., & Zhu, X. P. (2013). Identification of 'C andidatus P hytoplasma solani' Associated with Tree Peony Yellows Disease in China. *Journal of Phytopathology*, *161*(3), 197-200.

García, M. J., Lucena, C., Romera, F. J., Alcántara, E., & Pérez-Vicente, R. (2010). Ethylene and nitric oxide involvement in the up-regulation of key genes related to iron acquisition and homeostasis in Arabidopsis. *Journal of Experimental Botany*, *61*(14), 3885-3899.

Garnier M. (2000). The stolbur phytoplasma: an ubiquitous agent. *Comptes Rendus de l'Academie d'Agriculture de France*, *86*, 27–33.

Gatineau, F., Jacob, N., Vautrin, S., Larrue, J., Lherminier, J., Richard-Molard, M., & Boudon-Padieu, E. (2002). Association with the syndrome "basses richesses" of sugar beet of a phytoplasma and a bacterium-like organism transmitted by a Pentastiridius sp. *Phytopathology*, *92*(4), 384-392.

Grillet, L., Lan, P., Li, W., Mokkapati, G., & Schmidt, W. (2018). IRON MAN is a ubiquitous family of peptides that control iron transport in plants. *Nature plants*, *1*.

Guerinot, M. L., & Yi, Y. (1994). Iron: nutritious, noxious, and not readily available. *Plant Physiol.*, *104*, 815–20

Haas, H., Eisendle, M., & Turgeon, B. G. (2008). Siderophores in fungal physiology and virulence. *Annu. Rev. Phytopathol.*, *46*, 149-187.

Haber, F., & Weiss, J. (1934). The catalytic decomposition of hydrogen peroxide by iron salts. *Proc. R. Soc. Lond. Ser. A*, 147:332–51.

Hogenhout, S. A., & Loria, R. (2008). Virulence mechanisms of Gram-positive plant pathogenic bacteria. *Current opinion in plant biology*, *11*(4), 449-456.

Hoshi, A., Oshima, K., Kakizawa, S., Ishii, Y., Ozeki, J., Hashimoto, M., ... & Namba, S. (2009). A unique virulence factor for proliferation and dwarfism in plants identified from a phytopathogenic bacterium. *Proceedings of the National Academy of Sciences*, *106*(15), 6416-6421.

Hren, M., Nikolić, P., Rotter, A., Blejec, A., Terrier, N., Ravnikar, M., ... & Gruden, K. (2009). 'Bois noir'phytoplasma induces significant reprogramming of the leaf transcriptome in the field grown grapevine. *BMC genomics*, *10*(1), 1.

Ivanov, R., Brumbarova, T., & Bauer, P. (2012). Fitting into the harsh reality: regulation of iron-deficiency responses in dicotyledonous plants. *Molecular Plant*, *5*(1), 27-42.

Jakoby, M., Wang, H. Y., Reidt, W., Weisshaar, B., & Bauer, P. (2004). FRU (BHLH029) is required for induction of iron mobilization genes in Arabidopsis thaliana. *FEBS letters*, *577*(3), 528-534.

Jović, J., Cvrković, T., Mitrović, M., Krnjajić, S., Redinbaugh, M. G., Pratt, R. C., ... & Toševski, I. (2007). Roles of stolbur phytoplasma and Reptalus panzeri (Cixiinae, Auchenorrhyncha) in the epidemiology of Maize redness in Serbia. *European Journal of Plant Pathology*, *118*(1), 85-89.

Kang, H. G., Foley, R. C., Oñate-Sánchez, L., Lin, C., & Singh, K. B. (2003). Target genes for OBP3, a Dof transcription factor, include novel basic helix-loop-helix domain proteins inducible by salicylic acid. *The Plant Journal*, *35*(3), 362-372.

Kanehisa, M., Goto, S., Furumichi, M., Tanabe, M., & Hirakawa, M. (2010). KEGG for representation and analysis of molecular networks involving diseases and drugs. *Nucleic acids research*, *38*(suppl_1), D355-D360.

Kim, D., Pertea, G., Trapnell, C., Pimentel, H., Kelley, R., & Salzberg, S. L. (2013). TopHat2: accurate alignment of transcriptomes in the presence of insertions, deletions and gene fusions. *Genome biology*, *14*(4), R36.

Kobayashi, T., & Nishizawa, N. K. (2014). Iron sensors and signals in response to iron deficiency. *Plant Science*, *224*, 36-43.

Kube, M., Mitrovic, J., Duduk, B., Rabus, R., & Seemüller, E. (2012). Current view on phytoplasma genomes and encoded metabolism. *The Scientific World Journal*, *2012*.

Kube, M., Schneider, B., Kuhl, H., Dandekar, T., Heitmann, K., Migdoll, A. M., ... & Seemüller, E. (2008). The linear chromosome of the plant-pathogenic mycoplasma 'Candidatus Phytoplasma mali'. *Bmc Genomics*, *9*(1), 306.

Leeman, M., Den Ouden, F. M., Van Pelt, J. A., Dirkx, F. P. M., Steijl, H., Bakker, P. A. H. M., & Schippers, B. (1996). Iron availability affects induction of systemic resistance to Fusarium wilt of radish by Pseudomonas fluorescens. *Phytopathology*, *86*(2), 149-155.

Li, L., Cheng, X., & Ling, H. Q. (2004). Isolation and characterization of Fe (III)-chelate reductase gene LeFRO1 in tomato. *Plant molecular biology*, *54*(1), 125-136.

Ling, H. Q., Bauer, P., Bereczky, Z., Keller, B., & Ganal, M. (2002). The tomato fer gene encoding a bHLH protein controls iron-uptake responses in roots. *Proceedings of the National Academy of Sciences*, *99*(21), 13938-13943.

Ling, H. Q., Koch, G., Bäumlein, H., & Ganal, M. W. (1999). Map-based cloning of chloronerva, a gene involved in iron uptake of higher plants encoding nicotianamine synthase. *Proceedings of the National Academy of Sciences*, *96*(12), 7098-7103.

Liu, R., Dong, Y., Fan, G., Zhao, Z., Deng, M., Cao, X., & Niu, S. (2013). Discovery of genes related to witches broom disease in Paulownia tomentosa× Paulownia fortunei by a de novo assembled transcriptome. *PLoS One*, *8*(11), e80238.

Liu, Z., Zhao, J., & Liu, M. (2016). Photosynthetic responses to phytoplasma infection in Chinese jujube. *Plant Physiology and Biochemistry*, *105*, 12-20.

Long, T. A., Tsukagoshi, H., Busch, W., Lahner, B., Salt, D. E., & Benfey, P. N. (2010). The bHLH transcription factor POPEYE regulates response to iron deficiency in Arabidopsis roots. *The Plant Cell*, tpc-110.

López-Millán, A. F., Morales, F., Gogorcena, Y., Abadía, A., & Abadía, J. (2009). Metabolic responses in iron deficient tomato plants. *Journal of plant physiology*, *166*(4), 375-384.

Lu, Y. T., Li, M. Y., Cheng, K. T., Tan, C. M., Su, L. W., Lin, W. Y., ... & Yang, J. Y. (2014). Transgenic plants that express the phytoplasma effector SAP11 show altered phosphate starvation and defense responses. *Plant physiology*, *164*(3), 1456-1469.

Lucena, C., Waters, B. M., Romera, F. J., García, M. J., Morales, M., Alcántara, E., & Pérez-Vicente, R. (2006). Ethylene could influence ferric reductase, iron transporter, and H+-ATPase gene expression by affecting FER (or FER-like) gene activity. *Journal of Experimental Botany*, *57*(15), 4145-4154.

Luo, Y., Han, Z., Chin, S. M., & Linn, S. (1994). Three chemically distinct types of oxidants formed by iron-mediated Fenton reactions in the presence of DNA. *Proceedings of the National Academy of Sciences*, *91*(26), 12438-12442.

Maixner M. (1994). Transmission of German grapevine yellows (Vergilbungskrankheit) by the planthopper Hyalesthes obsoletus (Auchenorrhyncha:Cixiidae). *Vitis*, *33*, 103–104.

Martini, M., Musetti, R., Grisan, S., Polizzotto, R., Borselli, S., Pavan, F., & Osler, R. (2009). DNA-dependent detection of the grapevine fungal endophytes Aureobasidium pullulans and Epicoccum nigrum. *Plant Disease*, *93*(10), 993-998.

Masuda, T., Tanaka, A., & Melis, A. (2003). Chlorophyll antenna size adjustments by irradiance in Dunaliella salina involve coordinate regulation of chlorophyll a oxygenase (CAO) and Lhcb gene expression. *Plant molecular biology*, *51*(5), 757-771.

Mata, C.G., Lamattina, L., & Cassia, R.O. (2001). Involvement of iron and ferritin in the potato-Phytophthora infestans interaction. *Eur. J. Plant Pathol.*, *107*, 557–562.

Maurer, F., Müller, S., & Bauer, P. (2011). Suppression of Fe deficiency gene expression by jasmonate. *Plant Physiology and Biochemistry*, *49*(5), 530-536.

Mendoza-Cózatl, D. G., Xie, Q., Akmakjian, G. Z., Jobe, T. O., Patel, A., Stacey, M. G., ... & Schroeder, J. I. (2014). OPT3 is a component of the iron-signaling network between leaves and roots and misregulation of OPT3 leads to an over-accumulation of cadmium in seeds. Molecular plant, 7(9), 1455-1469.

Minolta. 1989. SPAD-502 owner's manual. Industrial Meter Div. Minolta Corp., Ramsey, N.J.

Morsomme, P., & Boutry, M. (2000). The plant plasma membrane H+-ATPase: structure, function and regulation. *Biochimica et Biophysica Acta (BBA)-Biomembranes*, *1465*(1), 1-16.

Mortazavi, A., Williams, B. A., McCue, K., Schaeffer, L., & Wold, B. (2008). Mapping and quantifying mammalian transcriptomes by RNA-Seq. *Nature methods*, *5*(7), 621.

Mou, H. Q., Lu, J., Zhu, S. F., Lin, C. L., Tian, G. Z., Xu, X., & Zhao, W. J. (2013). Transcriptomic analysis of paulownia infected by paulownia witches'-broom phytoplasma. *PLoS One*, *8*(10), e77217.

Msilini, N., Zaghdoudi, M., Govindachary, S., Lachaâl, M., Ouerghi, Z., & Carpentier, R. (2011). Inhibition of photosynthetic oxygen evolution and electron transfer from the quinone acceptor QA– to QB by iron deficiency. *Photosynthesis research*, *107*(3), 247-256.

Muller, P. Y., Janovjak, H., Miserez, A. R., & Dobbie, Z. (2002). Short technical report processing of gene expression data generated by quantitative real-time RT-PCR. *Biotechniques*, *32*(6), 1372-1379.

Munekage, Y., Hojo, M., Meurer, J., Endo, T., Tasaka, M., & Shikanai, T. (2002). PGR5 is involved in cyclic electron flow around photosystem I and is essential for photoprotection in Arabidopsis. Cell, 110(3), 361-371.

Musetti, R., Buxa, S. V., De Marco, F., Loschi, A., Polizzotto, R., Kogel, K. H., & van Bel, A. J. (2013). Phytoplasma-triggered Ca2+ influx is involved in sieve-tube blockage. *Molecular Plant-Microbe Interactions*, *26*(4), 379-386.

Musetti, R., Di Toppi, L. S., Martini, M., Ferrini, F., Loschi, A., Favali, M. A., & Osler, R. (2005). Hydrogen peroxide localization and antioxidant status in the recovery of apricot plants from European Stone Fruit Yellows. *European Journal of Plant Pathology*, *112*(1), 53-61.

Naranjo-Arcos, M. A., & Bauer, P. (2016). Iron Nutrition, Oxidative Stress, and Pathogen Defense. In *Nutritional Deficiency*. InTech.

Nechushtai, R., Conlan, A. R., Harir, Y., Song, L., Yogev, O., Eisenberg-Domovich, Y., ... & Luo, Y. (2012). Characterization of Arabidopsis NEET reveals an ancient role for NEET proteins in iron metabolism. *The Plant Cell*, tpc-112.

Neema, C., Laulhere, J.P. and Expert, D. (1993) Iron deficiency induced by chrysobactin in Saintpaulia leaves inoculated with Erwinia chrysanthemi. *Plant Physiol.*, *102*, 967–973.

Nejat, N., Cahill, D. M., Vadamalai, G., Ziemann, M., Rookes, J., & Naderali, N. (2015). Transcriptomics-based analysis using RNA-Seq of the coconut (Cocos nucifera) leaf in response to yellow decline phytoplasma infection. *Molecular genetics and genomics*, *290*(5), 1899-1910.

Nicol, J. W., Helt, G. A., Blanchard Jr, S. G., Raja, A., & Loraine, A. E. (2009). The Integrated Genome Browser: free software for distribution and exploration of genome-scale datasets. *Bioinformatics*, *25*(20), 2730-2731.

Orlovskis, Z., Canale, M. C., Haryono, M., Lopes, J. R. S., Kuo, C. H., & Hogenhout, S. A. (2017). A few sequence polymorphisms among isolates of Maize bushy stunt phytoplasma associate with organ proliferation symptoms of infected maize plants. *Annals of botany*, *119*(5), 869-884.

Oshima, K., Kakizawa, S., Nishigawa, H., Jung, H. Y., Wei, W., Suzuki, S., ... & Namba, S. (2004). Reductive evolution suggested from the complete genome sequence of a plant-pathogenic phytoplasma. *Nature genetics*, *36*(1), 27.

Oshima, K., Maejima, K., & Namba, S. (2013). Genomic and evolutionary aspects of phytoplasmas. *Frontiers in microbiology*, *4*, 230.

Pagliari, L., Buoso, S., Santi, S., Furch, A. C., Martini, M., Degola, F., ... & Musetti, R. (2017). Filamentous sieve element proteins are able to limit phloem mass flow, but not phytoplasma spread. *Journal of experimental botany*, *68*(13), 3673-3688.

Pagliari, L., Martini, M., Loschi, A., & Musetti, R. (2016). Looking inside phytoplasma-infected sieve elements: a combined microscopy approach using Arabidopsis thaliana as a model plant. *Micron*, *89*, 87-97.

Paolacci, A. R., Catarcione, G., Ederli, L., Zadra, C., Pasqualini, S., Badiani, M., ... & Ciaffi, M. (2017). Jasmonate-mediated defence responses, unlike salicylate-mediated responses, are involved in the recovery of grapevine from bois noir disease. *BMC plant biology*, *17*(1), 118.

Payne, S. M. (1993). Iron acquisition in microbial pathogenesis. *Trends in microbiology*, *1*(2), 66-69.

Pfaffl, M. W. (2001). A new mathematical model for relative quantification in real-time RT–PCR. *Nucleic acids research*, *29*(9), e45-e45.

Pracros, P., Renaudin, J., Eveillard, S., Mouras, A., & Hernould, M. (2006). Tomato flower abnormalities induced by stolbur phytoplasma infection are associated with changes of expression of floral development genes. *Molecular Plant Microbe Interactions*, *19*, 62-68.

Pushnik, J. C., & Miller, G. W. (1982). The effects of iron and light treatments on chloroplast composition and ultrastructure in iron-deficient barley leaves. *Journal of Plant Nutrition*, *5*(4-7), 311-321.

Quaglino, F., Zhao, Y., Casati, P., Bulgari, D., Bianco, P. A., Wei, W., & Davis, R. E. (2013). 'Candidatus Phytoplasma solani', a novel taxon associated with stolbur-and bois noir-related diseases of plants. *International journal of systematic and evolutionary microbiology*, *63*(8), 2879-2894.

Ravet, K., Touraine, B., Boucherez, J., Briat, J. F., Gaymard, F., & Cellier, F. (2009). Ferritins control interaction between iron homeostasis and oxidative stress in Arabidopsis. *The Plant Journal*, *57*(3), 400-412.

Robinson, N. J., Procter, C. M., Connolly, E. L., & Guerinot, M. L. (1999). A ferric-chelate reductase for iron uptake from soils. *Nature*, *397*(6721), 694.

Rodríguez-Celma, J., Pan, I., Li, W. D., Lan, P. D., Buckhout, T. J., & Schmidt, W. (2013). The transcriptional response of Arabidopsis leaves to Fe deficiency. *Frontiers in plant science*, *4*, 276.

Romera, F. J., Alcántara, E., & De La Guardia, M. D. (1992). Role of roots and shoots in the regulation of the Fe efficiency responses in sunflower and cucumber. *Physiologia Plantarum*, *85*(2), 141-146.

Römheld, V., & Marschner, H. (1986). Evidence for a specific uptake system for iron phytosiderophores in roots of grasses. *Plant Physiology*, *80*(1), 175-180.

Rosa, C., Margaria, P., Geib, S. M., & Scully, E. D. (2017). Novel insights into the elm yellows phytoplasma genome and into the metagenome of elm yellows-infected elms. In *In: Pinchot, Cornelia C.; Knight, Kathleen S.; Haugen, Linda M.; Flower, Charles E.; Slavicek, James M., eds. Proceedings of the American elm restoration workshop 2016; 2016 October 25-27; Lewis Center, OH. Gen. Tech. Rep. NRS-P-174. Newtown Square, PA: US Department of Agriculture, Forest Service, Northern Research Station: 49-67.* (pp. 49-67).

Roschzttardtz, H., Conéjéro, G., Curie, C., & Mari, S. (2009). Identification of the endodermal vacuole as the iron storage compartment in the Arabidopsis embryo. *Plant physiology*, *151*(3), 1329-1338.

Roschzttardtz, H., Conéjéro, G., Divol, F., Alcon, C., Verdeil, J. L., Curie, C., & Mari, S. (2013). New insights into Fe localization in plant tissues. *Frontiers in plant science*, *4*, 350.

Roschzttardtz, H., Séguéla-Arnaud, M., Briat, J. F., Vert, G., & Curie, C. (2011). The FRD3 citrate effluxer promotes iron nutrition between symplastically disconnected tissues throughout Arabidopsis development. *The Plant Cell*, tpc-111.

Rossi, G., Beni, C., Socciarelli, S., Marconi, S., Pastore, M., Del Vaglio, M., Gervasi, F. (2010) Mineral nutrition of pear and apricot trees cultivated in Southern Italy area damaged by phytoplasma microorganisms. *Acta Horticulturae*, *868*,433–438.

Santi, S., & Schmidt, W. (2009). Dissecting iron deficiency–induced proton extrusion in Arabidopsis roots. *New Phytol.*, *183*, 1072–84.

Santi, S., De Marco, F., Polizzotto, R., Grisan, S., & Musetti, R. (2013). Recovery from stolbur disease in grapevine involves changes in sugar transport and metabolism. *Frontiers in Plant Science*, *4*, 1–12.

Schikora, A., & Schmidt, W. (2001). Iron stress-induced changes in root epidermal cell fate are regulated independently from physiological responses to low iron availability. *Plant Physiology*, *125*(4), 1679-1687.

Schmidt, W. (1999). Mechanisms and regulation of reduction-based iron uptake in plants. *The New Phytologist*, *141*(1), 1-26.

Schmidt, W., Boomgaarden, B., & Ahrens, V. (1996). Reduction of root iron in Plantago lanceolata during recovery from Fe deficiency. *Physiologia Plantarum*, *98*(3), 587-593.

Schweigkofler, W., Cassar, A., & Stimpfl, E. (2008). Reduced levels of calcium and other mineral elements in grapevine leaves affected by Bois noir (BN). *Mitteilungen Klosterneuburg*, *58*, 117.

Segarra, G., Van der Ent, S., Trillas, I., & Pieterse, C. M. J. (2009). MYB72, a node of convergence in induced systemic resistance triggered by a fungal and a bacterial beneficial microbe. *Plant Biology*, *11*(1), 90-96.

Segond, D., Dellagi, A., Lanquar, V., Rigault, M., Patrit, O., Thomine, S., & Expert, D. (2009). NRAMP genes function in Arabidopsis thaliana resistance to Erwinia chrysanthemi infection. *The Plant Journal*, *58*(2), 195-207.

Selote, D., Samira, R., Matthiadis, A., Gillikin, J. W., & Long, T. A. (2015). Iron-binding E3 ligase mediates iron response in plants by targeting basic helix-loop-helix transcription factors. *Plant physiology*, *167*(1), 273-286.

Sivitz, A. B., Hermand, V., Curie, C., & Vert, G. (2012). Arabidopsis bHLH100 and bHLH101 control iron homeostasis via a FIT-independent pathway. *PloS one*, *7*(9), e44843.

Stacey, M. G., Patel, A., McClain, W. E., Mathieu, M., Remley, M., Rogers, E. E., ... & Stacey, G. (2008). The Arabidopsis AtOPT3 protein functions in metal homeostasis and movement of iron to developing seeds. *Plant physiology*, *146*(2), 589-601.

Stocking, C. R. (1975). Iron deficiency and the structure and physiology of maize chloroplasts. *Plant physiology*, *55*(4), 626-631.

Strand, Å., Asami, T., Alonso, J., Ecker, J. R., & Chory, J. (2003). Chloroplast to nucleus communication triggered by accumulation of Mg-protoporphyrinIX. *Nature*, *421*(6918), 79.

Sugio, A., MacLean, A. M., Grieve, V. M., & Hogenhout, S. A. (2011). Phytoplasma protein effector SAP11 enhances insect vector reproduction by manipulating plant development and defense hormone biosynthesis. *Proceedings of the National Academy of Sciences*, *108*(48), E1254-E1263.

Terry, N. (1980). Limiting factors in photosynthesis: I. Use of iron stress to control photochemical capacity in vivo. *Plant Physiology*, *65*(1), 114-120.

Terry, N., & Abadía, J. (1986). Function of iron in chloroplasts. *Journal of Plant Nutrition*, *9*(3-7), 609-646.

Tikkanen, M., & Aro, E. M. (2012). Thylakoid protein phosphorylation in dynamic regulation of photosystem II in higher plants. *Biochimica et Biophysica Acta (BBA)-Bioenergetics*, *1817*(1), 232-238.

Tomato Genome Consortium (2012). The tomato genome sequence provides insights into fleshy fruit evolution. *Nature*, *485*, 635–641.

Tran-Nguyen, L. T., Kube, M., Schneider, B., Reinhardt, R., & Gibb, K. S. (2008). Comparative genome analysis of "Candidatus Phytoplasma australiense" (subgroup tuf-Australia I; rp-A) and "Ca. Phytoplasma asteris" strains OY-M and AY-WB. *Journal of Bacteriology*, *190*(11), 3979-3991.

Trapnell, C., Hendrickson, D. G., Sauvageau, M., Goff, L., Rinn, J. L., & Pachter, L. (2013). Differential analysis of gene regulation at transcript resolution with RNA-seq. *Nature biotechnology*, *31*(1), 46.

Tsai, H. H., & Schmidt, W. (2017). Mobilization of iron by plant-borne coumarins. *Trends in plant science*, *22*(6), 538-548.

Tsai, H. H., Rodríguez-Celma, J., Ping, L., Wu, Y. C., Vélez-Bermúdez, I. C., & Schmidt, W. (2018). Scopoletin 8-Hydroxylase-Mediated Fraxetin Production is Crucial for Iron Mobilization. Plant physiology, pp-00178.

Valenta, V., Musil, M., & Mišiga, S. (1961). Investigations on European Yellows-type Viruses I. The Stolbur Virus. *Journal of Phytopathology*, *42*(1), 1–38.

Vandesompele, J., De Preter, K., Pattyn, F., Poppe, B., Van Roy, N., De Paepe, A., & Speleman, F. (2002). Accurate normalization of real-time quantitative RT-PCR data by geometric averaging of multiple internal control genes. *Genome biology*, *3*(7), research0034-1.

Verbon, E. H., Trapet, P. L., Stringlis, I. A., Kruijs, S., Bakker, P. A., & Pieterse, C. M. (2017). Iron and immunity. *Annual review of phytopathology*, *55*, 355-375.

Vert, G. A., Briat, J. F., & Curie, C. (2003). Dual regulation of the Arabidopsis high-affinity root iron uptake system by local and long-distance signals. *Plant Physiology*, *132*(2), 796-804.

Vigani, G., Faoro, F., Ferretti, A. M., Cantele, F., Maffi, D., Marelli, M., ... & Zocchi, G. (2015). Three-dimensional reconstruction, by TEM tomography, of the ultrastructural modifications occurring in Cucumis sativus L. mitochondria under Fe deficiency. *PloS one*, *10*(6), e0129141.

Wang, N., Cui, Y., Liu, Y., Fan, H., Du, J., Huang, Z., ... & Ling, H. Q. (2013). Requirement and functional redundancy of Ib subgroup bHLH proteins for iron deficiency responses and uptake in Arabidopsis thaliana. *Molecular plant*, *6*(2), 503-513.

Wang, Y. X., Hu, Y., Zhu, Y. F., Baloch, A. W., Jia, X. M., & Guo, A. X. (2018a). Transcriptional and physiological analyses of short-term Iron deficiency response in apple seedlings provide insight into the regulation involved in photosynthesis. *BMC genomics*, *19*(1), 461.

Wang, J., Song, L., Jiao, Q., Yang, S., Gao, R., Lu, X., & Zhou, G. (2018b). Comparative genome analysis of jujube witches'-broom Phytoplasma, an obligate pathogen that causes jujube witches'-broom disease. *BMC genomics*, *19*(1), 689.

Wang, H., Ye, X., Li, J., Tan, B., Chen, P., Cheng, J., ... & Feng, J. (2018c). Transcriptome profiling analysis revealed co-regulation of multiple pathways in jujube during infection by 'Candidatus Phytoplasma ziziphi'. *Gene*, *665*, 82-95.

Wei, W., Davis, R. E., Jomantiene, R., & Zhao, Y. (2008). Ancient, recurrent phage attacks and recombination shaped dynamic sequence-variable mosaics at the root of phytoplasma genome evolution. *Proceedings of the National Academy of Sciences*, *105*(33), 11827-11832.

Wei, W., Davis, R. E., Nuss, D. L., & Zhao, Y. (2013). Phytoplasmal infection derails genetically preprogrammed meristem fate and alters plant architecture. *Proceedings of the National Academy of Sciences*, *110*(47), 19149-19154.

Wei, W., Kakizawa, S., Suzuki, S., Jung, H. Y., Nishigawa, H., Miyata, S. I., ... & Namba, S. (2004). In planta dynamic analysis of onion yellows phytoplasma using localized inoculation by insect transmission. *Phytopathology*, *94*(3), 244-250.

Weinberg, E.D. (2000). Modulation of intramacrophage iron metabolism during microbial cell invasion. *Microbes Infect.*, *1*, 85–89.

Weintraub, P. G., & Beanland, L. (2006). Insect vectors of phytoplasmas. *Annu. Rev. Entomol.*, *51*, 91-111.

Weisburg, W. G., Tully, J. G., Rose, D. L., Petzel, J. P., Oyaizu, H., Yang, D., ... & Van Etten, J. (1989). A phylogenetic analysis of the mycoplasmas: basis for their classification. *Journal of bacteriology*, *171*(12), 6455-6467.

Welch, R. M., Norvell, W. A., Schaefer, S. C., Shaff, J. E., & Kochian, L. V. (1993). Induction of iron (III) and copper (II) reduction in pea (Pisum sativum L.) roots by Fe and Cu status: Does the root-cell plasmalemma Fe (III)-chelate reductase perform a general role in regulating cation uptake?. *Planta*, *190*(4), 555-561.

Winkelmann, G. (2007). Ecology of siderophores with special reference to the fungi. *Biometals*, *20*, 379–392.

Xue, C., Liu, Z., Dai, L., Bu, J., Liu, M., Zhao, Z., ... & Zhao, J. (2018). Changing Host Photosynthetic, Carbohydrate, and Energy Metabolisms Play Important Roles in Phytoplasma Infection. *Phytopathology*, *108*(9), 1067-1077.

Yu, G., Wang, L. G., Han, Y., & He, Q. Y. (2012). clusterProfiler: an R package for comparing biological themes among gene clusters. *Omics: a journal of integrative biology*, *16*(5), 284-287.

Yuan, Y. X., Zhang, J., Wang, D. W., & Ling, H. Q. (2005). AtbHLH29 of Arabidopsis thaliana is a functional ortholog of tomato FER involved in controlling iron acquisition in strategy I plants. *Cell research*, *15*(8), 613.

Yuan, Y., Wu, H., Wang, N., Li, J., Zhao, W., Du, J., ... & Ling, H. Q. (2008). FIT interacts with AtbHLH38 and AtbHLH39 in regulating iron uptake gene expression for iron homeostasis in Arabidopsis. *Cell research*, *18*(3), 385.

Zamioudis, C., Hanson, J., & Pieterse, C. M. (2014). β-Glucosidase BGLU42 is a MYB72-dependent key regulator of rhizobacteria-induced systemic resistance and modulates iron deficiency responses in Arabidopsis roots. *New Phytologist*, *204*(2), 368-379.

5. Discussion and conclusions

Field condition implies a large number of abiotic and biotic stresses, which interfere with each other. Especially in relation with poorly studied pathogens, such as the almost unculturable phytoplasmas (Contaldo *et al.*, 2012), managing the contemporaneous effect of multiple factors may lead to confusion or misinterpretations. For this reason, many researchers have tried to focus their investigations on precise and limited aspects, working with model plants in environment-controlled conditions (Bai *et al*., 2009; Pacifico *et al*., 2015; Pagliari *et al*., 2017). Nevertheless, plant response to a combination of two different stresses is unique and cannot be directly extrapolated from the response of plants to each of the different stresses applied individually (Mittler *et al*., 2006; Prasch and Sonnewald, 2015).

Considering that, in nature, plants may be simultaneously exposed to nutrient deficiencies and pathogen infection (Datnoff *et al.*, 2007; Dordas 2008; Huber *et al.*, 2012; Gupta *et al.*, 2017), we tried to give an original contribution to the research on phytoplasma diseases and plant response in the tripartite nutrient-plant-pathogen system. Phytoplasma diseases are often related to symptoms of nutritional deficiency, such as chlorosis, curling, and reddening. However, only few studies addressed the imbalance of mineral nutrients in plants following phytoplasma infections. Schweigkofler *et al*. (2008) showed that the Bois noir disease caused a reduction of the content of Ca and other mineral elements such as N, Mg, P, K, Mn, and Fe in different grape cultivars. In phytoplasma infected pear and apricot, imbalances in Fe/Mn and K/Mg ratio were reported (Rossi *et al.*, 2010). The fact that both Fe deficiency and phytoplasma infection are characterized by leaf yellowing, caused by a decrease of chlorophyll content, and alteration of expression of genes involved in photosynthesis (Mou *et al*. 2013; Rodriguez-Celma *et al*., 2013; Nejat *et al*., 2015; Xue *et al*., 2018; Wang *et al*., 2018a; Wang *et al*., 2018c), let us to speculate that phytoplasma may cause an alteration of Fe homeostasis.

In this study, the role of Fe in the interaction between '*Candidatus* Phytoplasma solani' ('*Ca*. P. solani') and *Solanum lycopersicum* (cultivar Micro-Tom) was studied, comparing healthy and phytoplasma-infected plants in Fe-sufficient and Fe-starved conditions. Tomato plant is widely used as model in the study of the interaction with '*Ca*. P. solani' (Pracros *et al.*, 2006; Machenaud *et al.*, 2007; Pracros *et al.*, 2007; Ahmad *et al.*, 2014; Buxa *et al.*, 2015; Aryan *et al.*, 2016; De Marco *et al.*, 2016). In controlled condition, tomato plants are infected by grafting. As a first set up, different grafting methods were tested, and results on their strengths and weaknesses were published in Buoso

and Loschi (2019). Moreover, tomato plant is employed in the study of *Strategy I* Fe uptake mechanism (Ivanov *et al.*, 2012). Thus, as second goal to reach, an efficient system that guaranteed concomitant presence of Fe-deficiency and phytoplasma symptoms was set up.

In the current study, I studied the relationships occurring between phytoplasma infection and Fe deficiency stress, analysing the problem from different perspectives (single stress and double stress) and with different technical approaches. Transcriptome profiling (by RNA-seq) of phytoplasma-infected and Fe-deficient leaves indicated that both stresses share some important targets, affecting photosynthesis and pigments synthesis and leading to the development of altered chloroplasts and chlorotic leaves. ICP-OES surveys and expression analyses of the genes involved in Fe uptake mechanism in the root showed that, in case of Fe-sufficient conditions, phytoplasma do not apparently interfere with the uptake, acquisition or long-distance transport of Fe. Nevertheless, Perls'-DAB staining revealed that phytoplasma presence in the phloem deals to a shift of Fe pools and an increase of Fe in the leaf phloem. In infected plants that undergo Fe deficiency, the pathogen titre is significantly decreased, suggesting that the pathogen does need a Fe-rich environment for its wellness and its replication capability.

Under Fe starvation, the expression of the genes involved in Fe-uptake is reduced in the infected plants, indicating a possible impairment in the communication of the Fe status between shoots and roots caused by the pathogen, possibly by the interference with the synthesis or transport of a promotive signal. It may be assumed that interference with phloem-based long-distance signalling has far-reaching consequences for the orchestration of root-mediated transport processes.

6. Acknowledgement

I owe a great debt of gratitude to many people for their human and scientific contribution to this work.

I would like to thank to my supervisor Dr. Simonetta Santi for the support of my PhD study and for her guidance all the time of project: she encouraged my research, my intuitions and my independence, allowing me to grow as scientist.

Dr. Wolfgang Schmidt for the "remote" but valuable contribution to the review of this work. His availability, advice and support were a certainty during the most critical phases.

Prof. Rita Musetti, not only for her assistance in electron microscopy investigations, but also for her insightful comments and encouragement.

Prof. Marta Martini for the support with phytoplasma quantification and for the careful supervision of the analyses.

The whole plant pathology group for having hosted me and my plant material in their greenhouse.

Dr. Laura Pagliari for giving me the opportunity to grow as a researcher, for being a competent and helpful collaborator and for her presence in trouble moments.

Alberto Loschi for teaching me the grafting techniques and especially for being my point of reference in these three years.

Dr. Fabio Marroni for his collaboration with the bioinformatic analyses and his precious tips.

Dr. Laura Zanin for her scientific expertise, for supporting me in times of discouragement and for always being passionate about research.

Dr. Alessandro Franco for sharing with me every single moment during the PhD and for the certainty of never being alone.

I thank all the valuable people who collaborated with me, giving a precious contribution to my research: Carla Calligaro, Dr. Barbara Piani and Dr. Alessandro Mattiello.

Last but not least, I would like to express my deepest gratitude to my family and friends. This work would not have been possible without their warm love, continued patience, and endless support.

7. Literature

Ahmad, J. N., Renaudin, J., & Eveillard, S. (2014). Expression of defence genes in stolbur phytoplasma infected tomatoes, and effect of defence stimulators on disease development. *European journal of plant pathology*, *139*(1), 39-51.

Albertazzi, G., Milc, J., Caffagni, A., Francia, E., Roncaglia, E., Ferrari, F., ... & Pecchioni, N. (2009). Gene expression in grapevine cultivars in response to Bois Noir phytoplasma infection. *Plant Science*, *176*(6), 792-804.

Al-Ghaithi, A. G., Hanif, M. A., Al-Busaidi, W. M., & Al-Sadi, A. M. (2016). Increased sodium and fluctuations in minerals in acid limes expressing witches' broom symptoms. *SpringerPlus*, *5*(1), 418.

Andersen, M. T., Liefting, L. W., Havukkala, I., & Beever, R. E. (2013). Comparison of the complete genome sequence of two closely related isolates of 'Candidatus Phytoplasma australiense' reveals genome plasticity. *BMC genomics*, *14*(1), 529.

Anderson, A. J., & Guerra, D. (1985). Responses of bean to root colonization with Pseudomonas putida in a hydroponic system. *Phytopathology*, *75*(9), 992-995.

Andrews, S. C., Robinson, A. K., & Rodríguez-Quiñones, F. (2003). Bacterial iron homeostasis. *FEMS microbiology reviews*, *27*(2-3), 215-237.

Arashida, R., Kakizawa, S., Hoshi, A., Ishii, Y., Jung, H. Y., Kagiwada, S., ... & Namba, S. (2008). Heterogeneic dynamics of the structures of multiple gene clusters in two pathogenetically different lines originating from the same phytoplasma. *DNA and cell biology*, *27*(4), 209-217.

Arie, T., Takahashi, H., Kodama, M., & Teraoka, T. (2007). Tomato as a model plant for plant-pathogen interactions. *Plant Biotechnology*, *24*(1), 135-147.

Aryan, A., Musetti, R., Riedle-Bauer, M., & Brader, G. (2016). Phytoplasma transmission by heterologous grafting influences viability of the scion and results in early symptom development in periwinkle rootstock. *Journal of Phytopathology*, *164*(9), 631-640.

Audenaert, K., Pattery, T., Cornelis, P., & Hofte, M. (2002). Induction of systemic resistance to Botrytis cinerea in tomato by Pseudomonas aeruginosa 7NSK2: role of salicylic acid, pyochelin, and pyocyanin. *Mol. Plant Microbe Interact.*, *11*, 1147–1156.

Aznar, A., Chen, N. W., Thomine, S., & Dellagi, A. (2015). Immunity to plant pathogens and iron homeostasis. *Plant Science*, *240*, 90-97.

Bai, X., Correa, V. R., Toruño, T. Y., Ammar, E. D., Kamoun, S., & Hogenhout, S. A. (2009). AY-WB phytoplasma secretes a protein that targets plant cell nuclei. *Molecular Plant-Microbe Interactions*, *22*(1), 18-30.

Bai, X., Zhang, J., Ewing, A., Miller, S. A., Radek, A. J., Shevchenko, D. V., ... & Hogenhout, S. A. (2006). Living with genome instability: the adaptation of phytoplasmas to diverse environments of their insect and plant hosts. *Journal of bacteriology*, *188*(10), 3682-3696.

Bakker, P. A., Pieterse, C. M., & Van Loon, L. C. (2007). Induced systemic resistance by fluorescent Pseudomonas spp. *Phytopathology*, *97*(2), 239-243.

Balk, J., & Pilon, M. (2011). Ancient and essential: the assembly of iron-sulfur clusters in plants. *Trends Plant Sci.*, *16*, 218–226.

Barash, I., Zion, R., Krikun, J., & Nachmias, A. (1988). Effect of iron status on Verticillium wilt disease and on in vitro production of siderophores by Verticillium dahliae. *Journal of plant nutrition*, *11*(6-11), 893-905.

Bashir, K., & Nishizawa, N. K. (2006). Deoxymugineic acid synthase: a gene important for Fe-acquisition and homeostasis. *Plant signaling & behavior*, *1*(6), 290-292.

Bauer, P., Ling, H. Q., & Guerinot, M. L. (2007). FIT, the FER-like iron deficiency induced transcription factor in Arabidopsis. *Plant Physiology and Biochemistry*, *45*(5), 260-261.

Belli, G., Bianco, P. A., and Conti, M. (2010). Grapevine yellows in Italy: past, present and future. *J. Plant Pathol.*, *92*, 303–326.

Bertaccini, A., & Duduk, B. (2009). Phytoplasma and phytoplasma diseases: a review of recent research. *Phytopathologia mediterranea*, *48*(3), 355-378.

Bertaccini, A., Duduk, B., Paltrinieri, S., & Contaldo, N. (2014). Phytoplasmas and phytoplasma diseases: a severe threat to agriculture. *American Journal of Plant Sciences*, *5*,1763–1788.

Bertamini, M., Grando, M. S., Muthuchelian, K., & Nedunchezhian, N. (2002b). Effect of phytoplasmal infection on photosystem II efficiency and thylakoid membrane protein changes in field grown apple (Malus pumila) leaves. *Physiological and molecular plant pathology*, *61*(6), 349-356.

Bertamini, M., Nedunchezhian, N., Tomasi, F., & Grando, M. S. (2002a). Phytoplasma [Stolbur-subgroup (Bois Noir-BN)] infection inhibits photosynthetic pigments, ribulose-1, 5-bisphosphate carboxylase and photosynthetic activities in field grown grapevine (Vitis vinifera L. cv. Chardonnay) leaves. *Physiological and Molecular Plant Pathology*, *61*(6), 357-366.

Boonrod, K., Munteanu, B., Jarausch, B., Jarausch, W., & Krczal, G. (2012). An immunodominant membrane protein (Imp) of 'Candidatus Phytoplasma mali' binds to plant actin. *Molecular Plant-Microbe Interactions*, *25*(7), 889-895.

Borisy, G. G., & Svitkina, T. M. (2000). Actin machinery: pushing the envelope. *Current opinion in cell biology*, *12*(1), 104-112.

Bosco, D., Galetto, L., Leoncini, P., Saracco, P., Raccah, B., & Marzachì, C. (2007). Interrelationships between "Candidatus Phytoplasma asteris" and its leafhopper vectors (Homoptera: Cicadellidae). *Journal of economic entomology*, *100*(5), 1504-1511.

Briat, J. F., Duc, C., Ravet, K., & Gaymard, F. (2010). Ferritins and iron storage in plants. *Biochimica et Biophysica Acta (BBA)-General Subjects*, *1800*(8), 806-814.

Brumbarova, T., & Bauer, P. (2005). Iron-mediated control of the basic helix-loop-helix protein FER, a regulator of iron uptake in tomato. *Plant Physiology*, *137*(3), 1018-1026.

Buoso, S., & Loschi, A. (2019). Micro-Tom Tomato Grafting for Stolbur-Phytoplasma Transmission: Different Grafting Techniques. In *Phytoplasmas* (pp. 9-19). Humana Press, New York, NY.

Buxa, S. V., Degola, F., Polizzotto, R., De Marco, F., Loschi, A., Kogel, K. H., ... & Musetti, R. (2015). Phytoplasma infection in tomato is associated with re-organization of plasma membrane, ER stacks, and actin filaments in sieve elements. *Frontiers in plant science*, *6*, 650.

Buysens, S., Heungens, K., Poppe, J., & Hofte, M. (1996). Involvement of pyochelin and pyoverdin in suppression of Pythium-induced damping-off of tomato by Pseudomonas aeruginosa 7NSK2. *Applied and Environmental Microbiology*, *62*(3), 865-871.

Cesco, S., Neumann, G., Tomasi, N., Pinton, R., & Weisskopf, L. (2010). Release of plant-borne flavonoids into the rhizosphere and their role in plant nutrition. *Plant and Soil*, *329*(1-2), 1-25.

Christeller, J. T., Farley, P. C., Ramsay, R. J., & Laing, W. A. (1998). Purification, characterization and cloning of an aspartic protease inhibitor from squash phloem exudate. *European Journal of Biochemistry*, *254*, 160–167.

Christensen, N. M., Axelsen, K. B., Nicolaisen, M., & Schultz, A. (2005). Phytoplasmas and Their Interactions with Their Hosts. *Trends in Plant Science*, *10*, 526-535.

Christensen, N. M., Nicolaisen, M., Hansen, M., & Schulz, A. (2004). Distribution of phytoplasmas in infected plants as revealed by real-time PCR and bioimaging. *Molecular Plant–Microbe Interactions*, *17*,1175–1184.

Colangelo, E. P., & Guerinot, M. L. (2004). The essential basic helix-loop-helix protein FIT1 is required for the iron deficiency response. *The Plant Cell*, *16*(12), 3400-3412.

Contaldo, N., Bertaccini, A., Paltrinieri, S., Windsor, H. M., & Windsor, G. D. (2012). Axenic culture of plant pathogenic phytoplasmas. *Phytopathol. Mediterr.*, *51*, 607–617.

Cordova, I., Jones, P., Harrison, N. A., & Oropeza, C. (2003). In Situ Detection of Phytoplasma DNA in Embryos from Coconut Palms with Lethal Yellowing Disease. *Molecular Plant Pathology*, *4*, 99-108.

Cui, Y., Chen, C. L., Cui, M., Zhou, W. J., Wu, H. L., & Ling, H. Q. (2018). Four IVa bHLH Transcription Factors Are Novel Interactors of FIT and Mediate JA Inhibition of Iron Uptake in Arabidopsis. *Molecular plant*, *11*(9), 1166-1183.

Curie, C., Alonso, J. M., Marie, L. E., Ecker, J. R., & Briat, J. F. (2000). Involvement of NRAMP1 from Arabidopsis thaliana in iron transport. *Biochemical Journal*, *347*(3), 749-755.

Curie, C., Cassin, G., Couch, D., Divol, F., Higuchi, K., Le Jean, M., ... & Mari, S. (2008). Metal movement within the plant: contribution of nicotianamine and yellow stripe 1-like transporters. *Annals of botany*, *103*(1), 1-11.

Curie, C., Panaviene, Z., Loulergue, C., Dellaporta, S. L., Briat, J. F., & Walker, E. L. (2001). Maize yellow stripe1 encodes a membrane protein directly involved in Fe (III) uptake. *Nature*, *409*(6818), 346.

Cvrkovic, T., Jovic, J., Mitrovic, M., Krstic, O., & Tosevski I. (2014). Experimental and molecular evidence of Reptalus panzeri as a natural vector of bois noir. *Plant Pathology*, *63*, 42–53.

Dannenhoffer, J. M., Suhr, S. C., & Thompson, G. A. (2001). Phloem-specific expression of the pumpkin fruit trypsin inhibitor. *Planta*, *212*, 155–162.

Datnoff, L. E., Elmer, W. H., & Huber, D. M. (2007). Mineral nutrition and plant disease. *American Phytopathological Society* (APS Press).

De Marco, F., Pagliari, L., Degola, F., Buxa, S. V., Loschi, A., Dinant, S., ... & Musetti, R. (2016). Combined microscopy and molecular analyses show phloem occlusions and cell wall modifications in tomato leaves in response to 'Candidatus Phytoplasma solani'. *Journal of microscopy*, *263*(2), 212-225.

De Oliveira, E., De Oliveira, C. M., Magalhães, P. C., De Andrade, C. L. T., & Hogenhout, S. A. (2005). Spiroplasma and Phytoplasma infection reduce kernel production and nutrient and water contents of several but not all maize cultivars [Zea mays L.]. *Maydica (Italy).*

De Oliveira, E., Magalhães, P. C., Gomide, R. L., Vasconcelos, C. A., Souza, I. R., Oliveira, C. M., ... & Schaffert, R. E. (2002). Growth and nutrition of mollicute-infected maize. *Plant disease*, *86*(9), 945-949.

De Vleesschauwer, D., & Höfte, M. (2009). Rhizobacteria-induced systemic resistance. *Advances in botanical research*, *51*, 223-281.

Deák, M., Horváth, G. V., Davletova, S., Török, K., Sass, L., Vass, I., ... & Dudits, D. (1999). Plants ectopically expressing the ironbinding protein, ferritin, are tolerant to oxidative damage and pathogens. *Nature biotechnology*, *17*(2), 192.

Dellagi, A., Brisset, M. N., Paulin, J. P., & Expert, D. (1998). Dual role of desferrioxamine in Erwinia amylovora pathogenicity. *Molecular plant-microbe interactions*, *11*(8), 734-742.

Dellagi, A., Rigault, M., Segond, D., Roux, C., Kraepiel, Y., Cellier, F., ... & Expert, D. (2005). Siderophore-mediated upregulation of Arabidopsis ferritin expression in response to Erwinia chrysanthemi infection. *The Plant Journal*, *43*(2), 262-272.

Desneux, N., Decourtye, A., & Delpuech, J. M. (2007). The sublethal effects of pesticides on beneficial arthropods. *Annu. Rev. Entomol.*, *52*, 81-106.

Desveaux, D., Singer, A. U., & Dangl, J. L. (2006). Type III effector proteins: doppelgangers of bacterial virulence. *Current opinion in plant biology*, *9*(4), 376-382.

DiDonato Jr, R. J., Roberts, L. A., Sanderson, T., Eisley, R. B., & Walker, E. L. (2004). Arabidopsis Yellow Stripe-Like2 (YSL2): a metal-regulated gene encoding a plasma membrane transporter of nicotianamine–metal complexes. *The Plant Journal*, *39*(3), 403-414.

Dinant, S., & Lemoine, R. (2010). The phloem pathway: new issues and old debates. *Comptes rendus biologies*, *333*(4), 307-319.

Doi, Y., Teranaka, M., Yora, K. & Asuyama, H. (1967). Mycoplasma or PLT Grouplike Microrganisms Found in the Phloem Elements of Plants Infected with Mulberry Dwarf, Potato Witches' Broom, Aster Yellows or Pawlownia Witches' Broom. *Japanese Journal of Phytopathology*, *33*, 259-266.

Dordas, C. (2008). Role of nutrients in controlling plant diseases in sustainable agriculture. A review. *Agronomy for sustainable development*, *28*(1), 33-46.

Du, J., Huang, Z., Wang, B., Sun, H., Chen, C., Ling, H. Q., & Wu, H. (2015). SlbHLH068 interacts with FER to regulate the iron-deficiency response in tomato. *Annals of botany*, *116*(1), 23-34.

Duduk, B., & Bertaccini, A. (2006). Corn with symptoms of reddening: new host of stolbur phytoplasma. *Plant Disease*, *90*(10), 1313-1319.

Durrett, T. P., Gassmann, W., & Rogers, E. E. (2007). The FRD3-mediated efflux of citrate into the root vasculature is necessary for efficient iron translocation. *Plant physiology*, *144*(1), 197-205.

Eckhardt, U., Marques, A. M., & Buckhout, T. J. (2001). Two iron-regulated cation transporters from tomato complement metal uptake-deficient yeast mutants. *Plant molecular biology*, *45*(4), 437-448.

Eide, D., Broderius, M., Fett, J., & Guerinot, M. L. (1996). A novel iron-regulated metal transporter from plants identified by functional expression in yeast. *Proceedings of the National Academy of Sciences*, *93*(11), 5624-5628.

Ember, I., Acs, Z., Munyaneza, J. E., Crosslin, J. M., & Kolber, M. (2011). Survey and molecular detection of phytoplasmas associated with potato in Romania and southern Russia. *European Journal of Plant Pathology*, *130*(3), 367-377.

Ember, I., Bodor, P., Zsófi, Z., Pálfi, Z., Ladányi, M., Pásti, G., ... & Bencsik, O. (2018). Bois noir affects the yield and wine quality of Vitis vinifera L. cv.'Chardonnay'. *European Journal of Plant Pathology*, 1-13.

Endeshaw, S. T., Murolo, S., Romanazzi, G., & Neri, D. (2012). Effects of Bois noir on carbon assimilation, transpiration, stomatal conductance of leaves and yield of grapevine (Vitis vinifera) cv. Chardonnay. *Physiologia plantarum*, *145*(2), 286-295.

Expert, D. (1999). Withholding and exchanging iron: interactions between Erwinia spp. and their plant hosts. *Annual review of phytopathology*, *37*(1), 307-334.

Fenton, H. (1894). Oxidation of tartaric acid in presence of iron. *J. Chem. Soc. Trans.*, *65*, 899–910.

Firrao, G., Garcia-Chapa, M., & Marzachi, C. (2007). Phytoplasmas: genetics, diagnosis and relationships with the plant and insect host. *Front. Biosci.*, *12*, 1353–1375.

Foissac, X., & Maixner, M. (2013). Spread of grapevine phytoplasma diseases. *New perspectives in phytoplasma disease management*, 28.

Fos, A., Danet, J. L., Zreik, L., Garnier, M., & Bové, J. M. (1992). Use of a monoclonal-antibody to detect the stolbur mycoplasma-like organism in plants and insects and to identify a vector in France. *Plant Disease*, *76*, 1092–1096.

Fourcroy, P., Sisó-Terraza, P., Sudre, D., Savirón, M., Reyt, G., Gaymard, F., ... & Briat, J. F. (2014). Involvement of the ABCG37 transporter in secretion of scopoletin and derivatives by Arabidopsis roots in response to iron deficiency. *New Phytologist*, *201*(1), 155-167.

Furch, A. C., Hafke, J. B., Schulz, A., & van Bel, A. J. (2007). Ca2+-mediated remote control of reversible sieve tube occlusion in Vicia faba. *Journal of Experimental Botany*, *58*(11), 2827-2838.

Galetto, L., Bosco, D., Balestrini, R., Genre, A., Fletcher, J., & Marzachì, C. (2011). The major antigenic membrane protein of "Candidatus Phytoplasma asteris" selectively interacts with ATP synthase and actin of leafhopper vectors. *PLoS One*, *6*(7), e22571.

Garau, R., Sechi, A., Prota, V. A., & Moro, G. (2007). Productive parameters in Chardonnay and Vermentino grapevines infected with "bois noir" and recovered in Sardinia. *Bulletin of insectology*, *60*(2), 233.

García, M. J., Lucena, C., Romera, F. J., Alcántara, E., & Pérez-Vicente, R. (2010). Ethylene and nitric oxide involvement in the up-regulation of key genes related to iron acquisition and homeostasis in Arabidopsis. *Journal of Experimental Botany*, *61*(14), 3885-3899.

Garnier M. (2000). The stolbur phytoplasma: an ubiquitous agent. *Comptes Rendus de l'Academie d'Agriculture de France*, *86*, 27–33.

Gatineau, F., Jacob, N., Vautrin, S., Larrue, J., Lherminier, J., Richard-Molard, M., & Boudon-Padieu, E. (2002). Association with the syndrome "basses richesses" of sugar beet of a phytoplasma and a bacterium-like organism transmitted by a Pentastiridius sp. *Phytopathology*, *92*(4), 384-392.

Guerinot, M. L., & Yi, Y. (1994). Iron: nutritious, noxious, and not readily available. *Plant Physiol.*, *104*, 815–20

Gupta, N., Debnath, S., Sharma, S., Sharma, P., & Purohit, J. (2017). Role of Nutrients in Controlling the Plant Diseases in Sustainable Agriculture. In *Agriculturally Important Microbes for Sustainable Agriculture* (pp. 217-262). Springer, Singapore.

Haas, H., Eisendle, M., & Turgeon, B. G. (2008). Siderophores in fungal physiology and virulence. *Annu. Rev. Phytopathol.*, *46*, 149-187.

Haber, F., & Weiss, J. (1934). The catalytic decomposition of hydrogen peroxide by iron salts. *Proc. R. Soc. Lond. Ser. A*, 147:332–51.

Haglund, C. M., & Welch, M. D. (2011). Pathogens and polymers: microbe–host interactions illuminate the cytoskeleton. *The Journal of cell biology*, *195*(1), 7-17.

Hartmann, T. (1999). Chemical ecology of pyrrolizidine alkaloids. *Planta*, *207*: 483–495.

Hayashi, H., Fukuda, A., Suzui, N., & Fujimaki, S. (2000). Proteins in the sieve tube-companion cell complexes: their detection, localization and possible functions. *Australian Journal of Plant Physiology*, *27*, 489–496.

Hogenhout, S. A., & Loria, R. (2008). Virulence mechanisms of Gram-positive plant pathogenic bacteria. *Current opinion in plant biology*, *11*(4), 449-456.

Hogenhout, S. A., & Segura, M. (2010). Phytoplasma genomics, from sequencing to comparative and functional genomics-What have we learnt. *Phytoplasmas: genomes, plant hosts and vectors*, 19-36.

Hogenhout, S. A., Oshima, K., Ammar, E. D., Kakizawa, S., Kingdom, H. N., & Namba, S. (2008). Phytoplasmas: bacteria that manipulate plants and insects. *Molecular Plant Pathology*, *9*(4), 403-423.

Hoshi, A., Oshima, K., Kakizawa, S., Ishii, Y., Ozeki, J., Hashimoto, M., ... & Namba, S. (2009). A unique virulence factor for proliferation and dwarfism in plants identified from a phytopathogenic bacterium. *Proceedings of the National Academy of Sciences*, *106*(15), 6416-6421.

Hren, M., Nikolić, P., Rotter, A., Blejec, A., Terrier, N., Ravnikar, M., ... & Gruden, K. (2009). 'Bois noir'phytoplasma induces significant reprogramming of the leaf transcriptome in the field grown grapevine. *BMC genomics*, *10*(1), 1.

Huber, D., Römheld, V., & Weinmann, M. (2012). Chapter 10—Relationship between nutrition, plant diseases and pests. In P. Marschner (Ed.), *Marschner's mineral nutrition of higher plants* (3rd ed.) (pp. 283–298). London U.K.: Academic Press.

Inoue, H., Kobayashi, T., Nozoye, T., Takahashi, M., Kakei, Y., Suzuki, K., ... & Nishizawa, N. K. (2009). Rice OsYSL15 is an iron-regulated iron (III)-deoxymugineic acid transporter expressed in the roots and is essential for iron uptake in early growth of the seedlings. *Journal of Biological Chemistry*, *284*(6), 3470-3479.

IRPCM, P., & Spiroplasma, W. T. P. T. G. (2004). 'Candidatus Phytoplasma', a taxon for the wall-less, nonhelical prokaryotes that colonize plant phloem and insects. *International Journal of Systematic and Evolutionary Microbiology*, *54*(Pt 4), 1243.

Ishiie, T., Doi, Y., Yora, K., & Asuyama, H. (1967). Suppressive effects of antibiotics of tetracycline group on symptom development of mulberry dwarf disease. *Japanese Journal of Phytopathology*, *33*(4), 267-275.

Ivanov, R., Brumbarova, T., & Bauer, P. (2012). Fitting into the harsh reality: regulation of iron-deficiency responses in dicotyledonous plants. *Molecular Plant*, *5*(1), 27-42.

Ivanova, G., Mitrev, S., & Arsov, E. (2017). New evidence for the stolbur phytoplasma development in pepper in Republic of Macedonia. *Comptes rendus de l'Acade'mie bulgare des Sciences*, *70*(11), 1609-1616.

Jakoby, M., Wang, H. Y., Reidt, W., Weisshaar, B., & Bauer, P. (2004). FRU (BHLH029) is required for induction of iron mobilization genes in Arabidopsis thaliana. *FEBS letters*, *577*(3), 528-534.

Jin, C. W., Chen, W. W., Meng, Z. B., & Zheng, S. J. (2008). Iron deficiency-induced increase of root branching contributes to the enhanced root ferric chelate reductase activity. *Journal of integrative plant biology*, *50*(12), 1557-1562.

Johnson, D. C., Dean, D. R., Smith, A. D., & Johnson, M. K. (2005). Structure, function, and formation of biological iron-sulfur clusters. *Annu. Rev. Biochem.*, *74*, 247–281.

Jones Jr, J. B. (1982). Hydroponics: its history and use in plant nutrition studies. *Journal of plant Nutrition*, *5*(8), 1003-1030.

Jović, J., Cvrković, T., Mitrović, M., Krnjajić, S., Redinbaugh, M. G., Pratt, R. C., ... & Toševski, I. (2007). Roles of stolbur phytoplasma and Reptalus panzeri (Cixiinae, Auchenorrhyncha) in the epidemiology of Maize redness in Serbia. *European Journal of Plant Pathology*, *118*(1), 85-89.

Jung, H. Y., Miyata, S. I., Oshima, K., Kakizawa, S., Nishigawa, H., Wei, W., ... & Namba, S. (2003). First complete nucleotide sequence and heterologous gene organization of the two rRNA operons in the phytoplasma genome. *DNA and cell biology*, *22*(3), 209-215.

Kakizawa, S., Oshima, K., Kuboyama, T., Nishigawa, H., Jung, H. Y., Sawayanagi, T., ... & Namba, S. (2001). Cloning and expression analysis of Phytoplasma protein translocation genes. *Molecular plant-microbe interactions*, *14*(9), 1043-1050.

Kang, H. G., Foley, R. C., Oñate-Sánchez, L., Lin, C., & Singh, K. B. (2003). Target genes for OBP3, a Dof transcription factor, include novel basic helix-loop-helix domain proteins inducible by salicylic acid. *The Plant Journal*, *35*(3), 362-372.

Khan, M. A., Castro-Guerrero, N. A., McInturf, S. A., Nguyen, N. T., Dame, A. N., Wang, J., ... & Mendoza-Cozatl, D. G. (2018). Changes in iron availability in Arabidopsis are rapidly sensed in the leaf vasculature and impaired sensing leads to opposite transcriptional programs in leaves and roots. *Plant, cell & environment*.

Kieu, N. P., Aznar, A., Segond, D., Rigault, M., Simond-Côte, E., Kunz, C., ... & Dellagi, A. (2012). Iron deficiency affects plant defence responses and confers resistance to Dickeya dadantii and Botrytis cinerea. *Molecular plant pathology*, *13*(8), 816-827.

Kim, S. A., Punshon, T., Lanzirotti, A., Li, L., Alonso, J. M., Ecker, J. R., ... & Guerinot, M. L. (2006). Localization of iron in Arabidopsis seed requires the vacuolar membrane transporter VIT1. *Science*, *314*(5803), 1295-1298.

Kimura, S., & Sinha, N. (2008). Tomato (Solanum lycopersicum): a model fruit-bearing crop. *Cold Spring Harbor Protocols*, *2008*(11), pdb-emo105.

Kobayashi, T., & Nishizawa, N. K. (2012). Iron uptake, translocation, and regulation in higher plants. *Annual review of plant biology*, *63*, 131-152.

Kube, M., Mitrovic, J., Duduk, B., Rabus, R., & Seemüller, E. (2012). Current view on phytoplasma genomes and encoded metabolism. *The Scientific World Journal*, *2012*.

Kube, M., Schneider, B., Kuhl, H., Dandekar, T., Heitmann, K., Migdoll, A. M., ... & Seemüller, E. (2008). The linear chromosome of the plant-pathogenic mycoplasma 'Candidatus Phytoplasma mali'. *Bmc Genomics*, *9*(1), 306.

Kumar, R. K., Chu, H. H., Abundis, C., Vasques, K., Chan-Rodriguez, D., Chia, J. C., ... & Walker, E. L. (2017). Iron-Nicotianamine transporters are required for proper long distance iron signaling. *Plant physiology*, pp-00821.

Lanquar, V., Lelièvre, F., Bolte, S., Hamès, C., Alcon, C., Neumann, D., ... & Barbier-Brygoo, H. (2005). Mobilization of vacuolar iron by AtNRAMP3 and AtNRAMP4 is essential for seed germination on low iron. *The EMBO journal*, *24*(23), 4041-4051.

Laulhere, J. P., & Briat, J. F. (1993). Iron release and uptake by plant ferritin: effects of pH, reduction and chelation. *Biochemical Journal*, *290*(3), 693-699.

Lee I. M., (1992). Mycoplasmas which infect plants and insects. In Mycoplasmas: *Molecular Biology and Pathogenesis*, ed. J Maniloff, RN McElhansey, LR Finch, JB Baseman, pp. 379–90. Washington, DC: Am. Soc. Microbiol.

Lee I. M., Gundersen-Rindal, D., Davis, R.E. & Bartoszyk, I. M. (1998). Revised classification scheme of phytoplasmas based on RFLP analysis of 16SrRNA and ribosomal protein gene sequences. *International Journal of Systematic Bacteriology*, *48*, 1153-1169.

Lee, I. M., Davis, R. E., & Gundersen-Rindal, D. E., (2000). Phytoplasma: phytopathogenic mollicutes. *Annu. Rev. Microbiol., 54*, 221–255.

Lee, I. M., Gundersen-Rindal, D. E., Davis, R. E., Bottner, K. D., Marcone, C., & Seemüller, E. (2004a). 'Candidatus Phytoplasma asteris', a novel phytoplasma taxon associated with aster yellows and related diseases. *International journal of systematic and evolutionary microbiology*, *54*(4), 1037-1048.

Lee, I. M., Martini, M., Marcone, C., & Zhu, S. F. (2004b). Classification of phytoplasma strains in the elm yellows group (16SrV) and proposal of 'Candidatus Phytoplasma ulmi' for the phytoplasma associated with elm yellows. *International Journal of Systematic and Evolutionary Microbiology*, *54*(2), 337-347.

Leeman, M., Den Ouden, F. M., Van Pelt, J. A., Dirkx, F. P. M., Steijl, H., Bakker, P. A. H. M., & Schippers, B. (1996). Iron availability affects induction of systemic resistance to Fusarium wilt of radish by Pseudomonas fluorescens. *Phytopathology*, *86*(2), 149-155.

Lemanceau, P., Expert, D., Gaymard, F., Bakker, P. A. H. M., & Briat, J. F. (2009). Role of iron in plant–microbe interactions. *Advances in botanical research*, *51*, 491-549.

Li, J., Wu, X. D., Hao, S. T., Wang, X. J., & Ling, H. Q. (2008). Proteomic response to iron deficiency in tomato root. *Proteomics*, *8*(11), 2299-2311.

Ling, H. Q., Bauer, P., Bereczky, Z., Keller, B., & Ganal, M. (2002). The tomato fer gene encoding a bHLH protein controls iron-uptake responses in roots. *Proceedings of the National Academy of Sciences*, *99*(21), 13938-13943.

Liu, J., Osbourn, A., & Ma, P. (2015). MYB transcription factors as regulators of phenylpropanoid metabolism in plants. *Molecular Plant*, *8*(5), 689-708.

Lohaus, G., Winter, H., Riens, B., & Heldt, H. W. (1995). Further studies of the phloem loading process in leaves of barley and spinach. The comparison of metabolite concentrations in the apoplastic compartment with those in the cytosolic compartment and in the sieve tubes. *Botanica Acta*, *108*, 270–275.

Long, T. A., Tsukagoshi, H., Busch, W., Lahner, B., Salt, D. E., & Benfey, P. N. (2010). The bHLH transcription factor POPEYE regulates response to iron deficiency in Arabidopsis roots. *The Plant Cell*, tpc-110.

Lu, Y. T., Li, M. Y., Cheng, K. T., Tan, C. M., Su, L. W., Lin, W. Y., ... & Yang, J. Y. (2014). Transgenic plants that express the phytoplasma effector SAP11 show altered phosphate starvation and defense responses. *Plant physiology*, *164*(3), 1456-1469.

Lucena, C., Waters, B. M., Romera, F. J., García, M. J., Morales, M., Alcántara, E., & Pérez-Vicente, R. (2006). Ethylene could influence ferric reductase, iron transporter, and H+-ATPase gene expression by affecting FER (or FER-like) gene activity. *Journal of Experimental Botany*, *57*(15), 4145-4154.

Lucena, J. J. (2000). Effect of bicarbonate, nitrate and other environmental factors on iron deficiency chlorosis. A rewiew. *Journal of Plant Nutrition.*, *23*, 1591 – 1606.

Luo, Y., Han, Z., Chin, S. M., & Linn, S. (1994). Three chemically distinct types of oxidants formed by iron-mediated Fenton reactions in the presence of DNA. *Proceedings of the National Academy of Sciences*, *91*(26), 12438-12442.

Machenaud, J., Henri, R., Dieuaide-Noubhani, M., Pracros, P., Renaudin, J., & Eveillard, S. (2007). Gene expression and enzymatic activity of invertases and sucrose synthase in Spiroplasma citri or stolbur phytoplasma infected plants. *Bulletin of Insectology*, *60*(2), 219.

MacLean, A. M., Orlovskis, Z., Kowitwanich, K., Zdziarska, A. M., Angenent, G. C., Immink, R. G., & Hogenhout, S. A. (2014). Phytoplasma effector SAP54 hijacks plant reproduction by degrading MADS-box proteins and promotes insect colonization in a RAD23-dependent manner. *PLoS biology*, *12*(4), e1001835.

MacLean, A. M., Sugio, A., Makarova, O. V., Findlay, K. C., Grieve, V. M., Tóth, R., ... & Hogenhout, S. A. (2011). Phytoplasma effector SAP54 induces indeterminate leaf-like flower development in Arabidopsis plants. *Plant Physiology*, *157*(2), 831-841.

Macur, R. E., Mathre, D. E., & Olsen, R. A. (1991). Interactions between iron nutrition and Verticillium wilt resistance in tomato. *Plant and soil*, *134*(2), 281-286.

Maixner M. (1994). Transmission of German grapevine yellows (Vergilbungskrankheit) by the planthopper Hyalesthes obsoletus (Auchenorrhyncha: Cixiidae). *Vitis*, *33*, 103–104.

Marcone, C., Lee, I. M., Davis, R. E., Ragozzino, A., & Seemüller, E. (2000). Classification of aster yellows group phytoplasmas based on combined analyses of rRNA and tuf gene sequences. *International Journal of Systematic and Evolutionary Microbiology*, *50*(5), 1703-1713.

Marschner, P. (2011). Marschner´s Mineral Nutrition of Higher Plants 3rd ed., Academic Press, London.

Mata, C.G., Lamattina, L., & Cassia, R.O. (2001). Involvement of iron and ferritin in the potato-Phytophthora infestans interaction. *Eur. J. Plant Pathol.*, *107*, 557–562.

Maurer, F., Müller, S., & Bauer, P. (2011). Suppression of Fe deficiency gene expression by jasmonate. *Plant Physiology and Biochemistry*, *49*(5), 530-536.

McCoy, R. E. (1989). Plant disease associated with mycoplasma-like organisms. *The mycoplasmas*, 5, 546-640.

Mendoza-Cózatl, D. G., Xie, Q., Akmakjian, G. Z., Jobe, T. O., Patel, A., Stacey, M. G., ... & Schroeder, J. I. (2014). OPT3 is a component of the iron-signaling network between leaves and roots and misregulation of OPT3 leads to an over-accumulation of cadmium in seeds. *Molecular plant*, *7*(9), 1455-1469.

Mittler, R. (2006). Abiotic stress, the field environment and stress combination. *Trends in plant science*, *11*(1), 15-19.

Mortvedt, J. J. (1991). Correcting iron deficiencies in annual and perennial plants: present technologies and future prospects. *Plant and Soil.*, *130*, 273-279.

Murray, C., & Christeller, J. T. (1995). Purification of a trypsin inhibitor (PFT1) from pumpkin fruit phloem exudate and isolation of putative trypsin and chymotrypsin inhibitor cDNA clones. *Biological Chemistry*, *276*, 281–287.

Musetti, R., Buxa, S. V., De Marco, F., Loschi, A., Polizzotto, R., Kogel, K. H., & van Bel, A. J. (2013). Phytoplasma-triggered Ca2+ influx is involved in sieve-tube blockage. *Molecular Plant-Microbe Interactions*, *26*(4), 379-386.

Naranjo-Arcos, M. A., & Bauer, P. (2016). Iron Nutrition, Oxidative Stress, and Pathogen Defense. In *Nutritional Deficiency*. InTech.

Neema, C., Laulhere, J.P. and Expert, D. (1993) Iron deficiency induced by chrysobactin in Saintpaulia leaves inoculated with Erwinia chrysanthemi. *Plant Physiol.*, *102*, 967–973.

Nishigawa, H., Miyata, S. I., Oshima, K., Sawayanagi, T., Komoto, A., Kuboyama, T., ... & Namba, S. (2001). In planta expression of a protein encoded by the extrachromosomal DNA of a phytoplasma and related to geminivirus replication proteins. *Microbiology*, *147*(2), 507-513.

Nouet, C., Motte, P., & Hanikenne, M. (2011). Chloroplastic and mitochondrial metal homeostasis. *Trends in plant science*, *16*(7), 395-404.

Nozoye, T., Nagasaka, S., Kobayashi, T., Takahashi, M., Sato, Y., Sato, Y., ... & Nishizawa, N. K. (2011). Phytosiderophore efflux transporters are crucial for iron acquisition in graminaceous plants. *Journal of Biological Chemistry*, *286*(7), 5446-5454.

Ohata, T., Kanazawa, K., Mihashi, S., Kishi-Nishizawa, N., Fushiya, S., Nozoe, S., ... & Mori, S. (1993). Biosynthetic pathway of phytosiderophores in iron-deficient graminaceous plants: development of an assay system for the detection of nicotianamine aminotransferase activity. *Soil Science and Plant Nutrition*, *39*(4), 745-749.

Opalski, K. S., Schultheiss, H., Kogel, K. H., & Hückelhoven, R. (2005). The receptor-like MLO protein and the RAC/ROP family G-protein RACB modulate actin reorganization in barley attacked by the biotrophic powdery mildew fungus Blumeria graminis f. sp. hordei. *The Plant Journal*, *41*(2), 291-303.

Orlovskis, Z., Canale, M. C., Haryono, M., Lopes, J. R. S., Kuo, C. H., & Hogenhout, S. A. (2017). A few sequence polymorphisms among isolates of Maize bushy stunt phytoplasma associate with organ proliferation symptoms of infected maize plants. *Annals of botany*, *119*(5), 869-884.

Oshima, K., Ishii, Y., Kakizawa, S., Sugawara, K., Neriya, Y., Himeno, M., ... & Namba, S. (2011). Dramatic transcriptional changes in an intracellular parasite enable host switching between plant and insect. *PLoS One*, *6*(8), e23242.

Oshima, K., Kakizawa, S., Nishigawa, H., Jung, H. Y., Wei, W., Suzuki, S., ... & Namba, S. (2004). Reductive evolution suggested from the complete genome sequence of a plant-pathogenic phytoplasma. *Nature genetics*, *36*(1), 27.

Oshima, K., Kakizawa, S., Nishigawa, H., Kuboyama, T., Miyata, S. I., Ugaki, M., & Namba, S. (2001). A plasmid of phytoplasma encodes a unique replication protein having both plasmid-and virus-like domains: clue to viral ancestry or result of virus/plasmid recombination?. *Virology*, *285*(2), 270-277.

Oshima, K., Maejima, K., & Namba, S. (2013). Genomic and evolutionary aspects of phytoplasmas. *Frontiers in microbiology*, *4*, 230.

Osler, R., Borselli, S., Ermacora, P., Ferrini, F., Loschi, A., Martini, M., ... & Loi, N. (2016). Transmissible tolerance to European stone fruit yellows (ESFY) in apricot: cross-protection or a plant mediated process?. *Phytoparasitica*, *44*, 203-211.

Osler, R., Borselli, S., Ermacora, P., Loschi, A., Martini, M., Musetti, R., & Loi, N. (2014). Acquired tolerance in apricot plants that stably recovered from European stone fruit yellows. *Plant Disease*, *98*(4), 492-496.

Pacifico, D., Galetto, L., Rashidi, M., Abbà, S., Palmano, S., Firrao, G., ... & Marzachì, C. (2015). Decreasing global transcript levels over time suggest phytoplasma cells enter stationary phase during plant and insect colonization. *Applied and environmental microbiology*, AEM-03096.

Pagliari, L., Buoso, S., Santi, S., Furch, A. C., Martini, M., Degola, F., ... & Musetti, R. (2017). Filamentous sieve element proteins are able to limit phloem mass flow, but not phytoplasma spread. *Journal of experimental botany*, *68*(13), 3673-3688.

Paolacci, A. R., Catarcione, G., Ederli, L., Zadra, C., Pasqualini, S., Badiani, M., ... & Ciaffi, M. (2017). Jasmonate-mediated defence responses, unlike salicylate-mediated responses, are involved in the recovery of grapevine from bois noir disease. *BMC plant biology*, *17*(1), 118.

Payne, S. M. (1993). Iron acquisition in microbial pathogenesis. *Trends in microbiology*, *1*(2), 66-69.

Pérez-López E., Luna-Rodríguez M., Olivier C.Y., & Dumonceaux T.J. (2016). The underestimated diversity of phytoplasmas in Latin America. *International Journal of Systematic and Evolutionary Microbiology*, *66*, 492–513.

Pieterse, C. M., Zamioudis, C., Berendsen, R. L., Weller, D. M., Van Wees, S. C., & Bakker, P. A. (2014). Induced systemic resistance by beneficial microbes. *Annual review of phytopathology*, *52*.

Pracros, P., Hernould, M., Teyssier, E., Eveillard, S., & Renaudin, J. (2007). Stolbur phytoplasma-infected tomato showed alteration of SlDEF methylation status and deregulation of methyltransferase genes expression. *Bulletin of Insectology*, *60*(2), 221.

Pracros, P., Renaudin, J., Eveillard, S., Mouras, A., & Hernould, M. (2006). Tomato flower abnormalities induced by stolbur phytoplasma infection are associated with changes of expression of floral development genes. *Molecular Plant Microbe Interactions*, *19*, 62-68.

Prasch, C. M., & Sonnewald, U. (2015). Signaling events in plants: stress factors in combination change the picture. *Environmental and Experimental Botany*, *114*, 4-14.

Punelli, F., Al Hassan, M., Fileccia, V., Uva, P., Pasquini, G., & Martinelli, F. (2016). A microarray analysis highlights the role of tetrapyrrole pathways in grapevine responses to "stolbur" phytoplasma, phloem virus infections and recovered status. *Physiological and Molecular Plant Pathology*, *93*, 129-137.

Quaglino, F., Zhao, Y., Casati, P., Bulgari, D., Bianco, P. A., Wei, W., & Davis, R. E. (2013). 'Candidatus Phytoplasma solani', a novel taxon associated with stolbur-and bois noir-related diseases of plants. *International journal of systematic and evolutionary microbiology*, *63*(8), 2879-2894.

Razin, S., Yogev, D., & Naot, Y. (1998). Molecular biology and pathogenicity of mycoplasmas. *Microbiol Mol Biol Rev*, *62*,1094–1156.

Rellán-Álvarez, R., Stastion, A. D. E., Giner-Martinez Sierra, J., Orduna, J., Orera, I., Rodriguez-Castrillon, J. A., ... & Alvarez-Fernandez, A. (2010). Identification of a tri-iron (III), tri-citrate complex in the xylem sap of iron-deficient tomato [Lycopersicon esculentum] resupplied with iron: new insights into plant iron long-distance transport. *Plant and Cell Physiology (Japan).*

Robinson, N. J., Procter, C. M., Connolly, E. L., & Guerinot, M. L. (1999). A ferric-chelate reductase for iron uptake from soils. *Nature*, *397*(6721), 694.

Rogers, E. E., & Guerinot, M. L. (2002). FRD3, a member of the multidrug and toxin efflux family, controls iron deficiency responses in Arabidopsis. *The Plant Cell*, *14*(8), 1787-1799.

Romanazzi, G., Murolo, S., & Feliziani, E. (2013). Effects of an innovative strategy to contain grapevine Bois noir: field treatment with resistance inducers. *Phytopathology*, *103*(8), 785-791.

Römheld, V. (1987). Different strategies for iron acquisition in higher plants. *Physiologia Plantarum.*, *70*(2), 231–234.

Römheld, V., & Marschner, H. (1986). Evidence for a specific uptake system for iron phytosiderophores in roots of grasses. *Plant Physiology*, *80*(1), 175-180.

Ruiz-Medrano, R., Xoconostle-Cazares, B., & Lucas, W. J. (2001). The phloem as a conduit for inter-organ communication. *Current Opinion in Plant Biology*, *4*, 202–209.

Rusjan, D., & Mikulic-Petkovsek, M. (2015). Phenolic responses in 1-year-old canes of V itis vinifera cv. C hardonnay induced by grapevine yellows (Bois noir). *Australian journal of grape and wine research*, *21*(1), 123-134.

Santi, S., & Schmidt, W. (2009). Dissecting iron deficiency–induced proton extrusion in Arabidopsis roots. *New Phytol.*, *183*, 1072–84.

Santi, S., De Marco, F., Polizzotto, R., Grisan, S., & Musetti, R. (2013a). Recovery from stolbur disease in grapevine involves changes in sugar transport and metabolism. *Frontiers in Plant Science*, *4*, 1–12.

Santi, S., Grisan, S., Pierasco, A., De Marco, F., & Musetti, R. (2013b). Laser microdissection of grapevine leaf phloem infected by stolbur reveals site-specific gene responses associated to sucrose transport and metabolism. *Plant, cell & environment*, *36*(2), 343-355

Schaper, U., & Seemüller, E. (1984). Recolonization of the stem of apple proliferation and pear decline-diseased trees by the causal organisms in spring/Wiederbesiedlung des Sprosses von triebsuchtkranken Apfelbäumen und verfallskranken Birnbäumen durch die Erreger im Frühjahr. *Zeitschrift für Pflanzenkrankheiten und Pflanzenschutz/Journal of Plant Diseases and Protection*, 608-613.

Schikora, A., & Schmidt, W. (2002). Formation of transfer cells and H+-ATPase expression in tomato roots under P and Fe deficiency. *Planta*, *215*(2), 304-311.

Schmidt, H., Günther, C., Weber, M., Spörlein, C., Loscher, S., Böttcher, C., ... & Clemens, S. (2014). Metabolome analysis of Arabidopsis thaliana roots identifies a key metabolic pathway for iron acquisition. *PLoS One*, *9*(7), e102444.

Schmidt, W. (1999). Mechanisms and regulation of reduction-based iron uptake in plants. *The New Phytologist*, *141*(1), 1-26.

Schweigkofler, W., Cassar, A., & Stimpfl, E. (2008). Reduced levels of calcium and other mineral elements in grapevine leaves affected by Bois noir (BN). *Mitteilungen Klosterneuburg*, *58*, 117.

Seemüller, E., Garnier, M., & Schneider, B. (2002). Mycoplasmas of plants and insects. In *Molecular Biology and Pathogenicity of Mycoplasmas* (pp. 91-115). Springer US.

Segond, D., Dellagi, A., Lanquar, V., Rigault, M., Patrit, O., Thomine, S., & Expert, D. (2009). NRAMP genes function in Arabidopsis thaliana resistance to Erwinia chrysanthemi infection. *The Plant Journal*, *58*(2), 195-207.

Selote, D., Samira, R., Matthiadis, A., Gillikin, J. W., & Long, T. A. (2015). Iron-binding E3 ligase mediates iron response in plants by targeting basic helix-loop-helix transcription factors. *Plant physiology*, *167*(1), 273-286.

Shin, L. J., Lo, J. C., Chen, G. H., Callis, J., Fu, H., & Yeh, K. C. (2013). IRT1 degradation factor1, a ring E3 ubiquitin ligase, regulates the degradation of iron-regulated transporter1 in Arabidopsis. *The Plant Cell*, tpc-113.

Sivitz, A. B., Hermand, V., Curie, C., & Vert, G. (2012). Arabidopsis bHLH100 and bHLH101 control iron homeostasis via a FIT-independent pathway. *PloS one*, *7*(9), e44843.

Socciarelli, S., Marconi, S., Rossi, G., Beni, C., Pastore, M., Del Vaglio, M., & Gervasi, F. (2008, May). Mineral nutrition of pear and apricot trees cultivated in Southern Italy area damaged by phytoplasma microorganisms. In *VI International Symposium on Mineral Nutrition of Fruit Crops 868* (pp. 433-438).

Sugio, A., MacLean, A. M., Grieve, V. M., & Hogenhout, S. A. (2011). Phytoplasma protein effector SAP11 enhances insect vector reproduction by manipulating plant development and defense hormone biosynthesis. *Proceedings of the National Academy of Sciences*, *108*(48), E1254-E1263.

Tarantino, D., Santo, N., Morandini, P., Casagrande, F., Braun, H. P., Heinemeyer, J., ... & Murgia, I. (2010). AtFer4 ferritin is a determinant of iron homeostasis in Arabidopsis thaliana heterotrophic cells. *Journal of plant physiology*, *167*(18), 1598-1605.

Terry, N., & Abadía, J. (1986). Function of iron in chloroplasts. *Journal of Plant Nutrition*, *9*(3-7), 609-646.

Tomato Genome Consortium. (2012). The tomato genome sequence provides insights into fleshy fruit evolution. *Nature*, *485*(7400), 635.

Tran-Nguyen, L. T., Kube, M., Schneider, B., Reinhardt, R., & Gibb, K. S. (2008). Comparative genome analysis of "Candidatus Phytoplasma australiense" (subgroup tuf-Australia I; rp-A) and "Ca. Phytoplasma asteris" strains OY-M and AY-WB. *Journal of Bacteriology*, *190*(11), 3979-3991.

Valenta, V., Musil, M., & Mišiga, S. (1961). Investigations on European Yellows-type Viruses I. The Stolbur Virus. *Journal of Phytopathology*, *42*(1), 1–38.

Van Bel, A. J., Helariutta, Y., Thompson, G. A., Ton, J., Dinant, S., Ding, B., & Patrick, J. W. (2013). Phloem: the integrative avenue for resource distribution, signaling, and defense. *Frontiers in plant science*, *4*, 471.

Verbon, E. H., Trapet, P. L., Stringlis, I. A., Kruijs, S., Bakker, P. A., & Pieterse, C. M. (2017). Iron and immunity. *Annual review of phytopathology*, *55*, 355-375.

Wang, N., Cui, Y., Liu, Y., Fan, H., Du, J., Huang, Z., ... & Ling, H. Q. (2013). Requirement and functional redundancy of Ib subgroup bHLH proteins for iron deficiency responses and uptake in Arabidopsis thaliana. *Molecular plant*, *6*(2), 503-513.

Wang, J., Song, L., Jiao, Q., Yang, S., Gao, R., Lu, X., & Zhou, G. (2018). Comparative genome analysis of jujube witches'-broom Phytoplasma, an obligate pathogen that causes jujube witches'-broom disease. *BMC genomics*, *19*(1), 689.

Wei, W., Davis, R. E., Nuss, D. L., & Zhao, Y. (2013). Phytoplasmal infection derails genetically preprogrammed meristem fate and alters plant architecture. *Proceedings of the National Academy of Sciences*, *110*(47), 19149-19154.

Wei, W., Kakizawa, S., Suzuki, S., Jung, H. Y., Nishigawa, H., Miyata, S. I., ... & Namba, S. (2004). In planta dynamic analysis of onion yellows phytoplasma using localized inoculation by insect transmission. *Phytopathology*, *94*(3), 244-250.

Weinberg, E.D. (2000). Modulation of intramacrophage iron metabolism during microbial cell invasion. *Microbes Infect.*, *1*, 85–89.

Weintraub, P. G., & Beanland, L. (2006). Insect vectors of phytoplasmas. *Annu. Rev. Entomol.*, *51*, 91-111.

Weisburg, W. G., Tully, J. G., Rose, D. L., Petzel, J. P., Oyaizu, H., Yang, D., ... & Van Etten, J. (1989). A phylogenetic analysis of the mycoplasmas: basis for their classification. *Journal of bacteriology*, *171*(12), 6455-6467.

Winkelmann, G. (2007). Ecology of siderophores with special reference to the fungi. *Biometals*, *20*, 379–392.

Xue, C., Liu, Z., Dai, L., Bu, J., Liu, M., Zhao, Z., ... & Zhao, J. (2018). Changing Host Photosynthetic, Carbohydrate, and Energy Metabolisms Play Important Roles in Phytoplasma Infection. *Phytopathology*, *108*(9), 1067-1077.

Ye, F., Albarouki, E., Lingam, B., Deising, H. B., & von Wirén, N. (2014). An adequate Fe nutritional status of maize suppresses infection and biotrophic growth of Colletotrichum graminicola. *Physiologia plantarum*, *151*(3), 280-292.

Yuan, Y. X., Zhang, J., Wang, D. W., & Ling, H. Q. (2005). AtbHLH29 of Arabidopsis thaliana is a functional ortholog of tomato FER involved in controlling iron acquisition in strategy I plants. *Cell research*, *15*(8), 613.

Yuan, Y., Wu, H., Wang, N., Li, J., Zhao, W., Du, J., ... & Ling, H. Q. (2008). FIT interacts with AtbHLH38 and AtbHLH39 in regulating iron uptake gene expression for iron homeostasis in Arabidopsis. *Cell research*, *18*(3), 385.

Zahavi, T., Sharon, R., Sapir, G., Mawassi, M., Dafny-Yelin, M., & Naor, V. (2013). The long-term effect of S tolbur phytoplasma on grapevines in the G olan H eights. *Australian journal of grape and wine research*, *19*(2), 277-284.

Zamboni, A., Zanin, L., Tomasi, N., Pezzotti, M., Pinton, R., Varanini, Z., & Cesco, S. (2012). Genome-wide microarray analysis of tomato roots showed defined responses to iron deficiency. *BMC genomics*, *13*(1), 101.

Zamioudis, C., Hanson, J., & Pieterse, C. M. (2014). β-Glucosidase BGLU42 is a MYB72-dependent key regulator of rhizobacteria-induced systemic resistance and modulates iron deficiency responses in Arabidopsis roots. *New Phytologist*, *204*(2), 368-379.

Zhai, Z., Gayomba, S. R., Jung, H. I., Vimalakumari, N. K., Piñeros, M., Craft, E., ... & Guerinot, M. L. (2014). OPT3 is a phloem-specific iron transporter that is essential for systemic iron signaling and redistribution of iron and cadmium in Arabidopsis. *The Plant Cell*, tpc-114.

Zhang, J., Hogenhout, S. A., Nault, L. R., Hoy, C. W., & Miller, S. A. (2004). Molecular and symptom analyses of phytoplasma strains from lettuce reveal a diverse population. *Phytopathology*, *94*(8), 842-849.

Zhao, J., Liu, & M. J. (2009) Variation of mineral element contents in Chinese jujube with witches' broom disease. *Acta Hortic*. *840*, 399–404.

Zhao, Y., & Davis, R. E. (2016). Criteria for phytoplasma 16Sr group/subgroup delineation and the need of a platform for proper registration of new groups and subgroups. *International journal of systematic and evolutionary microbiology*, *66*(5), 2121-2123.

Ziegler, H. (1975). Nature of transported substances. In *Transport in Plants I* (pp. 59-100). Springer, Berlin, Heidelberg.

Zimmermann, M. H., & Ziegler, H. (1975). List of sugars and sugar alcohols in sieve-tube exudates. *Transport in plants*, vol I Springer, Berlin Heidelberg New York, pp 480–496.

Zorzoli, R., Pratta, G. R., Rodríguez, G. R., & Picardi, L. A. Advances in Biotechnology: Tomato as a Plant Model System. *Functional Plant Science and Biotechnology*, *1*(1), 146-159.

Zouari, M., Abadía, A., & Abadía, J. (2001). Iron is required for the induction of root ferric chelate reductase activity in iron-deficient tomato. *Journal of plant nutrition*, *24*(2), 383-396.

8. Publications

8.1. Papers

1. Filamentous sieve element proteins are able to limit phloem mass flow, but not phytoplasma spread

Laura Pagliari, Sara Buoso, Simonetta Santi, Alexandra C.U. Furch, Marta Martini, Francesca Degola, Alberto Loschi, Aart J.E. van Bel and Rita Musetti

Journal of Experimental Botany, 2017, 68:(13)3673–3688, Doi: 10.1093/jxb/erx199

Abstract: In Fabaceae, dispersion of forisomes—highly ordered aggregates of sieve element proteins—in response to phytoplasma infection was proposed to limit phloem mass flow and, hence, prevent pathogen spread. In this study, the involvement of filamentous sieve element proteins in the containment of phytoplasmas was investigated in non- Fabaceae plants. Healthy and infected Arabidopsis plants lacking one or two genes related to sieve element filament formation—*AtSEOR1* (At3g01680), *AtSEOR2* (At3g01670), and *AtPP2-A1* (At4g19840)—were analysed. TEM images revealed that phytoplasma infection induces phloem protein filament formation in both the wild-type and mutant lines. This result suggests that, in contrast to previous hypotheses, sieve element filaments can be produced independently of *AtSEOR1* and *AtSEOR2* genes. Filament presence was accompanied by a compensatory overexpression of sieve element protein genes in infected mutant lines in comparison with wild-type lines. No correlation was found between phloem mass flow limitation and phytoplasma titre, which suggests that sieve element proteins are involved in defence mechanisms other than mechanical limitation of the pathogen.

Key words: Arabidopsis thaliana, combined microscopy, phloem mass flow, phytoplasmas, sieve element occlusion, sieve element proteins.

As second author, together with L. Pagliari (first author) I took care of plant material preparation, gene expression experiments and partial writing of the manuscript.

2. What Slows Down Phytoplasma Proliferation? Speculations on the Involvement of AtSEOR2 Protein in Plant Defence Signalling

Laura Pagliari*, Sara Buoso*, Simonetta Santi, Aart J.E. van Bel and Rita Musetti

***Laura Pagliari and Sara Buoso are contributed equally to this work.*

Plant signaling & behavior, 2018, 13(5), e1473666, Doi: 10.1080/15592324.2018.1473666

Abstract: Considering the crude methods used to control phytoplasma diseases, a deeper knowledge on the defence mechanisms recruited by the plant to face phytoplasma invasion is required. Recently, we demonstrated that Arabidopsis mutants lacking AtSEOR1 gene showed a low phytoplasma titre. In wild type plants AtSEOR1 and AtSEOR2 are tied in filamentous proteins. Knockout of the *AtSEOR1* gene may pave the way for an involvement of free AtSEOR2 proteins in defence mechanisms. Among the proteins conferring resistance against pathogenic bacteria, AtRPM1-interacting protein has been found to interact with AtSEOR2 in a high-quality, matrix-based yeast-two hybrid assay. For this reason, we investigated the expression levels of Arabidopsis *AtRIN4*, and the associated *AtRPM1* and *AtRPS2* genes in healthy and Chrysanthemum yellows-infected wild-type and Atseor1ko lines.

Key words: Arabidopsis thaliana; defence responses; phytoplasmas; sieve element proteins; RPM1-interacting protein

8.2. Abstracts

1. Dissecting the role of iron in the interaction between the host plant tomato and '*Candidatus* Phytoplasma solani'

Sara Buoso, Laura Pagliari, Rita Musetti, Wolfgang Schmidt, Simonetta Santi

19th International Symposium on Iron Nutrition and Interactions in Plants 2018

Abstract: Phytoplasmas are prokaryotic plant pathogens that colonize the sieve elements of the host plant phloem. Alteration in phloem function and impairment of assimilate translocation is one of the most dramatic effects, but mechanisms underlying plant host-phytoplasma interaction are still largely unexplored. In particular, no knowledge is available on the role of iron (Fe) in this interaction. Iron is an essential element for most living organisms, and competition for it can lead, as already observed in different pathosystems, to the development of an Fe-withholding response by plants that changes Fe distribution and trafficking [1]. Moreover, the signaling pathways regulating plant Fe uptake directly interact with the plant immune signaling network [2]. In the current study, we investigated on the role of Fe in the interaction between tomato (cv. Micro-Tom) and '*Candidatus* Phytoplasma solani' by analyzing control plants (H/+Fe), Fe-starved plants (H/-Fe), phytoplasma-infected plants (D/+Fe) and phytoplasma-infected / Fe-starved plants (D/-Fe). The expression of strongly Fe-regulated genes was analyzed in leaves, focusing on vein-enriched tissue. While the expression level of the *ferritin-1* gene dramatically decreased upon Fe-starvation but not in infected plants, *magnesium-chelatase subunit ChlH* and *nicotianamine synthase* (chln) were down-regulated under both stress conditions. Iron pools visualized by Perls' staining indicated local alterations of Fe distribution in the leaf lamina of plants subjected to stress conditions, visible by fewer iron spots in the mesophyll palisade cells of infected plants. Moreover, the total absence of Fe spots in xylem parenchyma cells could be interpreted as a further signal of Fe-deficiency, although Fe spots were localized to the phloem of both diseased (D) and healthy (H) plants in the presence of Fe. On the other hand, no significant difference in total leaf Fe concentration (analyzed by ICP-OES) emerged when comparing H and D plants under both nutritional conditions, whereas the Fe concentration in D/+Fe roots was 11% lower when compared to H/+Fe. These results prompted us to investigate if the observed changes in Fe homeostasis had an effect on the Fe acquisition mechanism at the root level. We analyzed the expression of genes involved in the Fe uptake of strategy I plants: the AtFIT ortholog FER, bHLH68, IRT1, FRO1, and the AtAHA2 ortholog LHA4. In presence of Fe in the nutrient solution, the expression of these genes did not change significantly, although high variability was observed among D plants. Surprisingly, phytoplasma infection under Fe-deficient conditions reduced

the expression of all the examined genes, except for FRO1. Determination of ferric chelate reduction activity (localized on agarose gel) was in line with the unaltered expression of this gene. In conclusion, phytoplasma appears to interfere with a long-distance signal triggering the Fe acquisition machinery involving FER/BHL68, IRT1 and LHA4, tuning the plant Fe uptake towards a permanent basal-level. Notably, in our system FRO1 seems to respond prevalently to a locally generated signal, suggesting multi-level regulation of Fe acquisition**.**

Keywords: Phytoplasma, phloem, iron homeostasis, iron deficiency

References: [1] Dellagi A et al. 2005, Plant J. 43: 262-272. [2] Pieterse CMJ et al. 2014 Annu. Rev. Phytopathol. 52:347–75